INTEGRATED PHASE BEHAVIOUR MODELLING OF PETROLEUM FLUIDS FOR COMPOSITIONAL SIMULATION OF RESERVOIR-SURFACE PROCESSES

by

FATHOLLAH GOZALPOUR

BSc Chem Eng, MSc Res Eng

Submitted for the Degree of Doctor of Philosophy in

PETROLEUM ENGINEERING

Department of Petroleum Engineering

Heriot-Watt University

Edinburgh, UK

July 1998

To my wife

for her **patience** and **encouragement**

TABLE OF CONTENTS

LIST OF SYMBOLS

a	attractive term, parameter of equation of state
A	$Pa / (RT)^2$
a'	attractive term, parameter of equation of state with no BIPs in the mixture
A',B',C',D'	coefficients of Eq 2.57 and their values are given in Table 2.6
A, B, C	coefficients of Eq 2.53 and their values are given in Table 2.2
A,B	coefficients of Eq 2.41
A_0, A_1, A_2	coefficients of Eq 2.44
B	Pb / (RT)
b	repulsive term (co-volume), parameter of equation of state
Bo	formation volume factor
C	Pc / (RT)
C	coefficient of Eq 2.43
c	third parameter of equation of state
C_1,C_2, C_3	coefficients of Eq 2.45
d	derivative operand (Eq 2.1)
d	positive correlation coefficient, Eq 2.55
d_1,d_2,d_3	coefficients of Eq 2.48
e	positive correlation coefficient, Eq 2.55
E',F'	coefficients of Eq 2.57 and their values are given in Table 2.6
e_1, e_2, e_3	check functions (Eqs 3.20, 3.21, 3.22)
f	fugacity
$F(\bar{x})$	objective function
g	gravitational acceleration
G	total Gibbs free energy
h	depth
k	binary interaction parameter
K	equilibrium ratio ($K_i=y_i / x_i$)

K_1, K_2, K_3	pure compound adjustable parameter in Eq 2.47b
K_{ver}	slope of temperature dependency of the attractive term (Eq 2.47a)
L, M, N	parameters of Eq 2.52
Lmax	upper limit, Eq 3.29
Lmin	lower limit, Eq 3.28
M	molecular weight
M	number of experimental data Eq 3.26
m	slope of temperature dependency of the attractive term (Eq 2.21)
m'	modified slope of temperature dependency of the attractive term (Eq 2.50)
$M(\omega)$	slope of temperature dependency of the attractive term (Eq 2.44)
m,n	empirical constants in Eq 2.46
m_m, n_n	coefficients of Eq 2.49
m_{Wilson}	slope of temperature dependency of the attractive term (Eq 2.39)
N	number of components in the mixture or each phase
n	number of moles of a component
N	number of regression parameters, Eq 3.26
N_p	number of data points
P	pressure
P	property, Eq 3.26
q_1	$\partial(nu)/\partial n_i$
q_2	$2nw\ \partial(nw)/\partial n_i$
R	universal gas constant
S	shift parameters in the PR EOS
S^0	numerical value of shift parameter at ω=0.
S^1	numerical value of shift parameter at ω=1.
SG	specific gravity
S_{int}	an adjustable parameter in shift parameter correlation, Fig. 2.19
S_{teta}	an adjustable parameter in shift parameter correlation, Fig. 2.19
T	temperature
U	Pu / (RT)

u, w	parameters in the general form of EOS, Eq A.2
V	molar volume
v	total volume (v=nV)
W	Pw / (RT)
w	weighing factor, Eq 3.26
$\overline{x}$	vector of regression variables
x	liquid mole fractions (composition)
X	regression parameter or calculated properties, Eq 3.27
y	vapour mole fractions (composition)
Z	compressibility factor
z	feed mole fractions (composition)
Z_{RA}	Rackett compressibility factor

Greek letters

α or $\alpha(T)$	temperature dependency of the attractive term in equation of state
α^0	numerical value of α at ω=0.
α^1	numerical value of α at ω=1.
γ	vapour phase fraction (relative to feed)
η	parameter of the PT EOS, Eq 2.32
μ	chemical potential
ρ	density
ϕ	fugacity coefficient
ω	acentric factor
Ω_{ac}	equation of state constant
Ω_b	equation of state constant
Ω_c	equation of state constant

Subscripts

c	critical
F	feed

i,j	component index
L	liquid
r	reduced (e.g., $T_r = T / T_c$)
sat	saturation point
V	vapour

Superscripts

L	liquid
V	vapour
P1,P2,...,Pm	phase identification (Eq 2.2)

Abbreviations

AAD%	average absolute percentage deviation $\sum_{i=1}^{N_p} 100 \times \lvert Cal./Exp. - 1 \rvert_i / N_p$
AD%	absolute percentage deviation $100 \times \lvert Cal./Exp. - 1 \rvert$
bbl	barrel
BDD	backward differential depletion
BIP	binary interaction parameter
BP	bubble point pressure
Cal	calculated
CCE	constant composition expansion
CGR	condensate gas ratio
Contam.	contaminated
CPU time	Central Processing Unit, computational time, s
CVD	constant volume depletion
DL	differential liberation
DP	dew point pressure
DSS	direct sampling system
%Dev.	percentage deviation
EOS	equation of state

Exp	experimental
frac.	fraction
FVF	formation volume factor
GLR	gas-liquid ratio
GOR	gas-oil ratio
IFT	interfacial tension
JY	Jhaveri-Youngren
Kh	equilibrium ratio of the heaviest component (plus fraction) in the mixture
Kl	equilibrium ratio of the lightest component (C_1) in the mixture
Liq.	liquid
LM	Levenberg-Marquardt
MBC	multiple backward contact
MFC	multiple forward contact
mPR	Peng-Robinson EOS with the new α function
MSCF	thousand standard cubic feet
MW	molecular weight
PR	Peng-Robinson
PR3	3-parameter modification of the Peng-Robinson
Press	pressure
PT	Patel-Teja
PVT	pressure-volume-temperature
QN	quasi-Newton
Res.	reservoir
RFC	rapid flash calculation
RFT	repeat formation tester
RK	Redlich-Kwong
SCF	standard cubic feet
Sat.	saturation
SCN	single carbon number (group)
Sep.	separator

Sp. Gr.	specific gravity
SRK	Soave-Redlich-Kwong
SS	successive substitution
STB	stock tank barrel
Temp.	temperature
VDW	van der Waals
VLE	vapour-liquid equilibrium
Vol.	volume
VPT	Valderrama modification of Patel and Teja
WFT	wireline formation tester
1D	one dimensional
2D	two dimensional

LIST OF TABLES

LIST OF FIGURES

ACKNOWLEDGEMENTS

I wish to express my gratitude and appreciation to Prof. Ali Danesh and Prof. Adrian C. Todd for their excellent supervision and technical guidance throughout this work. Their directions and ideas were very valuable for my work. Their professional support and encouragement made the completion of this work successful.

I am deeply grateful to Prof. Dabir H. Tehrani for his interest in this work and useful advice on various subjects related to my study.

The financial support of Heriot-Watt University through their full scholarship to conduct this study is gratefully acknowledged.

Thanks are extended to the personnel of Reservoir Fluid Project team in the Department of Petroleum Engineering, Heriot-Watt University for providing experimental data for this work. In particular, I appreciate the help of Mr. Keith Bell, Mr. Ken Malcolm, Mr. Alastair Reid for experimental measurements, Mr. Jim Pantling for fabricating the equipment and Dr. Bahman Tohidi for lab supervision.

I would also like to express my thanks to all my colleagues with whom I shared the office during this study.

The research on which this work is based was equally sponsored by the UK Department of Trade and Industry, BP Exploration Operating Company Ltd, Chevron Petroleum (UK) Ltd, Conoco (UK) Ltd, Elf (UK) Ltd, Marathon International (GB) Ltd, Mobil (North Sea) Ltd, Phillips Petroleum Co. (UK) Ltd and Total Oil Marine Plc which is gratefully acknowledged.

Finally, the patience and encouragement of my wife and my parents were very valuable to me during the course of this study.

ABSTRACT

Equations of state (EOS) are widely used in the petroleum industry, because of their simplicity and reliability in predicting phase equilibrium calculations. The main objective of this study was to develop an ability to model the phase behaviour of reservoir fluids over wide ranges of temperature and compositional changes with a single EOS. In this thesis, an integrated phase behaviour model, two practical tuning methods, two methods of recombining separator samples to determine the original reservoir fluid composition and contamination of fluid sample with an oil-based mud filtrate have been investigated.

In the developed method which allows integrated modelling of the fluid behaviour within the reservoir, flow lines and process facilities, the reservoir fluid can be described by a large number of components without significantly increasing the computational time. This provides adequate compositional information for surface processes without impeding compositional reservoir simulation.

The temperature dependency of the attractive term in EOS has been modified in this study to improve the EOS predictions over a wide range of temperature. The modification also extends the applicability of EOS to hydrocarbons heavier than those used originally in its development. A consistent method to determine the volume shift, as the third parameter, to improve phase density prediction has also been suggested.

Two practical tuning methods namely, conventional and integrated, have been developed. In the conventional method the properties of the heavy end are used as regression variables to fit the experimental data at reservoir and surface conditions. In the integrated tuning method, the temperature dependency of the attractive term for the liquid phase, along with the properties of the heavy end if required, are used as regression variables. The capability of the tuning methods have been demonstrated by comparing with other methods in matching the PVT data over wide ranges of temperature and compositional changes.

Two methods, separator and backward differential depletion (BDD), are applied to the collected samples of liquid and vapour from the separator to determine the initial reservoir fluid composition, using saturation pressure as the matching point. The effect of inaccuracies in collected separator gas and liquid samples on the determined reservoir fluid composition have been investigated. A method to adjust the collected gas-liquid ratio has been described and its ability in determining the initial reservoir fluid composition demonstrated for different types of saturated and depleted reservoirs.

Contamination with an oil-based mud filtrate can impair the collected samples of reservoir fluid. A simple and practical method has been developed to determine the original composition of the reservoir fluid from contaminated samples. The method is general and it can be applied to different types of reservoir fluids, and highly contaminated samples. The proposed method provides PVT data within an acceptable accuracy in most cases.

CHAPTER 1

INTRODUCTION

Compositional simulation is extensively used in the petroleum industry to model fluid phase behaviour within the reservoir, flow lines and surface facilities. The simulation results provide valuable information for reservoir management and can also be used to design a production plan and/or to assess economic viability of the field development. Phase behaviour models have a major contribution in compositional simulation. These models generally employ an equation of state (EOS) to determine the equilibrium conditions. EOS is an analytical expression which relates the fluid temperature to its volume and pressure.

The majority of the modern EOS are based upon the van der Waals[1] EOS. Since van der Waals, a number of modifications have been developed to improve the capability of the EOS in predicting the phase behaviour and volumetric properties of fluids. To accurately predict the experimental vapour pressure of pure compounds over a wide range of temperature change, it is essential that at least one of the parameters in EOS is considered to be temperature dependent. Introducing temperature dependency in the attractive term of EOS, significantly improves the phase behaviour prediction[2,3]. Several investigators[4,5] have proposed different functions for the temperature dependency of the attractive term to improve phase behaviour prediction for multicomponent systems.

The volumetric prediction of the original two-parameter EOS has been improved by introducing a third parameter, which affects the phase density prediction[6]. This method is particularly attractive as it adjusts the phase densities by shifting the pressure-volume curve along the volume axis without changing the phase equilibrium conditions determined by the unmodified two-parameter EOS. Using the third parameter might,

however, deteriorate the predicted densities at some conditions. This could occur for systems with a high concentration of supercritical compound(s), particularly methane. Using a constant shift parameter for light hydrocarbons, the phase densities cannot be predicted accurately[7].

EOS are basically developed for pure compounds. Their application was then extended to multicomponent systems by introducing mixing rules. Using mixing rules, the average parameters of EOS can be determined through pure compound critical properties. Binary interaction parameters (BIP) were considered in the mixing rules as adjusting parameters to match the experimental data.

The capability of the compositional models depends on the reliability of the EOS, which are used to perform the phase equilibrium calculations. To improve the compositional simulation prediction, the EOS parameters are adjusted to match the available experimental data, then they are used to predict the required information. Hence, tuning of EOS is another aspect of phase equilibrium calculations from a practical application perspective. The majority of tuning procedures suggest binary interaction parameters (BIP) as regression variables. It is believed that these parameters empirically cover the deficiencies of EOS rather than accounting for any physical interaction between molecules of hydrocarbon components. Other parameters, however, can be used instead of BIP. For example using the composition and properties of the heavy end in petroleum fluids, particularly gas condensates, as regression variables are justified as the heavy end in petroleum fraction is the least defined component[8]. When BIP are not used in the mixing rules of EOS, phase equilibrium calculation can be performed much faster than the conventional method[9].

Computational time of compositional reservoir simulation is an important factor in petroleum industry. In practice, thousands of grid blocks are generally used to model the real reservoirs. To determine the phase behaviour of fluids in every grid block an iterative flash calculation is employed to calculate the composition and volumetric properties of

equilibrated phases. Therefore, it is vital to perform the flash calculation as fast as possible. Using the conventional methods to perform the flash calculation, the number of equations that are solved in phase equilibrium, is directly related to the number of components describing the fluid. The computational time can be decreased by reducing the number of components and/or the number of equations in flash calculation. The number of components can be reduced by grouping them. Grouping[10] the reservoir fluid components may reduce the computational time but the approach is not suitable for integrated phase behaviour modelling where detailed compositional analysis may be required in the design and operation of separation facilities at surface. Reduction of the number of components by grouping could also have an adverse effect on the accuracy of phase calculations, particularly for gas condensates.

Phase behaviour models can also be used as powerful tools in other field applications, such as evaluation and improvement of reservoir fluid samples.

Bottom hole samples of reservoir fluid can be obtained from a well test, a drill stem test and/or wireline formation testers (WFT). WFT recover samples of reservoir fluid from formations at selected depths. They can also measure the variation of pressure as a function of depth in formations. Using bottom hole sampling methods, reliable samples can be obtained from undersaturated oil reservoirs. However, these information are generally hampered by contamination of the reservoir fluid with drilling mud filtrate. Mud filtrate invades the formation during the drilling process. If an oil-based mud was used in the drilling, the mud filtrate would be completely soluble with the formation fluid. Therefore, it would be almost impossible to separate the contaminants from the reservoir fluid. As running WFT is expensive and accurate reservoir fluid properties are needed in reservoir development, it would be highly desirable to determine the accurate composition and phase behaviour of the reservoir fluid from contaminated samples. Although, significant efforts have been made in the design of WFT to improve sample recovery, sample quality has improved only marginally[11].

Surface sampling is widely used in industry as it is less expensive and easy to handle in the laboratory. It can also be applied to sample oil and gas reservoirs. In surface sampling, once the well is stabilised, samples of the liquid and vapour are collected from the separator. The collected liquid and vapour samples are recombined in the laboratory at the measured producing gas-liquid ratio (GLR) to give a representative sample of in-situ reservoir fluid. The recombining proportion (GLR) strongly affects the quality of the recombined mixture. The well stabilisation can also be a problem, where, in tight reservoirs the stabilisation period may be as long as a month. Any inaccuracy in separation efficiency and in the measured GLR will directly affect the composition of the recombined fluid. Any carryover or carry through in the separation could cause unrepresentative samples being taken. The separation of gas and liquid during the process of sampling, before or during the sampling outside or within the sample taker could result in an unrepresentative fluid. For example, if high pressure rich gas from the separator is directed through a throttling valve to an empty sample taker, liquid may dropout on the way and may be trapped in the lines that lead to the sample taker. The sample could be unrepresentative.

The main objective of this study was to develop a capability to model the phase behaviour of reservoir fluids over wide ranges of temperature and composition with a single EOS. The method, which allows integrated modelling of the fluid within the reservoir, flow lines and process facilities is based on an approach which avoids using BIP. The fluid can then be described with a large number of components without significantly increasing the computational time.

The associated problems in reservoir fluid sampling were also investigated. The impact of contamination with oil-based mud filtrate on phase behaviour and properties of collected samples in bottom hole sampling were studied. The effect of erroneous GLR on the phase behaviour of the recombined sample was also examined.

This thesis consists of 6 chapters. This chapter begins with a brief review of phase behaviour models and outline of this study.

Chapter 2 describes the fundamental thermodynamic aspects of phase equilibrium calculation. A brief review of some popular EOS in the petroleum industry is discussed in this chapter. A new correlation developed in this study for the temperature dependency of the attractive term in the Peng-Robinson[12] (PR) EOS is presented. The developed function has compensated the lack binary interaction parameters (BIP) in the mixing rules, hence allowing the use of a rapid flash calculation (RFC) method in performing the phase equilibrium calculations. A new method is also proposed to determine the shift parameters of the PR EOS which improves phase density predictions. The developed functions are linear in acentric factor at constant reduced temperature and they can be extrapolated to heavy petroleum fractions.

Chapter 3 gives the application of a rapid flash calculation (RFC) in phase behaviour modelling of reservoir fluids. A modification is developed in this chapter to improve the robustness of the rapid flash calculation. The reliability and low computational time of the modified RFC method in performing phase spilt calculations are demonstrated for variety of fluids. Tuning of EOS and its application in the petroleum industry are also investigated in this chapter. Two developed practical tuning methods are explained in detail and applied to several model and real reservoir fluids. It is shown that phase behaviour models can be tuned against experimental data as effectively without using binary interaction parameters in the mixing rules.

Chapter 4 examines the effect of errors in surface sampling of reservoir fluids, on the phase behaviour of the recombined samples. Different types of reservoir fluids are sampled during the normal operational conditions. Two methods of adjusting the recombination ratio to match the saturation pressure are employed to determine the initial reservoir fluid composition. A method has been proposed to determine the representative reservoir fluid composition in saturated reservoirs.

Chapter 5 reports the results of an investigation on the contamination of bottom hole samples by mud filtrate. Different types of reservoir fluids were deliberately contaminated with an oil-based mud filtrate. A modelling approach is suggested to calculate the original reservoir fluid composition from contaminated samples. A phase behaviour model is calibrated against the experimental data of contaminated samples. The developed model is used to predict the properties of the original reservoir fluid, using the retrieved composition from contaminated samples.

The conclusions of this study and recommendations for future investigation are presented in Chapter 6.

REFERENCES

1. Van der Waals, J.D., (1873) : "*On the Continuity of the Liquid and Gaseous State*", PhD Dissertation, Sigthoff, Leiden.

2. Wilson, G.M., (1964) : "Vapour-Liquid Equilibria Correlated by Means of a Modified Redlich-Kwong Equation of State", *Adv. Cryog. Eng.*, **9**, 168-176.

3. Soave, G., (1972) : "Equilibrium Constants from a Modified Redlich-Kwong Equation of State", *Chem. Eng. Sci.*, **27**, 1197-1203.

4. Twu, C.H., Coon, J.E. and Cunningham, J.R., (1995) : "A New Generalised alpha Function for a Cubic Equation of State, Part 1. Peng-Robinson Equation", *Fluid Phase Equilibria*, **105**, 49-59.

5. Gozalpour, F., Danesh, A., Todd, A.C. and Tehrani, D.H., (1998) : "Rapid and Robust Phase Equilibrium Calculation to Model Fluids in Reservoir and Surface Processing", *Chem. Eng. Res. Des.*, in press.

6. Jhaveri, B.S. and Youngren, G.K., (1988) : "Three-Parameter Modification of the Peng-Robinson Equation of State to Improve Volumetric Predictions", *SPERE*, Aug., 1033-1040.

7. Gozalpour, F., Danesh, A., Tohidi, B., Todd, A.C. and Tehrani, D.H., (1998) : "Improved Modelling of Reservoir Fluid Phase Behaviour", Petroleum Geoscience and Engineering Conference, 20-21 April, London, UK.

8. Danesh, A., Gozalpour, F., Todd, A.C. and Tehrani, D.H., (1996) : "Reliable Tuning of Equation of State with No Binary Interaction Parameter", paper presented at the 17th International Workshop and Symposium, International Energy Agency Collaborative Project on EOR, Sept. 30-Oct. 2, Sydney, Australia.

9. Michelsen, M.L., (1986) : "Simplified Flash Calculations for Cubic Equations of State", *Ind. Eng. Chem. Process Des. Dev.*, **25**(1), 184-188.

10. Danesh, A., Xu, D.-H. and Todd, A.C., (1990) : "A Grouping Method to Optimise Oil Description for Compositional Simulation of Gas Injection Processes", SPE paper 20745, presented at the 65th Annual Technical Conference and Exhibition held in New Orleans, L.A., Sept. 23-26.

11. Michaels, J., Moody, M. and Shwe, S., (1995) : "Wireline Fluid Sampling", SPE 30610, presented at the SPE Annual Technical Conference and Exhibition held in Dallas, 22-25 October.

12. Peng, D.-Y. and Robinson, D.B., (1976) : "A New Two-Constant Equation of State", *Ind. Eng. Chem. Fundam.*, **15**(1), 59-64.

CHAPTER 2

APPLICATION OF EOS IN PHASE EQUILIBRIUM CALCULATIONS

2.1 INTRODUCTION

Phase equilibrium is of special interest in the petroleum industry as in many production operations. Many operations and processes in reservoir fluid production, such as design of surface facilities, reservoir production, pipeline and enhanced oil recovery processes consist of contacting different phases. To have an understanding of any one of them knowledge of phase equilibrium is vital. Equilibrium state is the conditions at which there is no tendency to depart spontaneously and cross the phase boundary. In the state of equilibrium, values of the properties are independent of time and they are stable[1]. Equilibrium requires balance of all potentials that may cause a change in the system. A true state of equilibrium may never be attained, as there is a continual change in surroundings. For practical purposes, the equilibrium state is presumed if changes can no longer be detected with available measuring devices.

In this chapter the criterion of phase equilibrium is introduced. Some well-known equations of state (EOS) are briefly described. The application of EOS to determine the phase equilibrium calculation using the equilibrium criteria is also discussed in this chapter. The importance of EOS parameters on determining phase equilibrium is also investigated and the temperature dependency of the attractive term is modified to improve EOS predictions over a wide range of temperature change. Finally, a new method is also developed in this study to determine the shift parameters of the Peng-Robinson[2] EOS which has improved phase density predictions.

2.2 CRITERIA OF EQUILIBRIUM

An important outcome of phase equilibrium thermodynamics is the determination of the distribution of every component among all the phases present at equilibrium. The thermodynamic solution to the phase equilibrium problem was obtained many years ago by Gibbs when he introduced the concept of chemical potential. Gibbs stated that a closed system attains equilibrium when the total Gibbs free energy (G), determined by its composition, pressure and temperature, was minimum[1].

$$dG = 0 \quad \text{and} \quad d^2G > 0 \tag{2.1}$$

Equation 2.1 leads to the fact that at equilibrium the chemical potential (μ) of each component, defined as the partial molar Gibbs energy, must be the same in every phase:

$$\mu_i^{P1} = \mu_i^{P2} = \ldots = \mu_i^{Pm} \qquad i = 1,2,\ldots,N \tag{2.2}$$

where the superscripts P1, P2, ..., Pm identify the phases and N is the number of components in the system.

Lewis[3] simplified the concept of chemical potential by expressing it in terms of fugacity:

$$d\mu_i = RTd\ln f_i \tag{2.3}$$

where f_i is known as fugacity of component i. R is the universal gas constant and T is the temperature. When all the phases are at the same temperature, substitution of Equation 2.3 for μ_i in Equation 2.2 gives:

$$f_i^{P1} = f_i^{P2} = \ldots = f_i^{Pm} \qquad i = 1,2,\ldots,N \tag{2.4}$$

For a specific case of vapour and liquid:

$$f_i^L = f_i^V \qquad i = 1,2,....,N \qquad (2.5)$$

Equation 2.5 reveals that to establish phase equilibrium between two phases the fugacity of each component in the liquid phase should be same as the fugacity of that component in the vapour phase.

2.3 FUGACITY AND FUGACITY COEFFICIENT

The fugacity of component i (f_i) in any phase can be determined from its fugacity coefficient (ϕ_i) defined in Equation 2.6:

$$f_i = \phi_i y_i P \qquad i = 1,2,...,N \qquad (2.6)$$

where P is the system pressure and y_i is the molar composition of component i in that phase. The fugacity coefficient is a function of temperature, pressure and composition of the phase. It can rigorously be related to the measurable variables using the following thermodynamic relation[4]:

$$\ln \phi_i = \frac{1}{RT} \int_v^\infty \left[\left(\frac{\partial P}{\partial n_i} \right)_{T,v,n_{j \neq i}} - \frac{RT}{v} \right] dv - \ln Z \qquad (2.7)$$

where v, Z and n_i are the total volume, compressibility factor and the number of moles of component i. Equation 2.7 can be solved using an equation which relates pressure, temperature, volume and composition that is, an equation of state (Section 2.4). The solution of Equation 2.7 is given in Appendix A.

2.4 EQUATION OF STATE (EOS)

Equations of state (EOS) are analytical expressions which relate the pressure to the temperature and the volume. As some of them provide an acceptable engineering

accuracy whilst maintaining the simplicity, they have been widely used in predicting phase behaviour of mixtures. The simplest EOS, which is the essence of all complex EOS, is the ideal gas law. The ideal gas equation is based on two assumptions:

1. The volume occupied by the molecules of gas is insignificant compared to the volume of the container and distance between the molecules.
2. There are no attractive or repulsive forces between the molecules and the walls of the container.

The ideal gas equation can mathematically be written as:

$$Pv = nRT \tag{2.8}$$

where, P, v, T and R are the pressure, volume, temperature and the universal gas constant, respectively. n is the number of moles of gas in the container. The equation can also be written in the form of molar volume (V=v/n) as follows:

$$PV = RT \tag{2.9}$$

Equation 2.8 can be used to reasonably describe the volumetric behaviour of a large number of gases at low pressures (atmospheric pressure). However, the volumetric behaviour of real gases deviates from the ideal behaviour at higher pressures. To apply the ideal gas equation to real gases a deviation factor, which is called compressibility factor (Z), is introduced in the ideal gas equation. The compressibility factor is defined as:

$$Z = \frac{PV}{RT} \tag{2.10}$$

At low pressures, the compressibility factor is close to unity (Z=1, ideal gas), however, as pressure increases system deviates from the ideal gas conditions and the compressibility factor differs from unity.

For an accurate description of phase behaviour of mixtures over wide ranges of temperature and pressure, more comprehensive EOS are required. The applicability of such EOS must not be restricted by presenting excessive mathematical difficulties in phase equilibrium calculations. Among all EOS, polynomial equations which are cubic in molar volume offer a compromise in generality and simplicity that are suitable to many proposes. Cubic EOS are in fact the simplest equations capable of representing both the liquid and the vapour phase behaviour.

2.5 CUBIC EOS

Cubic EOS are widely used in industry because of their simplicity and reliability in predicting the phase equilibrium. Basically, EOS have been developed for pure compounds and, then their application has been extended to mixtures. Although, many cubic EOS have been suggested, none of the available equations can be selected as the most superior one to predict all the properties at all conditions. Some reviews of cubic EOS have been presented[5-7]. A number of comparative studies[8-11] of cubic EOS in predicting the phase behaviour and volumetric properties of different types of fluids, have shown that certain equations can exhibit a higher capability at specific conditions. The reliability of these equations also vary for different fluid systems. The cubic EOS can reasonably predict the phase behaviour of fluids at conditions far from the critical point. However, approaching the critical point the EOS predictions deteriorate and become unreliable.

2.5.1 van der Waals (VDW) EOS

Johannes van der Waals[12] proposed his well known equation of state in 1873 where it became the basis of new and modern EOS. He used the ideal gas law as the basis for the development and tried to eliminate the two assumptions which were made in developing the ideal gas equation. Instead of considering the molecules of gas as infinite small spheres which their volume is insignificant compare to the volume of container, he supposed that the gas molecules occupy a significant fraction of the volume particularly at

higher pressures. This means the movement of gas molecules are restricted to a smaller volume which is v-nb. The parameter b is regarded as the correction to the volume due to the volume occupied by the molecules and n is the number of moles. The ideal gas law can then be written as:

$$P = \frac{nRT}{v - nb} \tag{2.11}$$

The right hand side of Equation 2.11 is called the repulsive term, since the correction is caused by the repulsive interaction between the molecules.

To eliminate the second assumption, attractive forces were also introduced in the ideal gas law. The attractive forces between the molecules reduce the frequency of collisions with the walls and the force of collisions with other molecules. As the pressure of gas depends on the mentioned collisions, the attractive term should be subtracted from the pressure. van der Waals pointed out that the correction in the pressure due to reduction in the frequency of the collisions can roughly be related to the molar concentration (n/v). Hence, he proposed the following correction for pressure reduction:

$$-a\left(\frac{n}{v}\right)^2$$

where 'a' is a fluid-dependent constant.

Addition of the attractive term to Equation 2.11, the final form of van der Waals EOS is:

$$P = \frac{nRT}{v - nb} - a\left(\frac{n}{v}\right)^2 \tag{2.12}$$

or in molar volume:

$$P = \frac{RT}{V - b} - \frac{a}{V^2} \tag{2.13}$$

Equation 2.13 can be written in the cubic polynomial form after a brief mathematical manipulation:

$$PV^3 - (bP + RT)V^2 + aV - ab = 0 \tag{2.14}$$

This equation shows that if a and b parameters are given, one can determine pressure as a function of molar volume at different temperatures. Fig. 2.1 shows the variation of pressure against volume at three different temperatures for pure substances. On the Figure, C is the critical point where $T=T_c$, $P=P_c$ and $V=V_c$. The right hand side of the critical point on saturation curve is saturated vapour (dew point) curve where the left hand part is saturated liquid curve (bubble point). For $T>T_c$ (T_2) the pressure is monotonously decreasing as a function of volume where Equation 2.14 has only one real root. For $T<T_c$ (T_1) the behaviour of pressure-volume is different. It can be seen from Equation 2.13 if V=b, pressure will be positive infinite. An increasing volume results in a dramatic decrease in pressure and the isotherm will form the pure liquid region and pass the saturated liquid curve into two phase region. After passing through a local minimum and a local maximum, then the isotherm monotonously decreases passing the saturated vapour curve into the single phase vapour region. This behaviour results in three roots at any pressure in Equation 2.14. The predicted volume by any cubic EOS for a system in two phase conditions, as shown in Fig. 2.1, is not of relevance to fluid equilibria. If the cubic EOS gives more than one positive real root for the volume, the highest value should be considered for the vapour phase calculations and the lowest for the liquid phase calculations.

The critical isotherm ($T=T_c$) shows an inflection point at the critical point. Mathematically it means that the first and second derivatives of the pressure with respect to the volume, are zero:

$$\left(\frac{\partial P}{\partial V}\right)_{T=T_c} = \left(\frac{\partial^2 P}{\partial V^2}\right)_{T=T_c} = 0 \qquad (2.15)$$

Applying these conditions to the cubic EOS (Eq 2.14), the values of a and b parameters in the equations can be determined.

Since van der Waals proposed his EOS, hundreds of EOS have been developed to improve the phase behaviour predictions of mixtures. Redlich and Kwong[13] (RK) used Clausius'[14] and Berthelot's[15] ideas and introduced a temperature dependency in the attractive term of the VDW EOS. Redlich and Kwong improved the phase behaviour prediction of the VDW EOS by dividing the 'a' parameter by the square root of temperature in the attractive term. It could not accurately predict the saturation pressure and phase equilibrium nor could it satisfactorily predict the liquid density. Soave[16], therefore, modified the RK EOS by replacing the term $a/\sqrt{T}$ with a more general temperature dependent term. Soave's modification (SRK) greatly improved vapour pressure predictions for several binary mixtures. The SRK EOS was quite capable of predicting vapour-liquid equilibrium conditions (temperature, pressure and compositions) for fluid mixtures but it was not very satisfactory for predictions of liquid compressibility (or liquid density). Therefore, Peneloux et al.[17] introduced a translation parameter along the volume axis which improved the liquid density prediction with no effect on predicted vapour-liquid equilibrium conditions by the original SRK EOS. The translation parameter was introduced as a third parameter (c) in the SRK EOS by matching the saturated liquid densities. Peng and Robinson[2] (PR) proposed a two parameter EOS to improve the predicted liquid density in comparison with the original SRK EOS (Peng-Robinson EOS will be discussed in full later on in this section). Jhaveri and Youngren[18], similar to Peneloux et al.[17], proposed a third parameter in the PR EOS to further improve the phase density predictions. Schmidt and Wenzel[19] investigated the SRK and the PR EOS in predicting the molar volume of pure compounds. They realised that the SRK EOS describes the liquid molar volume well at acentric factor equal to zero (ω=0.), whereas the PR EOS yields best results at ω=0.35. Based on this observation they introduced a

component dependent critical compressibility factor by incorporating the acentric factor in the VDW type equation. Patel and Teja[20] (PT) developed a three parameter cubic EOS with two adjustable parameters to characterise each particular fluid. They evaluated the parameters by minimising deviations in saturated liquid densities while simultaneously satisfying the equality of fugacities along the saturation curve. Valderrama[21] generalised the PT EOS and correlated the empirical parameters of the PT EOS in terms of the acentric factor and the critical compressibility factor. Valderrama's modification resulted in improvement in predicting the properties of polar and non-polar fluids. A brief discussion of the two EOS used in this study, is given here.

2.5.2 Peng-Robinson (PR) EOS and Its Modification

Peng and Robinson[2] proposed a modification on the original SRK EOS, to improve its liquid density as well as vapour pressure prediction, particularly for naturally occurring hydrocarbon systems. It is generally accepted that Z_c of pure substances should be close to 0.28. The original SRK EOS gives an unrealistic universal critical compressibility factor of 1/3 for all substances. To improve the critical compressibility prediction, Peng and Robinson modified the original SRK EOS as follows:

$$P = \frac{RT}{V-b} - \frac{a}{V(V+b)+b(V-b)} \qquad (2.16)$$

The PR EOS gives Z_c=0.307 at the critical point.

The attractive term in the PR EOS (a) is defined as follows:

$$a(T) = a_c\,\alpha(T_r) \qquad (2.17)$$

where a_c is the value of 'a' at the critical point and T_r is the reduced temperature (T/T_c). $\alpha(T_r)$ is the temperature dependency of the attractive term and it should be continuous and equal one at the critical point to ensure:

$$a(T_c) = a_c \tag{2.18}$$

a_c and b can be determined using the critical properties of the pure compounds:

$$a_c = 0.457235 \frac{R^2 T_c^2}{P_c} \tag{2.19}$$

$$b = 0.077796 \frac{RT_c}{P_c} \tag{2.20}$$

Soave[16] showed that $\alpha^{0.5}$ is linear with $T_r^{0.5}$ (T_r=T/T_c, reduced temperature) at constant acentric factor and proposed his famous function. Peng and Robinson used a similar form of α as proposed by Soave. Unlike Soave, who used only the critical point and the calculated vapour pressure at T_r=0.7 to correlate the α parameter, Peng and Robinson (PR) used the vapour pressure data of pure compounds from the normal boiling point to the critical point to determine the α parameter in the PR EOS:

$$\alpha = \left[1 + m(1 - T_r^{0.5})\right]^2 \tag{2.21}$$

where

$$m = 0.37464 + 1.54226\omega - 0.26992\omega^2 \tag{2.22}$$

The correlation was later expanded to improve predictions for heavier components[22]:

$$m = 0.379642 + 1.48503\omega - 0.1644\omega^2 + 0.016667\omega^3 \tag{2.23}$$

2.5.3 Patel and Teja (PT) EOS and Its Modification

Patel and Teja[20] (PT) proposed a 3-parameter cubic EOS by introducing two adjustable empirical parameters which can be determined from the liquid density and vapour

pressure data of pure compounds. They correlated the two empirical parameters in terms of the acentric factor:

$$P = \frac{RT}{V-b} - \frac{a_c\alpha(T)}{V(V+b)+c(V-b)} \tag{2.24}$$

where

$$a_c = \Omega_{ac}\frac{R^2T_c^2}{P_c} \tag{2.25}$$

$$b = \Omega_b\frac{RT_c}{P_c} \tag{2.26}$$

$$c = \Omega_c\frac{RT_c}{P_c} \tag{2.27}$$

Ω_b is the smallest positive root of Equation 2.28:

$$\Omega_b^3 + (2-3\eta)\Omega_b^2 + 3\eta^2\Omega_b - \eta^3 = 0 \tag{2.28}$$

An approximate value of Ω_b is given by:

$$\Omega_b = 0.32429\eta - 0.022005 \tag{2.29}$$

and

$$\Omega_c = 1 - 3\eta \tag{2.30}$$

$$\Omega_{ac} = 3\eta^2 + 3(1-2\eta)\Omega_b + \Omega_b^2 + (1-3\eta) \tag{2.31}$$

η can be evaluated from saturated liquid density data and it was correlated with the acentric factor:

$$\eta=0.329032-0.076799\omega+0.0211947\omega^2 \qquad (2.32)$$

Patel and Teja used Soave's α function (Eq 2.21) with slope m given in Equation 2.33:

$$m=0.45213+1.30982\omega-0.295937\omega^2 \qquad (2.33)$$

The 3-parameter PT EOS has shown to give satisfactory results for both vapour pressure and phase density predictions.

The acentric factor (ω) has extensively been used along with the critical temperature and critical pressure to correlate the parameters of the PT EOS. Solving an additional cubic equation for one of the three parameters of the EOS is an additional mathematical complexity which is not present in other common cubic EOS such as the Soave-Redlich-Kwong (SRK) or the PR equations. Therefore, Valderrama and Cisternas[23] and later Valderrama[21] proposed generalised correlations for the parameters in the PT EOS. They used the critical compressibility factor of pure compounds to correlate the parameters of the PT EOS where the necessity of solving any additional equation was eliminated.

$$\Omega_{ac}=0.66121-0.76105\ Z_c \qquad (2.34)$$

$$\Omega_b=0.02207+0.20868\ Z_c \qquad (2.35)$$

$$\Omega_c=0.57765-1.87080\ Z_c \qquad (2.36)$$

For slope m in α function (Eq 2.21):

$$m=0.46283+3.58230(\omega Z_c)+8.19417(\omega Z_c)^2 \qquad (2.37)$$

It has been shown that the phase behaviour and volumetric properties of real reservoir fluids during gas injection schemes can reasonably be modelled, using the Valderrama modification of Patel and Teja (VPT) EOS[24]. The VPT EOS also gives satisfactory results for vapour pressure and density prediction of non-polar as well as heavy and polar compounds.

2.6 PARAMETERS OF EOS

EOS are initially developed for pure compounds and their application is extended to the multicomponent systems by introducing mixing rules to determine the parameters of EOS for mixtures. Several investigators[16,17,18,25-29] have modified the parameters of EOS to improve phase behaviour and volumetric predictions for multicomponent systems. In this study the temperature dependency of the attractive term (a) is modified to improved the phase behaviour prediction at different temperatures. The repulsive term (b) was kept in its original form where it is assumed to be independent of temperature. A new method is developed to determine the third parameter (c) of the Peng-Robinson (PR) EOS which has improved the capability of the EOS in predicting the volumetric behaviour of mixtures.

2.6.1 The Attractive Term (a)

Review of α Function

Since van der Waals[12] developed his well known EOS over a century ago, a number of modifications have been proposed to improve the EOS predictions. The main concern has been to improve the volumetric prediction as well as phase equilibrium behaviour at different temperatures. To accurately reproduce the experimental vapour pressure of pure components over a wide range of temperature change, it is essential that at least one of the parameters in the cubic EOS are considered to be temperature dependent. The majority of scientists have suggested that introducing temperature dependency into the attractive term of EOS is sufficient to reproduce vapour pressure data of pure compounds.

Tsonopoulos and Prausnitz[5], and Abbott[6] reviewed the early methods for adjusting the EOS parameters to reasonably match the experimental vapour pressure data. Wilson[25] was one of the pioneers who modified Redlich-Kwong[13] (RK) EOS by introducing a temperature dependent parameter in the attractive term.

He defined the α parameter as a function of T_r and acentric factor (ω):

$$\alpha = T_r + m_{Wilson}(1-T_r) \tag{2.38}$$

He related the slope m_{Wilson} to the acentric factor by forcing the EOS to give reasonable values of the slope of the vapour pressure curve.

$$m_{Wilson}= 1.57+1.62\omega \tag{2.39}$$

Soave[16] used vapour pressure data and the definition of acentric factor to obtain his well-known α expression. Soave calculated the values of α parameter over a temperature range of $0.4<T_r<1.0$ for a number of light hydrocarbon compounds ($0.<\omega<0.5$). He demonstrated that $\alpha^{0.5}$ was a linear function of $\sqrt{T_r}$ and then proposed the α function as:

$$\alpha = \left[1 + m(1 - T_r^{0.5})\right]^2 \tag{2.21}$$

where m was expressed as a quadratic function of the acentric factor:

$$m=0.48+1.574\omega-0.176\omega^2 \tag{2.40}$$

Soave developed his α function more directly than Wilson, by matching the vapour pressure for non-polar compounds at $T_r=0.7$ (the definition of acentric factor). Soave's function gained wide-spread popularity due to its accuracy and simplicity and it was

adopted by many investigators[2,19,20,30,31] who changed only the m function (Eq 2.40) to accommodate it into their own equations of state.

Harmens and Knapp[32] added one more term to Soave's form to improve the temperature dependency of the attractive term at low temperatures for subcritical compounds:

$$\alpha = \left[1 + A(1 - T_r^{0.5}) - B(1 - \frac{1}{T_r})\right]^2 \qquad (2.41)$$

The parameters A and B were correlated with acentric factor by matching the experimental vapour pressure in the temperature range of $0.3 \leq T_r \leq 1.0$ and the volume along the critical isobar to about T_r=2.5.

Graboski and Daubert[33,34] found that Equation 2.21 was not capable to accurately predict the phase behaviour of hydrogen systems which is normally at high reduced temperatures. Therefore, they recommended an exponential form:

$$\alpha = 1.202 \exp(-0.30228 T_r) \qquad (2.42)$$

Equation 2.42 is expected to be accurate for hydrogen at $T_r \geq 2.5$.

Heyen[35] also recommended a similar exponential function:

$$\alpha = \exp\left[C(1 - T_r^n)\right] \qquad (2.43)$$

Adachi and Lu[36] examined three different types of α functions; Soave form, a logarithmic and a polynomial form. They applied the expressions to different EOS and they concluded that the logarithmic form was the most suitable one only for the VDW EOS. However, Soave's form and the polynomial form were preferred and gave similar results for the other tested EOS. Patel and Teja[20] also showed that Equations 2.42 and 2.43 did

not offer any advantages in comparison to the Soave's form, when applied to vapour pressures in typical reduced temperature ranges.

Yu and Lu[37] also proposed an exponential expression to describe the temperature dependency of the attractive term:

$$\log_{10}\alpha = M(\omega)(A_0 + A_1 T_r + A_2 T_r^2)(1 - T_r) \qquad (2.44)$$

They used vapour pressure data of pure compounds to determine the parameters in Equation 2.44 for subcritical compounds ($T_r \leq 1.0$). At $T_r > 1.0$, the parameters were determined, using vapour-liquid equilibrium values by minimising the deviations in the calculated bubble point pressure for mixtures in which the component of interest exists at its supercritical state.

The reviewed equations can satisfactorily predict the phase behaviour of non-polar compounds and they can be generalised in terms of acentric factor. The equations are also applicable for polar compounds provided that the parameters are determined from the actual vapour pressure of the polar substances and not correlated with acentric factor[38,39]. Although no general characteristic parameter exists for polar compounds that could replace the acentric factor, correlation with the reduced dipole moment may give satisfactory results[40,41].

Numerous equations with 1 to 3 empirical constants have been proposed to improve the ability of EOS in predicting the phase behaviour of polar compounds. Among them, Mathias and Copeman[42] developed a three-parameter α function:

$$\alpha = \left[1 + C_1(1 - \sqrt{T_r}) + C_2(1 - \sqrt{T_r})^2 + C_3(1 - \sqrt{T_r})^3\right]^2 \qquad (2.45)$$

Equation 2.45 reduces to Soave's form when $C_2=C_3=0$. The additional parameters were considered to correlate the vapour pressure of highly polar substances like water and methanol.

Soave[43] modified his earlier α function and gave a two-parameter correlation for polar compounds:

$$\alpha = 1 + m(1 + T_r) + n(\frac{1}{T_r} - 1) \tag{2.46}$$

where m and n are empirical constants which can be derived by correlating the experimental vapour pressure data.

Stryjek and Vera[44] developed a three-parameter α function to accurately reproduce the vapour pressure of ninety compounds including polar and non-polar substances:

$$\alpha = \left[1 + K_{ver}(1 - T_r^{0.5})\right]^2 \tag{2.47a}$$

$$K_{ver} = K_0 + \left[K_1 + K_2(K_3 - T_r)(1 - T_r^{0.5})\right](1 + T_r^{0.5})(0.7 - T_r) \tag{2.47b}$$

where K_1, K_2 and K_3 are pure compound adjustable parameters.

Androlakis et al.[45] investigated several two- and three-parameter forms of the α function considering their capability in predicting the experimental data and extrapolating to low temperatures. They suggested a three-parameter form for subcritical compounds:

$$\alpha = 1 + d_1(1 - T_r^{2/3}) + d_2(1 - T_r^{2/3})^2 + d_3(1 - T_r^{2/3})^3 \tag{2.48}$$

For supercritical compounds they recommended an one-parameter exponential expression providing a smooth transition between sub and supercritical regions. Melhem et al.[46] also discussed several forms of the temperature dependency of the attractive term. They

recommended a two-parameter equation that correlates the experimental data with similar accuracy as that of Soave's function[43] but extrapolates better to supercritical temperatures.

$$\ln\alpha = m_m(1-T_r)+n_m(1-\sqrt{T_r})^2 \qquad (2.49)$$

A list of m_m and n_m parameters were supplied for more than 100 compounds by authors.

Danesh et al.[47] demonstrated that modifying the value of α function in the PR EOS for supercritical hydrocarbon components, would improve its capability in predicting the phase behaviour of multicomponent mixtures. The modification was expressed by replacing slope m in Soave's function (Eq 2.21) with m':

$$m'=1.21\ m \qquad (2.50)$$

The reviewed α functions show that the tendency is going in the direction of more complex equations with higher order function of the acentric factor. Soave's form (Eqs 2.21 and 2.40) reveals that α is a fourth order function of the acentric factor, where the developed α function by Robinson and Peng[22] is a sixth order function of the acentric factor. The numerical values in Soave's form are derived from the vapour pressure of a limited number of hydrocarbons up to an acentric factor of 0.5. Examination of Equations 2.21 and 2.40, reveals that a questionable assumption is being made in the extrapolation of a fourth order polynomial equation in acentric factor (ω) to heavy hydrocarbons or petroleum fractions. Equation 2.21 performs well for light hydrocarbons at values of reduced temperature from 0.7 to 1.0, but it becomes unreliable at all temperatures for compounds with large acentric factors[48].

It has been shown that α is linearly related to acentric factor (ω) at constant reduced temperature in subcritical region (Fig. 2.2). Based on this linearity, Twu et al.[48]

developed an α function, using the numerical α values of compounds over wide ranges of acentric factor and reduced temperatures (T_r).

$$\alpha = \alpha^0 + \omega(\alpha^1 - \alpha^0) \tag{2.51}$$

α^0 and α^1 are values of α parameter at ω=0. and ω=1.0 respectively. α^0 and α^1 have been correlated with T_r by a three parameter correlation:

$$[\alpha] = T_r^{N(M-1.)} e^{L(1.-T_r^{NM})} \tag{2.52}$$

$$[\alpha] \ : \ \alpha^0 \text{ or } \alpha^1$$

where the parameters L, M and N are unique to each component and have been determined from the regression of pure compounds vapour pressure. Twu et al. generalised Equation 2.52 and reported two sets of parameters for L, M and N for subcritical and supercritical compounds.

Twu et al.'s correlation was used along with the PR EOS to predict the vapour pressure of 24 polar and non-polar compounds over a wide range of temperature from the triple point to the critical point. The results (Table 2.1) showed that they improved vapour pressure prediction of pure compounds (excluding water) comparison to the Soave's form. However, using Twu et al.'s correlation along with the PR EOS to predict the phase behaviour of multicomponent petroleum mixtures, offered no significant advantage over Soave's function. As Twu et al. used only one binary mixture (H_2-C_1) to correlate the α function for supercritical compounds, his expression may not be capable of modelling the complex behaviour of petroleum fluids with two or more components in supercritical region.

Investigating Twu et al.'s correlation also showed that it was not a flexible function particularly for supercritical compounds. Using the parameters of Equation 2.52 (N, M

and / or L) as regression variables to match the experimental data, revealed that even with 20% changes in N, M and / or L parameters, the experimental data could not be matched.

A New α Function

Twu et al.'s α function significantly improved the vapour pressure prediction of pure compounds. However, the improvement in predicting the saturation pressure of multicomponent systems, particularly petroleum fluids was less striking. This can be due to the treatment of supercritical component behaviour in the mixture, where Twu et al. used only one binary system to correlate the α parameter for supercritical compounds. Based on the observed linearity of α parameter with acentric factor at constant T_r, a new α correlation is determined, which is more reliable for supercritical compounds. Taking α as a linear function of ω at constant T_r any of the constant T_r lines can be drawn, by knowing at least two points of that line. The experimental vapour pressure[49] of C_1 (ω=0.011), nC_{12} (ω=0.5752) and nC_{20} (ω=0.907) were used to correlate the α function for subcritical compounds. The vapour pressure of each compound over a wide range of temperature ($0.5 \le T_r < 1.0$) was individually matched, using the α parameter as a regression variable in this work. The calculated α values of each compound were plotted and correlated with a third degree polynomial. These are shown in Figs. 2.3-2.5. They show that third degree polynomials could be applied to correlate the α parameters of different compounds very accurately. To generalise the third degree polynomial of α function, the matched α values were plotted versus the acentric factor for constant T_r's (Fig. 2.6). The constant T_r lines are drawn, which are used to determine the loci of α^0 (α at ω=0.) and α^1 (α at ω=1.0) at different values of T_r. The calculated α^0 and α^1 values were then plotted versus T_r, and were each correlated with a third degree polynomial (Fig. 2.7). Hence, the α parameter of compounds at subcritical conditions can be determined, using Equation 2.51 along with the proposed Equation in this thesis (Eq 2.53), which is used to calculate α^0 and α^1.

$$\alpha = \alpha^0 + \omega(\alpha^1 - \alpha^0) \tag{2.51}$$

$$[\alpha] = 1 + A(T_r - 1) + B(T_r - 1)^2 + C(T_r - 1)^3 \qquad (2.53)$$

$$[\alpha] \;:\; \alpha^0 \text{ or } \alpha^1$$

The values of A, B and C coefficients are given in Table 2.2. It should be noted, this method has been applied to the Peng-Robinson (PR) EOS, however, the method is general and it can be applied to any EOS.

For supercritical compounds (with T_r>1.), Twu et al. used the experimental data of H_2-C_1 binary system to determine a generalised α function. Accepting the linearity of α with acentric factor in supercritical region, the same form of equation (Eq 2.53) was applied to correlate the α values with T_r in that region. Instead of one binary system which was considered by Twu et al. (H_2-C_1), a number of binary and multicomponent systems over a wide range of temperature were used to correlate the α function for supercritical compounds. It should be mentioned that no binary interaction parameters (BIP, Eq 3.1) were used in the phase equilibrium calculation of binary and multicomponent systems. It is believed that BIP, at least for hydrocarbon mixtures, cover the deficiencies of EOS rather than account for the interaction between molecules of hydrocarbon compounds. It has also been shown, using no BIP in the EOS, enables us to describe the reservoir fluid by a large number of components without significantly increasing the computational time. Therefore, the modelling approach is based on avoiding the use of BIP in the mixing rules of EOS (this issue has comprehensively been discussed in Chapter 3).

The vapour pressure of C_1-C_3, C_1-nC_4 and C_1-nC_{16} binary systems within a temperature range of $1.0 \le T_{r,C1} < 3.5$ were matched, using the α parameter of C_1 as a regression variable. The numerical α values of supercritical compounds, C_1 and C_2, which were determined by matching the measured saturation pressure of model fluids, were also considered in correlation of the α function at supercritical conditions. The regressed α values were plotted and correlated with a third degree polynomial (Fig. 2.8). The experimental data of four binary systems (H_2-C_1, H_2-nC_4, H_2-nC_6 and H_2-nC_{16}) over a wide range of temperature ($2.5 \le T_{r,H2} < 20$) were also used to determine the α function

of H_2 in supercritical conditions (Fig. 2.9). Finally, the α function of CO_2 at supercritical conditions was determined, by matching the vapour pressure of CO_2-nC_{10} and CO_2-nC_{16} binary systems within temperature range of $1.2 \leq T_{r,CO2} < 2.2$, using the α parameter of CO_2 as a regression variable. The regressed α values were plotted and correlated with a third degree polynomial, as shown in Fig. 2.10.

The correlated α functions of the above mentioned compounds (C_1, H_2 and CO_2) were used to determine the generalised α function for supercritical compounds. Many α values were generated at different acentric factors (mainly at the acentric factors which correspond to C_1, H_2 and CO_2) and reduced temperatures, using the correlated α functions. The generated α values were used to draw the constant T_r lines and these lines were applied to determine the loci of α^0 and α^1 at different T_r's in supercritical region. The calculated α^0 and α^1 values were plotted and individually correlated with third degree polynomials (Fig. 2.11). The A, B and C coefficients of these polynomials for supercritical compounds (Eq 2.53) are given in Table 2.2.

To investigate the linearity of α parameter with acentric factor at near critical point ($0.9<T_r<1.0$), five compounds (C_1, nC_5, nC_{12}, nC_{15} and nC_{20}) at subcritical temperatures were selected. The vapour pressures of these compounds in the temperature range $0.9 \leq T_r \leq 0.98$ were matched, using the α parameter as a regression variable. The matched α values were plotted versus acentric factor at constant T_r (Fig. 2.12). Fig. 2.12 shows that α deviates from linearity at near critical conditions (say $T_r \geq 0.94$).

The behaviour of the new α function was investigated and compared with Soave's (Eq 2.21) and Twu et al.'s correlation for supercritical compounds at high T_r values. The new α function showed a more pronounced change with acentric factor at constant T_r leading to a negative values at very high temperatures. For reservoir fluids such behaviour occurs at temperature above 720°C, which is well outside the practical range.

The new α function was applied to the PR EOS to predict the vapour pressure and saturation pressure of pure compounds and multicomponent mixtures, respectively. The capability of the new α function was demonstrated in comparison to the other leading α functions in the literature.

Three models, the original PR α function[22], Twu et al.[48] and the new α function were used along with the Peng-Robinson (PR) EOS to predict the vapour pressure of 24 pure polar and non-polar compounds. The average absolute percentage deviation (AAD%) between experimental and predicted vapour pressures over all points from the triple point to the critical point by the original PR α function, Twu et al. and the new α function were 3.89%, 2.07% and 1.69%, respectively. The AAD% in predicting the vapour pressure of individual pure compounds is presented in Table 2.1. In general, the deviation in predicting vapour pressure is comparable with that of the experimental data. The exception is the vapour pressure of water, which is significantly higher than the experimental error. The reason is the α parameter of water significantly deviates from the isotherm lines at low temperatures ($T_r \leq 0.5$), as shown in Fig. 2.2. However, at higher temperatures ($T_r > 0.5$), the determined α values of water coincide with the isotherm lines and its phase behaviour can accurately be predicted. The isotherm $T_r = 0.5$ associates with a temperature of 50°C, which is well below the temperature of a typical reservoir.

To compare the AAD% in predicting the saturation pressure of model and real reservoir fluids, four methods namely the original PR α function, Twu et al.'s α correlation, m' (Eq 2.50) and the new α function were used with the PR EOS. The m' method was included in this comparison as authors[47] have claimed that their modification has improved the phase behaviour prediction without using any BIP in the mixing rules. Different types of fluids covering a range of black oil to lean gas condensate samples were studied to evaluate the reliability of the new α function for supercritical compounds. In this study the critical properties of pseudo components of real reservoir fluids were estimated using the perturbation expansion correlation[50]. For the literature data where the fluid heavy end was reported only as C_{7+} (or C_{10+}) fraction, the gamma distribution

function was used to describe the heavy end, as proposed by Whitson[51], and split it into a number of pseudo components, up to C_{20}.

The predicted saturation pressure of 5- and 20-component model gas condensate samples (GMX89-1 and GMX90-1) at different temperatures are plotted in Figs. 2.13 and 2.14, where the original PR α function (with and without BIP), Twu et al.'s function (without BIP), m' and the new α function along with the PR EOS were used to perform the phase equilibrium calculation. The superiority of the new α function is quite obvious, particularly at low temperatures.

Fig. 2.15 shows the experimental and predicted dew point pressures of gas condensate JOCBS-5 at different temperatures by the four methods. As shown, the PR EOS with the new α function predicts the saturation pressure at all temperatures better than any of the other models.

It should be noted that the developed binary interaction parameter (BIP) set for any EOS should generally be used only for that EOS. No BIP set have been reported for Twu et al.'s α function in multicomponent phase behaviour calculations. Therefore, Twu et al.'s correlation was used with no BIP in the PR EOS to predict the saturation pressure of the fluids.

The average absolute percentage deviation (AAD%) between experimental and predicted saturation pressure of 32 fluids including, gas condensates and volatile oils, by the PR EOS using the original α function with and without BIP, m' (Eq 2.50) and the new α function were 7.4%, 12.9%, 6.3% and 4.5% respectively. As no BIP set has been reported for Twu et al.'s α function, the model was not included in this comparison. The results are summarised in Table 2.3.

2.6.2 The Third Parameter (c)

The capability of two-parameter cubic EOS in predicting the liquid density has been improved[17,18] by introducing a third parameter (c). This method is particularly attractive as it does not change the phase equilibrium conditions determined by the unmodified two-parameter EOS, but it affects the phase densities by shifting the phase envelope along the volume axis.

Peneloux et al.[17] introduced the volume translation to the SRK EOS and markedly improved the liquid density prediction. They correlated the third parameter (c_i) with Z_{RA} (called Rackett compressibility factor) by matching the saturated liquid densities of pure compounds. Jhaveri and Youngren[18] adopted Peneloux et al.'s method and defined a dimensionless shift parameter , S, to calculate the third parameter (c) of the PR EOS.

$$S = \frac{c}{b} \tag{2.54}$$

where b is the repulsive (co-volume) parameter of the PR EOS. The numerical values of the shift parameter were determined by matching the molar volume of well defined hydrocarbons at datum temperature (T_r=0.7). For well-defined hydrocarbons lighter than normal heptane, they matched the saturated liquid densities whereas for heavier hydrocarbons the molar volume at standard conditions were matched. Hence, they gave constant values for the shift parameter of light hydrocarbons up to normal heptane (Table 2.4), but proposed Equation 2.55 to calculate the shift parameter of heavier hydrocarbons.

$$S = 1 - \frac{d}{M^e} \tag{2.55}$$

M is the molecular weight and d and e are adjustable parameters that can be used as regression variables to match the experimental densities. The shift parameter of different types of compounds, n-alkanes, n-alkylcyclohexanes and n-alkylbenzenes can be

calculated by introducing relative numerical values of d and e coefficients in Equation 2.55. These values are given in Table 2.5.

The inclusion of the third parameter might deteriorate the predicted density at some conditions. This could occur for systems with high concentration of supercritical compound(s), particularly methane. Using a constant shift parameter for light hydrocarbons, the phase densities may not be predicted accurately.

To improve the density prediction, the shift parameter of several pure hydrocarbons were determined in this thesis within a wide temperature range. The shift parameter was used as a regression variable to match the liquid density at standard conditions if the pressure was below the normal boiling point, and at the saturation pressure at and above the normal boiling pressure. The numerical values of shift parameter are plotted against acentric factor at constant T_r in Fig. 2.16. It shows that the shift parameter is a linear function of acentric factor at constant T_r. The isotherms were used to determine the loci of S^0 (S at ω=0.) and S^1 (S at ω=1.) at different T_r values. The calculated S^0 and S^1 values are plotted against T_r and correlated with fifth degree polynomials (Figs. 2.17 and 2.18). Hence, the shift parameter of subcritical compounds can be calculated from the following equations;

$$S = S^0 + \omega\,(S^1 - S^0) \tag{2.56}$$

$$[S] = A' + B'T_r + C'T_r^2 + D'T_r^3 + E'T_r^4 + F'T_r^5 \tag{2.57}$$

$[S]$: S^0 or S^1

S^0 and S^1 can be calculated from Equation 2.57 with coefficients given in Table 2.6. Equation 2.56 can be applied in EOS calculation in the temperature range of $0.3<T_r<0.94$ for subcritical compounds. Due to lack of saturated liquid density data for supercritical components, the above method cannot be applied to determine the shift parameter of supercritical components . Therefore, the isotherm T_r=0.7 is used in Equations 2.56 and

2.57 to calculate the shift parameters of the supercritical components. Equation 2.56 will then reduce to the following Equation for supercritical components;

$$S = -0.147617 + 0.420093\ \omega \qquad (2.58)$$

The proposed method is used to determine the phase densities of different types of fluids and its superiority in comparison to the Jhaveri and Youngren method has been demonstrated[52]. Examples will be given in this section.

The reliability of the new shift parameter correlation was checked against the experimental densities of 5- and 20-component model gas condensates (GMX89-1 and GMX90-1) at different temperatures. The tuning results of the developed method in this thesis have been compared with those of the Jhaveri and Youngren (JY) method. In the JY method, d and e parameters (Eq 2.55) were considered as tuning variables. In the new method, two parameters are introduced in the correlation (Eqs 2.56 and 2.57) which are schematically described in Fig. 2.19. S_{int} is used to adjust the intercept of the isotherm lines with Y-axis. S_{teta} is applied to change the slope of the isotherm lines with respect to X-axis.

The 5-component model gas condensate (GMX89-1) was used to perform a constant composition expansion (CCE) test at 30 and 80°C, where the predicted liquid and vapour densities are plotted in Figs. 2.20 and 2.21, respectively. As they show, both methods have reasonably matched the liquid densities, however, the tuning results of the new method in matching the gas densities are better than those of the JY method.

The results of fitting the liquid and vapour densities of the 20-component model gas condensate (GMX90-1) from CCE test at 93.3 and 121.1°C are plotted in Figs. 2.22 and 2.23, respectively. The tuning results of the two methods are in good agreement with those measured values at 121.1°C. As the critical point is approached (by reducing the temperature, Fig. 2.22), neither of the two methods could reasonably match the liquid

densities. However, the new method has matched the gas densities better than the JY method.

The results demonstrated that applying the developed method in this thesis with variable shift parameters for light hydrocarbons, can improve modelling of the phase densities of the hydrocarbon mixtures.

2.7 CONCLUSIONS

To improve phase behaviour predictions, modifications have been made in determining the temperature dependency of the attractive term (α parameter) and the third parameter of the Peng-Robinson EOS.

Vapour pressure data of pure compounds and saturation pressure data of binary and multicomponent model systems which, include supercritical component(s), have been used to develop a new α function to replace the existing temperature correlation of the Peng-Robinson (PR) EOS, as the most widely used equation. The new α function (Eqs 2.51 and 2.53) provides more reasonable values for supercritical components, such as methane, and account for the omitted binary interaction parameters. The new α function is linearly related to the acentric factor at constant reduced temperature, hence it can be extrapolated to heavy petroleum fractions with high acentric factors and low reduced temperatures. The modification improved the prediction of vapour pressure of pure compounds, reducing the average absolute percentage deviation (AAD%) from 3.89% for the original PR α function, to 1.69% for the new function. The AAD% of 12.9%, in predicting the saturation pressure of 32 model and real reservoir fluids over a wide range of temperature by the original PR (BIP=0.), was reduced to 4.5%, using the PR with the new α function (Eqs 2.51 and 2.53).

The phase density predictions of the Peng-Robinson EOS have been improved by producing a new correlation to determine the shift parameters of pure hydrocarbon

compounds. The new shift parameter correlation (Eqs 2.56 and 2.57) is linear with acentric factor at constant reduced temperature, hence it can be extrapolated to heavy petroleum fractions. The reliability of the new shift parameter correlation was evaluated against the experimental data of model reservoir fluids, with successful results.

REFERENCES

1. Prausnitz, J.M., Lichtenthaler, R.N. and de Azevedo, E.G., (1986) : *Molecular Thermodynamics of Fluid-Phase Equilibria*, Second Edition, Prentice-Hall Inc.

2. Peng, D.Y. and Robinson, D.B., (1976) : "A New Two-Constant Equation of State", *Ind. Eng. Chem. Fundam.*, **15**(1), 59-64.

3. Lewis, G.N. and Randall, M., (1961) : *Thermodynamics* (revised : Pitzer, K.S. and Brewer, L.), McGraw-Hill Book Co., New York.

4. Edmister, W.C. and Lee, B.I., (1984) : *Applied Hydrocarbon Thermodynamics*, second Edition, Gulf Publishing Co., Houston, Texas.

5. Tsonopoulos, C. and Prausnitz, J.M., (1969) : "Equations of State. A Review for Engineering Applications", *Cryogenics*, **9**, 315-327.

6. Abbott, M.M., (1979) : "Cubic Equations of State : an Interactive Review", *Am. Chem. Soc. Advan. Chem. Ser.*, 182, 47-70.

7. Martin, J.J., (1979) : "Cubic Equation of State - Which?", *Ind. Eng. Chem. Fundam.*, **18**(2), 81-97.

8. Danesh, A., Xu, D.-H. and Todd, A.C., (1991) : "Comparative Study of Cubic Equations of State for Predicting Phase Behaviour and Volumetric properties of Injection Gas-Reservoir Oil Systems", *Fluid Phase Equilibria*, **63**, 259-278.

9. Ahmed, T., (1988) : "Comparative Study of Eight Equations of State for Predicting Hydrocarbon Volumetric Phase Behaviour", *SPERE*, Feb., 337-348.

10. Firoozabadi, A., (1988) : "Reservoir-Fluid Phase Behaviour and Volumetric Prediction with Equation of State", *JPT*, **40**(4), 397-406.

11. Adachi, Y., Sugie, H. and Lu, B.C.-Y., (1984) : "Evaluation of Cubic Equation of State", *J. Chem. Eng. Japan*, **17**(6), 624-631.

12. van der Waals, J.D., (1873) : "*On the Continuity of the Liquid and Gaseous State*", PhD Dissertation, Sigthoff, Leiden.

13. Redlich, O. and Kwong, J.N.S., (1949) : "On the Thermodynamics of Solutions. V-An Equation of State. Fugacities of Gaseous Solutions", *Chem. Reviews*, **44**, 233-244.

14. Clausius, R., (1880) : *Ann. Phys. Chem.*, **9**, 337.

15. Berthelot, D.J., (1899) : *J. Phys.*, **3**, 263.

16. Soave, G., (1972) : "Equilibrium Constants from a Modified Redlich-Kwong Equation of State", *Chem. Eng. Sci.*, **27**, 1197-1203.

17. Peneloux, A., Rauzy, E. and Freze, R., (1982) : "A Consistent Correction for Redlich-Kwong-Soave Volumes", *Fluid Phase Equilibria*, **8**, 7-23.

18. Jhaveri, B.S. and Youngren, G.K., (1988) : "Three-Paramter Modification of the Peng-Robinson Equation of State to Improve Volumetric Predictions", *SPERE*, Aug., 1033-1040.

19. Schmidt, G. and Wenzel, H., (1980) : "A Modified van der Waals Type Equation of State", *Chem. Eng. Sci.*, **35**, 1503-1512.

20. Patel, N.C. and Teja, A.S., (1982) : "A New Cubic Equation of State for Fluids and Fluid Mixtures", *Chem. Eng. Sci.*, **37**(3), 463-473.

21. Valderrama, J.O., (1990) : "A Generalized Patel-Teja Equation of State for Polar and non-Polar Fluids and Their Mixtures", *J. Chem. Eng. Japan*, **23**(1), 87-91.

22. Robinson, D.B. and Peng, D.Y., (1978) : "The Characterization of the Heptanes and Heavier Fractions for the GPA Peng-Robinson Programs", GPA Research Report, RR-28, Project 756, University of Alberta, Edmonton, Alberta, Canada.

23. Valderrama, J.O. and Cisternas, L.A., (1986) : "A Cubic Equation of State for Polar and Other Complex Mixtures", *Fluid Phase Equilibria*, **29**, 431-438.

24. Danesh, A., Xu, D.-H. and Todd, A.C., (1990) : "An Evaluation of Cubic Equations of State for Phase Behaviour Calculations Near Miscibility Conditions", SPE/DOE paper 20267, presented at the Seventh Symposium on Enhanced Oil Recovery held in Tulsa, Oklahoma, April 22-25.

25. Wilson, G.M., (1964) : "Vapour-Liquid Equilibria Correlated by Means of a Modified Redlich-Kwong Equation of State", *Adv. Cryog. Eng.*, **9**, 168-176.

26. Joffe, J., Schroeder, G.M. and Zudkevitch, D., (1970) : "Vapour-Liquid Equilibria with the Redlich-Kwong Equation of State", *AIChE J.* **16**, 496-498.

27. Chang, S.D. and Lu, B.C.-Y., (1970) : "Prediction of Partial Molar Volumes of Normal Fluid Mixtures", *Can. J. Chem. Eng.*, **48**, 261-266.

28. Salim, P.H. and Trebble, M.A., (1991a) : "Thermodynamic Property Prediction from the Trebble-Bishnoi-Salim Equation of State", *Fluid Phase Equilibria*, **65**, 41-57.

29. Salim, P.H. and Trebble, M.A., (1991b) : "A Modified Trebble-Bishnoi Equation of State : Thermodynamic Consistency Revisited", *Fluid Phase Equilibria*, **65**, 59-71.

30. Adachi, Y., Lu, B.C.-Y. and Sugie, H., (1983) : "Three-Parameter Equations of State", *Fluid Phase Equilibria*, **13**, 133-142.

31. Watson, P., Cascella, M., May, D., Salerno, S. and Tassios, D., (1986) : "Prediction of Vapour Pressure and Saturated Volumes with a simple Equation of State. Part I : The VdW-711 EOS", *Fluid Phase Equilibria*, **27**, 35-52.

32. Harmens, A. and Knapp, H., (1980) : "Three Parameter Cubic Equation of State for Normal Substances", *Ind. Eng. Chem. Fundam.*, **19**, 291-294.

33. Graboski, M.S. and Daubert, T.E., (1978) : "A Modified Soave Equation of State for Phase Equilibrium Calculations. 1. Hydrocarbon Systems", *Ind. Eng. Chem. Process Des. Dev.*, **17**, 443-448.

34. Graboski, M.S. and Daubert, T.E., (1979) : "A Modified Soave Equation of State for Phase Equilibrium Calculations. 1. Systems Containing Hydrogen", *Ind. Eng. Chem. Process Des. Dev.*, **18**, 300-306.

35. Heyen, G., (1980) : "A Cubic Equation of State with Extended Range of Application", Chapter 15 in : *Chemical Engineering Thermodynamics*, p. 175-185. Ann Arbor Science.

36. Adachi, Y. and Lu, B.C.-Y., (1984) : "Simplest Equation of State for Vapour-Liquid Equilibrium Calculation : A Modification of the van der Waals Equation", *AIChE J*, **30**, 991-993.

37. Yu, J.M. and Lu, B.C.-Y., (1987) : "A Three-Parameter Cubic Equation of State for Asymmetric Mixture Density Calculations", *Fluid Phase Equilibria*, **34**, 1-19.

38. Robinson, D.B., Peng, D.-Y. and Chung, S.Y.-K., (1985) : "The Development of the Peng-Robinson Equation and Its Application to Phase Equilibrium in a System Containing Methanol", *Fluid Phase Equilibria*, **24**, 25-41.

39. Georgeton, G.K., Smith, R.L. Jr. and Teja, A.S., (1986) : "Application of Cubic Equation of State to Polar Fluids and Fluid Mixtures", ACS Symposium Series, Volume 300 : *Equations of State, Theories and Applications*, American Chemical Society, Washington DC, 434-451.

40. Guo, T.M., Kim, H., Lin, H.M. and Chao, K.-C., (1985) : "Cubic Chain-of-Rotators Equation of State. 2. Polar Substances", *Ind. Eng. Chem. Proc. Des. Dev.*, **24**, 764-767.

41. Guo, T.M., Lin, H.M. and Chao, K.-C., (1985) : "Cubic Chain-of-Rotators Equation of State. 3. Mixtures of Polar Substances", *Ind. Eng. Chem. Proc. Des. Dev.*, **24**, 768-773.

42. Mathias, P.M. and Copeman, T.W., (1983) : "Extension of the Peng-Robinson Equation of State to Polar Fluids and Fluid Mixtures", *Fluid Phase Equilibria*, **13**, 91-108.

43. Soave, G., (1984) : "Improvement of the van der Waals Equation of State". *Chem. Eng. Sci.*, **39**, 357-369.

44. Stryjek, R. and Vera, J.H., (1986) : "PRSV2 : A Cubic Equation of State for Accurate Vapour-Liquid Equilibria Calculations", *Canadian J. Chem. Eng.*, **64**, 820-826.

45. Androulakis, I.P., Kalospiros, N.S. and Tassios, D.P., (1989) : "Thermophysical Properties of Pure Polar and Non-Polar Compounds with a Modified vdW-711 Equation of State", *Fluid Phase Equilibria*, **45**, 135-163.

46. Melhem, G.A., Saini, R. and Goodwin, B.M., (1989) : "A Modified Peng-Robinson Equation of State", *Fluid Phase Equilibria*, **47**, 189-237.

47. Danesh, A., Xu, D.-H., Tehrani, D.H. and Todd, A.C., (1995) : "Improving Predictions of Equation of State by Modifying Its Parameters for Super Critical Components of Hydrocarbon Reservoir Fluids", *Fluid Phase Equilibria*, **112**, 45-61.

48. Twu, C.H., Coon, J.E. and Cunningham, J.R., (1995) : "A New Generalised alpha Function for a Cubic Equation of State, Part 1. Peng-Robinson Equation", *Fluid Phase Equilibria*, **105**, 49-59.

49. Daubert, T.E. and Danner, R.P., (1990) : "*Data Compilation - Physical and Thermodynamic Properties of Pure Compounds*", Taylor and Francis, Washington, USA.

50. Twu, C.H., (1984) : "An Internally Consistent Correlation for Predicting the Critical Properties and Molecular Weights of Petroleum and Coal-Tar Liquids", *Fluid Phase Equilibria*, **16**, 137-150.

51. Whitson, C.H., (1983) : "Characterizing Hydrocarbon Plus Fraction", *SPEJ*, Aug., 683-694.

52. Danesh, A., Tehrani, D.H., Todd, A.C., Tohidi, B., Gozalpour, F., Malcolm, K., Reid, A., Bell, K., Elghayed, K. and Burgass, R., (1997) : "Phase Behaviour and Properties of Reservoir Fluids", paper presented at the Department of Trade and Industry, IOR Symposium, London, June.

Table 2.1 : AAD% of Predicted Vapour Pressure of Pure Compounds.

Comp.	Temp. Range (K)	Error % Exp. *	Error % PR	Error % Twu et al.	Error % This work**
C1	68.60 - 186.75	< 1.0	6.231	5.364	3.053
C2	106.86 - 299.21	< 1.0	2.349	0.932	1.346
C3	129.44 - 362.43	< 3.0	3.727	1.243	0.873
n-C4	148.79 - 416.62	< 3.0	3.174	2.371	1.456
n-C5	164.39 - 460.31	< 3.0	4.430	2.298	0.712
C6	203.04 - 497.45	< 3.0	4.613	1.123	1.515
C7	216.08 - 529.40	< 3.0	3.544	1.737	0.578
C8	227.48 - 557.33	< 3.0	3.546	2.520	1.149
C9	237.84 - 582.71	< 3.0	5.004	1.626	0.643
C10	247.08 - 605.35	< 3.0	5.049	2.887	1.077
C11	274.77 - 626.22	< 3.0	5.352	0.917	1.298
C12	276.36 - 644.84	< 3.0	4.777	1.932	1.257
C13	283.50 - 661.50	< 1.0	5.430	1.136	1.167
C14	297.99 - 679.14	< 3.0	7.057	0.711	2.762
C15	318.60 - 693.84	< 3.0	3.580	0.939	0.883
C16	325.35 - 708.54	< 3.0	4.861	0.923	2.105
C17	331.20 - 721.28	< 5.0	2.698	1.116	0.748
C18	336.15 - 732.06	< 5.0	2.401	1.449	0.684
C19	348.68 - 742.84	< 5.0	2.765	1.020	1.174
C20	360.96 - 752.64	< 5.0	1.803	3.297	2.385
H_2S	205.44 - 366.06	< 3.0	2.754	2.733	3.202
H_2O	258.85 - 634.19	< 0.2	4.237	7.843	6.962
CO	73.11 - 130.26	< 3.0	3.421	3.373	2.861
CO_2	228.14 - 298.11	< 1.0	0.437	0.094	0.633
AAD%			3.885	2.066	1.688

* Estimated errors of experimental data.

** Using the new α function.

Table 2.2 : Values of A, B and C Parameters in Eq 2.53.

Parameter	$T_r \leq 1.0$		$T_r > 1.0$	
	α^0	α^1	α^0	α^1
A	-0.4568138	-1.7581060	-0.6701814	-1.5599740
B	-0.2951492	0.8365879	0.4072234	0.4812347
C	-0.6336781	-1.428765	-0.0948269	-0.1504902

Table 2.3 : Percentage Deviation in Predicted Saturation Pressure.

Fluid	Type	T (°C)	Sat. Press Exp. (psia)	% Dev. in Sat. Press.			
				PR ($k_{ij}=0$)	PR ($k_{ij}\neq0$)	m' (Eq 2.50)	This Work
GC1	r-gc	121	6836	-20.7	-13.1	-12.4	-11.0
gc5	r-gc	140	6200	-12.2	-1.9	-2.7	-2.3
GCA94-1	r-gc	110	5330	-8.7	-0.5	+0.5	+3.1
boa	sy-bo	100	2942	-15.3	-5.1	-7.3	-4.0
bob	sy-bo	100	2238	-14.1	-0.8	-6.4	-3.1
voa	sy-vo	100	4754	-8.0	+3.3	-1.0	+3.4
vob	sy-vo	100	4743	-9.5	+3.4	-1.0	+3.2
boc	r-bo	100	2598	-15.8	-11.2	-7.3	-3.9
voc	r-vo	100	5065	-19.5	-9.4	-10.9	-7.8
oil7	sy-o	60	3119	-15.3	-0.3	-8.5	-0.9
o8	r-o	82.2	2535	-24.8	-11.6	-17.6	-12.1
bod	r-bo	55	1708	-18.5	-7.4	-11.3	-3.7
boe	r-bo	104.4	2635	-11.2	-2.9	-4.6	-0.7
bof	r-bo	100	1365	-9.0	+0.2	-0.1	+2.4
o1	r-o	100	2598	-15.8	-12.2	-7.4	-4.0
Starling-B	sy-gc	101.1	3795	-12.1	-5.7	-5.2	-2.1
Starling-B	sy-gc	121.1	3515	-7.6	-1.4	-0.1	+1.1
Starling-A	sy-gc	93.9	3842	-12.6	-7.6	-5.6	-1.7
Whit-Torp	r-gc	137.8	6765	-11.1	+2.6	-0.9	-0.3
McCain	r-o	104.4	2635	-11.3	+2.2	-2.1	-0.9
bo9	r-bo	96.6	2300	-14.4	-3.5	-6.6	-1.9
Jacoby S-3	r-gc	93.3	4022	-9.6	+3.6*	-0.8	+3.3
Jacoby S-6	r-gc	93.3	5020	-21.9	-16.7	-15.1	-11.7
Jacoby S-7	r-gc	93.3	5118	-25.6	-20.1	-19.3	-16.1
Pedersen-1	r-gc	96.6	4090	-10.4	+15.5	-2.9	+1.1
Pedersen-3	r-gc	143.0	6527	-15.0	-5.6	-5.7	-5.6
Pedersen-4	r-vo	142.2	5665	-3.5	+12.4	+7.5	+7.9
Pedersen-4	r-vo	151.1	5646	-2.4	+13.1	+8.8	+8.6

Table 2.3 : Continued ...

Fluid	Type	T (°C)	Sat. Press Exp. (psia)	% Dev. in Sat. Press.			
				PR (k_{ij}=0.)	PR ($k_{ij}\neq$0.)	m' (Eq 2.50)	This Work
Pedersen-4	r-gc	163.3	5594	-7.4	+14.5*	+3.3	+3.2
Pedersen-4	r-gc	170.0	5568	-6.0	+15.0*	+4.9	+3.5
Pedersen-5	r-vo	140.0	4788	-6.1	+9.6	+4.4	+4.8
Hoffman	r-vo	93.9	3840	-17.9	-4.6	-8.6	-4.2
AAD%				**12.92**	**7.41**	**6.28**	**4.49**

* Bubble Point Prediction

- Keys :

r : real reservoir fluid
gc : gas condensate
sy : model fluid
bo : black oil
vo : volatile oil
o : oil
AAD% : average absolute percentage deviation

Table 2.4 : Shift Parameters for Hydrocarbons.

Component	Shift Parameter (S)
Methane	-0.1540
Ethane	-0.1002
Propane	-0.08501
i-Butane	-0.07935
n-Butane	-0.06413
i-Pentane	-0.04350
n-Pentane	-0.04183
n-Hexane	-0.01478

Table 2.5 : Shift Parameter Correlation Coefficients for Hydrocarbons Heavier Than Hexane (Eq 2.55).

Component Type	d	e
n-Alkanes	2.258	0.1823
n-Alkylcyclohexanes	3.004	0.2324
n-Alkylbenzenes	2.516	0.2008

Table 2.6 : Numerical Values of Coefficients of Eq 2.57.

Parameter	S^0	S^1
A'	-1.7135	-0.02818
B'	15.210	6.73570
C'	-55.889	-33.94500
D'	99.290	73.56000
E'	-86.482	-74.23100
F'	29.823	28.62200

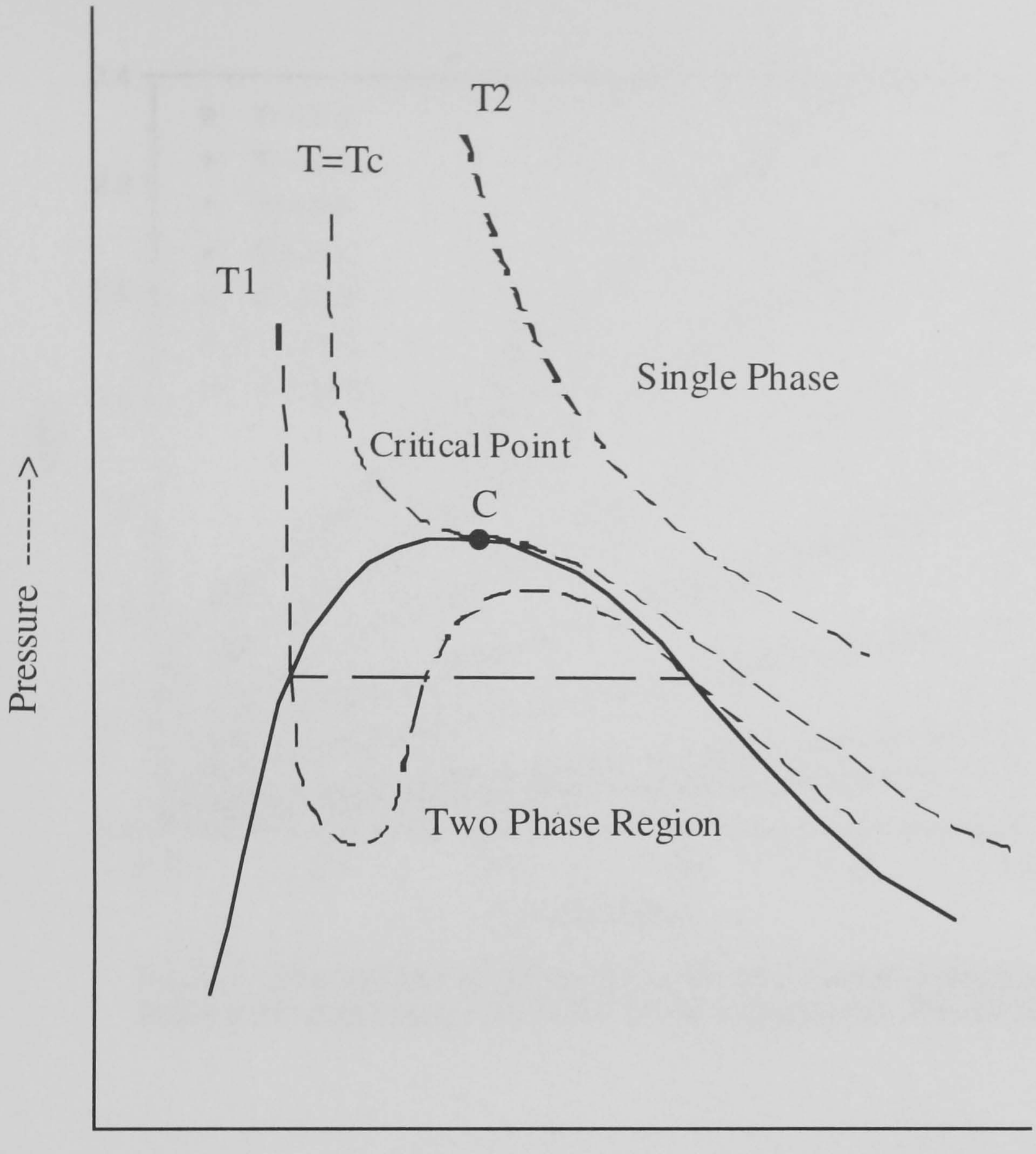

Fig. 2.1 - Phase Diagram of Pure Fluid

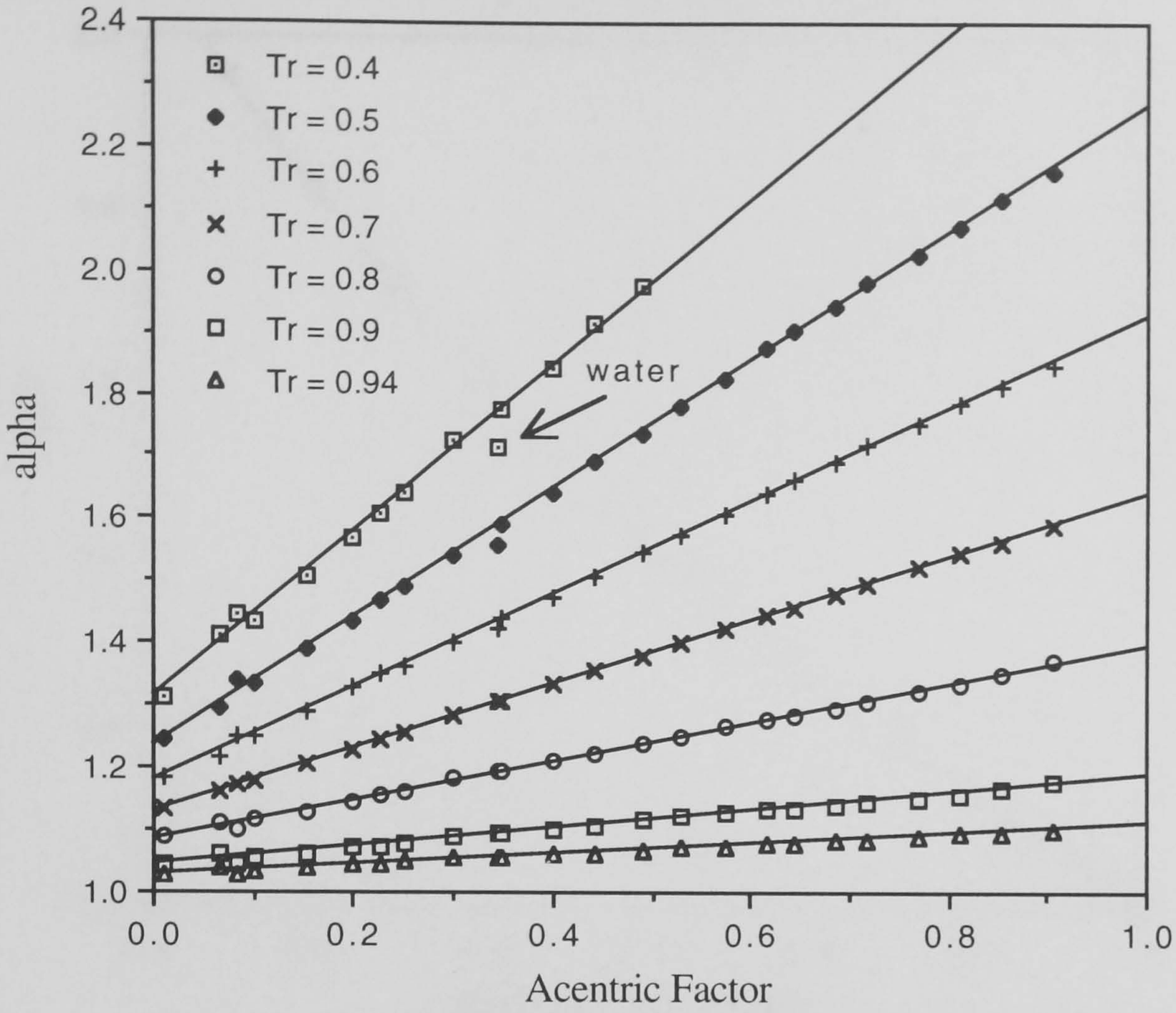

Fig. 2.2 - Dependence of alpha on the Acentric Factor at Several Reduced Temperatures, for Sub Critical Compounds, PR3 EOS.

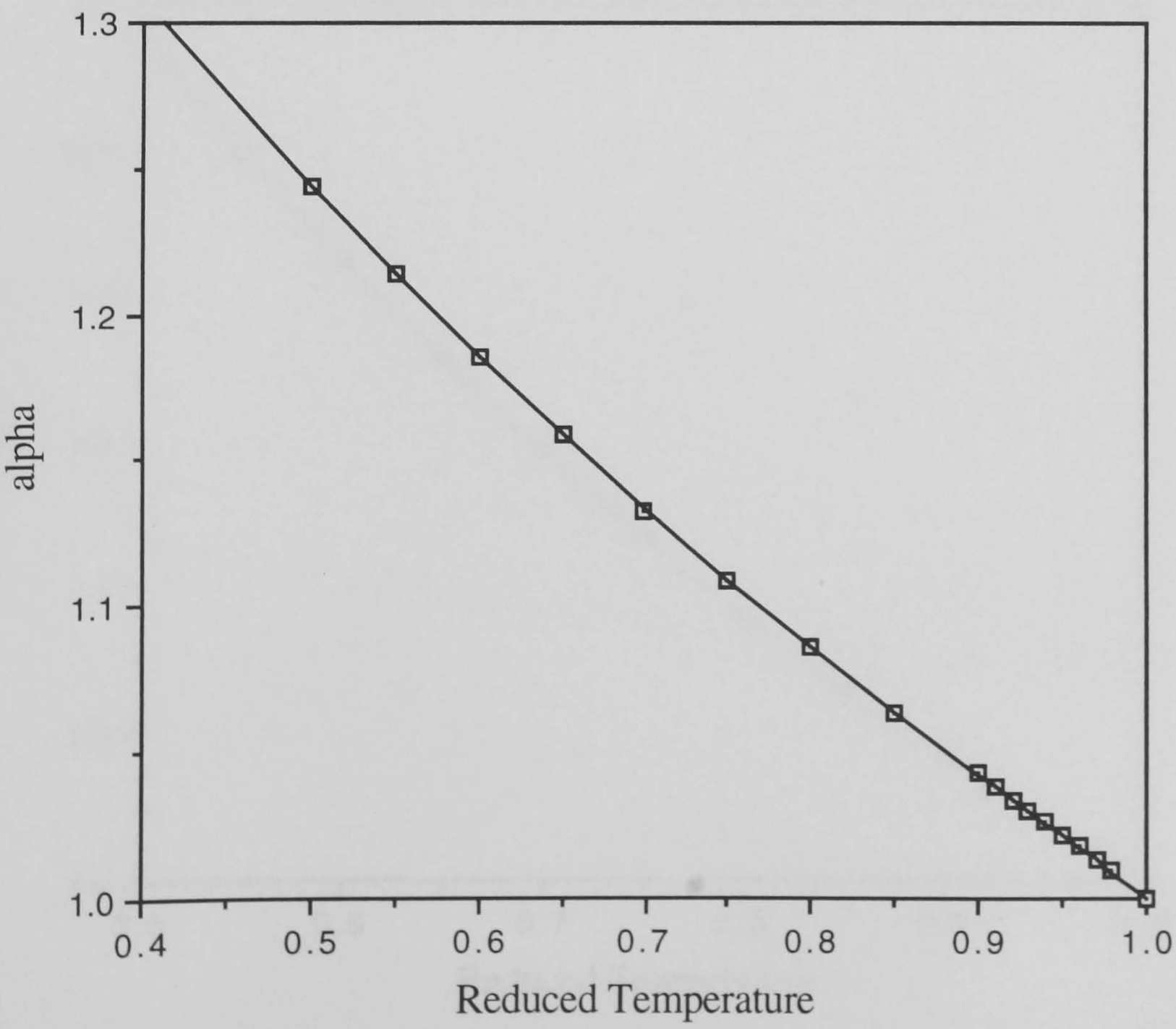

Fig. 2.3 - Alpha Parameter of Pure Methane.

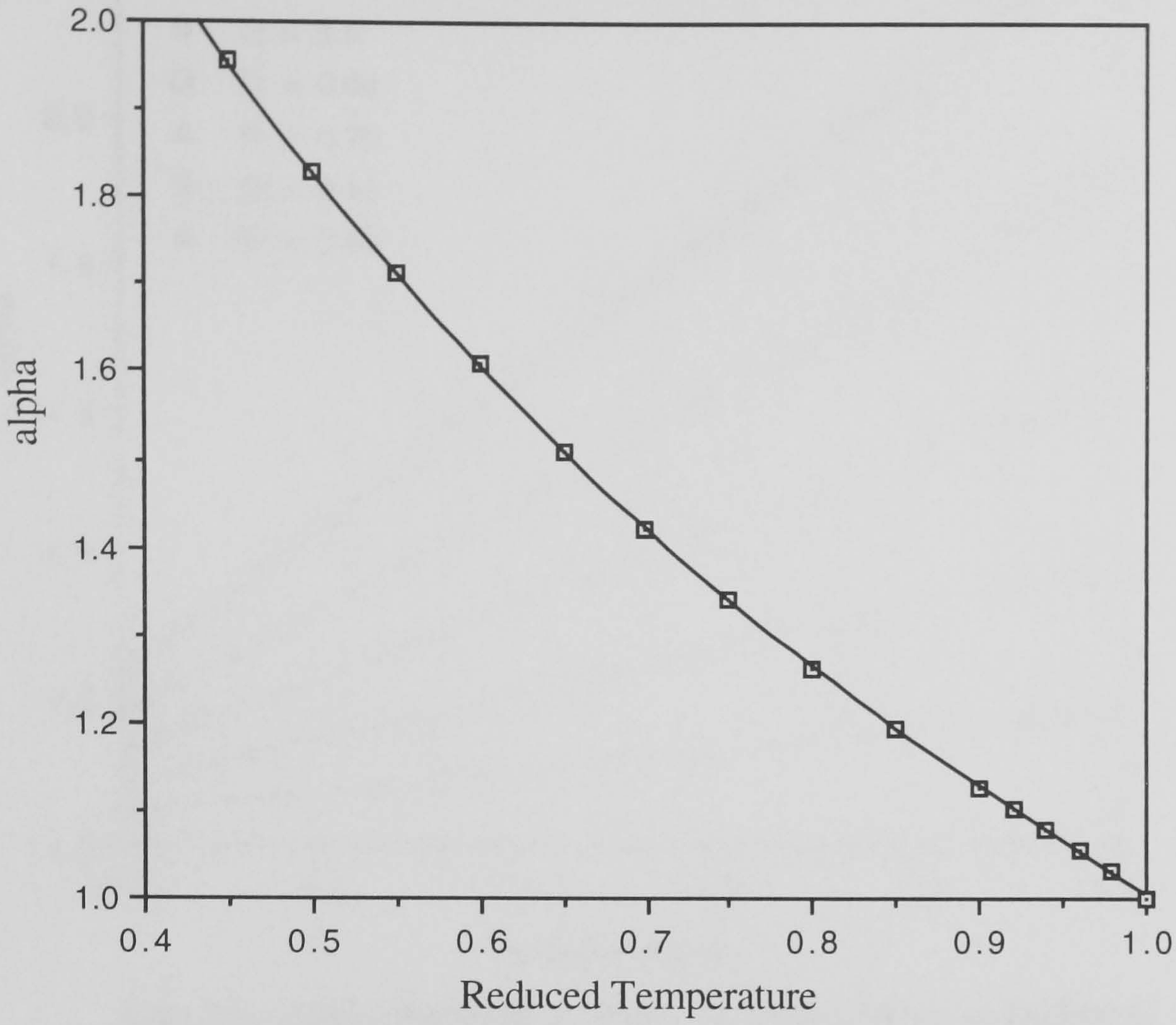

Fig. 2.4 - Alpha Parameter of Pure n-Dodecane (C12H26).

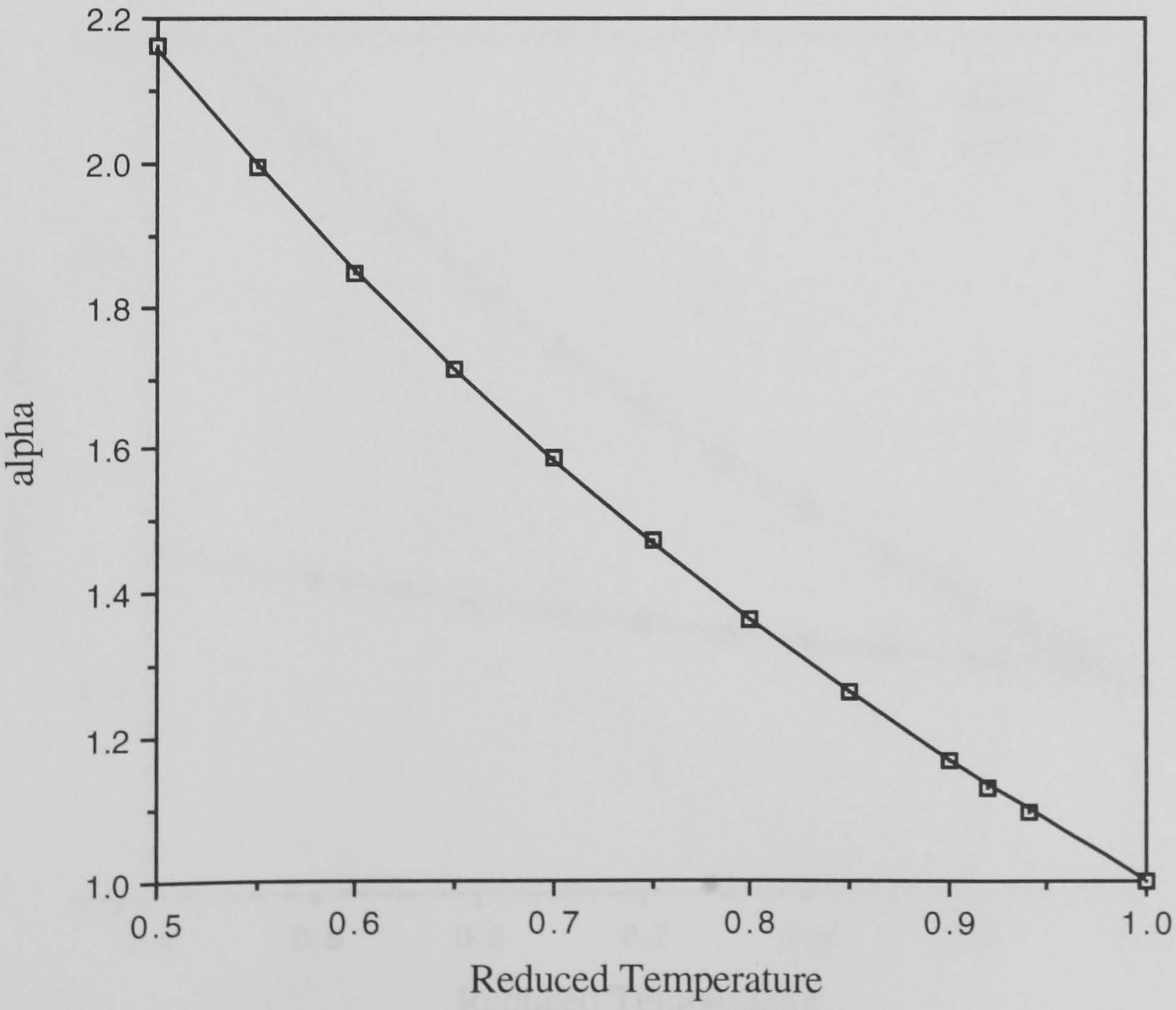

Fig. 2.5 - Alpha Parameter of Pure n-C20H42.

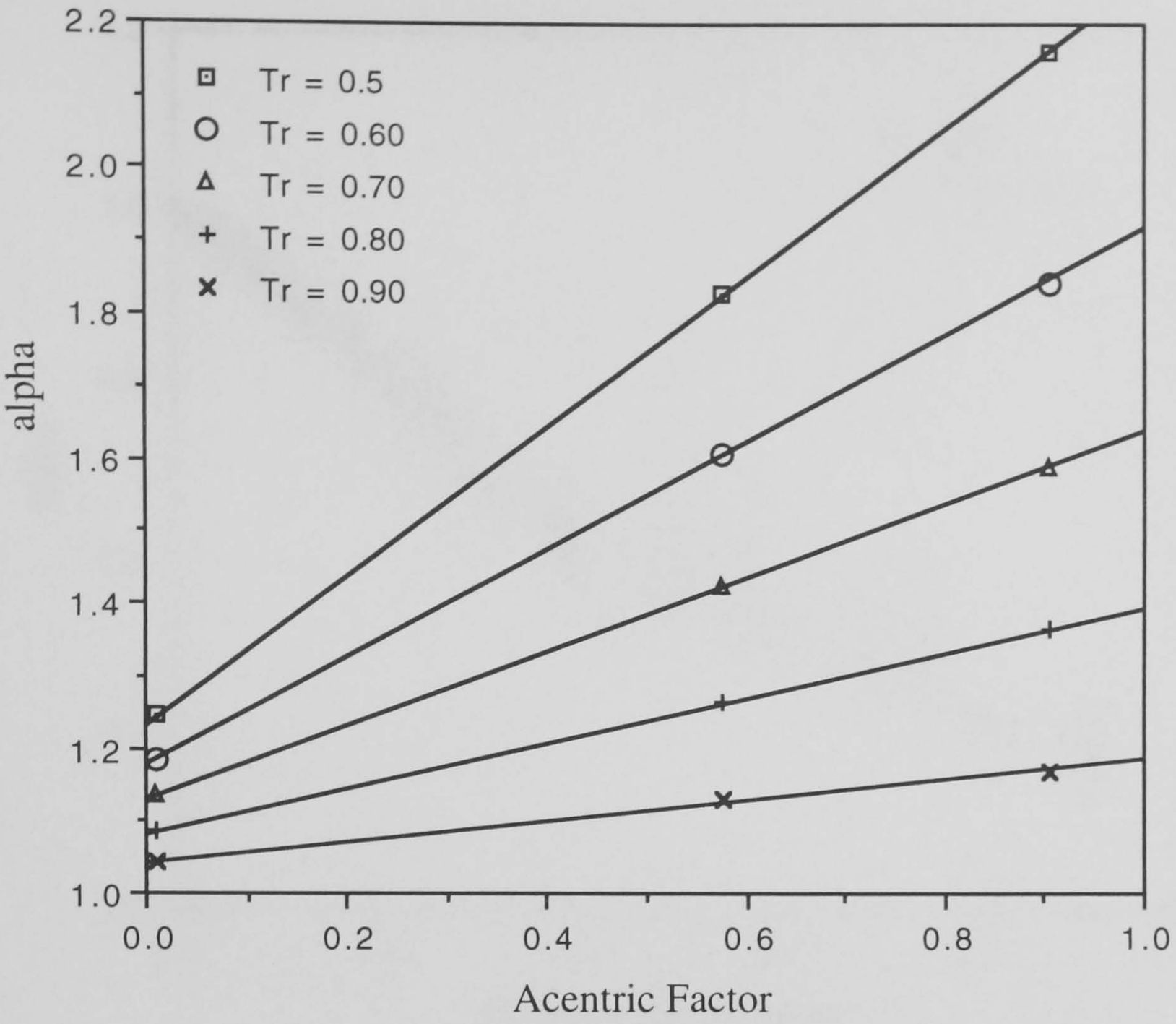

Fig. 2.6 - Alpha Parameter versus Acentric Factor at Different Reduced Temperatures.

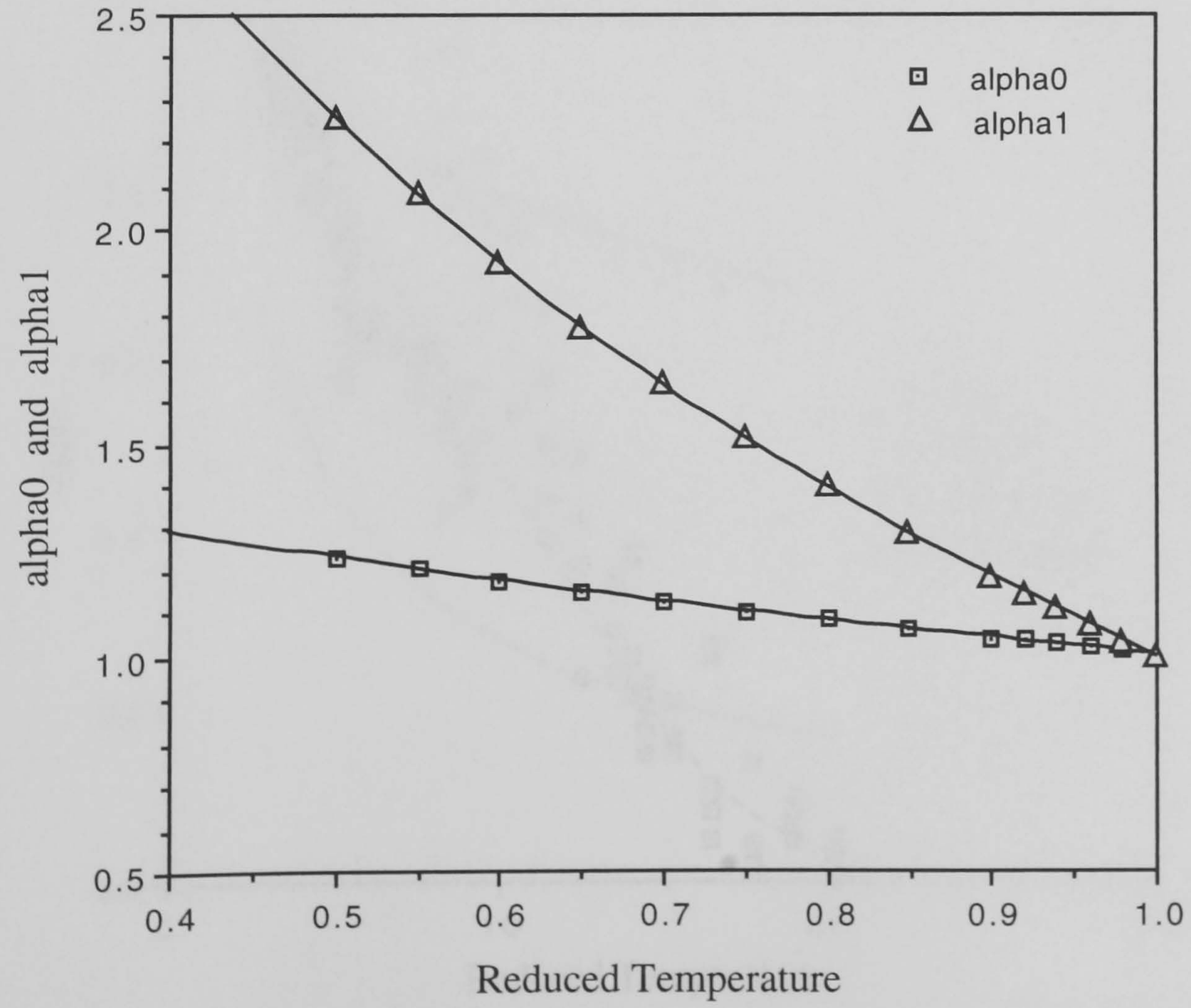

Fig. 2.7 - alpha0 and alpha1 versus Reduced Temperature.

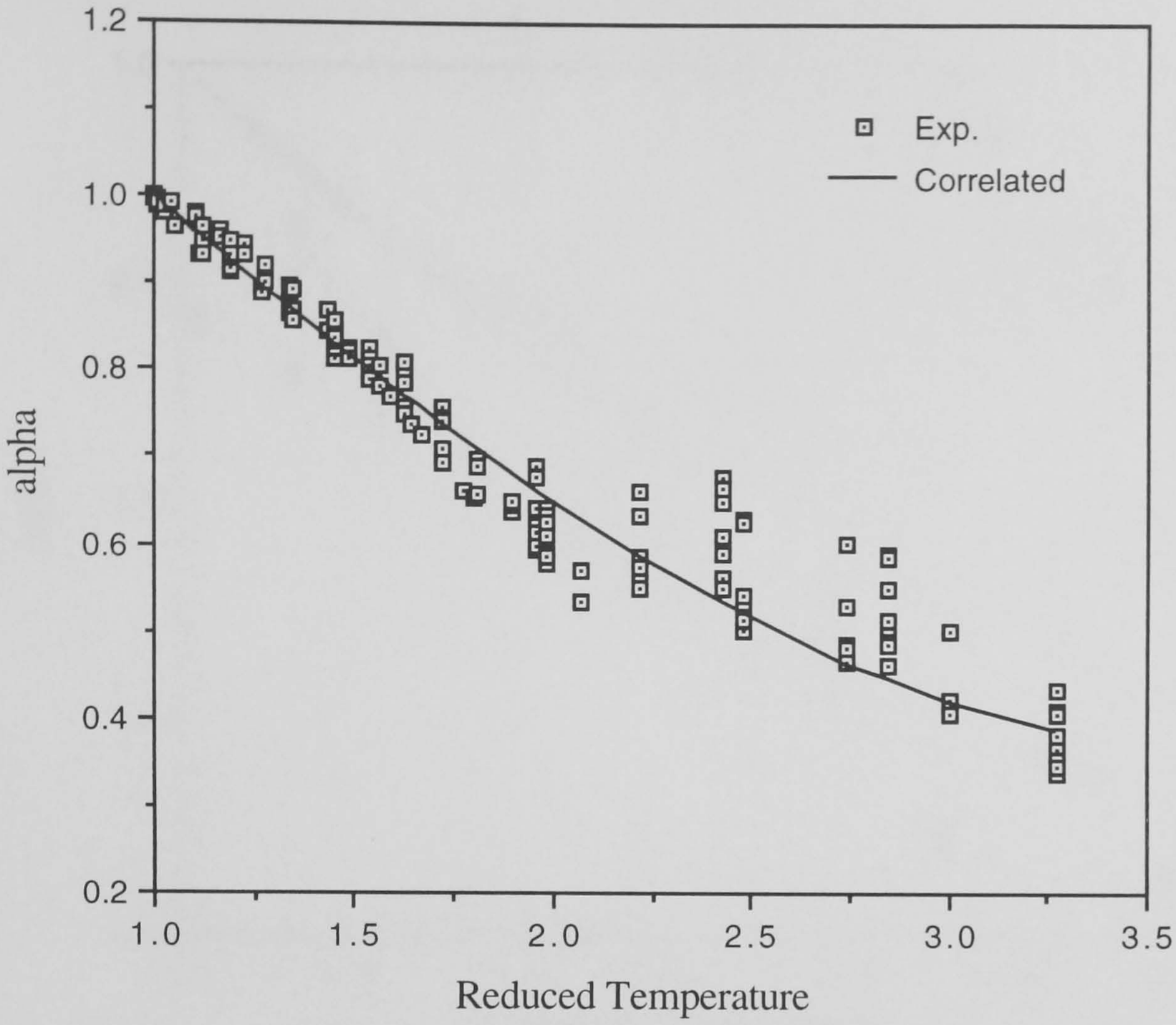

Fig. 2.8 - Supercritical Alpha Parameter of C1 from Various Binary Systems.

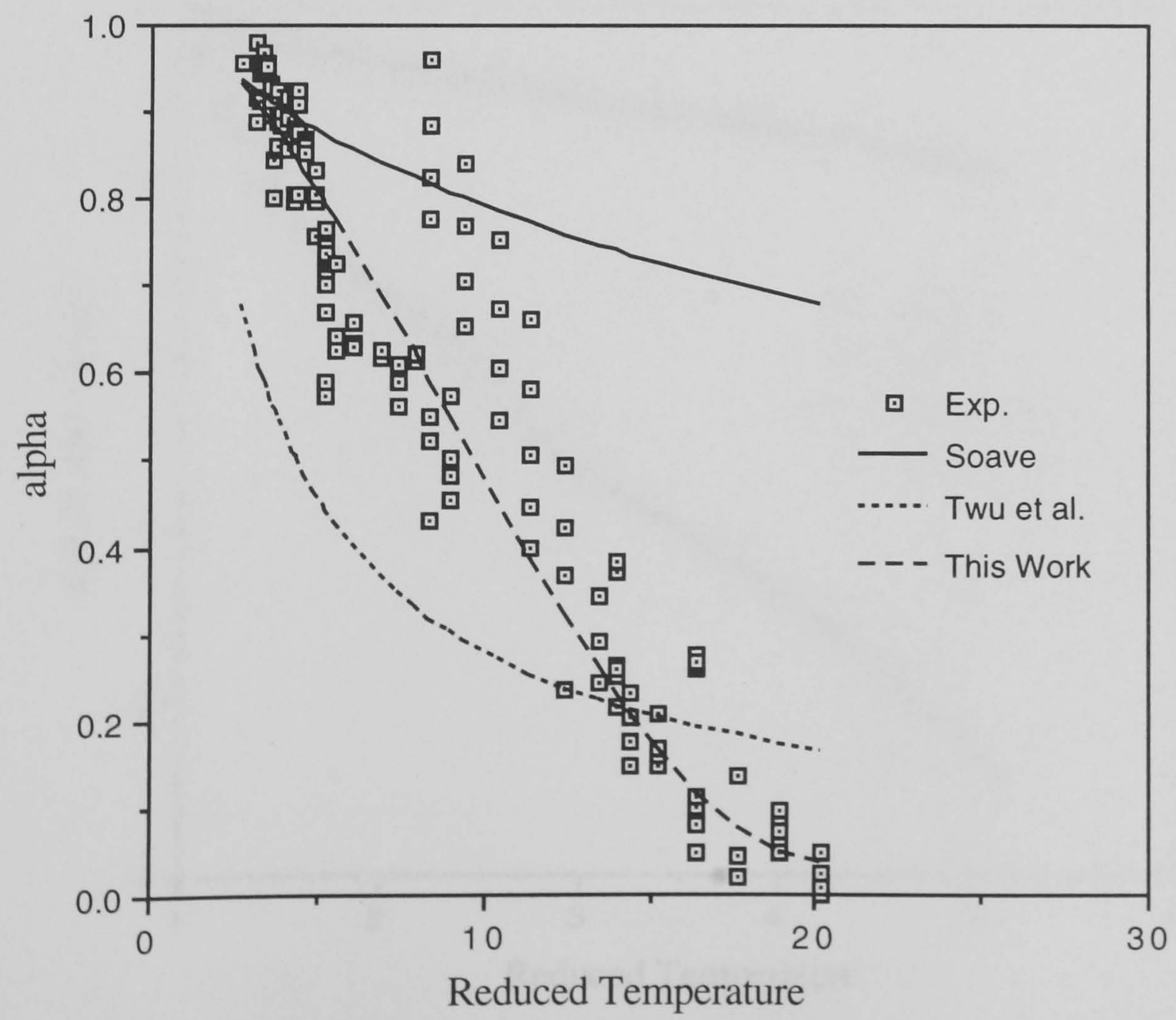

Fig. 2.9 - Supercritical Alpha Parameter of H2 from Various Binary Systems.

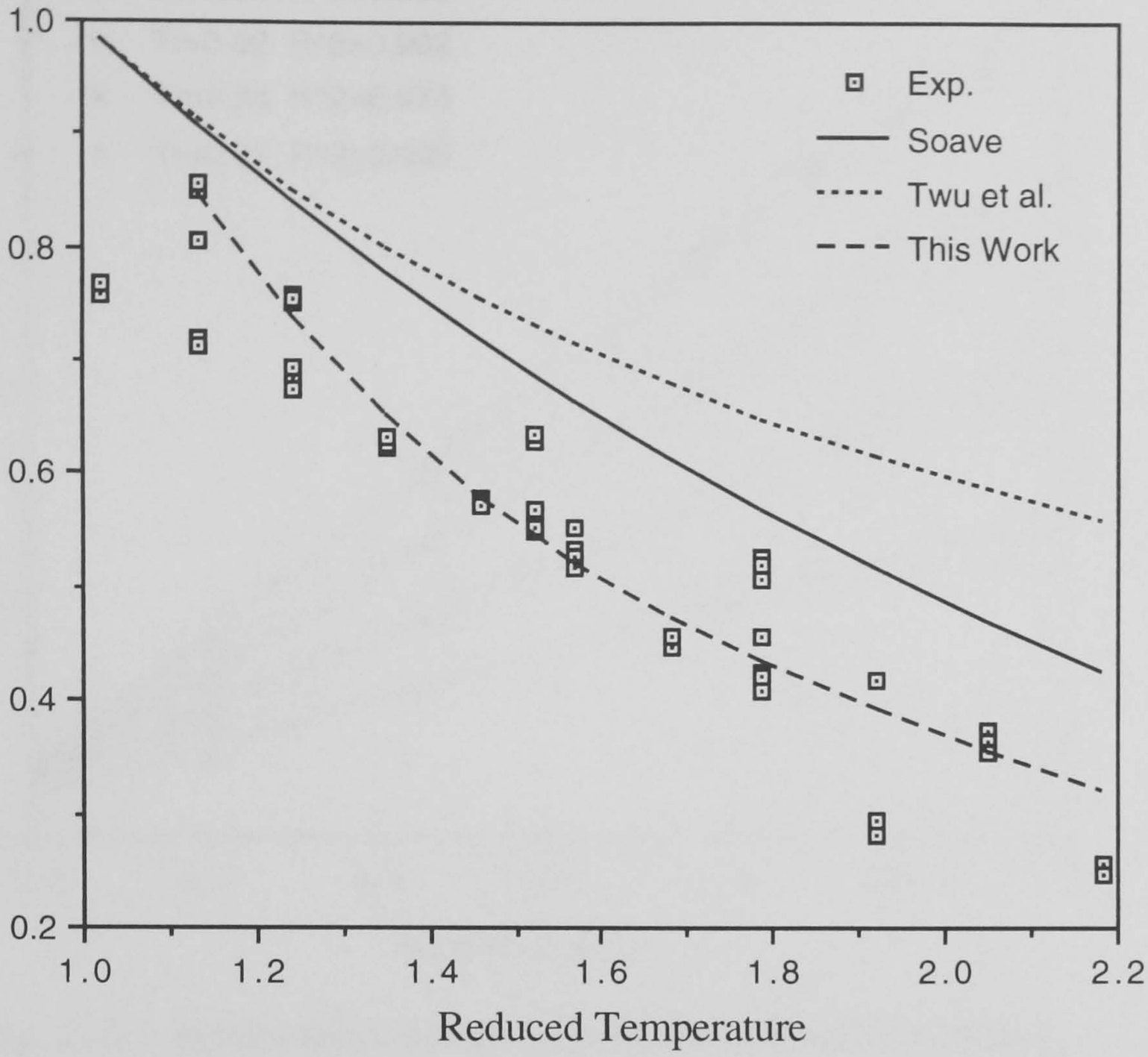

Fig. 2.10 - Supercritical Alpha Parameter of CO2 from Various Binary Systems.

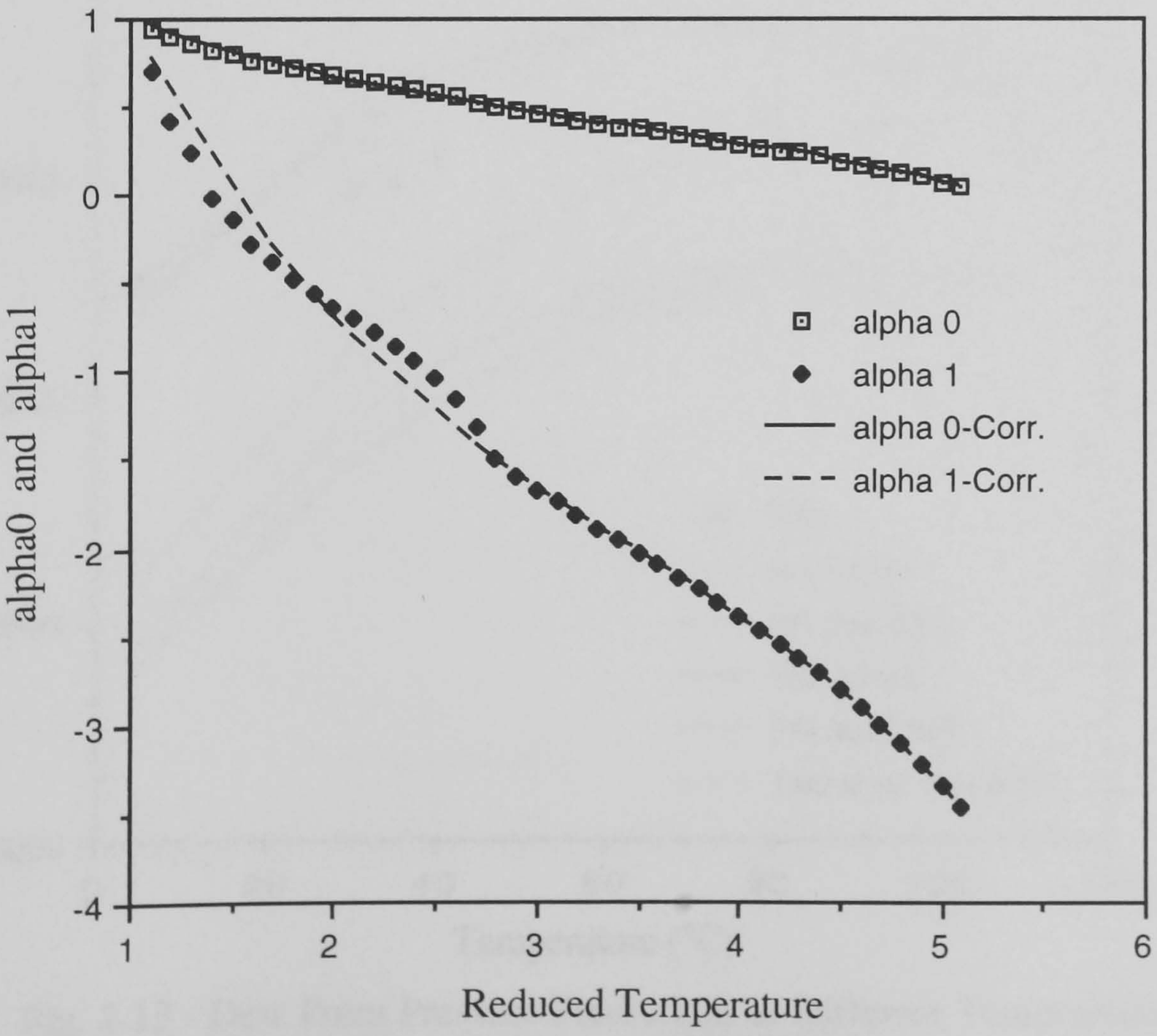

Fig. 2.11 - alpha0 and alpha1 versus Reduced Temperature.

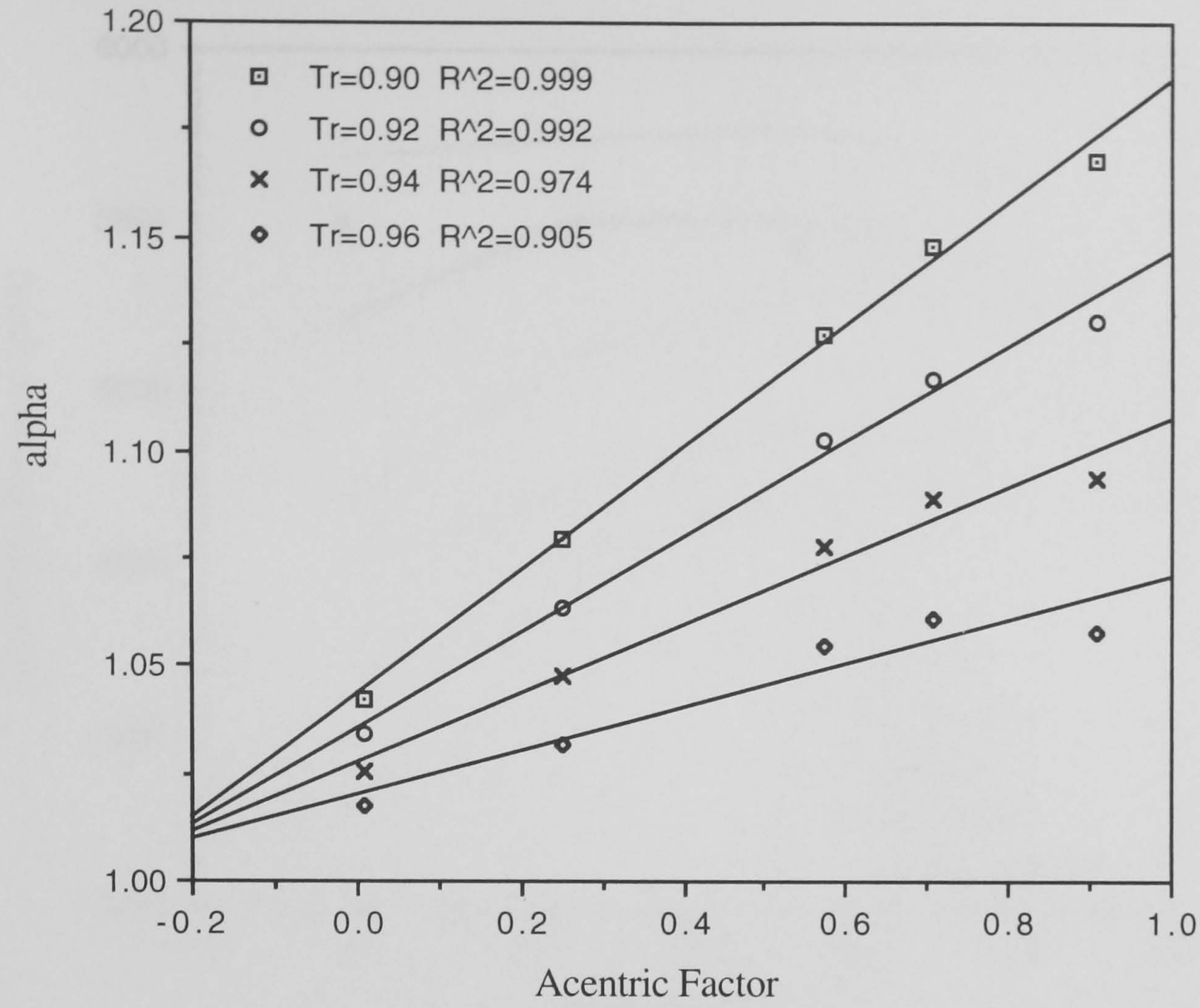

Fig. 2.12 - alpha versus Acentric Factor at Near Critical Region.

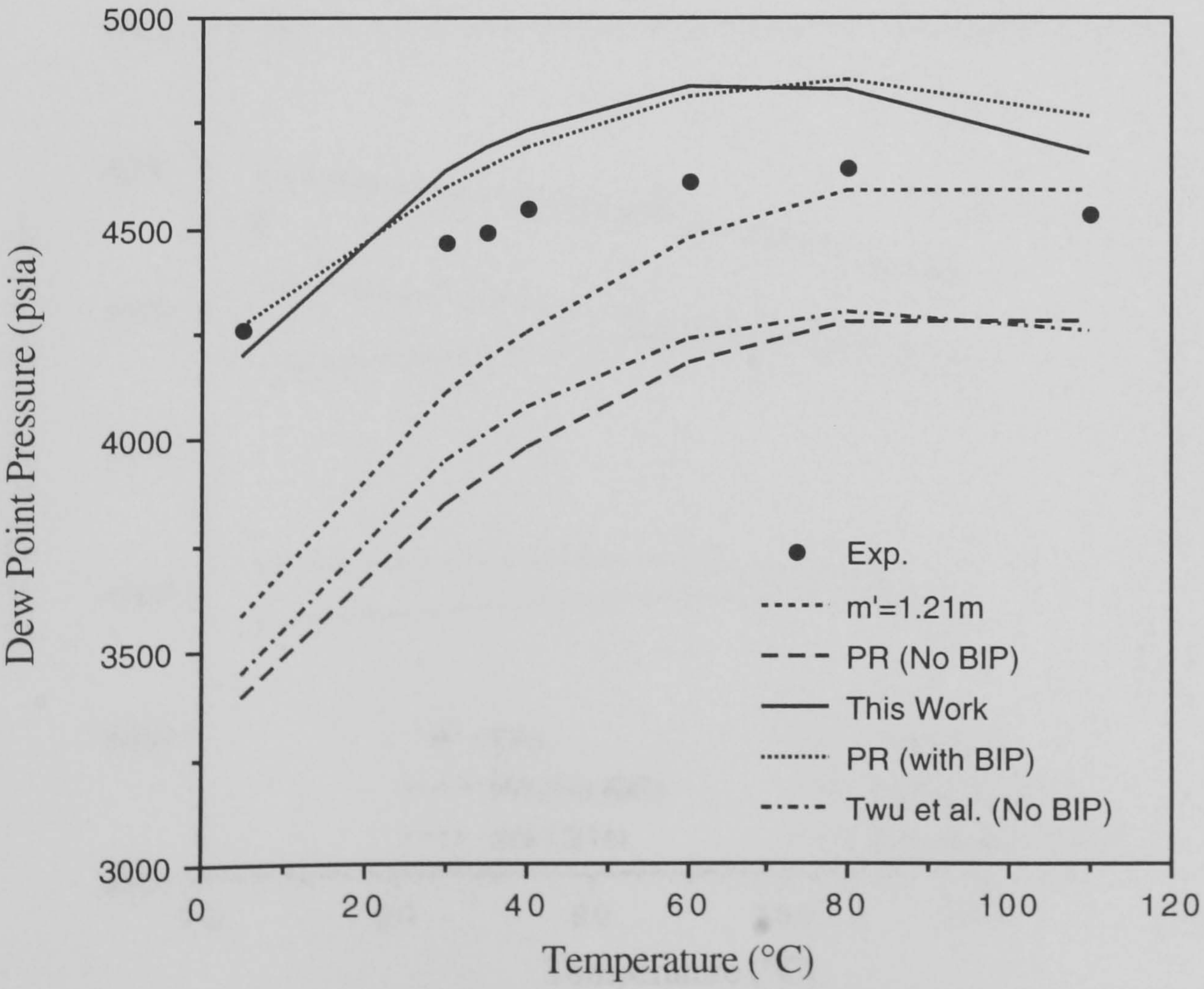

Fig. 2.13 - Dew Point Pressure Predictions at Different Temperatures, 5-component Model Gas Condensate (GMX89-1).

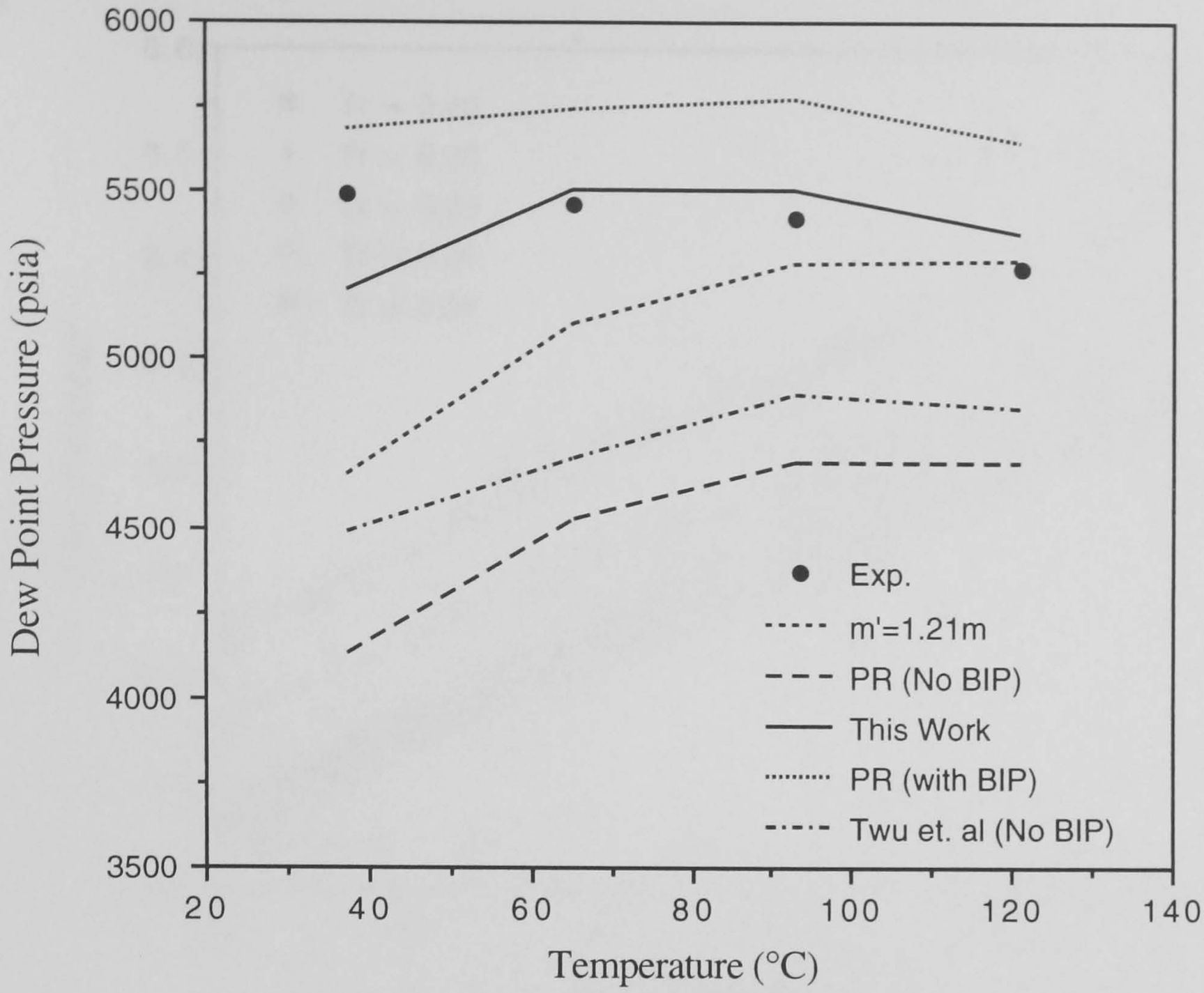

Fig. 2.14 - Dew Point Pressure Predictions at Different Temperatures, 20-component Model Gas Condensate (GMX90-1).

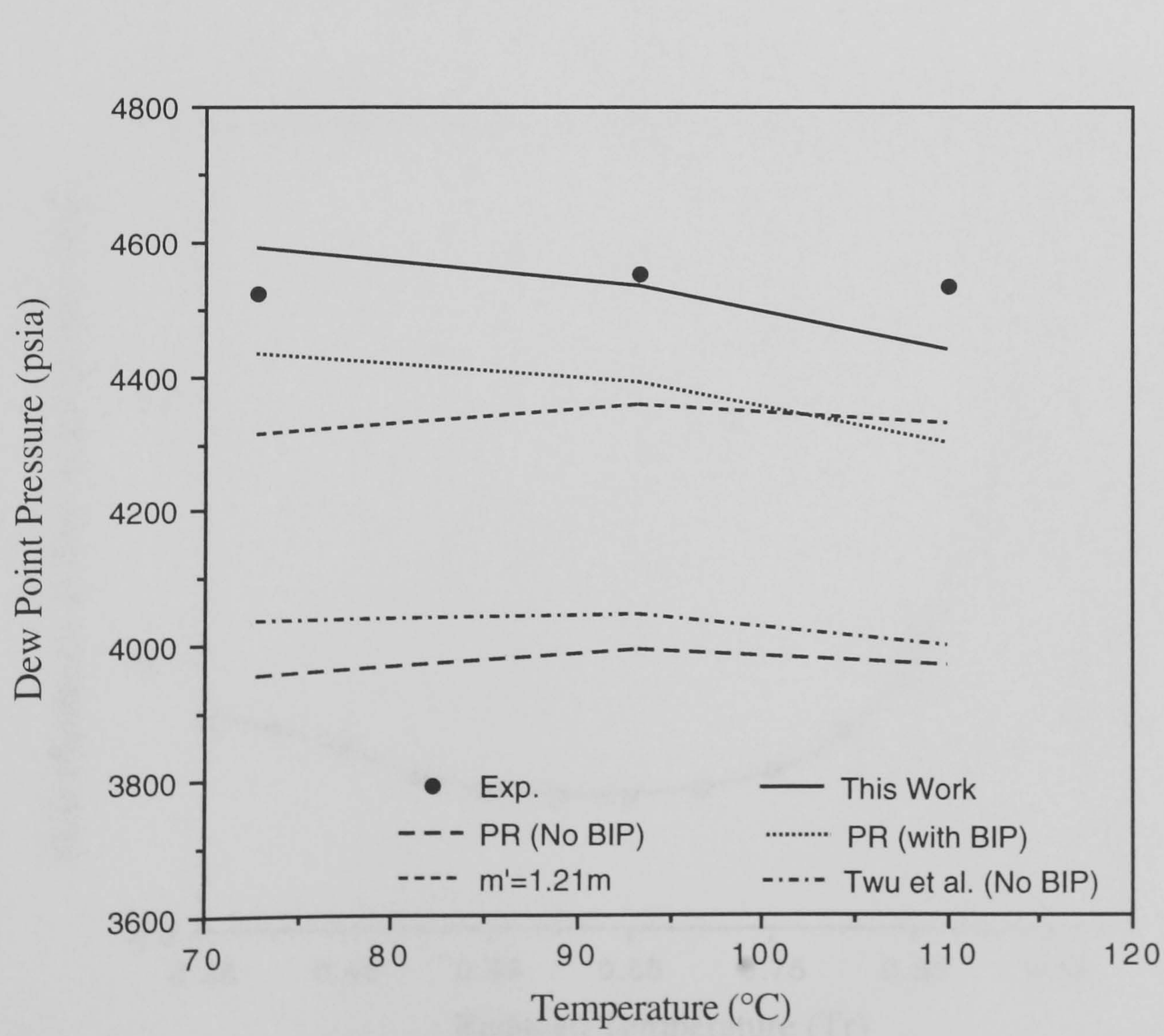

Fig. 2.15 - Dew Point Pressure Predictions at Different Temperatures, Gas Condensate JOCBS-5.

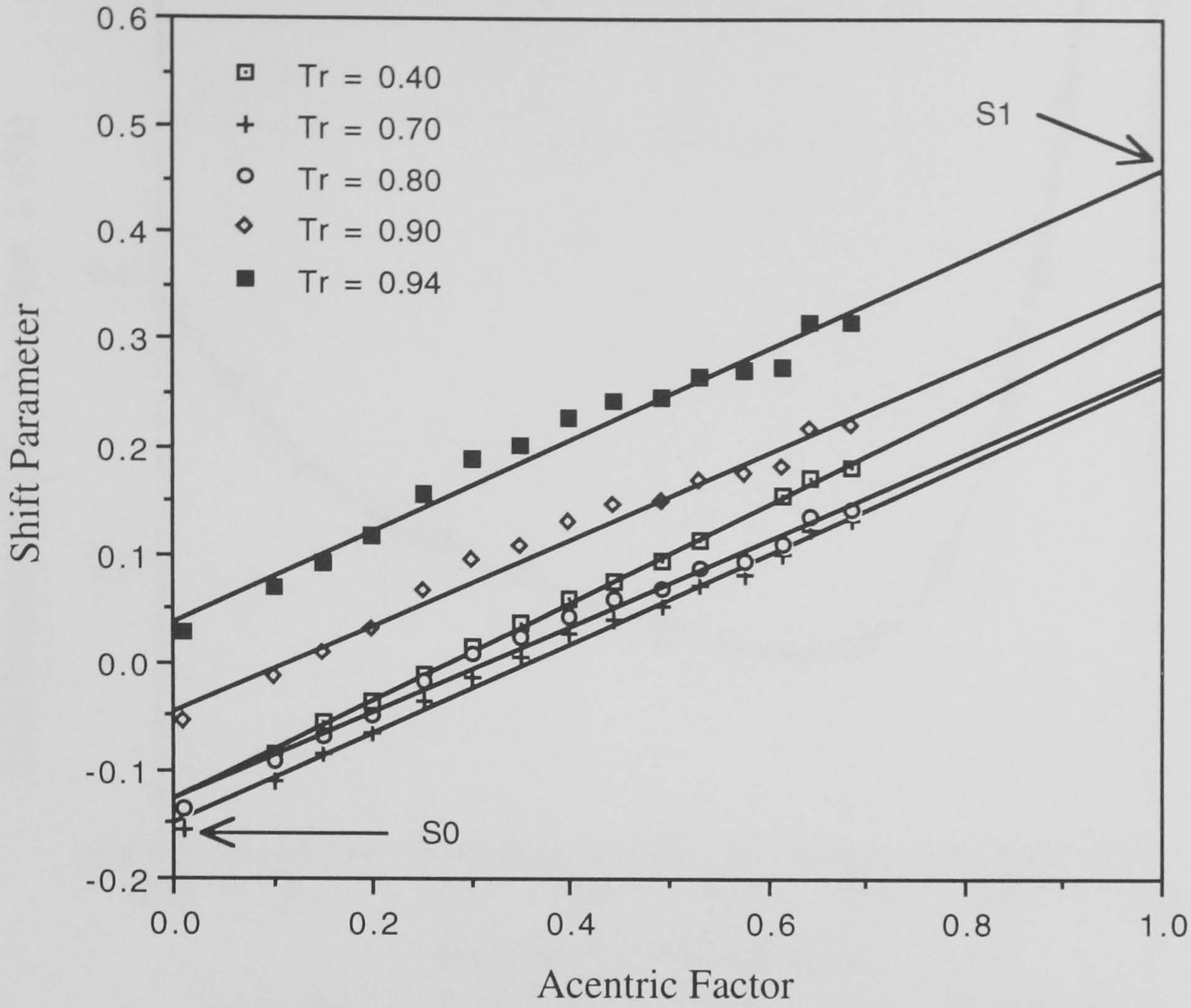

Fig. 2.16 - Dependence of Shift Parameter on the Acentric Factor at Several Reduced Temperatures, PR3 EOS.

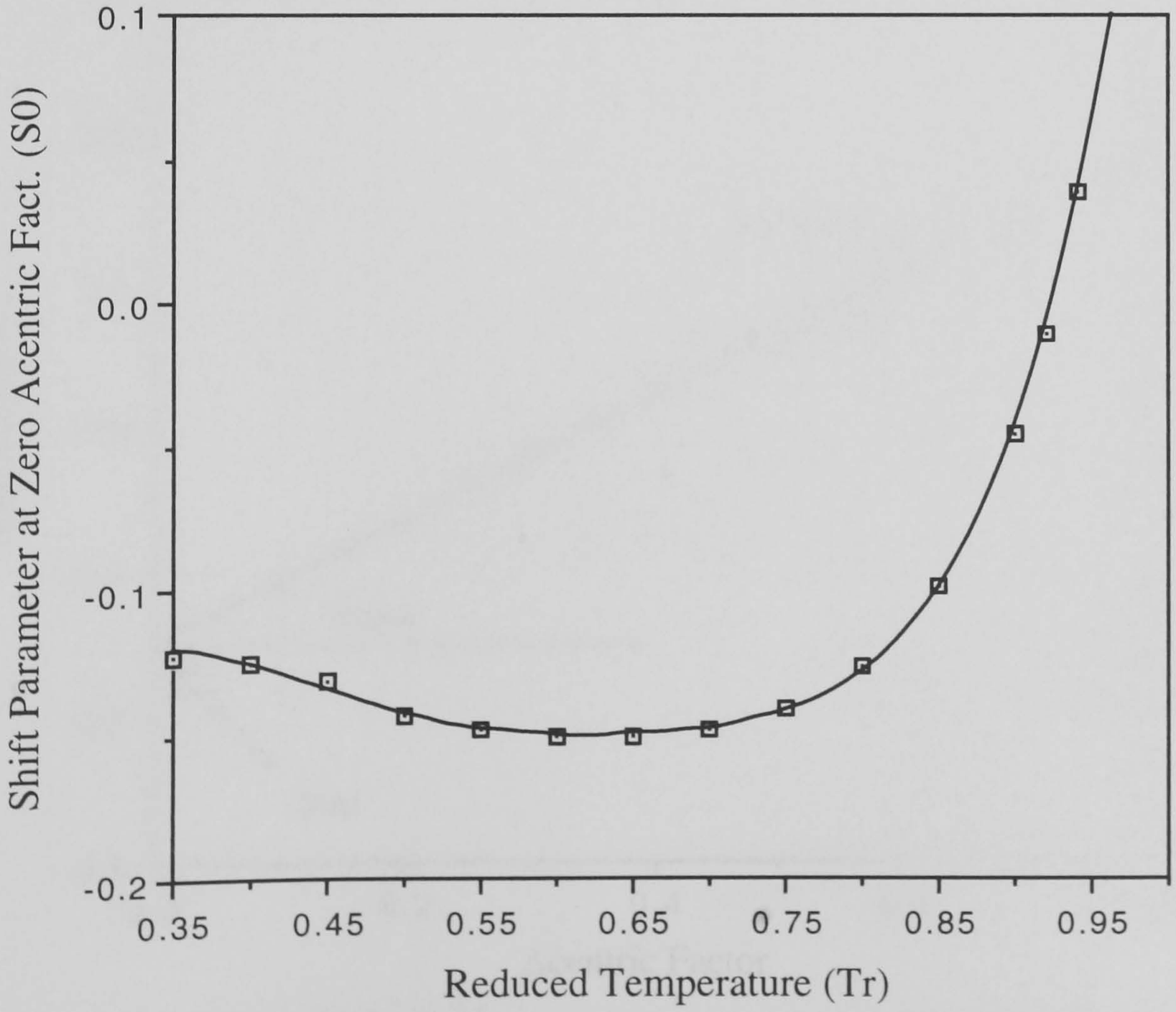

Fig. 2.17 - Shift parameter at Acentric Factor Equal Zero versus Reduced Temperature.

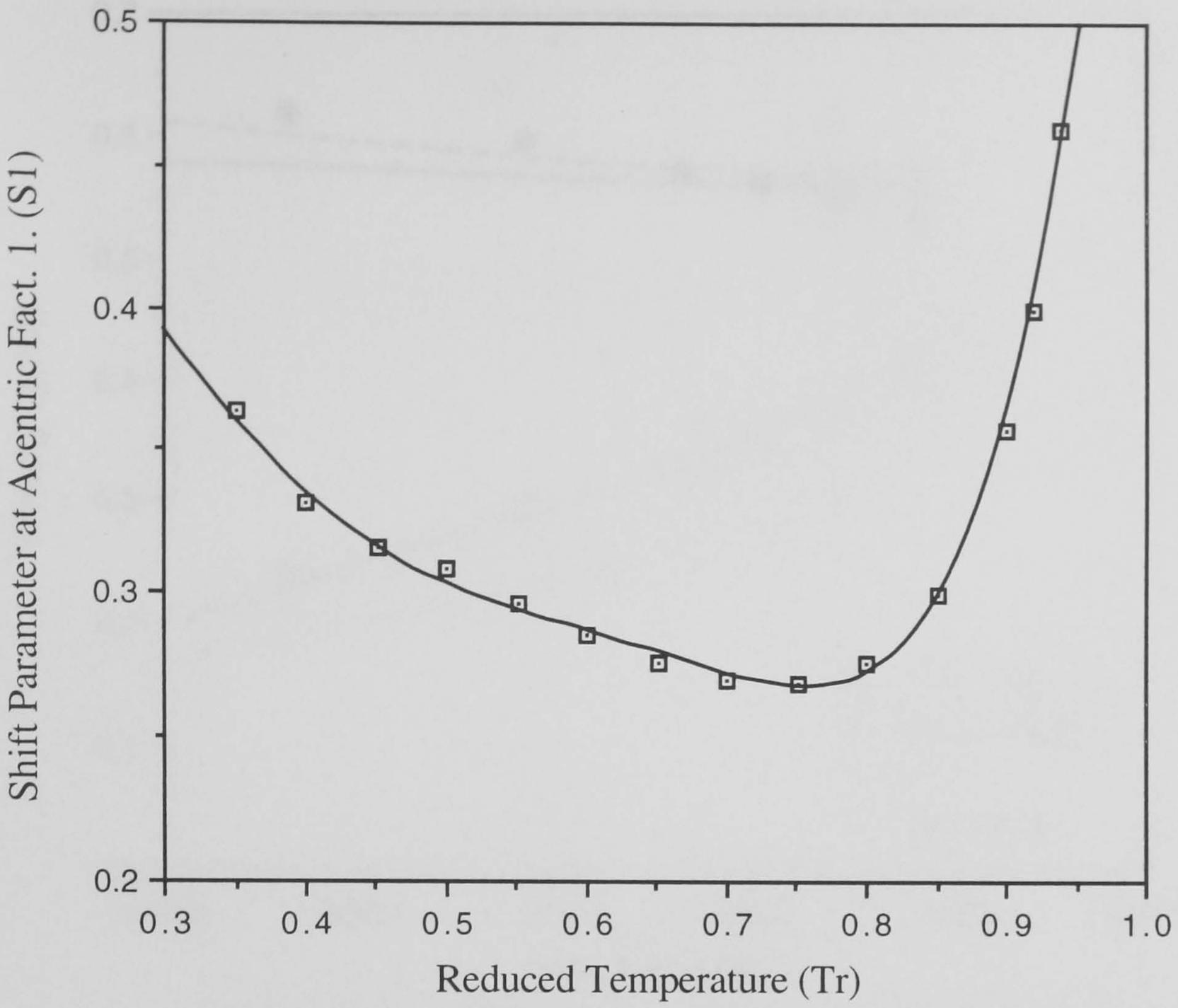

Fig. 2.18 - Shift Parameter at Acentric Factor Equal One versus Reduced Temperature.

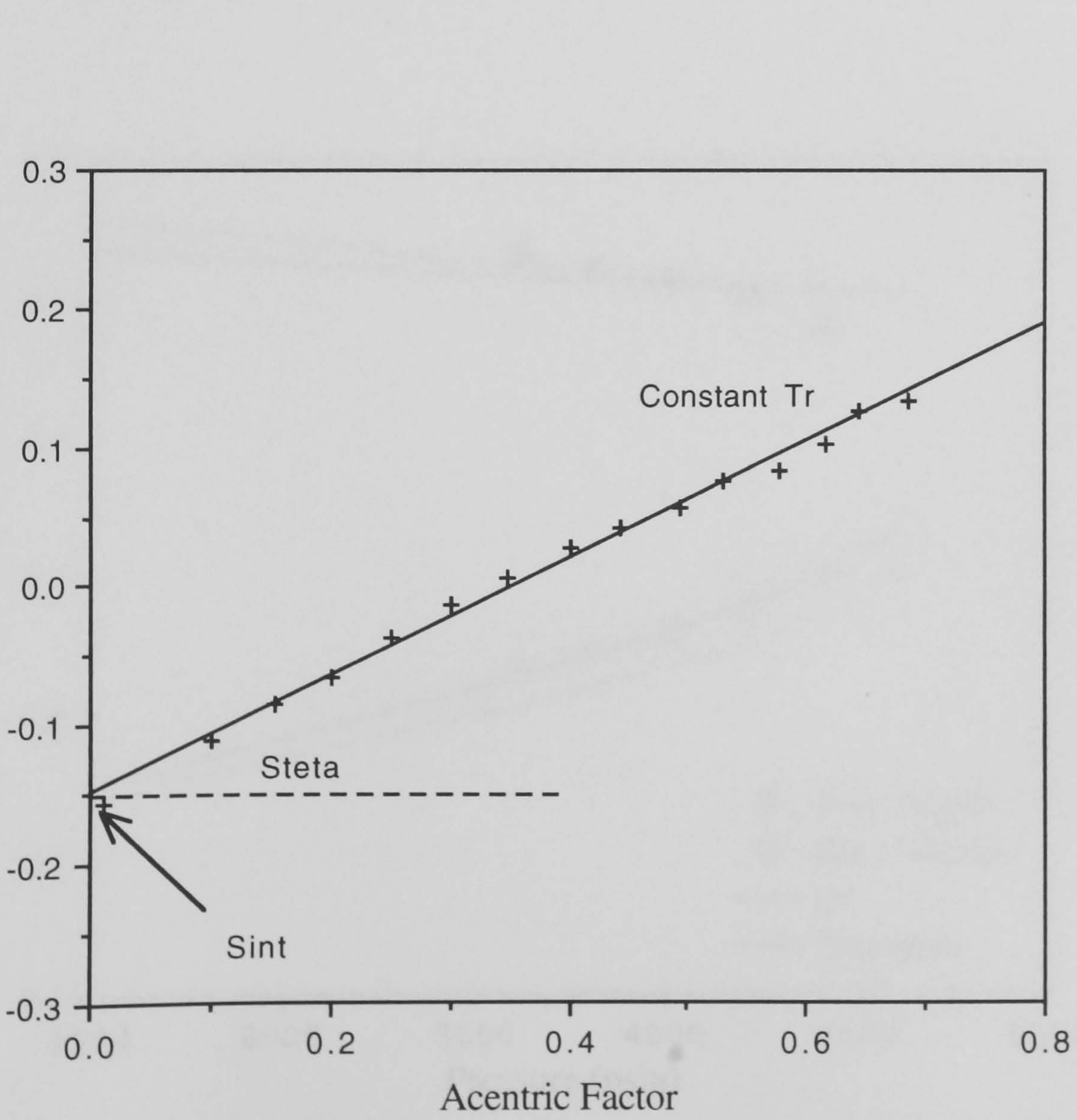

Fig. 2.19 - Adjustable Parameters in the New Shift Parameter Correlation, PR3 EOS.

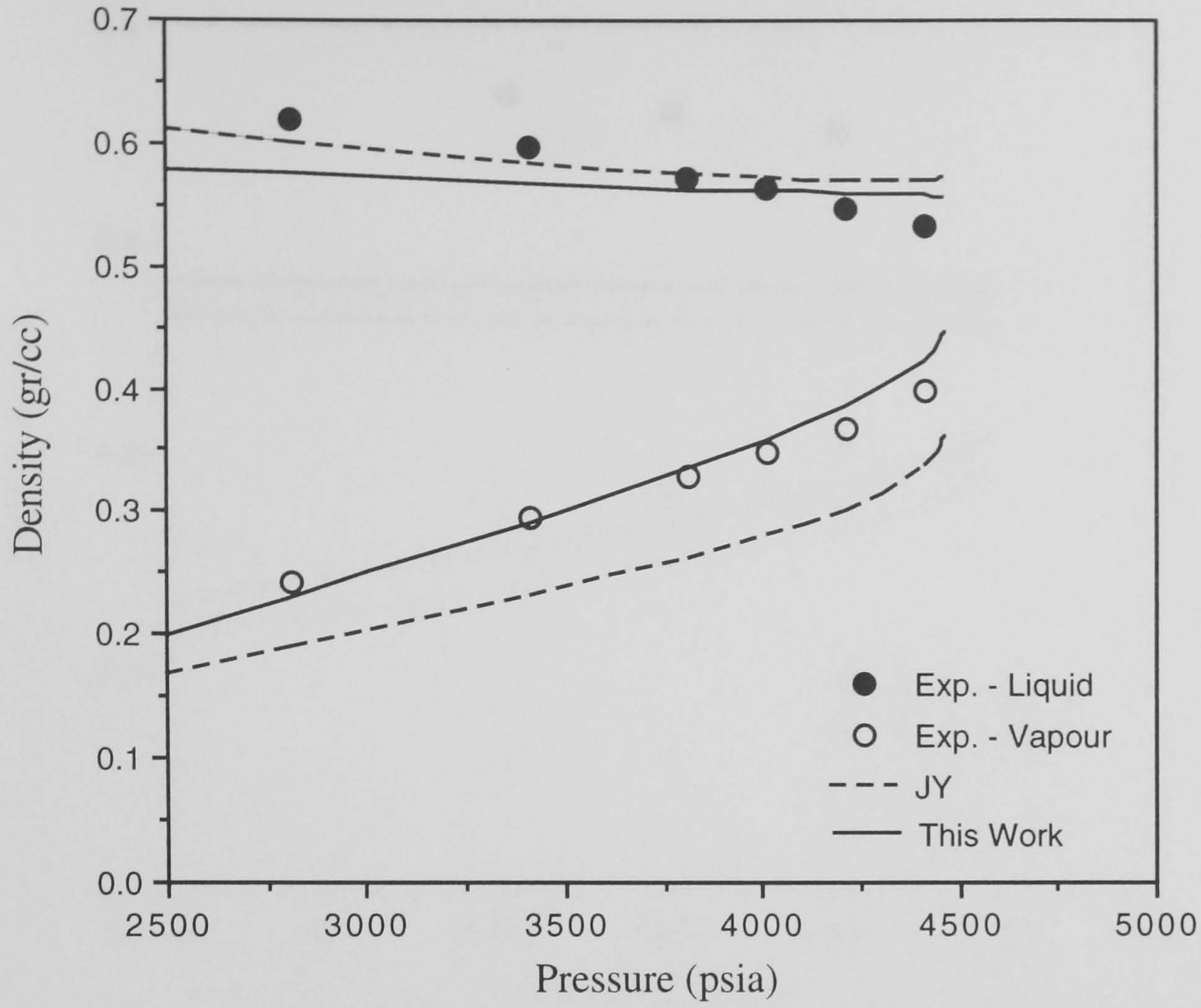

Fig. 2.20 - Phase Densities versus Pressure, Constant Composition Expansion (CCE) Test at 30°C, 5-component Model Gas Condensate (GMX89-1).

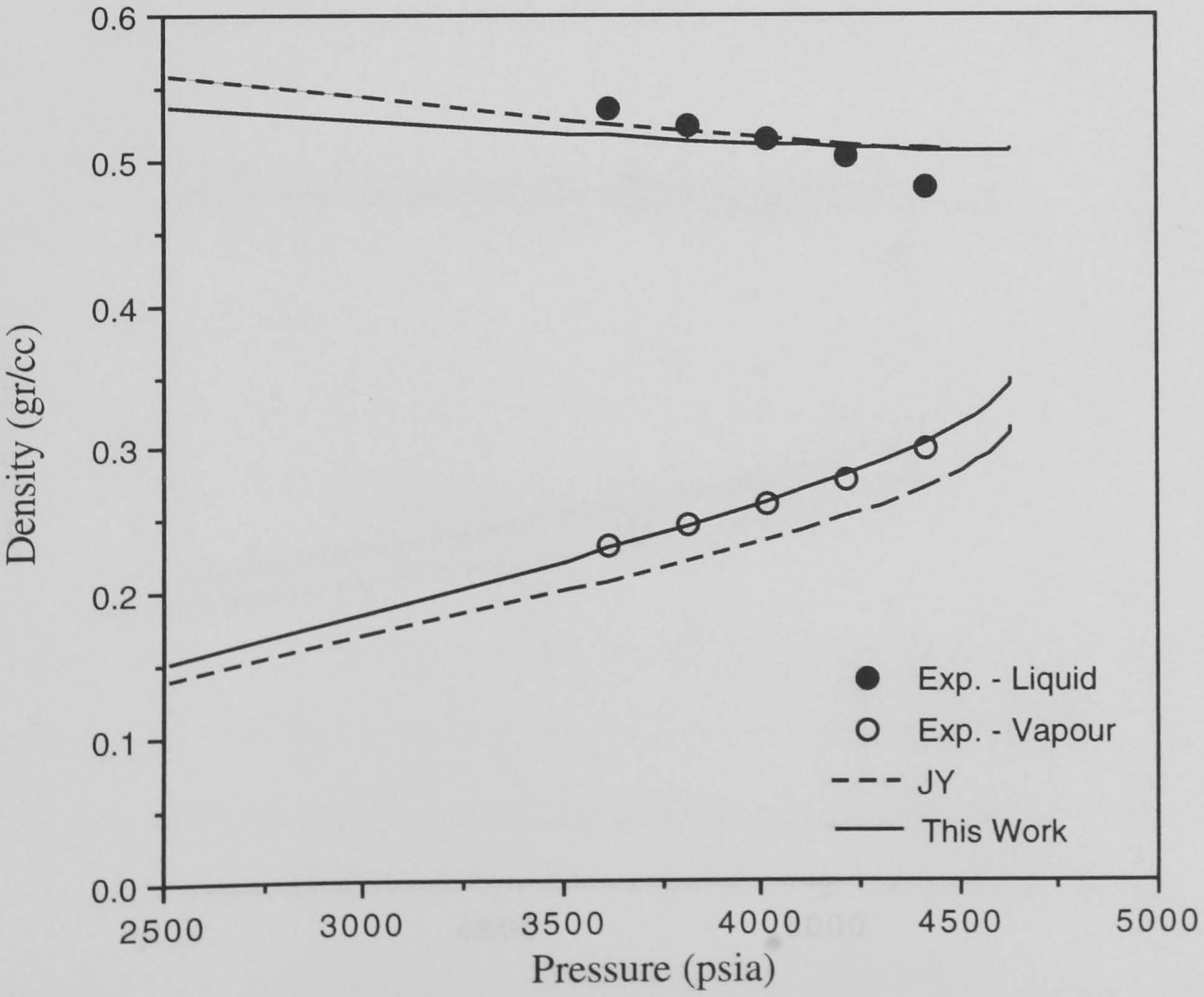

Fig. 2.21 - Phase Densities versus Pressure, Constant Composition Expansion (CCE) Test at 80°C, 5-component Model Gas Condensate (GMX89-1).

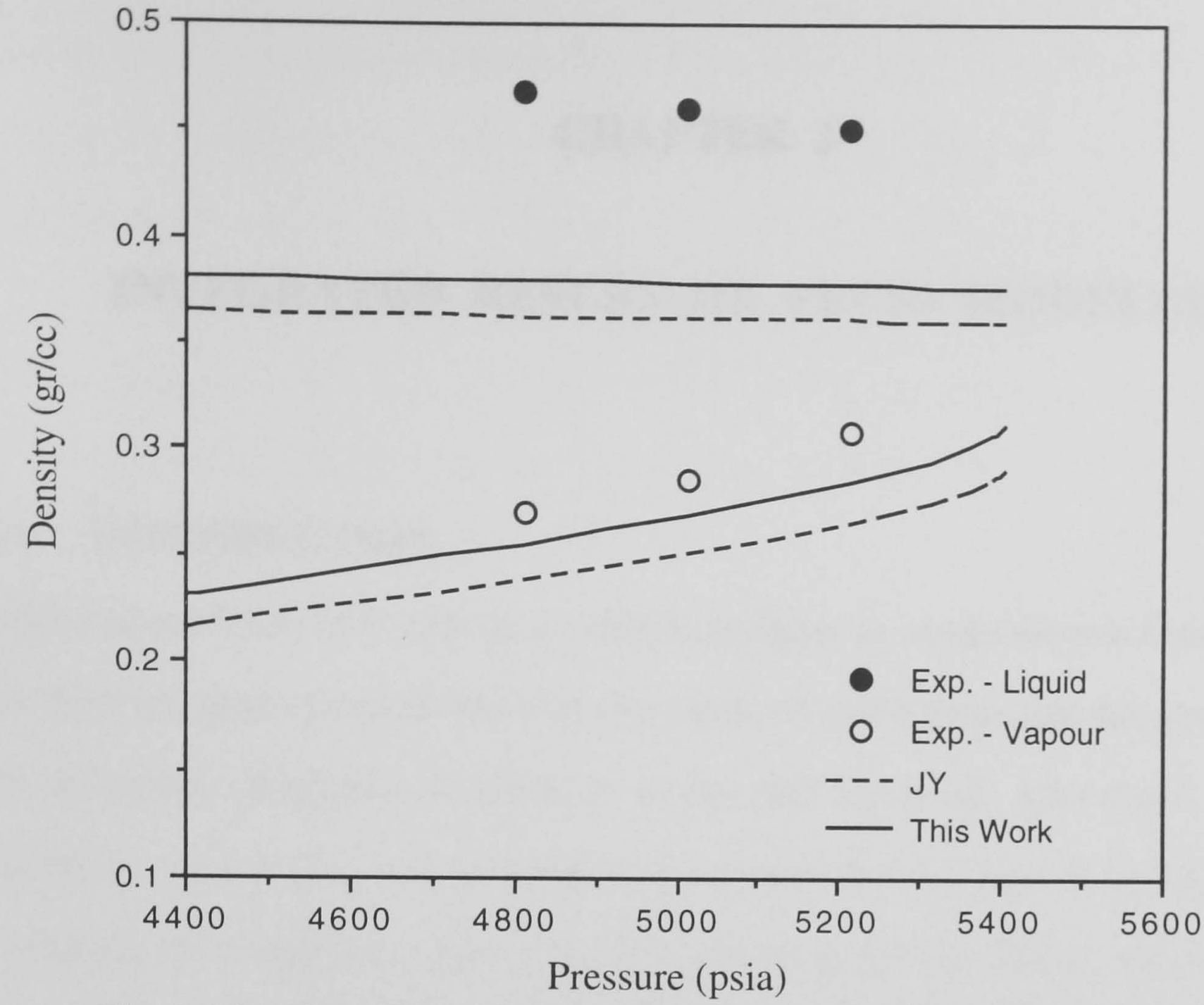

Fig. 2.22 - Phase Densities versus Pressure, Constant Composition Expansion (CCE) Test at 93.3°C, 20-component Model Gas Condensate (GMX90-1).

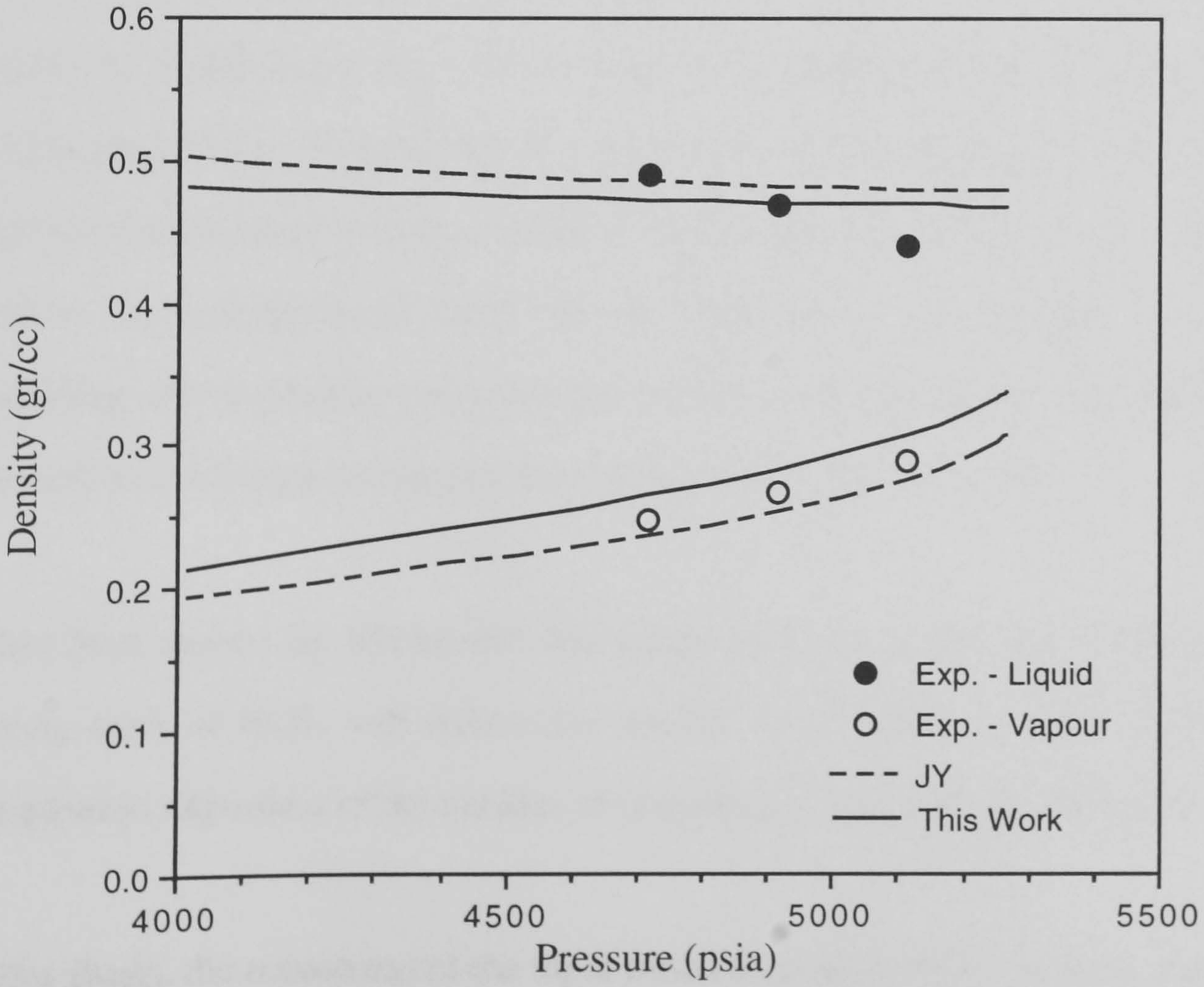

Fig. 2.23 - Phase Densities versus Pressure, Constant Composition Expansion (CCE) Test at 121.1°C, 20-component Model Gas Condensate (GMX90-1).

CHAPTER 3

INTEGRATED RESERVOIR FLUID MODELLING

3.1 INTRODUCTION

Computational time (CPU time) is an important factor in compositional simulation. Real reservoirs are generally modelled with thousands of grid blocks and the phase behaviour and volumetric properties of fluids in every grid block are determined, using flash calculation. At any time step an iterative flash calculation is required for each grid block to calculate the compositions and volumetric properties of equilibrated phases. Hence, it is essential to reduce CPU time of flash calculations as much as possible.

In conventional methods the number of equations that are solved in flash calculation, is directly related to the number of components describing the fluid. Any reduction in the number of components and / or the number of equations could therefore decrease the computational time. The number of components can be reduced by grouping them. This approach has extensively been studied in the literature[1,2]. Grouping of fluid components reduces the computational time, but the approach is not suitable for an integrated modelling, where detailed compositional information on produced reservoir fluids may be required in the design and operation of fluid processes at the surface[3].

It has been shown by Michelsen[4] that using no binary interaction parameters (BIP) in mixing rules of EOS, will reduce the number of equations to three without additional complexity, regardless of the number of components (rapid flash calculation).

In this thesis, the robustness of the rapid flash calculation (RFC) method was investigated by using different types of fluids (black oils and gas condensates) at different temperatures to perform a constant composition expansion (CCE) test. The effect of the

number of components on computational time was also investigated using different methods to perform phase behaviour calculations. The original rapid flash calculation (RFC) method was modified to improve its robustness for gas condensate systems.

BIP are generally used as regression variables in tuning processes. Omitting BIP from the mixing rules, may reduce the flexibility of the EOS in matching the experimental data of fluids in compositional models. Therefore, two practical tuning methods are developed in this study without using any BIP in the mixing rules of EOS. The methods were applied to a number of real reservoir and model fluids over wide ranges of temperature and compositional changes.

3.2 MIXING RULES

The semi-empirical cubic EOS have basically been developed for pure compounds. Their application has been extended to multicomponent mixture by introducing mixing rules to determine the average parameters of EOS. Several mixing rules have been proposed to improve the EOS predictions for mixtures. However, the following classical mixing rules, also called the conventional random van der Waals mixing rules, are the most common and have extensively been used in multicomponent systems:

$$a = \sum_{i=1}^{N}\sum_{j=1}^{N} x_i x_j (a_i a_j)^{0.5}(1-k_{ij}) \tag{3.1}$$

$$b = \sum_{i=1}^{N} x_i b_i \tag{3.2}$$

$$c = \sum_{i=1}^{N} x_i c_i \tag{3.3}$$

x_i and N are the mole fraction of component i and the total number of components in the mixture, respectively. The a_i, b_i, and c_i are the EOS parameters of component i which can be determined from critical properties and the system temperature. The

parameter k_{ij} is an empirically determined correction factor to improve the predictive capability of the EOS. It is called binary interaction parameter (BIP), characterising the interaction between component i and component j in the mixture. The BIP are commonly assumed to be independent of temperature, composition and density for hydrocarbon components[5]. As the interaction parameter is determined by matching the predicted values with experimental data, it should be considered as an adjusting parameter rather than a rigorous physical parameter. Therefore, no general BIP equations or data set are available to be used in phase equilibrium calculation of multicomponent systems. The developed BIP set are specific to a particular EOS and therefore should be used only for that EOS.

A comparative study of ten EOS[6] indicated that the Valderrama[7] modification of Patel and Teja (VPT) EOS with no BIP was more successful than the others with pertinent BIP in modelling the phase behaviour of reservoir fluids. The success of the VPT EOS with no BIP in predicting the phase behaviour, strengthens the view that these parameters mostly cover the deficiencies of EOS rather than accounting for the interaction between molecules of hydrocarbon compounds. Omitting BIP from mixing rules of EOS may reduce the flexibility of the EOS in tuning the phase behaviour of the reservoir fluids. However, it[8] will be shown that EOS can reliably be tuned to the experimental data without using any BIP.

3.3 PHASE EQUILIBRIUM CALCULATIONS

3.3.1 Bubble Point and Dew Point

Bubble point is the condition where the system is all liquid with presence of an infinitesimally small amount of vapour. For the bubble point, the criterion of equilibrium (Eq 2.5) must be satisfied, as well as the following Equations:

$$x_i = z_i \qquad i = 1,2,....,N \qquad (3.4)$$

$$\sum_{i=1}^{N} y_i = \sum_{i=1}^{N} K_i x_i = 1.0 \qquad (3.5)$$

where x_i, y_i and z_i are the mole fraction of component i in the liquid, the vapour and the feed streams, respectively. N is the number of components and K_i is the equilibrium ratio (K-value) of component i in the mixture, which can be determined from fugacity coefficients as follows:

$$K_i = \frac{y_i}{x_i} = \frac{\phi_i^L}{\phi_i^V} \qquad i = 1,2,...,N \qquad (3.6)$$

Superscripts L and V denote the liquid and vapour phases.

Dew point is the condition where the whole system is in the vapour with presence of an infinitesimally small droplet of liquid. For the dew point calculation, the following equations should be satisfied along with the criterion of equilibrium (Eq 2.5):

$$y_i = z_i \qquad i = 1,2,...,N \qquad (3.7)$$

$$\sum_{i=1}^{N} x_i = \sum_{i=1}^{N} \frac{y_i}{K_i} = 1.0 \qquad (3.8)$$

The bubble point and dew point pressure are generally determined at a known temperature in petroleum industry. Bubble point pressure of real reservoir fluids is a monotonic function of temperature. It means that the bubble point pressure increases with increase in the temperature. However, the dew point pressure of gas condensates is not generally a monotonic function of temperature. Gas condensate mixtures also exhibit two dew point pressures at the same temperature (Fig. 3.1). The higher dew point pressure which is called *retrograde dew point*, can be calculated by satisfying Equations 2.5 and 3.7 as well as the following Equation[9]:

$$\sum_{i=1}^{N} x_i = \frac{1}{\sum_{i=1}^{N} \frac{y_i}{K_i}} = 1 \qquad (3.9)$$

The low dew point pressure is generally of little significance for real gas condensate systems, unless for lean mixtures at high temperatures.

3.3.2 Flash Calculation

Flash calculations are mostly applied to determine the vapour-liquid equilibrium conditions at fixed pressure and temperature in reservoir studies. Given the feed composition (z_i), one should determine the liquid (x_i) and the vapour (y_i) compositions as well as the vapour fraction (γ) from phase equilibrium calculation. Since the vapour and liquid phases are in equilibrium the criterion of equilibrium (Eq 2.5) must be satisfied. Applying component material balance for one mole of feed:

$$z_i = \gamma y_i + (1-\gamma)x_i \qquad i = 1,2,...,N \qquad (3.10)$$

Substituting the K-values (Eq 3.6) in Equation 3.10 and solving for x_i and y_i, gives:

$$x_i = \frac{z_i}{1+(K_i-1)\gamma} \qquad i = 1,2,...,N \qquad (3.11)$$

$$y_i = \frac{K_i z_i}{1+(K_i-1)\gamma} \qquad i = 1,2,...,N \qquad (3.12)$$

Equations 3.11 and 3.12 can also be written in terms of liquid fraction.

Combining Equations 3.11 and 3.12 gives:

$$\sum_{i=1}^{N}(y_i - x_i) = \sum_{i=1}^{N} \frac{(K_i - 1)\, z_i}{1+(K_i-1)\gamma} = 0.0 \qquad (3.13)$$

Equation 3.13 which is known as the Rachford-Rice equation, can be solved for γ by iterations. Then, the determined γ is substituted in Equations 3.11 and 3.12 to calculate the composition of two phases.

Flash separation calculation is applied in compositional reservoir simulators to determine the composition of equilibrated phases in every grid block. Hence, performing the flash separation calculation in the minimum possible time, is important in reservoir simulation. The computational time (CPU) of flash calculation drastically increases with increase in the number of equations to be solved in phase equilibrium calculation. In conventional flash formulation, 2N+1 equations (Eqs 2.5, 3.10 and 3.13) should be solved to determine 2N+1 unknowns (γ, x_i and y_i), where N is the number of components in the mixture. It is shown (Section 3.4) that the number of equations in phase equilibrium calculation can be reduced to three / four with no additional complexity and regardless of the number of components describing the mixture. Therefore, the flash calculation can be performed much faster than the conventional methods.

3.4 RAPID FLASH CALCULATION (RFC)

Michelsen[4] showed that using no BIP in mixing rules of cubic EOS, the number of equations will reduce to three regardless of number of components describing the fluids. Hence, the flash calculation can be carried out much faster than when the conventional methods are used. If BIP are set to zero in mixing rules, Equation 3.1 will reduce to:

$$a = \sum_{i=1}^{N}\sum_{j=1}^{N} x_i x_j (a_i a_j)^{0.5} = (a')^2 \qquad (3.14)$$

where $a_i = (a_i')^2$

Multiplication of the material balance, Equation 3.10, by a_i' and summation, result in:

$$\sum_{i=1}^{N} z_i a_i' = \gamma \sum_{i=1}^{N} y_i a_i' + (1-\gamma) \sum_{i=1}^{N} x_i a_i' \qquad (3.15)$$

$$a_F' = \gamma a_V' + (1-\gamma) a_L' \qquad (3.16)$$

and in the same way:

$$b_F = \gamma b_V + (1-\gamma) b_L \qquad (3.17)$$

These relations imply that in equilibrated phases, given the parameters of one phase, one can determine the parameters of the other phase. In the rapid flash calculation method (RFC) as suggested by Michelsen[4], the vapour phase parameters (a_V' and b_V) are estimated, then, they are used to determine the liquid phase parameters from the following equations;

$$a_L' = \frac{a_F' - \gamma a_V'}{1-\gamma} \quad , \quad b_L = \frac{b_F - \gamma b_V}{1-\gamma} \qquad (3.18)$$

The liquid and vapour compositions can be calculated by introducing the equilibrium ratios (K_i) in Equation 3.10;

$$x_i = \frac{z_i}{1+\gamma (K_i - 1)} \quad , \quad y_i = \frac{z_i K_i}{1+\gamma (K_i - 1)} \qquad (3.19)$$

The computational procedure can then be summarised as follows;

(1) At the given temperature and pressure, determine the a_i' and b_i .

(2) Calculate the a_F' and b_F , using the determined parameters from step (1).

(3) Estimate a_V' , b_V and γ.

(4) Evaluate a'_L and b_L from Equation 3.18.

(5) Determine the equilibrium ratios, using the calculated fugacity coefficients from phase equilibrium calculation (Appendix B).

(6) Calculate x_i and y_i from Equation 3.19.

(7) Evaluate the check functions;

$$e_1 = \sum_{i=1}^{N}(y_i - x_i) \tag{3.20}$$

$$e_2 = \sum_{i=1}^{N} y_i\, a'_i - a'_v \tag{3.21}$$

$$e_3 = \sum_{i=1}^{N} y_i\, b_i - b_v \tag{3.22}$$

If the above equations are all equal zero (that is, less than a pre-defined tolerance), the phase distribution at equilibrium has been determined. If not, iterate from step 3 with an improved estimate of a'_v, b_v and γ. The Newton-Raphson method was used to solve the above equations in this study.

In this thesis, the original rapid flash calculation (RFC) method as described above was applied to perform phase equilibrium calculations using different types of fluids, including volatile oil and gas condensates. The results showed that the original RFC method may fail to converge for gas condensate systems. Performing stability analysis[10], to get better initial guess before each stage of CCE test, did not help the convergence.

An analysis of the results showed that vapour phase parameters estimation was good for determining the phase behaviour of oils whereas, phase equilibrium calculation would diverge if it was applied to gas condensates. The original RFC method was modified in

this thesis to improve its convergence for gas condensate systems. In the modified RFC method the vapour phase parameters were calculated using the estimated liquid phase parameters[3]. Using the liquid parameters estimation, the equations in the original RFC method are applicable with a minor change, where Equation 3.18 should be replaced by Equation 3.23;

$$a'_v = \frac{a'_F - (1-\gamma)\, a'_L}{\gamma} \quad , \quad b_v = \frac{b_F - (1-\gamma)\, b_L}{\gamma} \tag{3.23}$$

Also the check functions, Equations 3.21 and 3.22, should be replaced by Equations 3.24 and 3.25, respectively;

$$e_2 = \sum_{i=1}^{N} x_i\, a'_i - a'_L \tag{3.24}$$

$$e_3 = \sum_{i=1}^{N} x_i\, b_i - b_L \tag{3.25}$$

In conventional flash formulation 2N+1 equations (Eqs 2.5, 3.10 and 3.13) should be solved to determine 2N+1 unknowns (liquid and vapour phase composition and vapour fraction of the system). N is the number of components in the mixture. Introducing equilibrium ratios (K-factor, $K_i = y_i / x_i$), 2N+1 equations can be reduced to N+1 equations. However, in the rapid flash calculation the number equations to be solved is reduce to three as given in Eqs 3.20, 3.21 and 3.22. These equations are generally solved by using successive substitution (SS) or Newtonian type methods.

To investigate the robustness of the RFC method and also to compare the computational time of different methods to carry out a certain PVT test, a number of oil and gas condensate mixtures were used. Phase equilibrium calculation was made using the modified PR EOS without BIP (mPR)[3].

It should be noted that flash calculations are performed using the original RFC method. that is, using the estimated vapour phase parameters to calculate the liquid phase parameters. If the phase equilibrium calculation fails to converge, then the modified RFC method will be used. In the modified RFC method the vapour phase parameters are determined using the estimated liquid phase parameters.

Three methods, SS and a quasi-Newton (QN) to solve conventional flash formulation, and the RFC method were used to carry out a 12 stage constant composition expansion (CCE) test, using different types of fluids with different number of components. Whatever method applied to perform the phase equilibrium calculation, the SS method was used to determine the saturation pressure at the first stage of the CCE test. The calculated K-factors of each stage were considered as the initial guess in the subsequent stage of CCE test. All the three methods converged successfully, using oils (black oil and volatile oil) to perform CCE test. It should be mentioned that in approaching the critical region, the dependency of the QN and RFC methods on the initial guess become much severe. It means that if the system is near the critical point, the initial guess should be close enough to the final solution, whereas for systems far from the critical point the domain of initial guess is much wider than the previous case. By comparison it was found that the convergence of the RFC method was as good as the QN method when it was applied to determine the phase equilibrium and volumetric properties of oils.

The convergence results of carrying out the 12 stage CCE test using different methods to perform the phase equilibrium calculation are given in Table 3.1. It should be noted that the vapour phase parameters estimation was applied with oils where the liquid phase parameters estimation was used with gas condensates, when the RFC method was applied in phase distribution calculation. Table 3.1 shows that the RFC method is as robust as the QN method for oil systems and it is somewhat superior in gas condensate systems. Also it can be seen that the modified RFC method converged to the solution if the initial K-factors were good enough, where in some cases due to poor convergence in saturation pressure calculation, the calculated K-factors in the first stage were not satisfactory to be

used in the subsequent calculations. Hence, the RFC method has not converged in those cases.

The computational time for performing the 12 stage CCE test using black oil and volatile oil systems are compared in Fig. 3.2 (CPU time based on Sun workstation Sparc 2). It can be seen that the computational time of the quasi-Newton (QN) method is two orders of magnitude (at least) greater than the other two methods. It also shows that approaching the critical region, the computational time will increase, which is more severe with the QN method than the other methods. The CPU time of the successive substitution (SS) and rapid flash calculation (RFC) methods in carrying out the 12 stage CCE test are compared in Fig. 3.3. As it is shown, the RFC method is clearly faster than the SS method in phase equilibrium calculations of black oil and volatile oil systems. It should be noted that the improvement in computational time depends on the mathematical method used to solve the governing equations.

The CPU time of a single flash calculation using a 17-component volatile oil (LRX89-3) and a 20-component model gas condensate (GMX90-1) is illustrated in Figs. 3.4 and 3.5, respectively. They show that approaching the single liquid phase region, the computational time of the QN method will sharply increase, whereas it does not have much effect on the computational time of the other methods, particularly the RFC method.

To compare the robustness of the three methods (i.e., SS, QN and RFC methods) in phase behaviour calculation, a volatile oil (57.53% C_1) was used to perform a multiple forward contact test (MFC) at 100°C. Pure methane was injected into the system as an injection gas at 6092 psia (420 bar), where after 12 stages, miscibility was achieved. The calculated K-values from each stage was used as the initial guess for the next stage. The original approach of estimating the vapour phase parameters was used in the RFC method to perform the MFC test.

The calculated K-values at each stage are shown in Fig. 3.6 for the mixture component identified by their molecular weights. The QN method failed to converge at the third stage, which is still far from the critical point. The RFC method did not meet the convergence criteria at the stage six. The SS method converged to the near miscible solution at stage 12, as indicated by the equilibrium ratio of almost equal one for all the components.

The density of equilibrated phases and the interfacial tension (IFT) between two phases are illustrated in Figs. 3.7 and 3.8, respectively. The above Figures indicate that the RFC method is more robust than QN in approaching near critical conditions. The SS method is however superior to both, as it converged even at conditions where the densities of both phases were almost equal with near zero IFT.

The CPU time of flash calculation at each stage, using different methods to perform phase equilibrium calculation, is shown in Fig. 3.9. It is evident that the RFC method is much faster than the other two methods, particularly QN.

3.5 TUNING OF EOS

The capability of compositional models highly depends on the efficiency of the EOS which are used to perform phase equilibrium calculations. Also, the accuracy of EOS predictions strongly depends on reliable input data. Although, EOS and the quality of input data have improved over years, tuning of EOS for a specific fluid at specific conditions is still very attractive.

Real reservoir fluids consist of thousands of components that are normally characterised by a limited number of component groups (pseudo components). The properties of these pseudo components, such as critical pressure and temperature and acentric factor, are determined from generalised correlations using limited measured data on these pseudo components. The deficiencies of generalised correlations in accurate prediction of critical

properties for pseudo components along with the major limitations and errors in measurements for real reservoir fluids often lead to poor predictions. Hence tuning of EOS, by changing the adjustable parameters to match available experimental data have become a common procedure for compositional studies.

The tuning of EOS is a non-linear regression problem. Several non-linear optimisation methods have been used by investigators[11-14], the modified Levenberg-Marquardt[15] (LM) method is known as a standard non-linear regression method. In this study the modified LM method has been used and the derivatives of the objective function with respect to regression variables are calculated by numerical methods.

The main aim of this study is to develop a tuning method to predict the phase behaviour and volumetric properties of real reservoir fluids within wide ranges of temperature and compositional changes, without using BIP in mixing rules of EOS. Using no BIP, the reservoir fluids can be described by a large number of components without increasing the computational time of the phase equilibrium calculations (Section 3.4).

In this study, two tuning methods have been developed and applied to a number of reservoir fluids. The tested fluids are selected to cover the different variety of real reservoir fluids, from black oils to lean gas condensates. Majority of conventional PVT test data for oil and gas condensate mixtures such as constant composition expansion (CCE), constant volume depletion (CVD), separator test, differential liberation (DL), gas injection and gas cycling test were matched, using EOS parameter(s) as regression variable(s). The results showed that the developed tuning method could provide reliable predictions of the phase behaviour of fluids with temperature and compositional changes.

3.5.1 Non-linear Regression Model

Tuning of EOS is a non-linear optimisation problem. To match the experimental data with an EOS, an objective function which is defined as a weighted sum of squared deviations of experimental and calculated values, should be minimised.

$$F(\bar{x}) = \sum_{i=1}^{M}\left[w_i\left(\frac{P_i^{cal}}{P_i^{exp}} - 1.0\right)\right]^2 \qquad (3.26)$$

where M is the number of experimental data to be matched, P_i^{cal} and P_i^{exp} are calculated and experimental values of a property P, w_i is weighing factor and $F(\bar{x})$ is the objective function with $\bar{x} = (x_1, x_2, ..., x_N)^T$ which is the vector of the regression parameters. N is the number of regression parameters. The values of regression parameters $\bar{x}$ are determined by optimising the objective function.

Weight factors are used to indicate the importance and reliability of measured properties. Higher weight factors should be always applied to more important properties if accurately measured. In phase equilibrium calculations, the saturation pressure is the most important property, where the compositions of equilibrated phases are the least reliable ones. Hence, the saturation pressure and the compositions should be weighed by the highest and the lowest values, respectively. The weight factors which have been used in this study are 40, 20, 5, and 1 for saturation pressure, density, volume and composition, respectively.

Limits of regression parameters are important in minimising the objective function. Wide limits of regression parameters provide more flexibility for matching the experimental data. However, they could lead to non-physical values for the tuned parameters. The range of tuning parameters can be determined from the accuracy of measured input data, generalised correlations used to predict fluid properties and the accuracy of fluid sampling. The majority of physical property correlations use two of the three following properties - the molecular weight, specific gravity and boiling point - to calculate other properties. Any error in measurement of these properties will affect the calculated critical properties from generalised correlations. The density can be measured typically within an error band of less than ± 0.0001 gr/cm^3 and the molecular weight of SCN (single carbon number) groups is determined by the freezing point depression method within ± 2.

Hence, the maximum deviation in measured molecular weight could be 2%, but Pedersen[12] considered 10% for adjusting molecular weight in her regression method. It has also been suggested[16] that molecular weight could be changed within 15%. Similarly, the range of tuning for measured specific gravities which were reported to within ±1% (for plus fraction)[17], could be up to 5% for single carbon numbers (SCN) and as high as 10% for plus fraction. The reason for the above wide ranges, which appear to be excessive in comparison with the error band, is the unreliability of generalised correlations used to determine critical properties for EOS calculations.

The consistency of properties calculated from generalised correlations, using the tuned parameters, should also be checked. The critical temperature, acentric factor and boiling point temperature increase with molecular weight, whereas the critical pressure decreases with molecular weight. Xu et al.[16] have suggested a dynamic constraint method (dynamic lower and upper limits) for determining the lower and upper limits of regression variables. The boundary values of each component are calculated, using the updated values of regression variables of the two adjacent components. Also the regression parameters should meet one of the following constraints for all components:

$$X_{i-1} < X_i < X_{i+1} \qquad \text{or} \qquad X_{i-1} > X_i > X_{i+1} \tag{3.27}$$

where, X is component property and i is component index. There are several samples for which the reported specific gravities do not obey the above criteria (3.27).

Hence, a new method has been developed in this thesis to keep the consistency in the calculated properties with anomalous variation of reported specific gravities (the specific gravity of single carbon i+1 could be lower than that of i)[18]. In the developed method, the lower limit of the first single carbon number (say C_6 in this example) and the upper limit of the last component (plus fraction, say C_{20+}) are set to be 0.95 and 1.1, respectively. It means that the specific gravity of C_6 could decrease by 5% while the specific gravity of the last component (plus fraction) could increase by 10%. The lower

and upper limits of other single carbon numbers (C_7-C_{19}) are calculated from the following correlations.

$$L\min_i = \frac{0.3(SG_i - SG_{i-1}) + SG_{i-1}}{SG_i} \tag{3.28}$$

$$L\max_i = \frac{0.7(SG_{i+1} - SG_i) + SG_i}{SG_i} \tag{3.29}$$

$$i = C_7, C_8, \ldots, C_{n-1}$$

where SG is the specific gravity and Lmin and Lmax are the lower and upper limits of specific gravity variation, respectively.

It should be noted that specific gravities that are used in the above correlations are the reported experimental values. In other words, they will not change, by changing the specific gravities of components as regression variables.

3.5.2 Minimum Number of Regression Variables

To optimise an objective function, different non-linear regression methods can be used to determine the values of regression parameters in the optimum of the objective function. In tuning of EOS, the least number of regression parameters should be selected to match the experimental data. Using more regression variables, matching the experimental data would be more convenient, however, the danger of converging to a local minimum instead of a global value becomes more probable.

Mathematically, introducing more regression variables in optimisation problems, more local minimum would be generated in the solution domain which could be quite problematic in running the programme through all of them to the global minimum.

In this study, the minimum number of regression variables have been used in tuning calculations to reduce the risk of converging to a local minimum.

3.5.3 Selection of Parameters for Tuning

Several parameters have been nominated as regression variables. The critical properties of pseudo components as well as binary interaction parameters (BIP) have been used in tuning of EOS by different investigators.

A sensitivity analysis were performed on EOS parameters[16]. The effect of specific gravity (SG), fluid composition, molecular weight (MW, hence composition as well), BIP, attractive term (a), repulsive term (b) and the third parameter of pseudo components were investigated on saturation pressure, gas and liquid densities, gas and liquid volumes and gas and liquid composition at equilibrium. As the sensitivity of predicted results to various input information could vary for different types of fluids, a wide range of petroleum reservoir fluids including black and volatile oils, near critical fluid and gas condensate mixtures were analysed. All the results indicate that the specific gravity, followed by the repulsive term 'b' and the attractive term 'a' in EOS are the most effective variables in EOS phase equilibrium calculation[16].

BIP are the most widely used regression variables in the EOS tuning. While there are sets of BIP for various EOS, it is treated as a fitting variable in mixing rules of EOS to match the experimental data. As the BIP value has little to do with the extent of physical interaction between the molecules and is used as a matching factor, it will obscure the deficiencies of EOS. By using no BIP in mixing rule of EOS, not only the computational time can highly be reduced but also the deficiencies of EOS will be revealed. The parameters of EOS can then be modified to improve its predictions (Chapter 2).

The EOS parameters are highly dependent on the fluid compositions. It seems that the concentration of the plus fraction is the most doubtful information among the reported compositions. Hence, for non-complex cases such as matching the experimental data at one temperature, the composition and the specific gravity of plus fraction can be used as regression variables. Due to the low concentration of the plus fraction in the vapour

phase, using the plus fraction properties as the regression variable, the vapour phase properties cannot significantly be affected.

It was concluded earlier that the attractive term 'a' in EOS is one of the most effective variables in EOS prediction. Due to the temperature dependent nature of 'a' parameter, it can be used as a powerful regression variable to match the experimental data at different temperatures from reservoir conditions to surface conditions. Hence, for complex fluids and processes such as matching the experimental data of rich gas condensates and/or near critical fluids within wide ranges of temperature and compositional changes, the temperature dependency of the attractive term (α) of sub and supercritical components in the liquid phase can be selected as regression variables. Adjusting the α parameter of components in the liquid phase is justifiable where the attraction between molecules in the liquid phase are different from that of the vapour phase. Obviously, the composition and physical properties of plus fraction can also be used as regression variables in addition to the mentioned parameters.

3.5.4 Tuning Approach

The three parameter modification of the Peng-Robinson[19] (PR3) EOS is used in this study for bench marking as it is the most widely used equation in the oil industry. Also the Valderrama[7] modification of Patel and Teja (VPT) and the new modification of PR (mPR, Chapter 2) EOS are employed for comparison with the PR3 EOS in some cases. All interaction parameters are set to be zero, which will reduce the number of equations to be solved and hence the CPU time.

The critical properties of pseudo components are calculated by the perturbation expansion correlations[20]. The boiling point temperature of the plus fraction (which are used in the perturbation expansion method), is determined from the Riazi-Daubert[21] correlation using the reported values of specific gravity and molecular weight. The Lee-Kesler[22] correlation is used to determine the acentric factor of the pseudo components of real reservoir fluids.

Two tuning approaches have been developed depending on the complexity of the phase behaviour modelling. To tune the EOS to experimental results at reservoir and surface temperatures, the specific gravity and composition of plus fraction as well as the shift parameters of the SCN groups and the plus fraction are used as regression variables. This is called in this work as "conventional tuning".

In complex cases where the experimental data within wide ranges of temperature and compositional changes should be matched, the temperature dependency of the attractive term (α) of EOS is adjusted. This is called in this work as "integrated tuning" as it can be used to reasonably predict the phase equilibrium of fluids within reservoir, flow lines and process facilities. The regression variables in the conventional method (specific gravity and composition of plus fraction along with shift parameters of pseudo components) can also be used in addition to the α parameter. In model fluids, the properties of components are known, therefore, the conventional tuning approach cannot be applied to these type of fluids.

The above tuning methods were evaluated for a wide range of model fluids as well as real reservoir fluids. As the application of compositional models is mainly for volatile systems, the selected fluids were limited to volatile oil and gas condensate samples.

3.5.5 Conventional Tuning

The conventional tuning method was applied to two volatile fluids, a volatile oil (LRX89-1) and a gas condensate (GCX89-1), and were successfully matched with the experimental data. All reported experimental data of the volatile oil (LRX89-1) included constant composition expansion (CCE), differential liberation (DL), multiple forward contact (MFC) and multiple backward contact (MBC) test at 100°C and separator test results were matched simultaneously, using the PR3 EOS with no BIP. Also the CCE and constant volume depletion (CVD) results of the gas condensate (GCX89-1) at 121°C were simultaneously matched, using the PR3 and the VPT EOS with no BIP. All the PVT tests which have been used in this study are described in Appendix C.

Volatile Oil (LRX89-1)

The volatile oil (LRX89-1) contains 57.53% methane with a saturation pressure of 5065 psia (34.9 MPa) at 100°C. Several laboratory tests were performed on this oil. The constant composition expansion (CCE) and the differential liberation (DL) tests were carried out at 100°C. The volatile oil was also used to perform a four stage multiple forward contact (MFC) and a three stage multiple backward contact (MBC) tests with methane injection at 5114 psia (35.27 MPa) and 100°C. A three stage separator test was also performed at 20.5°C[23].

The experimental results were used as matching values in tuning of EOS. The relative volume (V/V_{sat}), liquid saturations, saturation pressure and saturation density were selected from CCE test, whereas the solution gas-oil ratio, relative oil volume, total relative volume and gas Z-factor were used from differential liberation (DL) test. Liquid volumes and densities along with gas volumes and densities, measured in the multiple contact tests, and formation volume factor, stock tank specific gravity and liberated gas-oil ratio were selected from separator test for the tuning of EOS.

The compositions of equilibrated phases at multiple contacts were not used as matching values because of their unreliability. The laboratory has also noted problems for the second and third contacts in the multiple backward contact (MBC) test[24]. Probably the added methane was more than what was recorded.

To match all of the above mentioned experimental data the concentration of plus fraction was adjusted from 3.81 to 4.53 mole%. Also, the specific gravity of plus fraction along with the shift parameters of single carbon groups (SCN) and plus fraction were adjusted (see Section 2.6.2 for shift parameter definition).

Three companies (A, B and C) have also performed the tuning exercise on the same fluid in a comparative study[24]. All of them used the PR EOS with BIP used as the regression

variable. In order to be consistent with the companies, only the 3-parameter Peng-Robinson (PR3) EOS was tuned to the experimental data in this work.

In Fig. 3.10, the fit to liquid volume / total volume in the CCE test by this work is compared with those of the companies results. At low pressures this work gives better match to the experimental data, however at high pressures it is as good as other models.

The liberated gas oil ratio in the differential liberation (DL) test is presented in Fig. 3.11. At high pressures all models have similar predictions compared to experimental data, where again, at low pressures this work gives better results. Among the companies' studies, model A gives better match than the other two models. The improvement has been attributed to the treatment of density[24]. The calculated relative volume in the DL test, with as good as results of model A which is superior to other models, is illustrated in Fig. 3.12. The predicted compressibility factor of effluent gas by the tuned models in the DL test, was also investigated. The results are given in Fig. 3.13. All models had similar results compared to the experimental Z-factor. At low pressures all models predicted the Z-factor better than the high pressures conditions. The deviation (compressibility) factor of the liberated gas could not be matched very well in this work. This might be due to the very low concentration of the plus fraction in the effluent gas.

The mass and the densities of vapour and liquid phases in the multiple forward contact (MFC) test have also been fitted by different models. The mass of liquid were matched very well by all models, however, model B and this work fitted the mass of gas better than the other models. The tuning results of the EOS models in matching the phase densities are given in Fig. 3.14. The companies' models have under-tuned both the gas and liquid densities. This work has given the best fit to the gas density, where the liquid densities have been slightly over-tuned. However, by comparison the liquid density has been predicted as good as B and C models.

Fig. 3.15 presents the models' fit to the multiple backward contact (MBC) experimental data. The mass of liquid has been fitted very well at the first contact, by the companies, but slightly deteriorated at the next contacts. This work has matched the mass of liquid better than others, particularly in the second and the third contacts. Also, in fitting the mass of gas, this work has been superior to the others, particularly at the first and the second contacts. Gas densities of the MBC test were also matched similarly by companies, where the results of this work was superior, particularly at the first and the last contacts.

The average absolute percentage deviation (AAD%) of separator test results is presented in Table 3.2. It was noted that both models B and C ignored this data in the tuning[24]. The overall average absolute percentage deviations are 8.6, 13.1 and 9.9 for A, B and C respectively, where it is only 4.8 for this work.

All measured PVT data of the volatile oil (LRX89-1) are successfully fitted, using the conventional tuning method without any BIP as demonstrated above. In the next section, the capability of the developed tuning approach is examined against the experimental data of a gas condensate system.

Gas Condensate (GCX89-1)

The experimental data of gas condensate (GCX89-1) were matched, using the PR3 and the VPT EOS with no BIP's. The gas condensate (GCX89-1) exhibited a dew point pressure of 6836 psia at reservoir temperature of 121°C. The CCE and constant volume depletion (CVD) tests were performed at 121°C. Relative volume and liquid dropout from the CCE and compressibility factor of produced gas, volume of retrograde liquid and cumulative gas production from the CVD tests were used as matching experimental data.

The plus faction was split into four pseudo components, using the Whitson[25] method. The specific gravity of the last pseudo component along with shift parameters of single carbon groups and pseudo components (PR EOS only) were used as tuning parameters.

The tuned and predicted (no tuning) relative volume in CCE test, using the PR3 and the VPT EOS, are presented in Fig. 3.16. The CVD experimental data were also matched and the results are illustrated in Figs. 3.17 and 3.18. Fig. 3.17 shows that due to the error in predicted dew point pressure by the untuned PR3, the model has predicted less gas at high pressures in comparison to the other models.

The tuning of the PR EOS has resulted in a good match to the experimental data. Also the experimental data has been predicted very well by the VPT EOS, with no adjustment. The PR3 EOS with no tuning, has however failed to predict the experimental data.

The results of this study (volatile oil LRX89-1 and gas condensate GCX89-1) demonstrate that the EOS can successfully be fitted to the experimental data of volatile systems without using any BIP in phase equilibrium calculations.

3.5.6 Integrated Tuning

In the integrated tuning approach the temperature dependency of the attractive term (α) of EOS in the liquid phase is adjusted to match the PVT data of fluids over wide ranges of temperature and compositional changes. The attractive term of the EOS consists of the 'a' parameter ($a = \alpha a_c$) of EOS divided by the squared value of molar volume ($\alpha a_c / V^2$). The molar volume of the vapour phase is generally larger than that of the liquid phase. If the α parameter of components in the vapour phase is adjusted, its effect on the phase behaviour of the system will be less pronounced, as the α value is divided by a large value (vapour phase molar volume). However, the phase behaviour of the system can largely be affected by adjusting the α parameter of components in the liquid phase. Adjusting the α parameter of the components in the liquid phase is physically justified, as the effect of temperature on attraction between molecules in the liquid phase is expected to be different from that of the vapour phase. Approaching the critical point, the attraction between molecules in the liquid phase becomes similar to that of the vapour phase, therefore, the adjusted α parameter should approach that of the vapour at the critical point.

As it was seen in developing the new α function (see Section 2.6.1), the correlated α function for the supercritical components did not match all experimental α values very well. The developed α function for subcritical components, however, reasonably fitted the experimental α values. This suggests that the α parameter of the sub and supercritical components should be adjusted independently in the tuning process.

The developed integrated tuning method in this study is comparable to other leading tuning approaches in the literature. Coats and Smart[14] suggested that using the Ω_a and Ω_b parameters of methane and plus fraction in EOS (see Section 2.5) as regression variables. Adjusting the Ω_a parameter of methane and plus fraction is equivalent to changing the α parameter of those components. In the integrated tuning approach, the α parameter of all supercritical and subcritical components, instead of just the lightest and heaviest components, are used as regression variable. It should be mentioned that the correction to the α parameter of sub and supercritical components in the liquid phase are considered as a function of temperature (reduced temperature) in this study.

The capability of the integrated tuning method was investigated for well-defined systems, that is model fluids. The properties of components in model fluids are fully defined, therefore, the α parameter of the sub and supercritical components in the liquid phase can only be used as a regression variable. The CCE test results of two model gas condensate samples were matched over a wide range of temperature change. The modified Peng-Robinson (mPR) and the Valderrama modification of Patel and Teja (VPT) EOS with no BIP were used to perform phase equilibrium calculations.

The integrated tuning approach was also applied to two real gas condensate samples. In the case of real reservoir fluids the properties of plus fraction can also be adjusted in addition to the α parameter. All available experimental data including, constant composition expansion (CCE) test at different temperatures, constant volume depletion (CVD), methane injection, separator test, condensate accumulation near the well bore,

methane cycling and CCE test on depleted vapour tests were simultaneously matched, using the VPT and the mPR EOS with no BIP. The PVT tests which were used in this work are described in Appendix C. Some selected examples will be given in this section.

5-component Model Gas Condensate (GMX89-1)

Two batches of this model gas condensate (GMX89-1) were prepared and tested at different temperatures. This fluid was used to carry out several CCE tests over a wide range of temperature, 110°C, 80°C, 60°C, 40°C, 30°C and 5°C. This temperature range covers medium-rich gas condensate behaviour with maximum liquid dropout of 16% at 110°C to very rich gas condensate with a maximum liquid dropout of 44% at 5°C which is very close to the critical point.

The new modification of PR (mPR) and the VPT EOS with no BIP were used to perform the phase equilibrium calculations. The saturation pressure and liquid dropout in the CCE tests at different temperatures were matched. The results of tuned and untuned EOS at 110, 40 and 5°C are illustrated in Figs. 3.19 through 3.21. The experimental data within the wide range of temperature are reasonably matched by both EOS, except at 5°C where at this temperature the fluid was very close to the critical point. Also at 5°C phase equilibrium calculation did not meet the required tolerance of mathematical calculation. The results show that phase behaviour of model fluids can reasonably be determined over a wide range of temperature change by adjusting the α parameters of components in the liquid phase.

The ratios of the tuned α parameter of sub and supercritical components in the liquid phase to the original α parameter (untuned) are plotted against reduced temperature for the mPR and the VPT EOS in Figs. 3.22 and 3.23, respectively. They show that approaching the critical point the mentioned ratios converge to unity. It means, the attraction between molecules in the liquid phase going to be same as the attraction between molecules of the vapour phase, as expected. Fig. 3.22 shows that in some cases it is possible to keep the correction to the α parameter of subcritical components constant,

while changing the α parameter of the supercritical components to match the experimental data. In Fig. 3.23, the ratios of the tuned α parameter of sub and supercritical components in the liquid phase to the original α parameter for the VPT EOS deviated from unity at 5°C (T_r=1.16). At this temperature due to the fluid being close to the critical point, phase equilibrium calculation did not meet the required tolerance of mathematical calculation.

This demonstrates that phase behaviour models can reasonably be tuned to experimental data of model fluids over a wide range of temperatures without using any BIP. The developed tuning approach was successfully applied to the mPR and the VPT EOS in this study, however, the developed method is general and it can be applied to any other EOS. The reliability of the integrated tuning approach was also investigated by matching the experimental data of a 20-component model gas condensate (GMX90-1). The results are discussed in following section.

20-component Model Gas Condensate (GMX90-1)

A 20-component model gas condensate (GMX90-1) was prepared and tested at different temperatures. Four sets of CCE test experimental data have been reported at 121.1°C, 93.3°C, 65.5°C and 37.7°C by the laboratory. The maximum liquid dropout at 121.1°C was measured at 22% which raised to 40% at 37.7°C. Experimental results showed that reducing the temperature, the fluid would change from a medium-rich gas condensate to a very rich gas condensate at the near critical point. The mPR and the VPT EOS with no BIP were applied to match the liquid dropout as well as saturation pressure in the CCE test at different temperatures.

The tuning results of the two EOS were in good agreement with those experimentally measured values, particularly at high temperatures where the system was not very close to the critical point. The tuned and predicted (no tuning) results of the EOS in performing CCE tests at 121.1°C and 37.7°C are plotted in Figs. 3.24, and 3.25, respectively. As it

shows the tuning results deteriorate at 37.7°C, particularly for the VPT EOS, due to the fluid being close to the critical point at this conditions.

The ratios of the tuned α parameter of sub and supercritical components in the liquid phase to the original α parameter are plotted in Fig. 3.26 for the VPT EOS. Approaching the critical point the ratios converge to unity, as it was also seen for the 5-component model gas condensate (GMX89-1). Fig. 3.26 also shows that the correction to the α parameter almost changes linearly with reduced temperature for the VPT EOS.

The PVT data of two model fluids have been successfully matched over a wide range of temperature by adjusting the α parameter of sub and supercritical components in the liquid phase. For some tuning cases the correction to the α parameter of subcritical components can be kept constant while changing the α parameter of supercritical components to match the experimental data. The tuned α values of sub and supercritical components in the liquid phase converge to unity as the critical point is approached. This agrees with the physics of the molecules in the liquid phase, that is, the attraction between molecules in the liquid phase is the same as that of the vapour phase at the critical point.

In the next sections, the developed tuning approach in this study is used to match a comprehensive experimental data set of two real reservoir fluids over wide ranges of temperature and compositional changes.

Near Critical Fluid (NCF)

A Near Critical fluid (NCF) was used to carry out CCE tests over a wide temperature range, 140°C to 25°C. At 140°C, the Near Critical fluid (NCF) exhibits a medium-rich gas condensate behaviour with a maximum liquid dropout of 27%, whereas at 25°C it behaves as a very volatile oil. Hence, the temperature range covers from the gas condensate region, passing through the critical point to volatile oil phase behaviour. The Near Critical fluid (NCF) was also used to perform a constant volume depletion (CVD) test and a seven stage methane injection at 100°C. Some unconventional PVT tests, such

as condensate accumulation near the well bore at 5000 psia and methane cycling test at 4000 psia, were conducted at 100°C. A two stage separator test and a constant composition expansion (CCE) test on depleted vapour were carried out at 37.8°C (see Appendix C for the description of the PVT tests).

The Valderrama modification of Patel and Teja (VPT) and the modified Peng-Robinson (mPR) EOS with no BIP were applied to match the saturation pressure and liquid dropout in the CCE tests at various temperatures. The tuning and prediction (no tuning) results of the EOS are shown in Figs. 3.27 through 3.29. Results show that there is good agreement between the predictions of the tuned models and experimental data at all temperatures, except at 25°C which is very close to the critical point. Neither of the two untuned EOS could reasonably predict the saturation pressure and volumetric data, particularly the mPR could not predict the fluids as gas condensate at temperatures lower than 120°C. At 25°C, the results of untuned VPT EOS were highly erroneous, therefore, they are not included in the comparison. The results clearly illustrate the capability of the integrated tuning method to model phase behaviour of real reservoir fluids over a wide range of temperature change.

The experimental results of a seven stage methane injection into the Near Critical fluid (NCF) at 100°C were also modelled. The predicted and tuning results of the EOS models at stages three and five are presented in Figs. 3.30 and 3.31 where, 0.1285 and 0.3928 moles methane were injected into one mole Near Critical fluid (NCF), respectively. In Fig. 3.32, the variation of saturation pressure with methane injection is plotted. Results show that the tuned EOS can reasonably predict the saturation pressure and volumetric properties of the Near Critical fluid (NCF) during methane injection study. Further more, the tuned EOS were used to predict the volumetric behaviour of the Near Critical fluid (NCF) in a methane cycling test. A CVD test was performed to deplete the fluid to 4000 psia. Then, the CVD test was stopped and pure methane was injected into the cell to simulate a methane cycling process into a partially depleted reservoir (methane cycling test is described in Appendix C). The results of performing a methane cycling test at 4000

psia and 100°C, using the tuned EOS is shown in Fig. 3.33. The tuned EOS have given a good fit to the reported experimental data. The results demonstrate that the integrated tuning approach can successfully be used to model phase behaviour of fluids during gas injection and gas cycling processes where composition of fluids can dramatically change with the injection of gas into the system.

The mPR and the VPT EOS with no BIP were used to model the results of a two stage separator test from 5000 psia to 3000 psia (then stock tank) at 37°C. The results are given in Table 3.3. The average absolute percentage deviation (AAD%) in predicting the experimental data of separator test by the untuned mPR and VPT EOS were 3.8 and 7.0, respectively. Tuning of the EOS reduced the AAD% to 0.9 and 2.9 for the mPR and the VPT EOS, respectively. Although, the Near Critical fluid (NCF) is very close to the critical point at this temperature, the measured phase behaviour and volumetric properties of the Near Critical fluid (NCF) from the separator test are reasonably matched by the two EOS. This shows the capability of the developed tuning method in matching the experimental data of near critical fluids at surface conditions.

To simulate condensate accumulation near the well bore, an unconventional PVT test was performed at 100°C and 4550 psia (see Appendix C). In this test, a known amount of the Near Critical fluid (NCF) was charged into the cell at 100°C and it was depleted to 4550 psia. The saturation pressure and liquid fraction of mixture were measured at every stage after a certain amount of the single phase (100°C and 5000 psia) Near Critical fluid (NCF) was injected into the cell and pressure was stabilised. The predicted saturation pressure by the tuned EOS were in good agreement with those of the reported experimental data. The liquid fractions of the mixture from the condensate accumulation near the well bore test, are plotted versus cumulative volume of injected single phase Near Critical fluid (NCF) in Fig. 3.34. Both EOS models have reasonably predicted the liquid fraction of the mixture in the condensate accumulation near the well bore test.

The ratios of the tuned α parameter of sub and supercritical components in the liquid phase to those of the original ones are plotted against reduced temperature for the VPT EOS in Fig. 3.35. It shows that approaching the critical point the ratios converge to unity, which means the attraction between molecules in the liquid phase becomes the same as the vapour phase at the critical point. As it is shown in Fig. 3.35, a linear function can be fitted to the α values.

The results demonstrate the capability of the integrated tuning method to model phase behaviour of real reservoir fluids over wide ranges of temperature and compositional changes. The developed method can reasonably predict phase behaviour of fluids during gas injection and gas cycling processes, where a large compositional change can occur with the injection of the gas into the system. The α parameter of the sub and supercritical components can independently be adjusted to tuned the EOS. The tuned α parameters can be correlated against the reduced temperature of the mixture. The results are also in line with the conclusions of the model fluids, that is, the tuned α parameter of sub and supercritical components in the liquid phase converge to unity at the critical point.

Gas Condensate GCA94-1

Gas condensate (GCA94-1) was used to carry out constant composition expansion (CCE) tests at 110, 80, 50 and 37.8°C. The volumetric behaviour of this fluid was also measured by performing a constant volume depletion (CVD), three stage methane injection, condensate accumulation near the well bore and methane cycling tests at 110°C. A two stage separator test from saturation pressure to 3000 psia and a CCE test on depleted vapour at 37.8°C were carried out in the laboratory.

The tuned and untuned results of CCE test at 110°C and 50°C are given in Figs. 3.36 and 3.37, respectively. They show while the untuned EOS have not predicted the results satisfactorily, the tuned models have given reasonable match to the reported experimental data. This demonstrates the capability of the developed approach to model phase behaviour of fluids over a wide range of temperature change.

The tuned EOS were applied to predict the saturation pressure and volumetric properties of a three stage methane injection at 110°C. The results of tuned and untuned EOS at the second stage where 0.3119 moles methane were injected into the gas condensate (GCA94-1) are given in Fig. 3.38. The variation of saturation pressure of the mixture with methane injection is plotted in Fig. 3.39. The results show that the integrated tuning method is capable of modelling of fluid phase behaviour during gas injection processes where a large compositional change can occur with the injected gas into the system.

The tuned EOS to the experimental data of constant composition expansion (CCE) test at 110°C were used to predict the results of a constant volume depletion (CVD) test at 110°C. The results are given in Fig. 3.40. It shows that the tuned EOS to the CCE test data can reasonably predict the volumetric properties of the fluid in the CVD test at the same temperature.

The mPR and the VPT EOS with no BIP were used to predict the results of a CCE test at 37.8°C as shown in Fig. 3.41. A tail effect can be seen in the reported experimental data. The mPR EOS was tuned to saturation pressure about 350 psia under the reported saturation pressure (5480 psia) at 37.8°C. The tuned VPT EOS did not offer a major improvement in comparison to the untuned case in predicting the volumetric properties of the fluid at this temperature.

In the Near Critical fluid (NCF) study, a condensate accumulation near the well bore test, which is an unconventional PVT test, was performed to simulate condensate behaviour around the well bore. The test was also carried out on the gas condensate (GCA94-1) at 110°C and 3000 psia. A CVD test was performed to deplete the fluid from saturation pressure to 3000 psia prior to gas inflow testing in four stages. A CCE test was conducted at each stage. The results at the second stage of condensate accumulation near the well bore test with a total gas inflow volume of 52.62% pore volume, are demonstrated in Fig. 3.42. Neither of the untuned EOS could predict the results of this

test. The results of performing a CCE test at every stage showed that the predicted liquid dropouts were in good agreement with those experimental values at the first and second stages. Adding further single phase fluid into the system (to simulate gas inflow), at the later stages, the critical point was approached, therefore, the quality of the predictions were deteriorated. The variation of saturation pressure with gas inflow to the system, is given in Fig. 3.43. The tuned EOS have given reasonable match to the variation of the saturation pressure, particularly at the later stages of the test. Taking the correction to the α parameter of the components in the liquid phase as a function of reduced temperature has resulted in the observed improvements in modelling the phase behaviour of these complex systems.

The gas condensate (GCA94-1) was used to perform a CVD test at 110°C from saturation pressure to 3000 psia in six stages. Then the vapour phase at 3000 psia and 110°C was transferred to the VLE rig, where a CCE test was performed at 37.8°C. The tuned EOS were used to predict the phase behaviour of the mixture. The results are shown in Fig. 3.44. The tuned VPT EOS has given good predictions to the liquid fraction values, particularly at pressures close to the saturation pressure.

A service company had also carried out a three stage gas injection test, using the gas condensate (GCA94-1). The composition of injected gas is given in Table 3.4. The results at the third stage where 0.739 moles gas is injected into the gas condensate (GCA94-1), are illustrated in Fig. 3.45. The results show that the liquid dropout predictions deteriorated at low pressures (less than 2000 psia). The same trend was also observed in the CCE test results of the original fluid as shown in Fig. 3.36.

The results of study on the gas condensate (GCA94-1) supports the conclusions of the Near Critical fluid (NCF) and the model fluids cases. The integrated tuning method is capable of modelling phase behaviour of fluids over wide ranges of temperature and compositional changes. The tuned EOS to experimental data of CCE test can reasonably predict the volumetric properties of the fluid in a CVD test at the same temperature. The

integrated tuning method is general and it can be applied to any EOS where it was successfully applied to the mPR and the VPT EOS in this study.

3.6 CONCLUSIONS

A rapid flash calculation (RFC) method has been investigated. In the RFC method the number of equations to be solved in phase equilibrium calculation is reduced to three for a two parameter EOS. Three methods, successive substitution (SS) and a quasi-Newton (QN) method to solve conventional flash formulation and the RFC method were used to simulate various reservoir processes including constant composition expansion (CCE) and multiple contact gas injection tests for a large number of gas condensate and oil samples. It has been found that the convergence of the RFC method is as good as the QN method when it was applied to determine the phase equilibrium of oil systems. Approaching the critical region, the dependency of the QN and the RFC methods on the initial guess becomes more critical. The application of the RFC method to gas condensate systems resulted in lack of convergence in most cases. In the original RFC method, the two parameters of EOS for the vapour phase are initially assumed and iterated. The method has been modified in this study by iterating on EOS parameters for the liquid phase. The modified RFC method has been found even more robust than the QN method for gas condensate systems.

It has been shown in this study that, the computational time of flash calculations using the RFC method is markedly lower than those of the conventional ones in all cases. The results also showed that when approaching the critical region, the computational time increased, more severely with the QN method than the other methods.

An important contribution of this study has been the demonstration of the fact that EOS can be tuned as effectively without using binary interaction parameters (BIP), hence allowing the use of the rapid flash calculation in phase equilibrium calculations.

Two practical tuning methods, conventional and integrated, have been developed and applied to different types of fluids using EOS with no BIP to perform phase behaviour calculations. In the conventional tuning method, which is used to tune the phase behaviour model at reservoir and surface temperatures, the properties of the heavy end are used as the regression variables. In the integrated tuning model, the temperature dependency of the attractive term (α parameter) in EOS for the liquid phase, along with properties of the heavy end if required, are used as regression variables. This method is recommended for near critical fluids, particularly over wide ranges of temperature and compositional changes. In the case of two-parameter EOS, such as the Peng-Robinson (PR) EOS, the shift parameters of pseudo components can be treated as regression variables. The methods have been applied to a number of fluids, including model and real reservoir fluids.

The capability of the developed tuning methods have been illustrated by matching the measured PVT data of volatile systems, e.g. volatile oil and gas condensates. For model fluids with known component properties, the integrated tuning method has successfully fitted the experimental data over a wide range of temperature change.

The conventional tuning method has been applied to match a comprehensive experimental data set of a volatile oil sample. The data set comprised various PVT tests, including constant composition expansion (CCE), differential liberation (DL), four stage multiple forward contact (MFC), three stage multiple backward contact (MBC) and a three stage separator test. The original Peng-Robinson EOS (with no BIP), including the third parameter, was simultaneously tuned to the reported data set and the results have been compared with those of the other investigators reported in the literature. The results show that the developed model with no BIP has clearly been more successful than all other models to simulate each and all the experimental data. The conventional method has also been applied to fit the experimental data of a gas condensate system. The experimental results of a CCE and a constant volume depletion (CVD) tests were simultaneously regressed. The PR and the Valderrama modification of Patel-Teja (VPT) EOS were used

to perform the phase equilibrium calculations. The capability of the tuned models in predicting the phase behaviour of the gas condensate have been demonstrated.

The capability of the integrated tuning method to determine the phase behaviour of model and real reservoir fluids over wide ranges of temperature and compositional changes has been demonstrated. The α parameter of the sub and supercritical components in the liquid phase can independently be adjusted to tuned the EOS. The tuned α parameters can be correlated against the reduced temperature of the mixture. For some tuning cases the correction to the α parameter of subcritical components can be kept constant while changing the α parameter of supercritical components. The tuned α values of sub and supercritical components in the liquid phase converge to unity as the critical point is approached. This agrees with the physics of the molecules in the liquid phase, that is, the attraction between molecules in the liquid phase is same as that of the vapour phase at the critical point. The integrated tuning method is comparable to other leading tuning approaches in the literature, such as the Coats and Smart tuning method.

The developed tuning approaches in this study are general and they can be applied to any EOS. The methods were successfully applied to the PR and the VPT EOS in this study.

REFERENCES

1. Danesh, A., Xu, D.-H. and Todd, A.C., (1990) : "A Grouping Method to Optimise Oil Description for Compositional Simulation of Gas Injection Processes", SPE paper 20745, presented at the 65th Annual Technical Conference and Exhibition held in New Orleans, L.A., Sept. 23-26.

2. Xu, D.-H., (1990) : "*Phase Behaviour Modelling of Hydrocarbon Systems for Compositional Reservoir Simulation of Gas Injection Processes*", PhD Dissertation, Heriot-Watt University, Edinburgh, UK.

3. Gozalpour, F., Danesh, A., Todd, A.C. and Tehrani, D.H., (1998) : "Integrated Phase Behaviour Modelling of Fluids in Reservoir-Surface Processes Using Equation of State", SPE/DOE paper 39630, proceeding of the 11th Symposium on Improved Oil Recovery held in Tulsa, Oklahoma, April 19-22.

4. Michelsen, M.L., (1986) : "Simplified Flash Calculations for Cubic Equations of State", *Ind. Eng. Chem. Process Des. Dev.*, **25**(1), 184-188.

5. Prausnitz, J.M., Lichtenthaler, R.N. and de Azevedo, E.G., (1986) : *Molecular Thermodynamics of Fluid-Phase Equilibria*, 2nd Edition, Prentice-hall Inc.

6. Danesh, A., Xu, D.-H. and Todd, A.C., (1991) : "Comparative Study of Cubic Equations of State for Predicting Phase Behaviour and Volumetric properties of Injection Gas-Reservoir Oil Systems", *Fluid Phase Equilibria*, **63**, 259-278.

7. Valderrama, J.O., (1990) : "A Generalized Patel-Teja Equation of State for Polar and Non-Polar Fluids and Their Mixtures", *J. Chem. Eng. Japan*, **23**(1), 87-91.

8. Danesh, A., Gozalpour, F., Todd, A.C. and Tehrani, D.H., (1996) : "Reliable Tuning of Equation of State with No Binary Interaction Parameter", paper presented at the 17th International Workshop and Symposium, International Energy Agency Collaborative Project on EOR, Sept. 30-Oct. 2, Sydney, Australia.

9. Gozalpour, F., (1993) : *Compositional Description and Tuning of Equation of State for Predicting PVT Behaviour of Oil*, MSc Thesis, University of Petroleum Industry, Ahvaz, Iran.

10. Michelsen, M.L., (1982) : "The Isothermal Flash Problem. Part I. Stability", *Fluid Phase Equilibria*, **9**, 1-19.

11. Agarwal, R.K., Li, Y.K. and Nghiem, L., (1990) : "A Regression Technique With Dynamic Parameter Selection for Phase Behaviour Matching", *SPERE*, Feb., 115-119.

12. Pedersen, K.S., Thomassen, P. and Fredenslund, A., (1988) : "On the Dangers of "Tuning" Equation of State Parameters", *Chem. Eng. Sci.*, **43**(2), 269-278.

13. Gani, R. and Fredenslund, A., (1987) : "Thermodynamics of Petroleum Mixtures Containing Heavy Hydrocarbons : An Expert Tuning System", *Ind. Eng. Chem. Res.* **26**(7), 1304-1312.

14. Coats, K.H. and Smart, G.T., (1986) : "Application of a Regression-Based EOS PVT Program to Laboratory Data", *SPERE*, May, 277-299.

15. Marquardt, D.W., (1963) : "An Algorithm for Least-Squares Estimation of Non-linear Parameters", *J. Soc. Indust. Appl. Math.*, June, **11**(2), 431-441.

16. Final Report, Reservoir Fluid Studies, July 1993 (Vol. I). Heriot-Watt University, Department of Petroleum Engineering, Report No : PVT/93/2.

17. Osjard, E.H., Ronningsen, H.P. and Tau, L., (1985) : "Distribution of Weight, Density, and Molecular Weight in Crude Oil Derived from Computerized Capillary GC Analysis", *J. High Res. Chromat. & Chromat. Commun.*, Oct., **8**, 683-690.

18. Final Report, Reservoir Fluid Studies, January 1997. Heriot-Watt University, Department of Petroleum Engineering, Report No : PVT/97/1.

19. Jhaveri, B.S. and Youngren, G.K.. (1988) : "Three-Parameter Modification of the Peng-Robinson Equation of State to Improve Volumetric Predictions", *SPERE*, Aug., 1033-1040.

20. Twu, C.H., (1984) : "An Internally Consistent Correlation for Predicting the Critical Properties and Molecular Weights of Petroleum and Coal-Tar Liquids", *Fluid Phase Equilibria*, **16**, 137-150.

21. Riazi, M.R. and Daubert, T.E., (1987) : "Characterization Parameters for Petroleum Fractions", *Ind. Eng. Chem. Res.*, **26**(4), 755-759.

22. Lee, B.I., and Kesler, M.G., (1975) : "A Generalized Thermodynamic Correlation Based on Three-Parameter Corresponding States", *AIChE J.*, **21**, 510-527.

23. Final Report, Reservoir Fluid Studies, June 1990. Heriot-Watt University, Department of Petroleum Engineering, Report No : PVT/90/1.

24. Merrill, R.C., Hartman, K.J. and Creek, J.L., (1994) : "A Comparison of Equation of State Tuning Methods", SPE paper 28589, proceeding of the 69th Annual Technical Conference and Exhibition held in New Orleans, L.A., Sept. 25-28.

25. Whitson, C.H., (1983) : "Characterizing Hydrocarbon Plus Fraction", August, *SPEJ.*, 683-694.

Table 3.1 : Convergence Results of Carrying Out 12 Stage CCE Test.

Name	No. Comp.	Fluid Type	T (°C)	SS	QN	RFC This Work
McCain	3	Black Oil	71.1	C	C	C
LME88-1	7	Black Oil	60.0	C	C	C
LRG88-1	9	Black Oil	55.0	C	C	C
LRL88-1	13	Black Oil	100.0	C	C	C
LRX89-2	13	Volatile Oil	100.0	C	C	C
LRL88-1	17	Black Oil	100.0	C	C	C
LRX89-3	17	Volatile Oil	100.0	C	C	C
LRL88-1	22	Black Oil	100.0	C	C	C
LRX89-4	22	Volatile Oil	100.0	C	C	C
GCA94-1	24	Gas Condensate	110.0	C	C	C
GMX90-1	20	Gas Condensate	121.1	C	N	C
GMX90-1	20	Gas Condensate	93.3	P	N	N
GMX90-1	20	Gas Condensate	65.5	P	N	N
GMX89-1	5	Gas Condensate	110.0	C	C	C
GMX89-1	5	Gas Condensate	80.0	C	N	C
GMX89-1	5	Gas Condensate	60.0	C	N	C
GMX89-1	5	Gas Condensate	30.0	P	N	N
NCF	24	Gas Condensate	140.0	C	N	N
NCF	24	Gas Condensate	120.0	P	N	N
NCF	24	Gas Condensate	100.0	P	N	N

C : Converged

N : No convergence

P : Poor convergence

SS : Successive Substitution Method

QN : Quasi-Newton Method

RFC : Rapid Flash Calculation Method

Table 3.2 : Absolute Percentage Deviation of Separator Test Results Volatile Oil LRX89-1.

Source	GoR	F.V.F.	Stock Tank Gravity	**Over all**
Model A	10.1	8.8	6.9	**8.6**
Model B	20.6	16.0	2.7	**13.1**
Model C	17.1	12.2	0.3	**9.9**
This work	6.6	7.5	0.2	**4.8**

Table 3.3 : Two Stage Separator Test (5000 to 3000 psia) at 37.0°C - Near Critical Fluid (NCF).

Model	Sat. Press. psia	GOR. SCF/SCF*	Liq. Density at 3000 psia gr / cc	Bo Sep. bbl / STB	Stock Tank Sp. Gr.	**AAD%**
Exp.	4446	1022	0.594	3.874	0.792	
Untuned mPR	5025	1016	0.586	3.725	0.790	**3.8**
Untuned VPT	5445	1022	0.601	3.595	0.758	**7.0**
Tuned mPR	4425	1025	0.603	3.953	0.793	**0.9**
Tuned VPT	4695	1021	0.595	3.705	0.759	**2.9**

* at 14.7 psia and 15.5°C.

Table 3.4 : Composition of Injection Gas.

Component	**Mole %**
C1	85.06
C2	11.77
C3	3.17

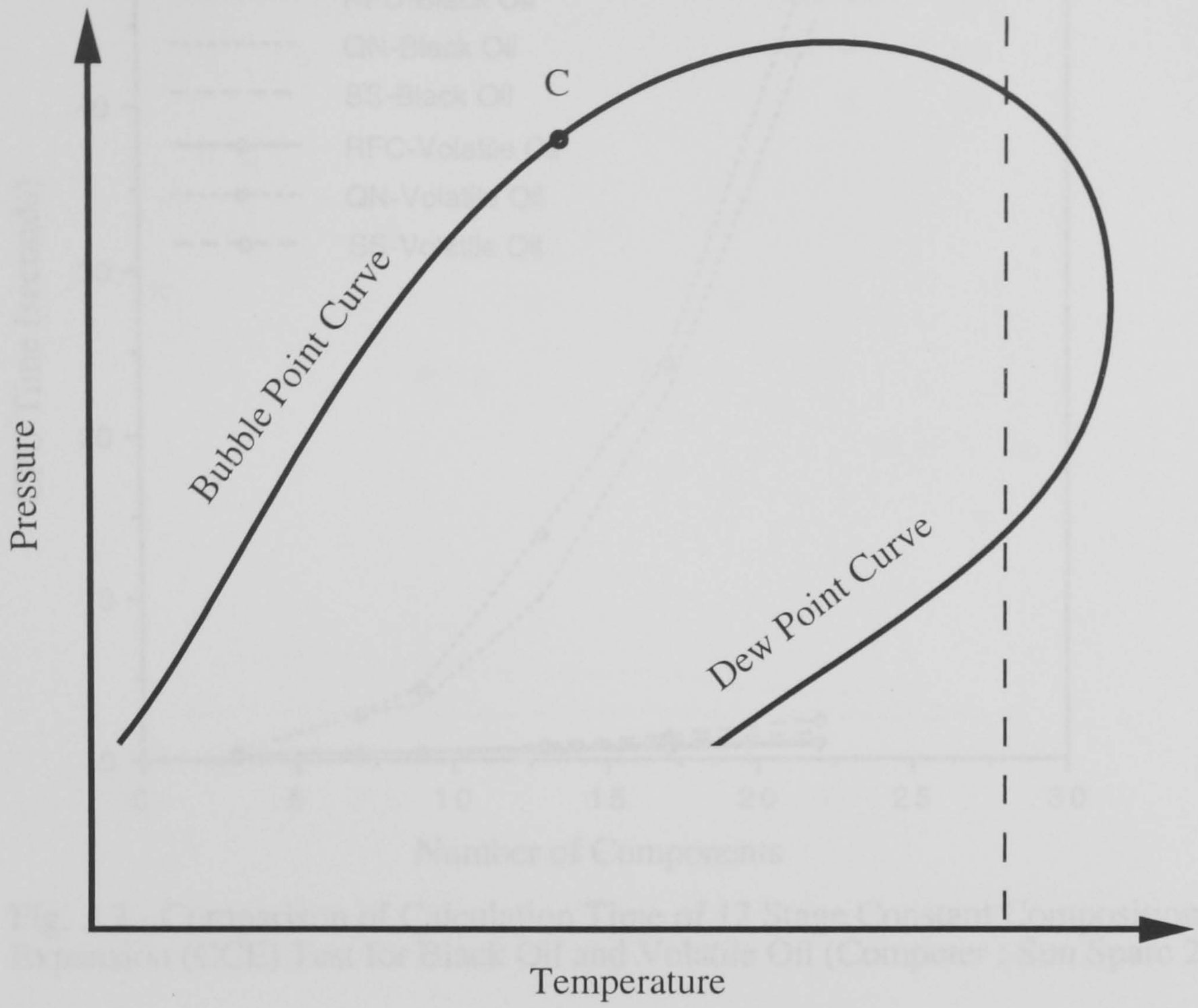

Fig. 3.1 - Saturation Pressure Variation of Petroleum Fluids with Temperature.

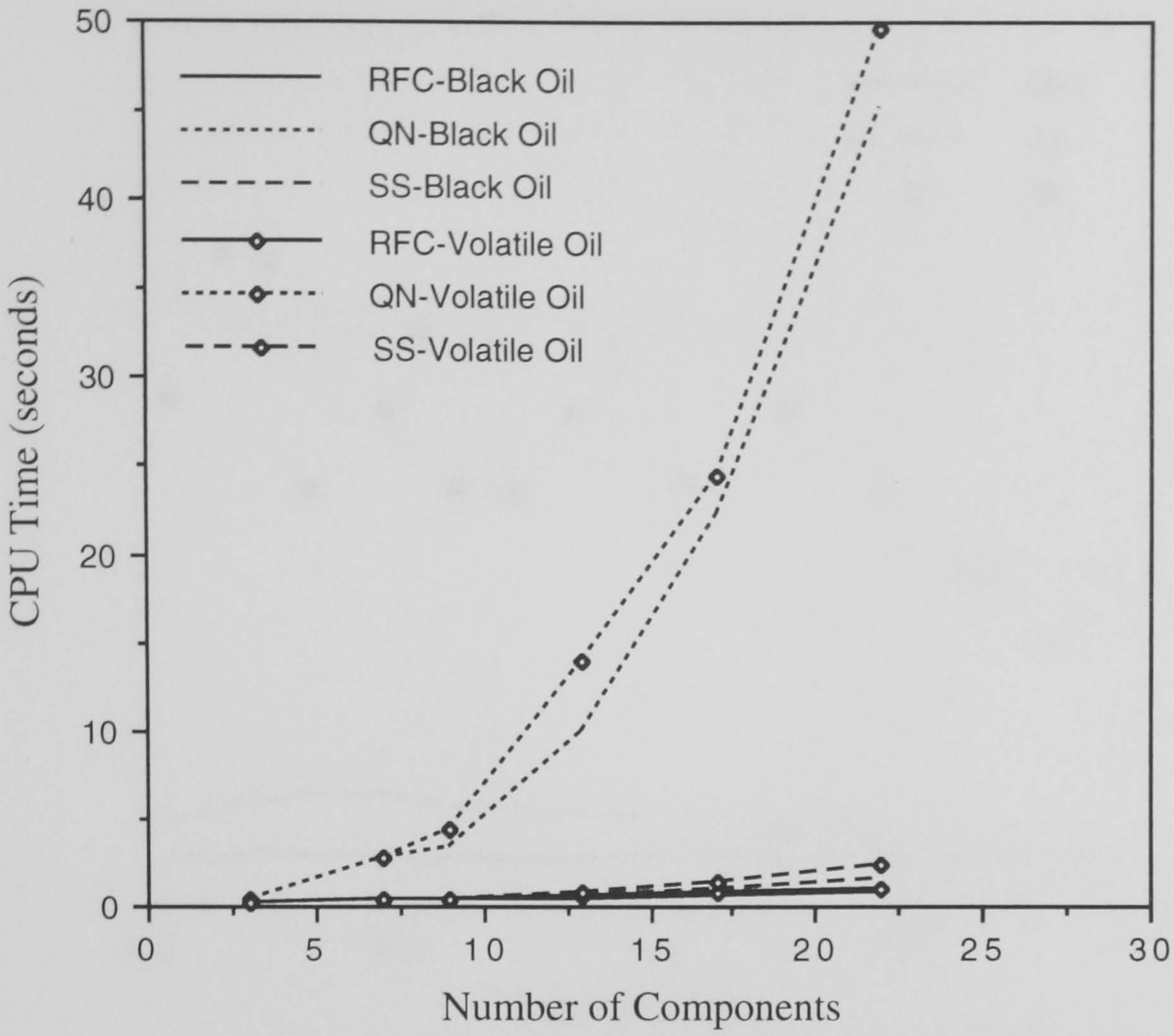

Fig. 3.2 - Comparison of Calculation Time of 12 Stage Constant Composition Expansion (CCE) Test for Black Oil and Volatile Oil (Computer : Sun Sparc 2).

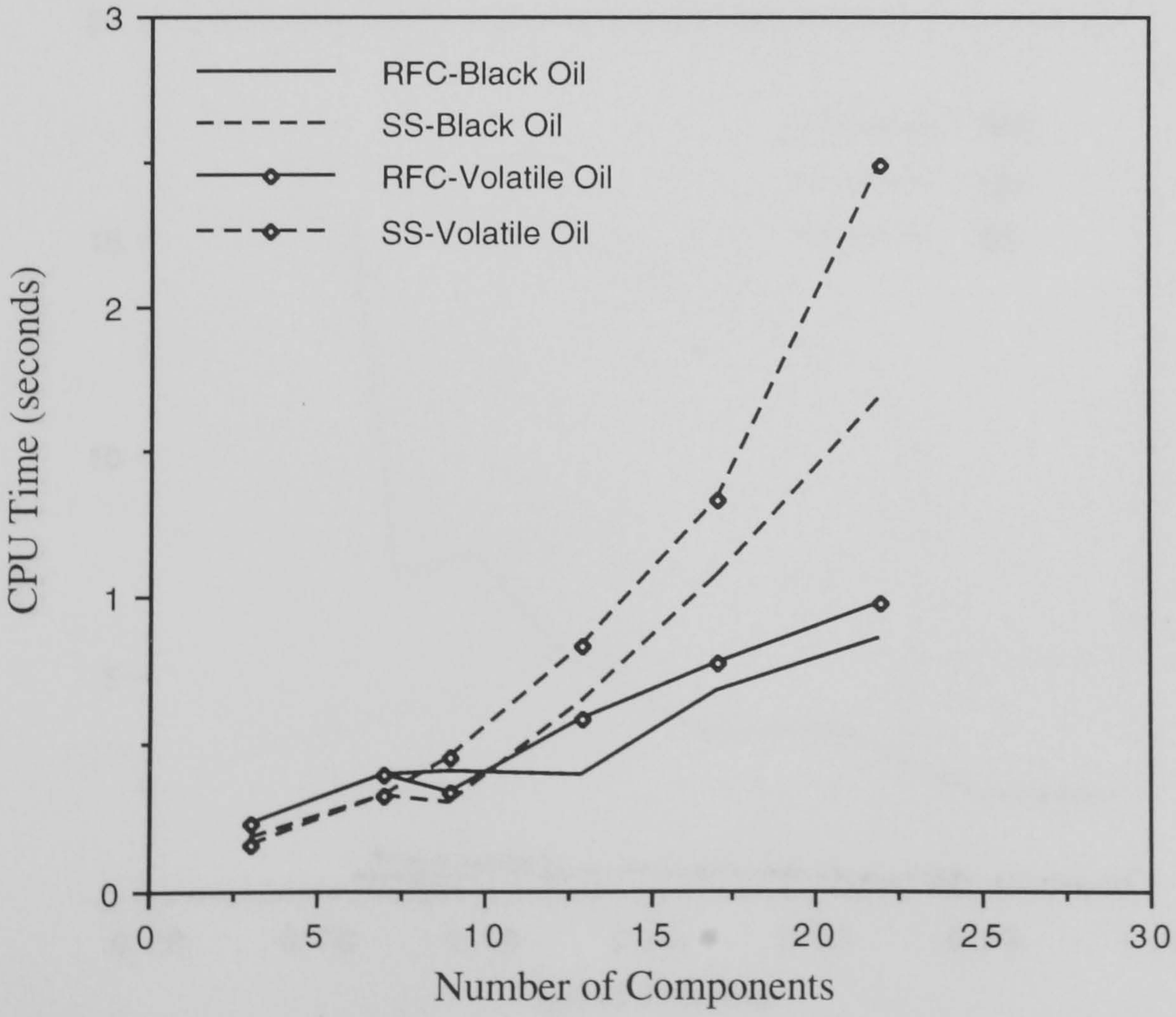

Fig. 3.3 - Comparison of Calculation Time of 12 Stage CCE Test for Black Oil and Volatile Oil, SS and RFC Methods (Expanded scale for the lower curves of Fig. 3.2, Computer : Sun Sparc 2).

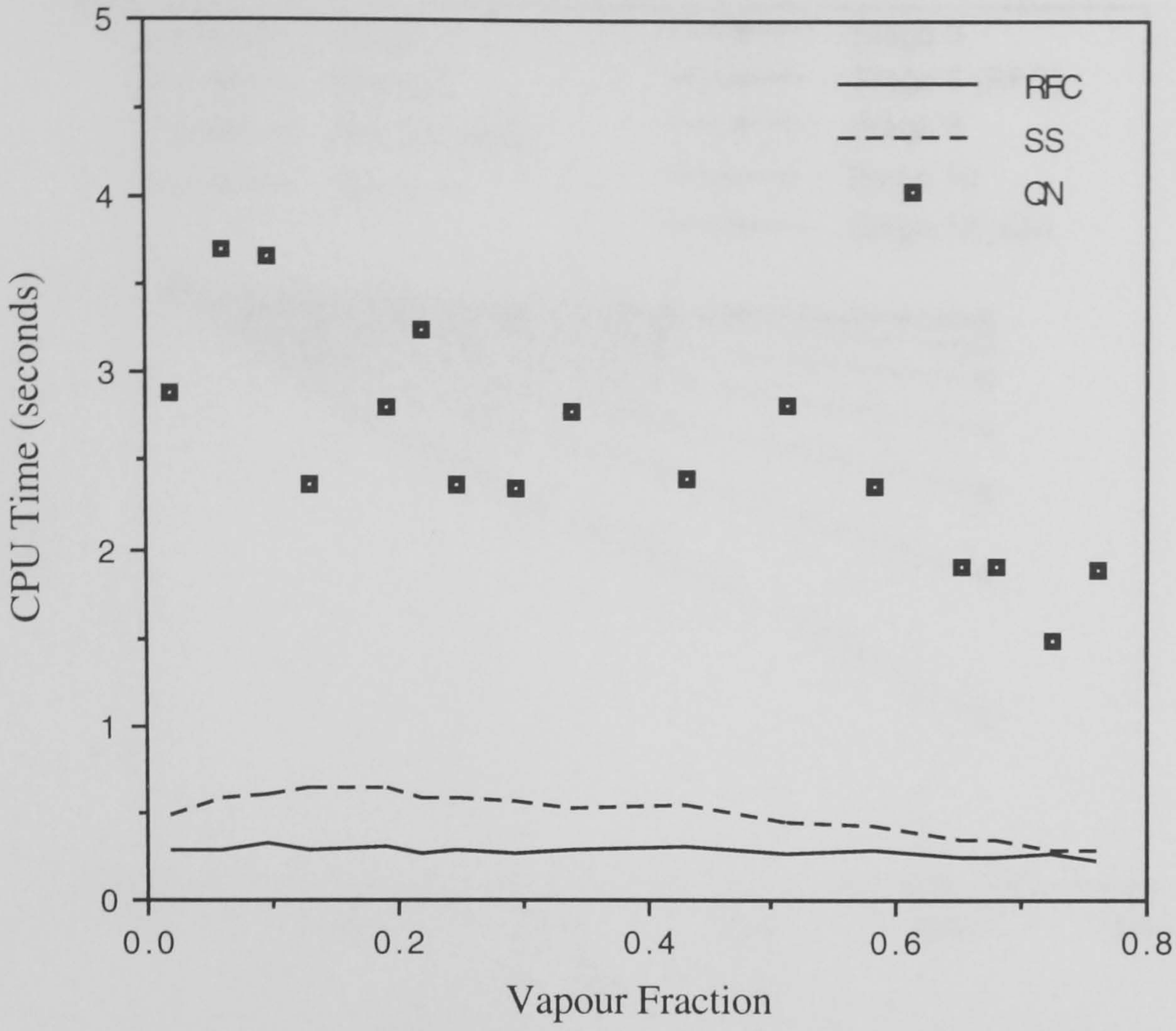

Fig. 3.4 - CPU Time of a Single Flash Calculation, Using 17-components Volatile Oil (LRX89-3, Computer : Sun Sparc 2).

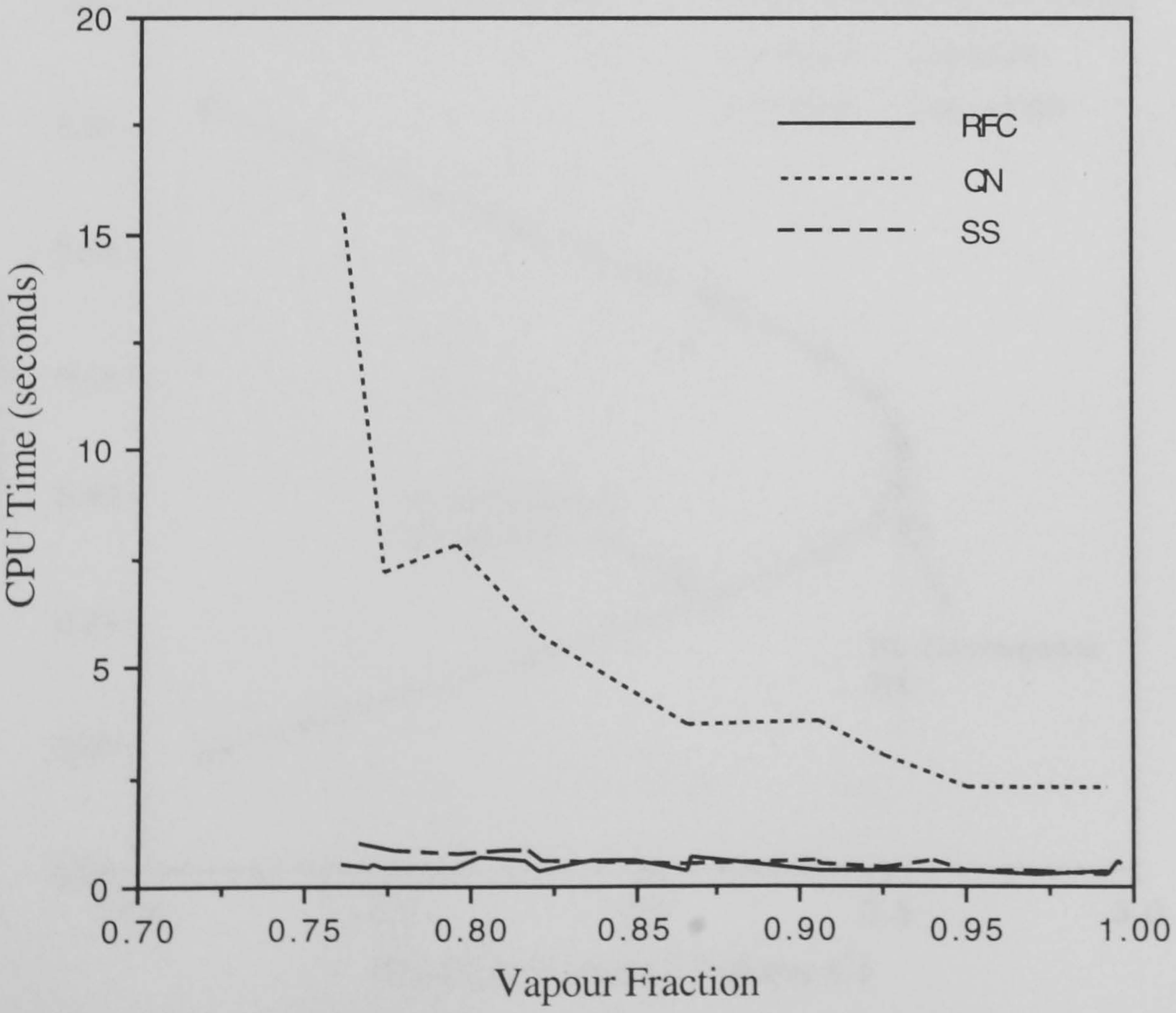

Fig. 3.5 - CPU Time of a Single Flash Calculation, Using 20-components Model Gas Condensate (GMX90-1, Computer : Sun Sparc 2).

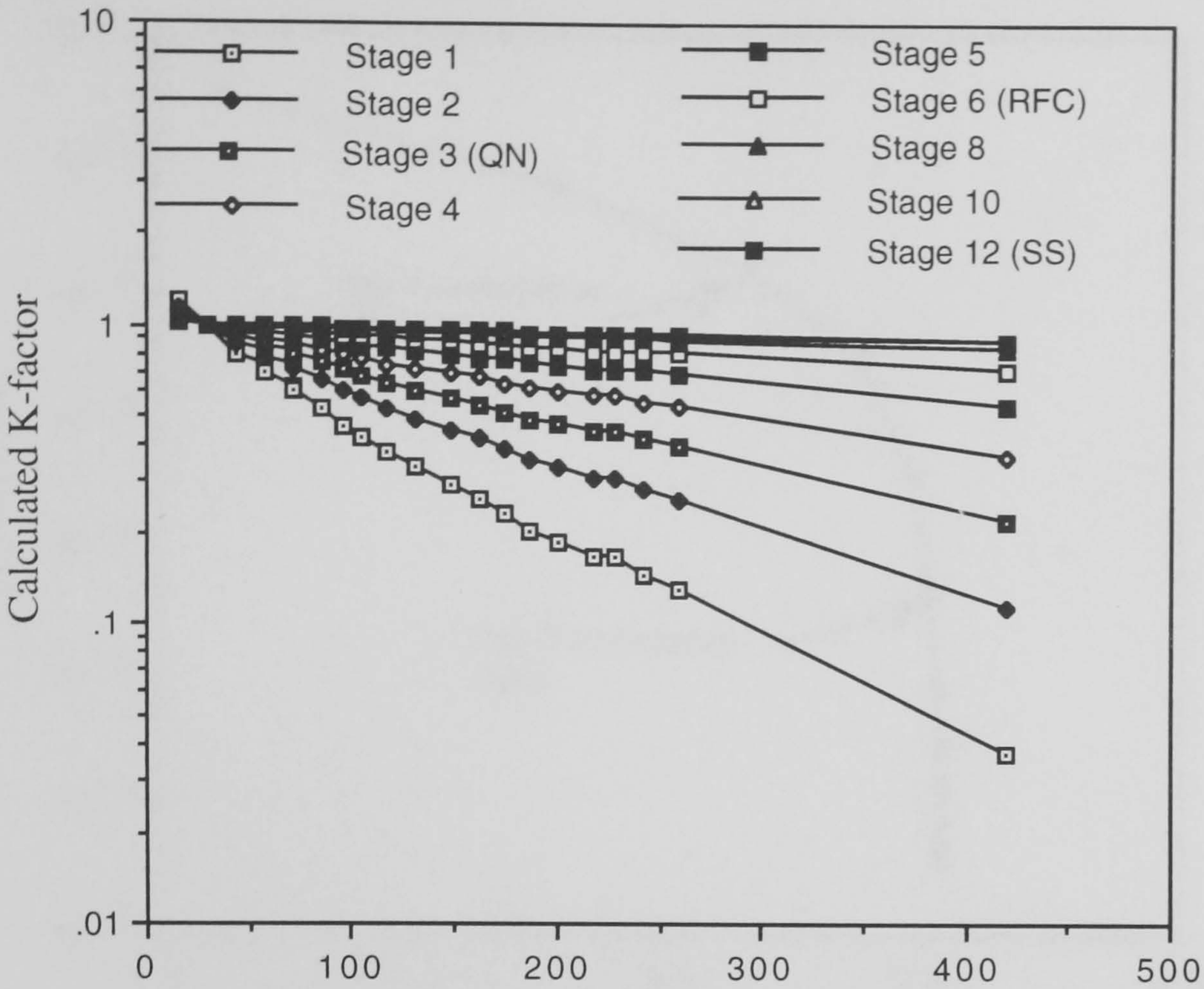

Fig. 3.6 - Calculated K-factors versus Molecular Weight, Forward Contact, Volatile Oil / Methane at 6092 psia and 100°C.

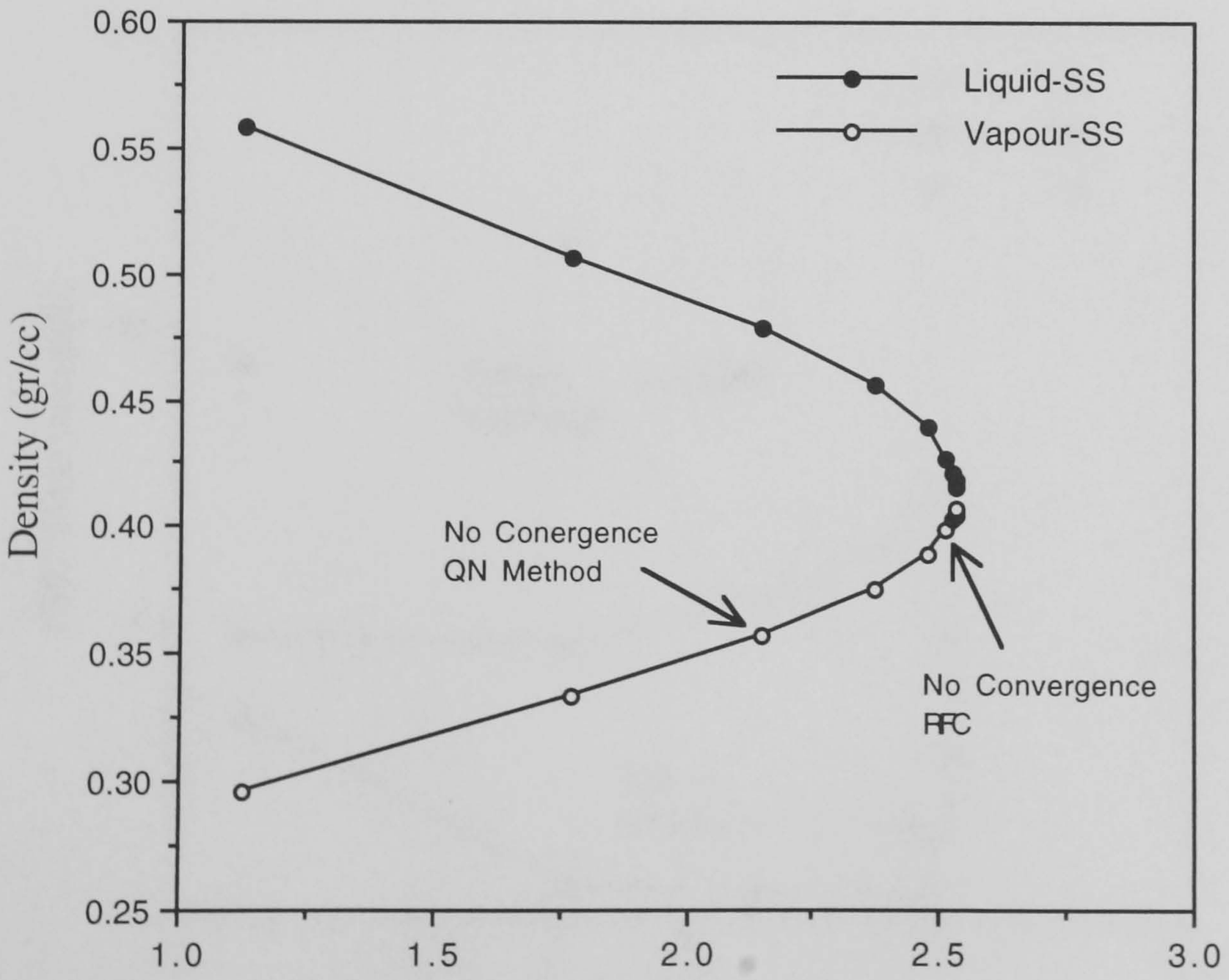

Fig. 3.7 - Density of Equilibrated Phases versus Total Volume of Contacted Oil, Forward Contact, Volatile Oil / Methane at 6092 psia and 100°C.

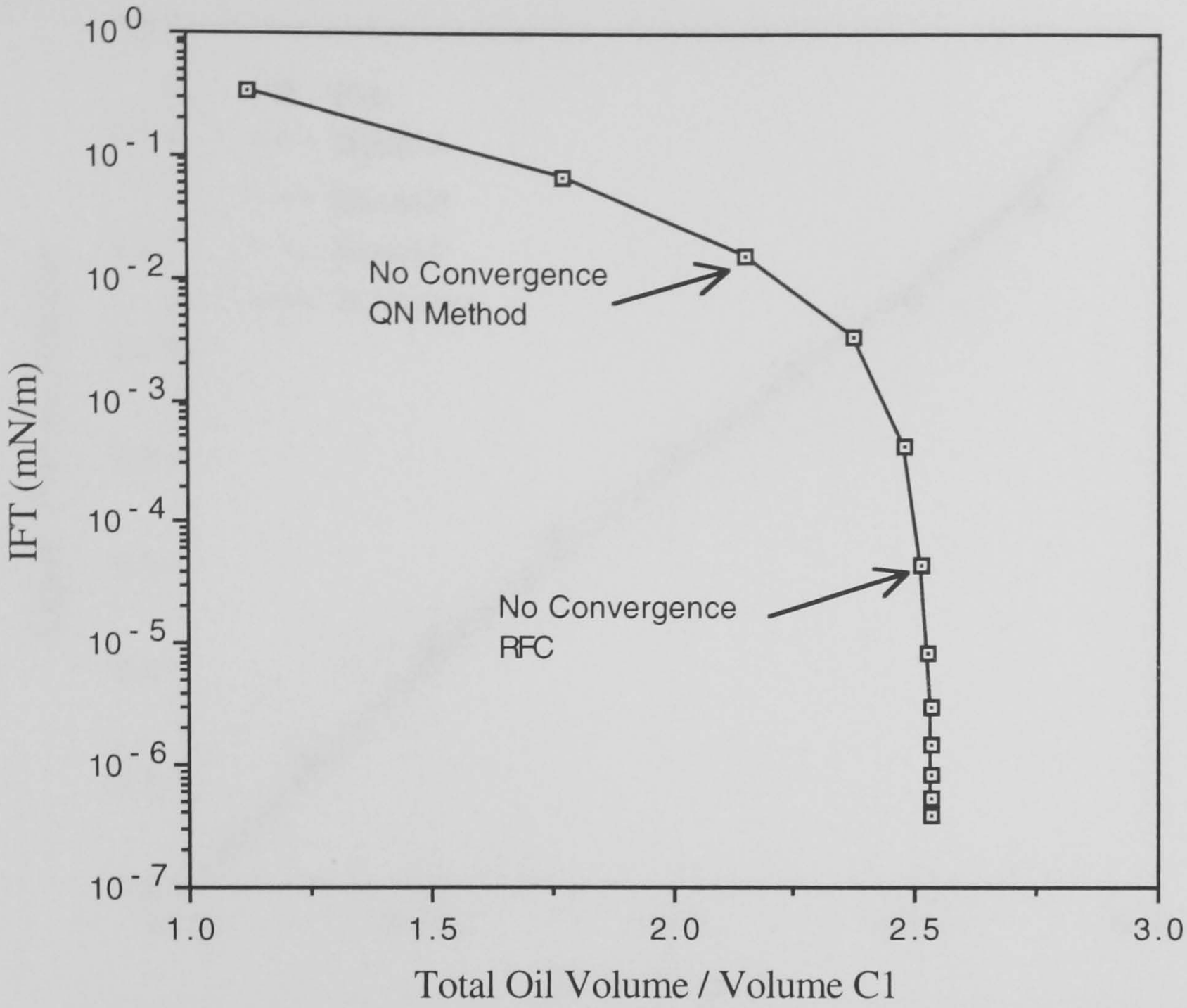

Fig. 3.8 - Interfacial Tension versus Total Volume of Contacted Oil, Forward Contact, Volatile Oil / Methane at 6092 psia and 100°C.

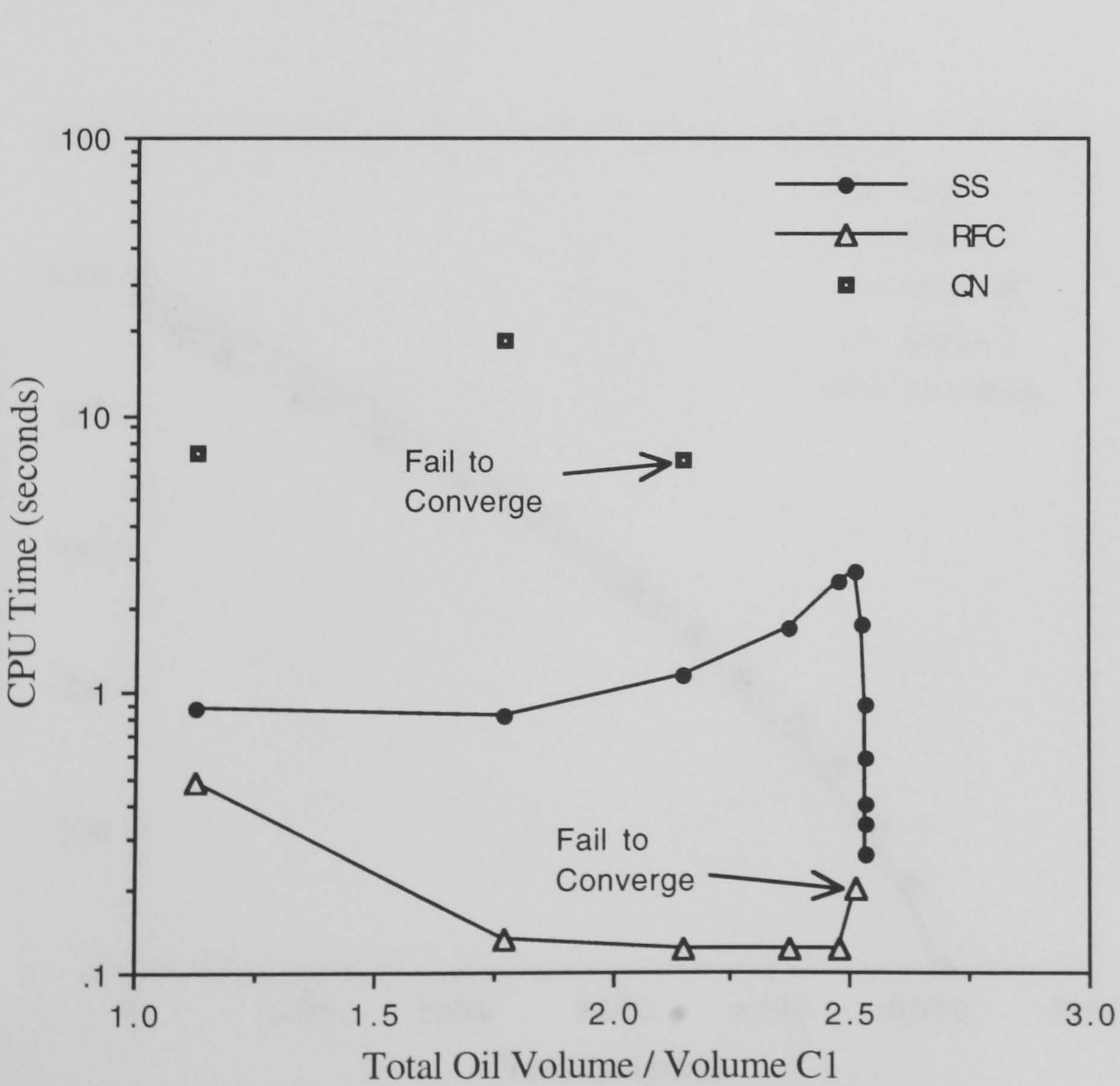

Fig. 3.9 - Comparison of Flash Calculation CPU Time for Different Methods, Forward Contact, Volatile Oil / Methane at 6092 psia and 100°C (Computer : Sun Sparc 2).

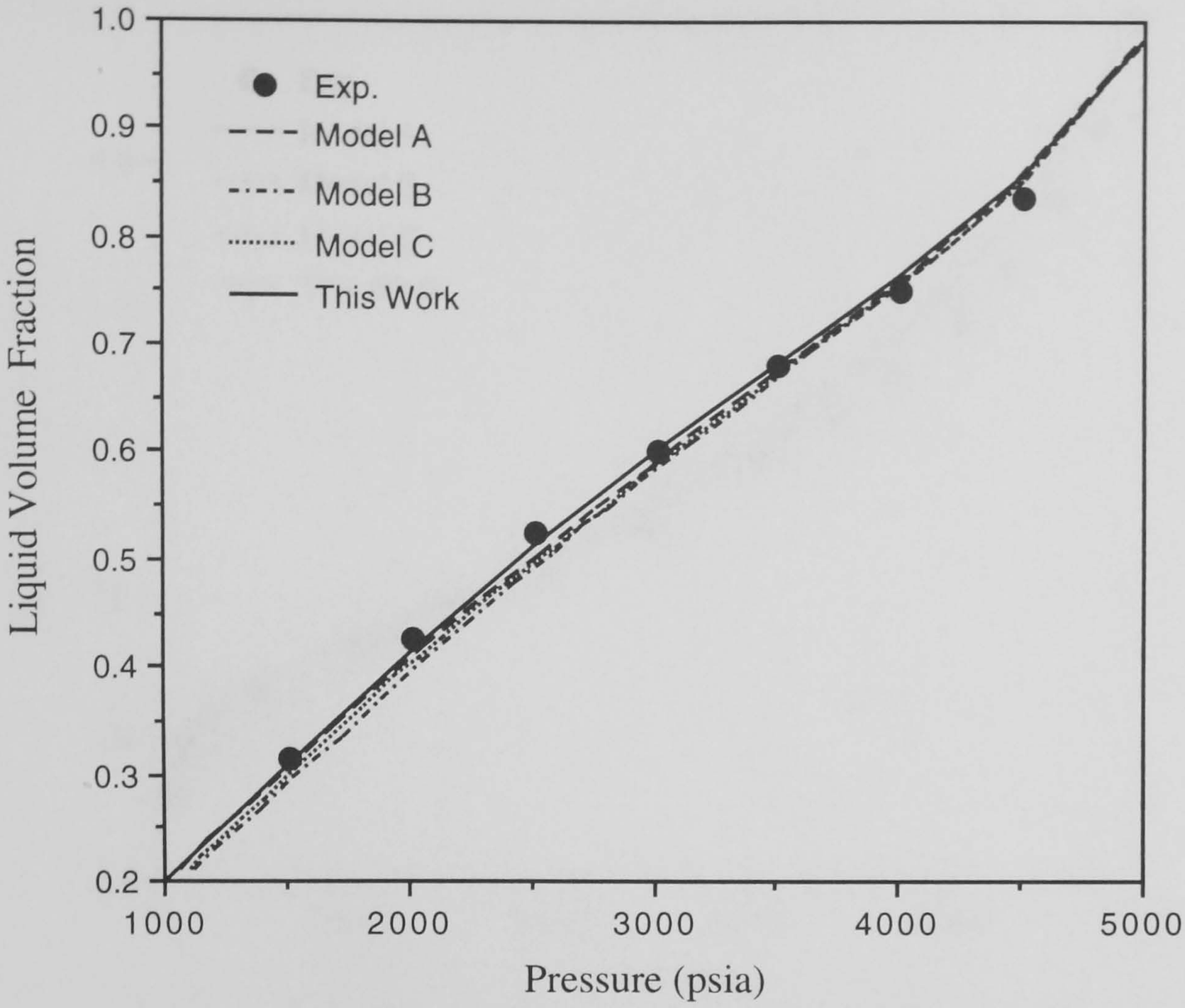

Fig. 3.10 - Variations of Liquid Volume Fraction Relative to Total Volume in Constant Composition Expansion (CCE), Volatile Oil LRX89-1.

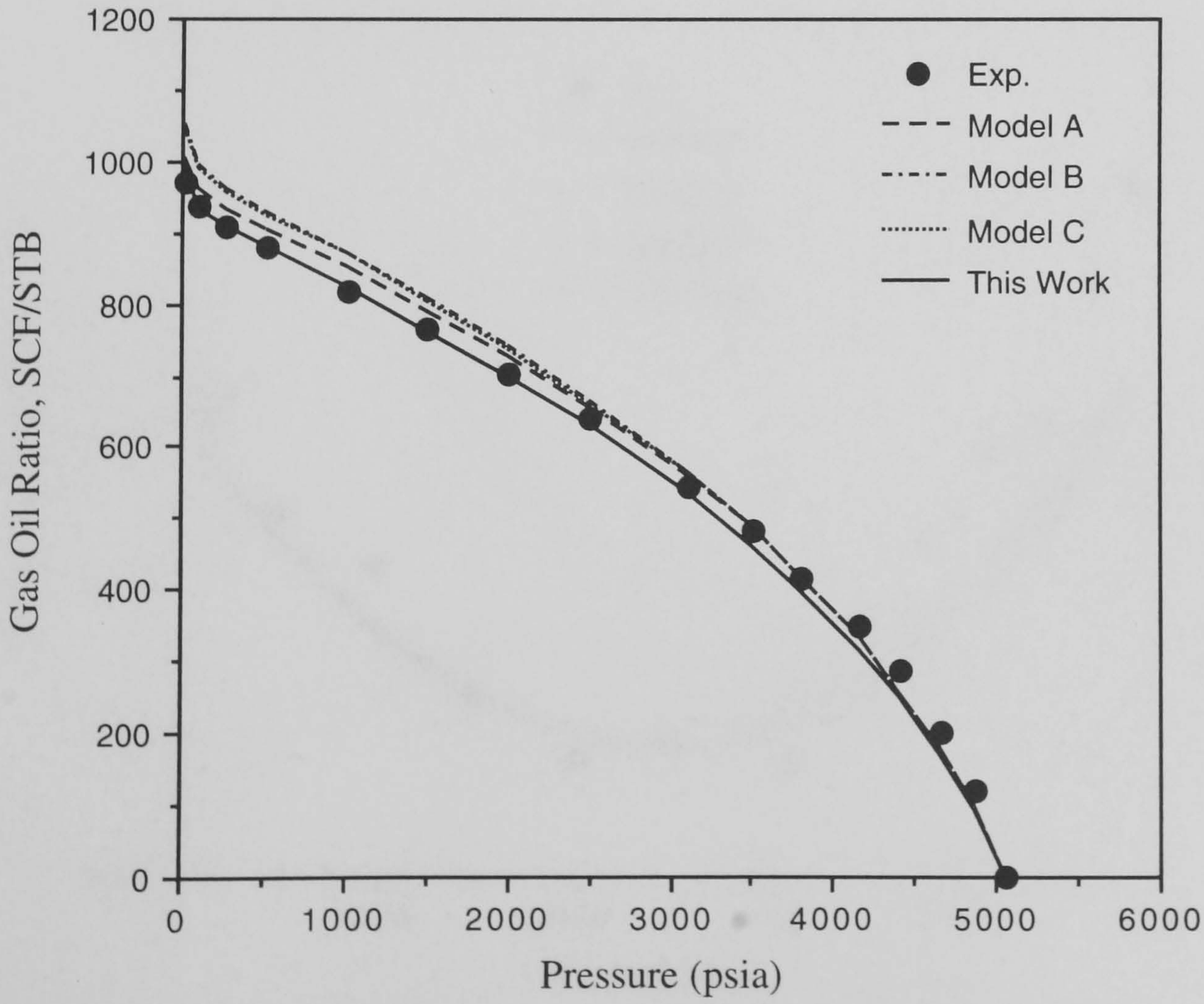

Fig. 3.11 - Variations of Gas-Oil Ratio with Pressure in Differential Liberation (DL) Test, Volatile Oil LRX89-1.

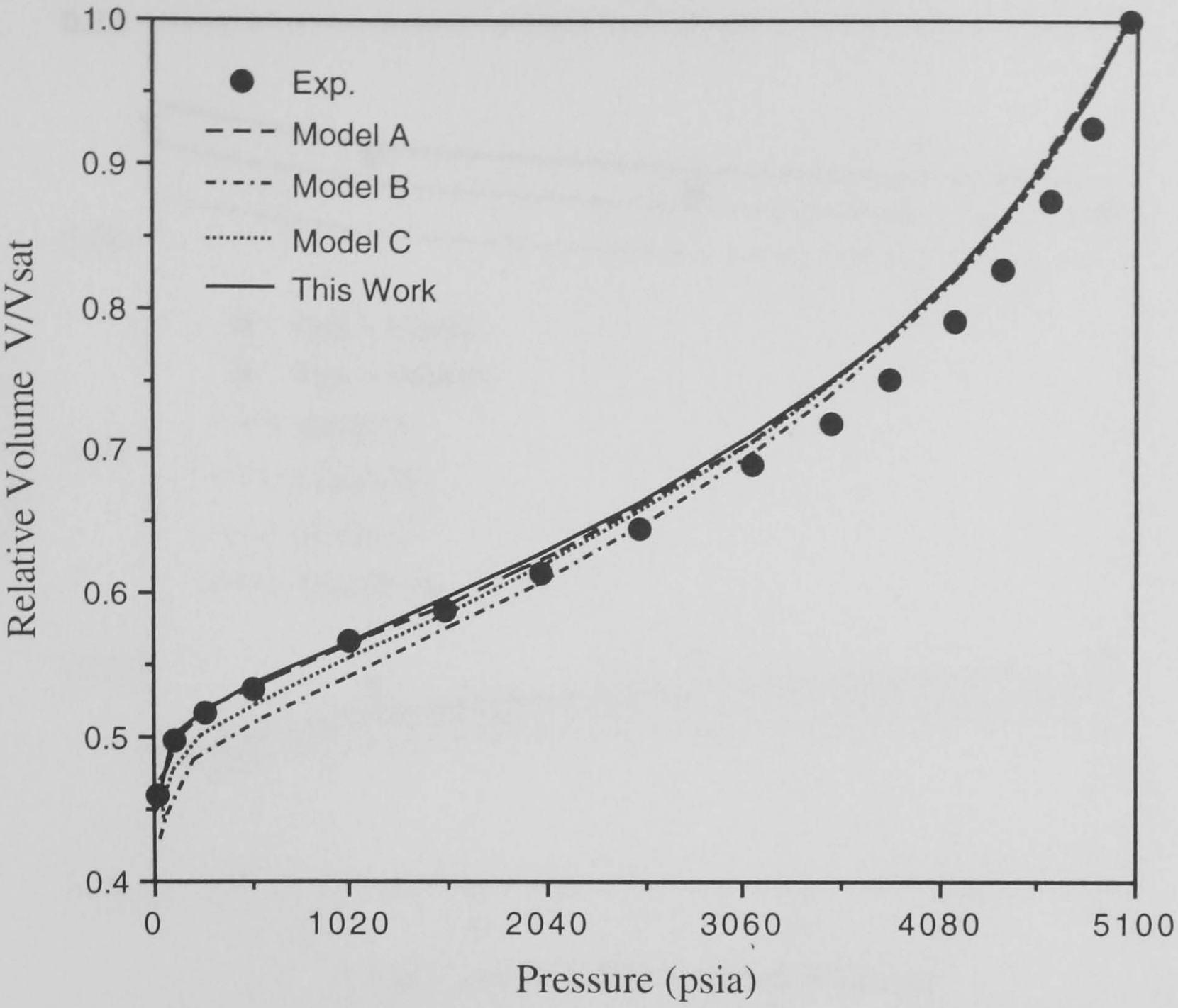

Fig. 3.12 - Variations of Liquid Volume Fraction Relative to Saturation Volume in Differential Liberation (DL) Test, Volatile Oil LRX89-1.

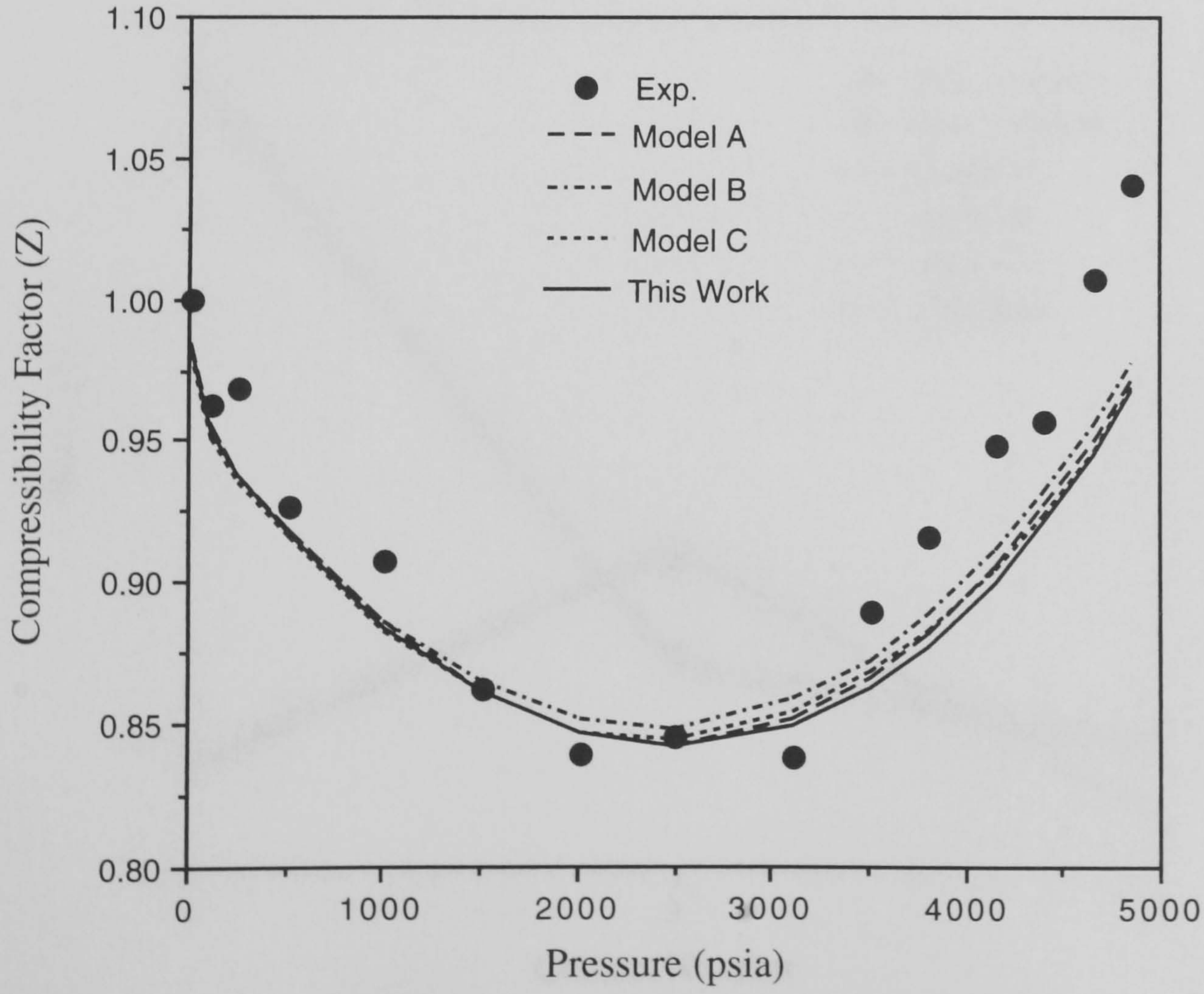

Fig. 3.13 - Variation of Compressibility Factor of Liberated Gas in Differential Liberation (DL) Test, Volatile Oil LRX89-1.

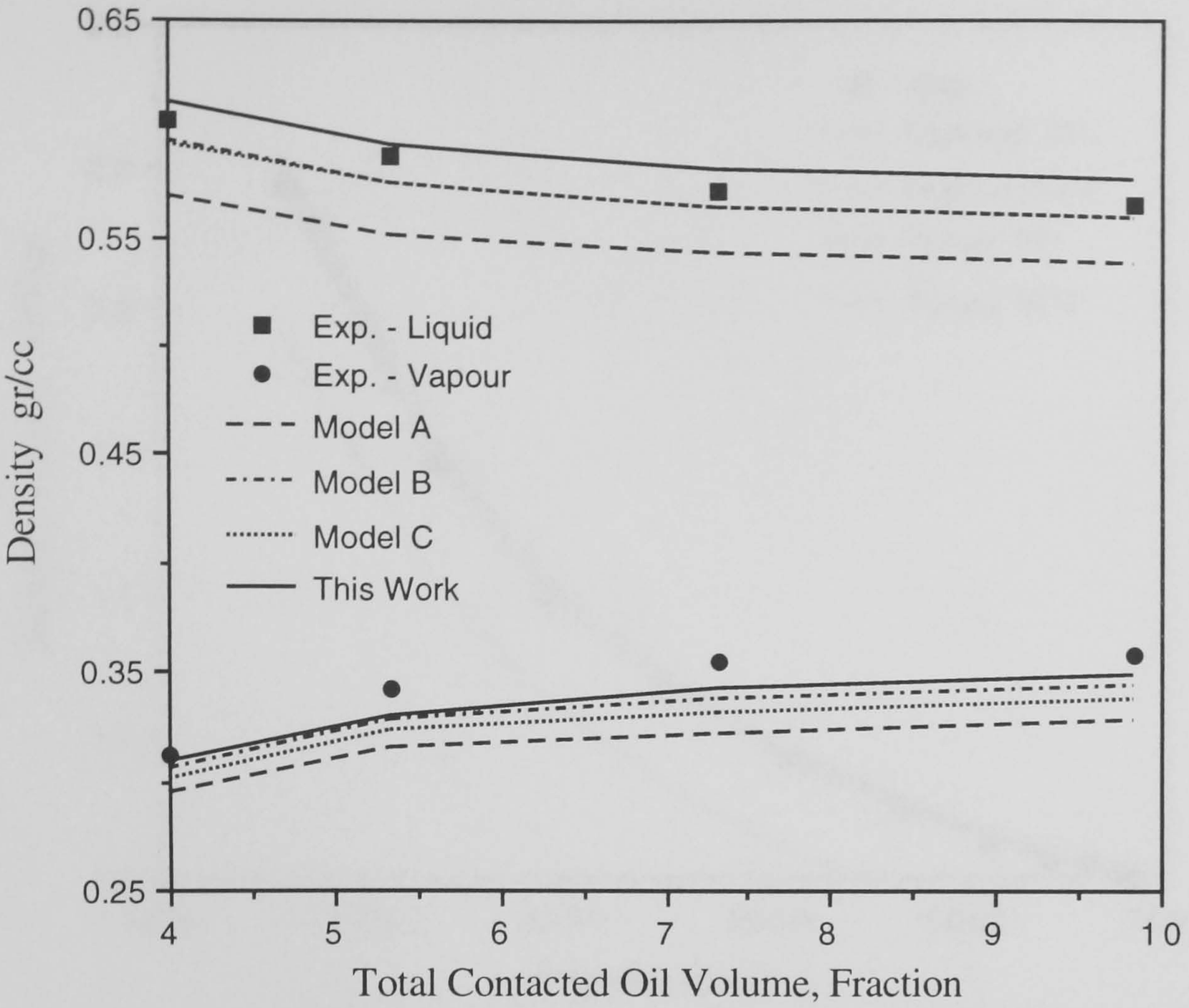

Fig. 3.14 - Variations of Liquid and Gas Density with Ratio of Total Contacted Oil to Injected Advancing Methane Volume at 5114 psia in Multiple Forward Contact Test, Volatile Oil LRX89-1.

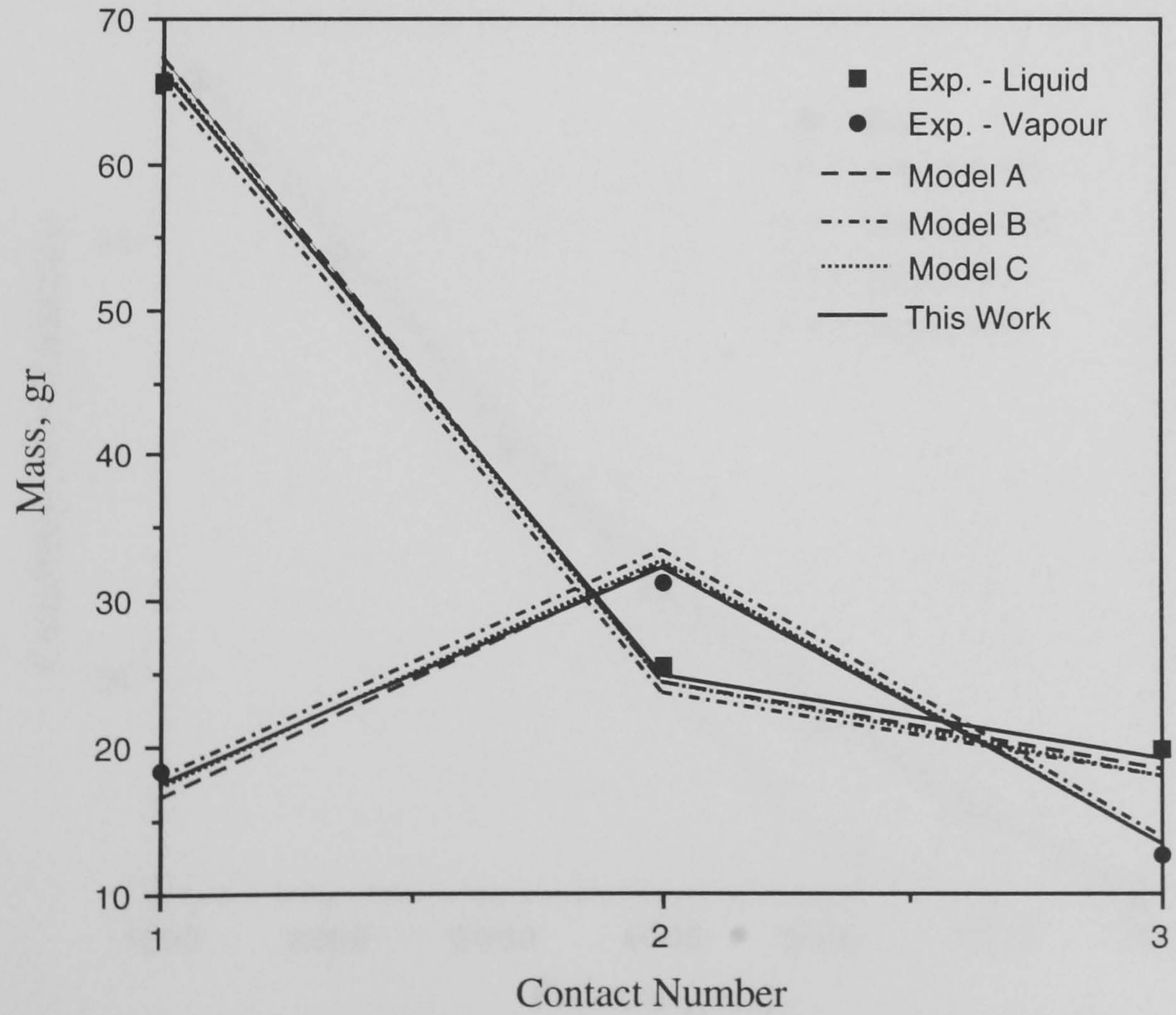

Fig. 3.15 - Variations of Mass of Liquid and Gas in Multiple Backward Contacts Test, Volatile Oil LRX89-1.

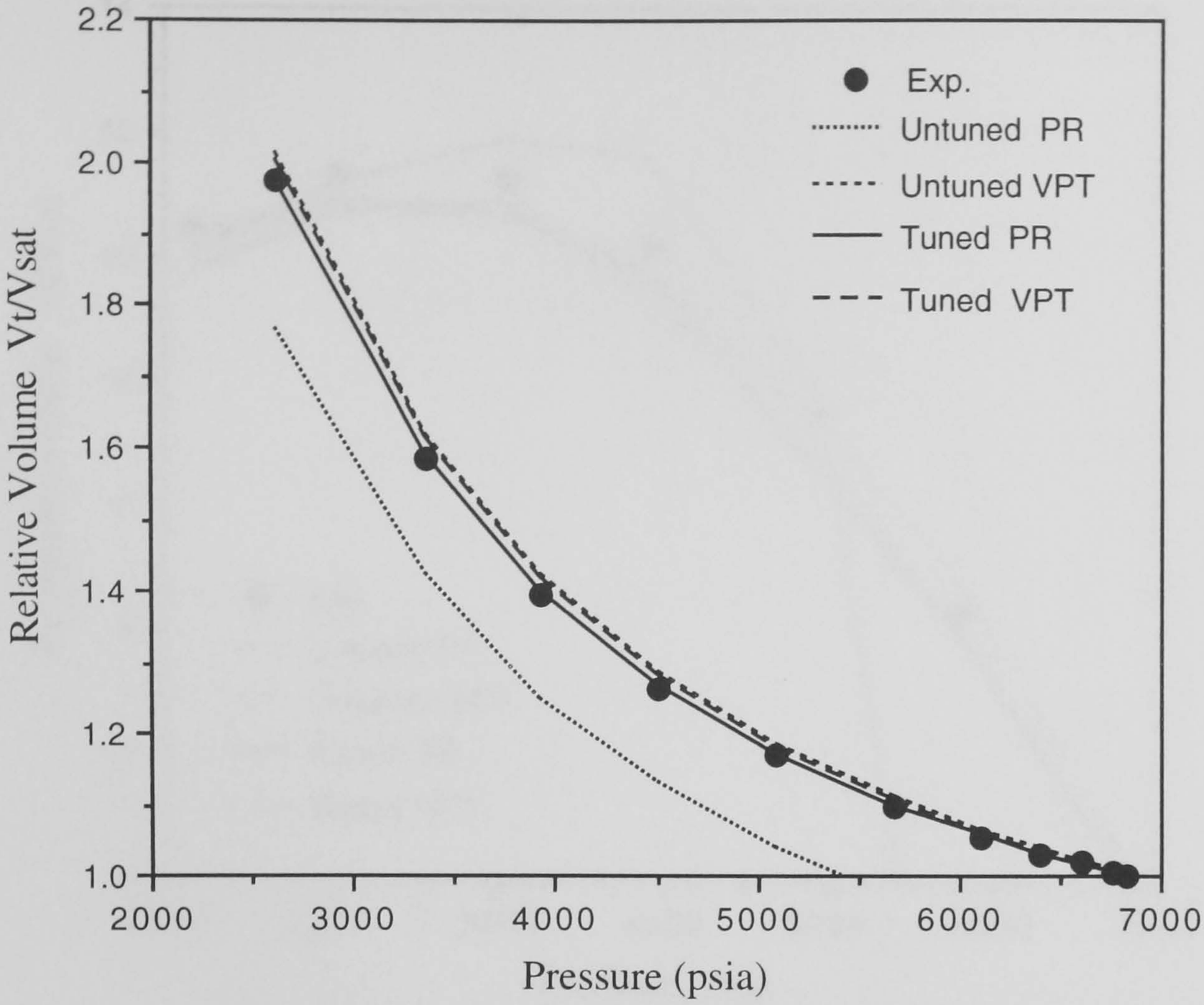

Fig. 3.16 - Variations of Relative Volume in Constant Composition Expansion (CCE) Test, Gas Condensate GCX89-1.

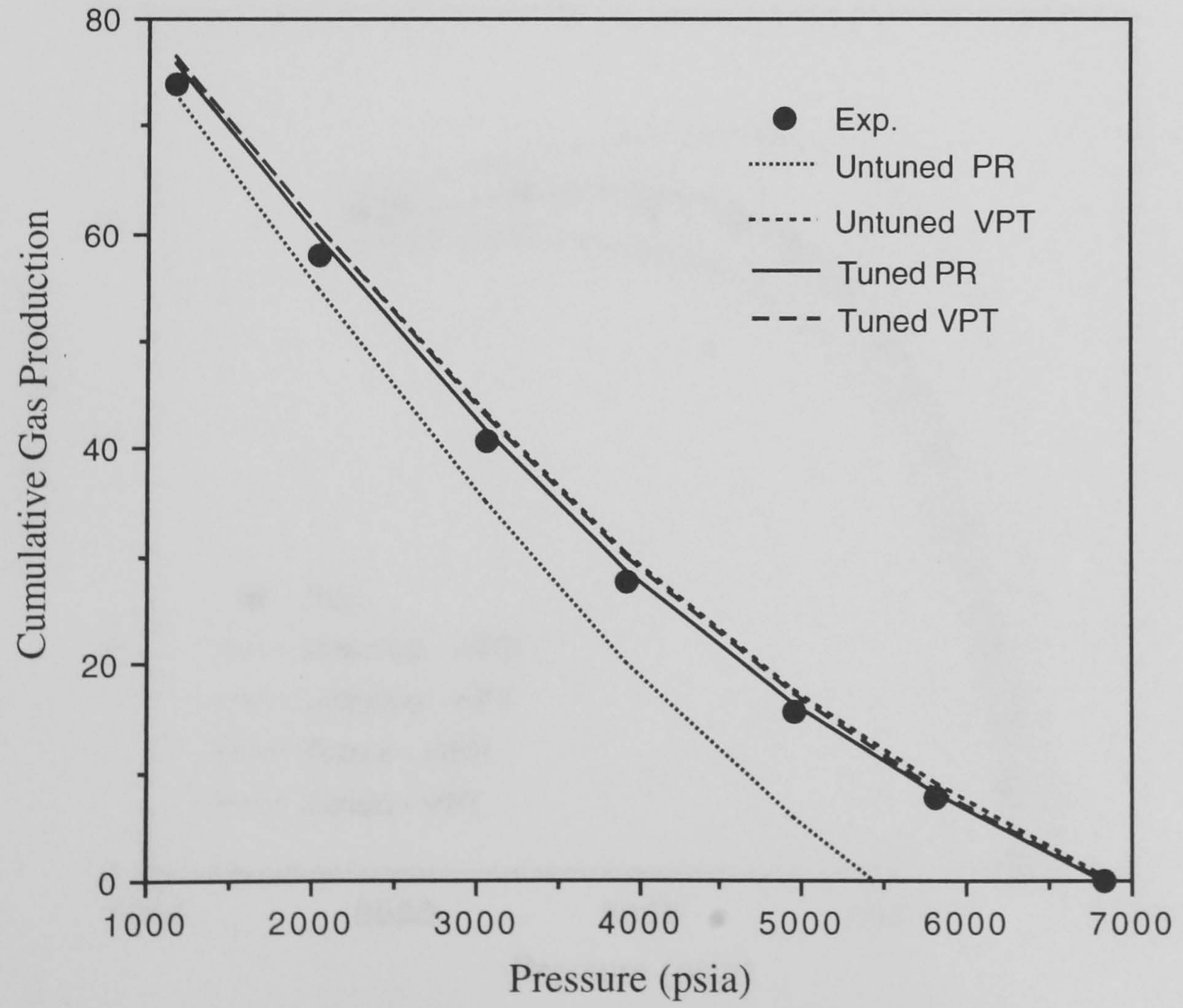

Fig. 3.17 - Cumulative Gas Production of Gas Condensate GCX89-1 in Constant Volume Depletion (CVD) Test.

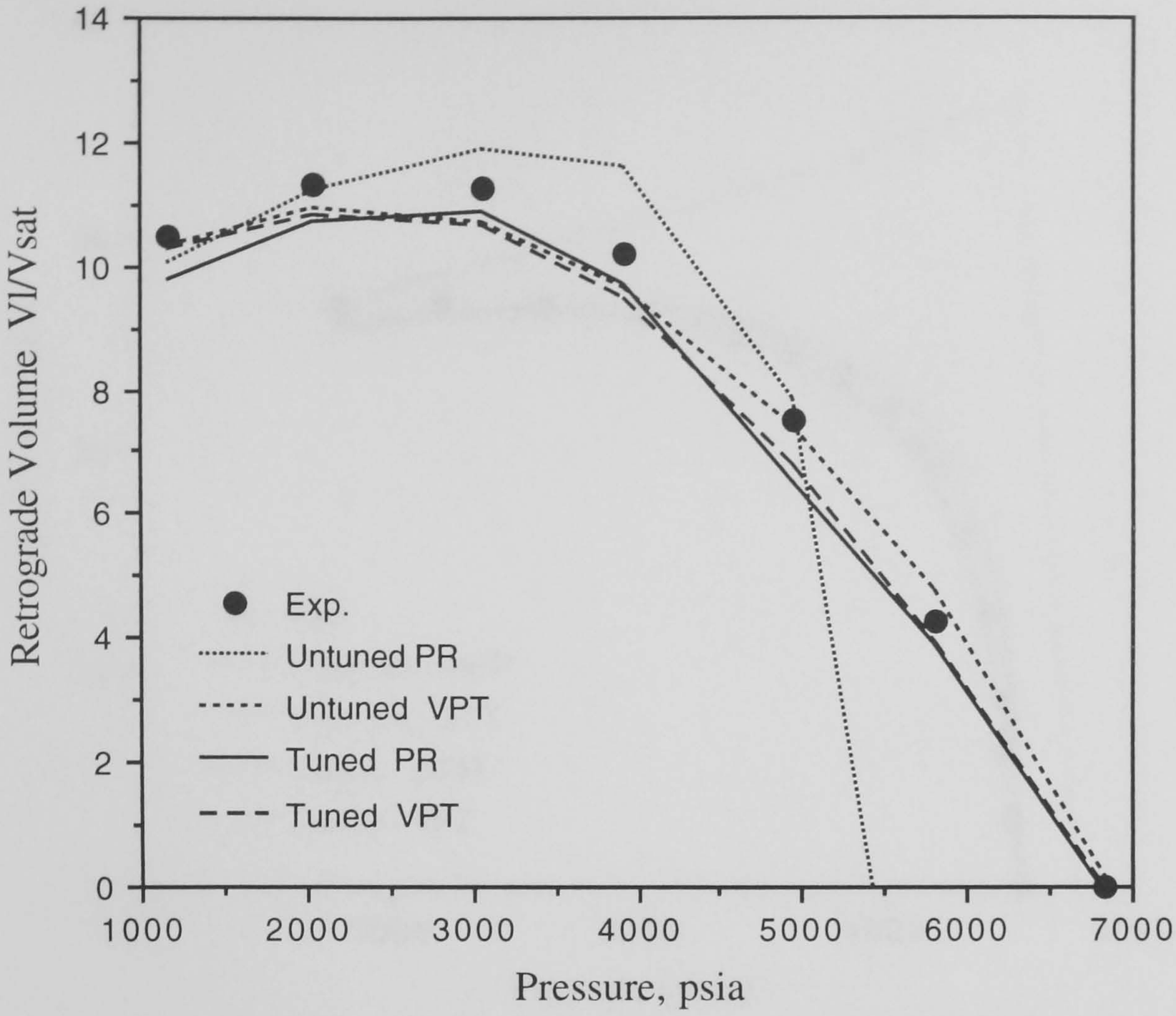

Fig. 3.18 - Variations of Liquid Volume Fraction Relative to Saturation Volume of Gas Condensate GCX89-1 in CVD Test.

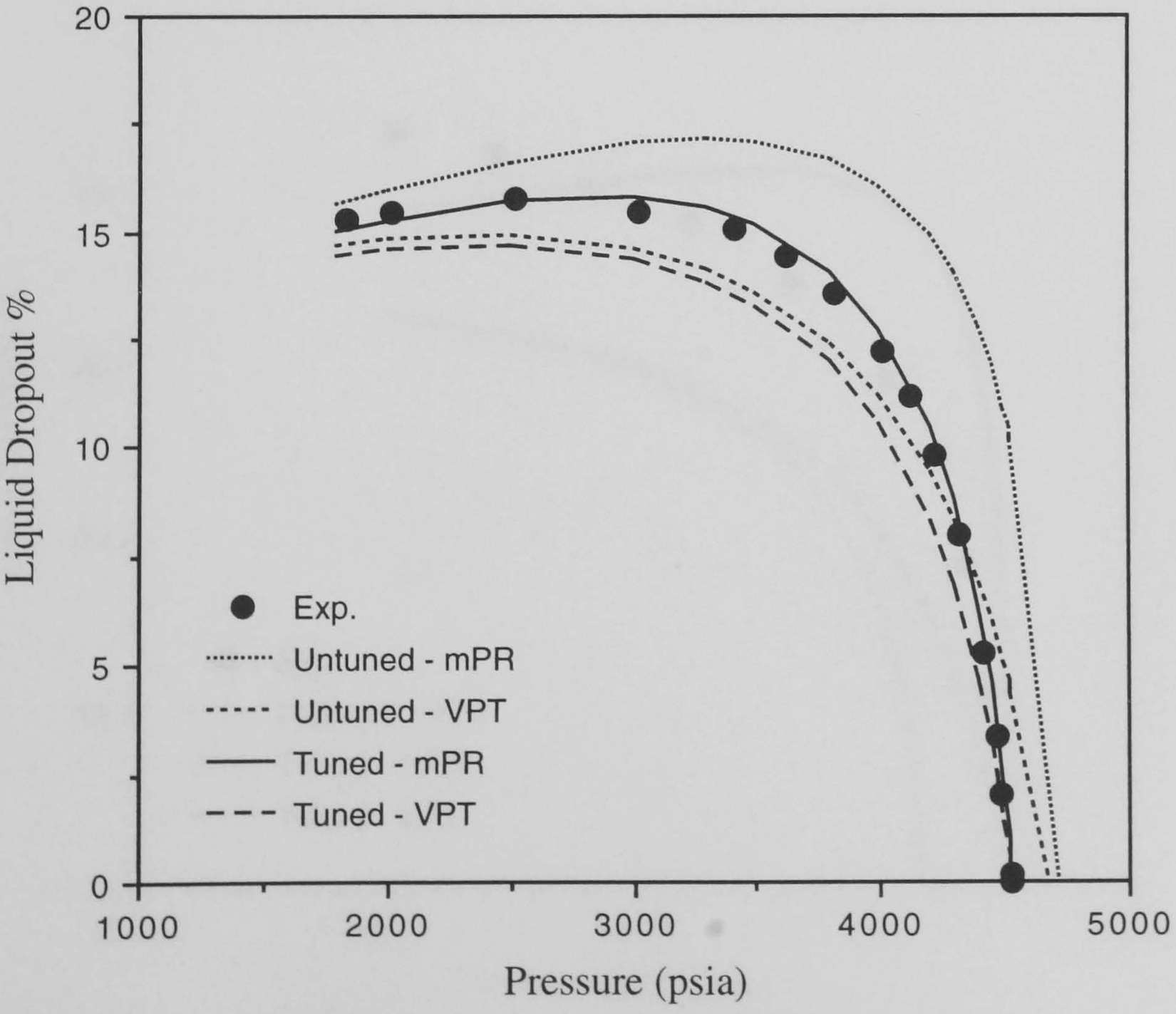

Fig. 3.19 - Liquid Dropout of 5-component Model Gas Condensate (GMX89-1) at 110°C.

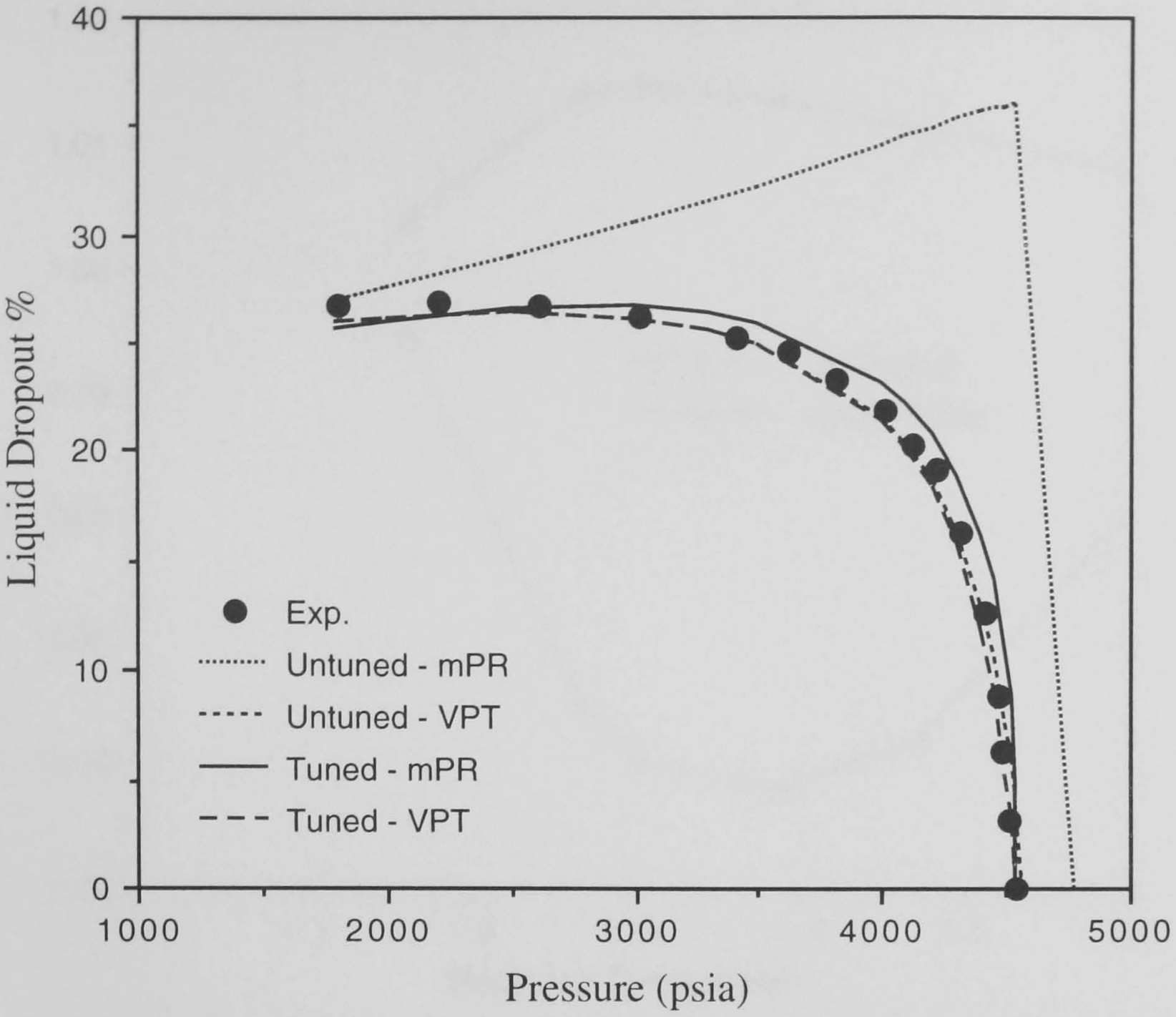

Fig. 3.20 - Liquid Dropout of 5-component Model Gas Condensate (GMX89-1) at 40°C.

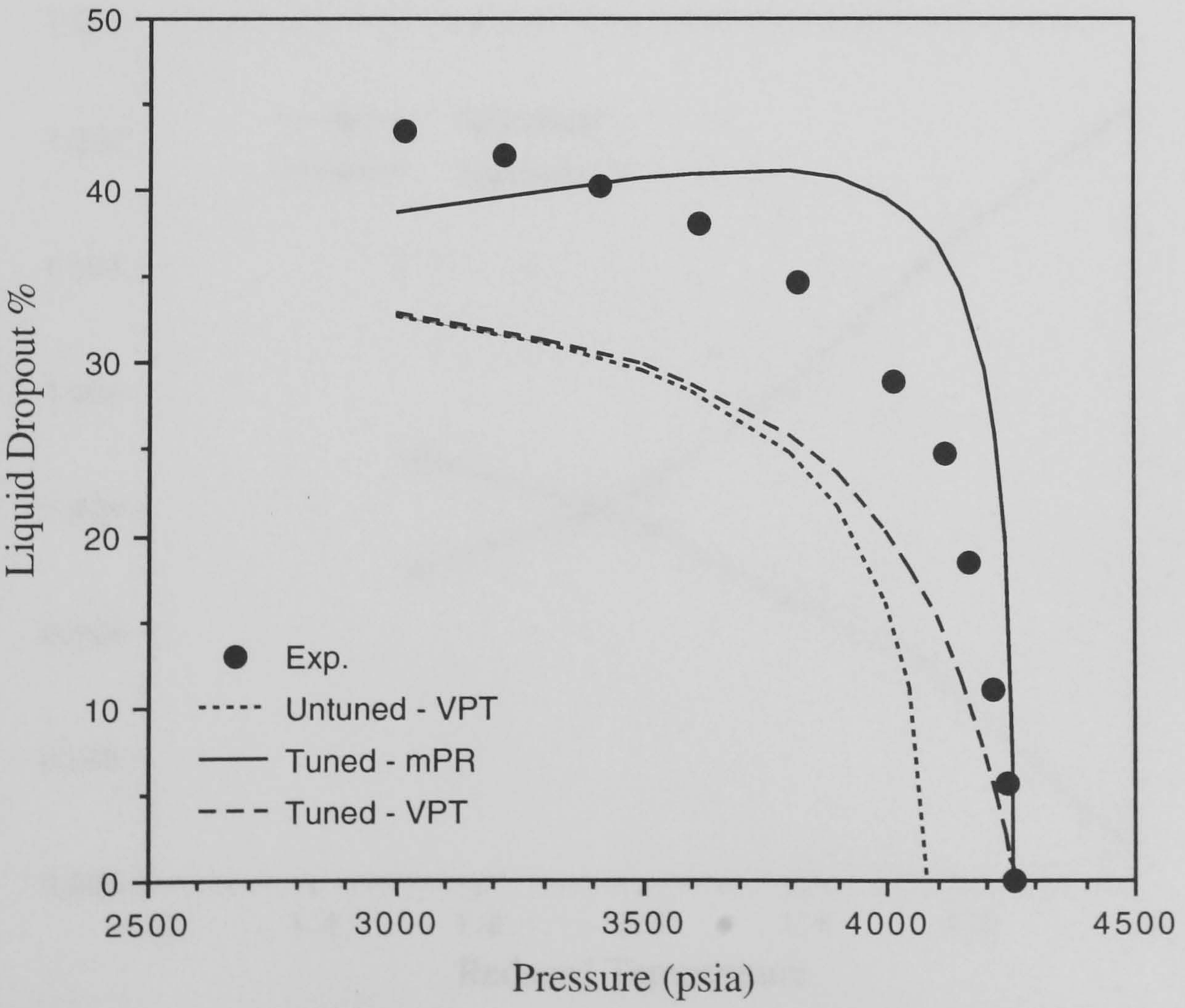

Fig. 3.21 - Liquid Dropout of 5-component Model Gas Condensate (GMX89-1) at 5°C.

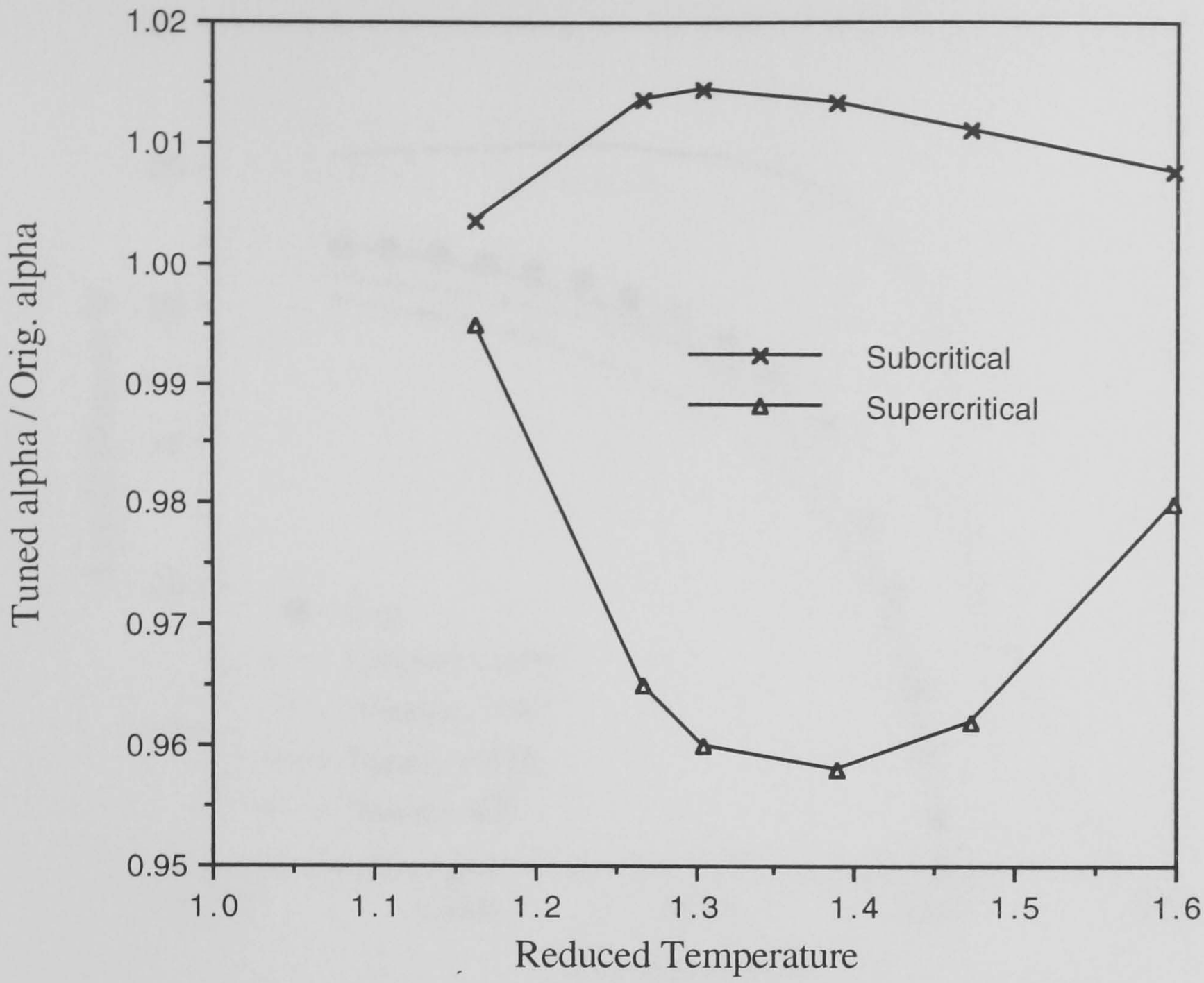

Fig. 3.22 - Variation of Tuned alpha Parameter of Sub and Supercritical Components in the Liquid Phase with Reduced Temperature, 5-component Model Gas Condensate (GMX89-1), mPR EOS.

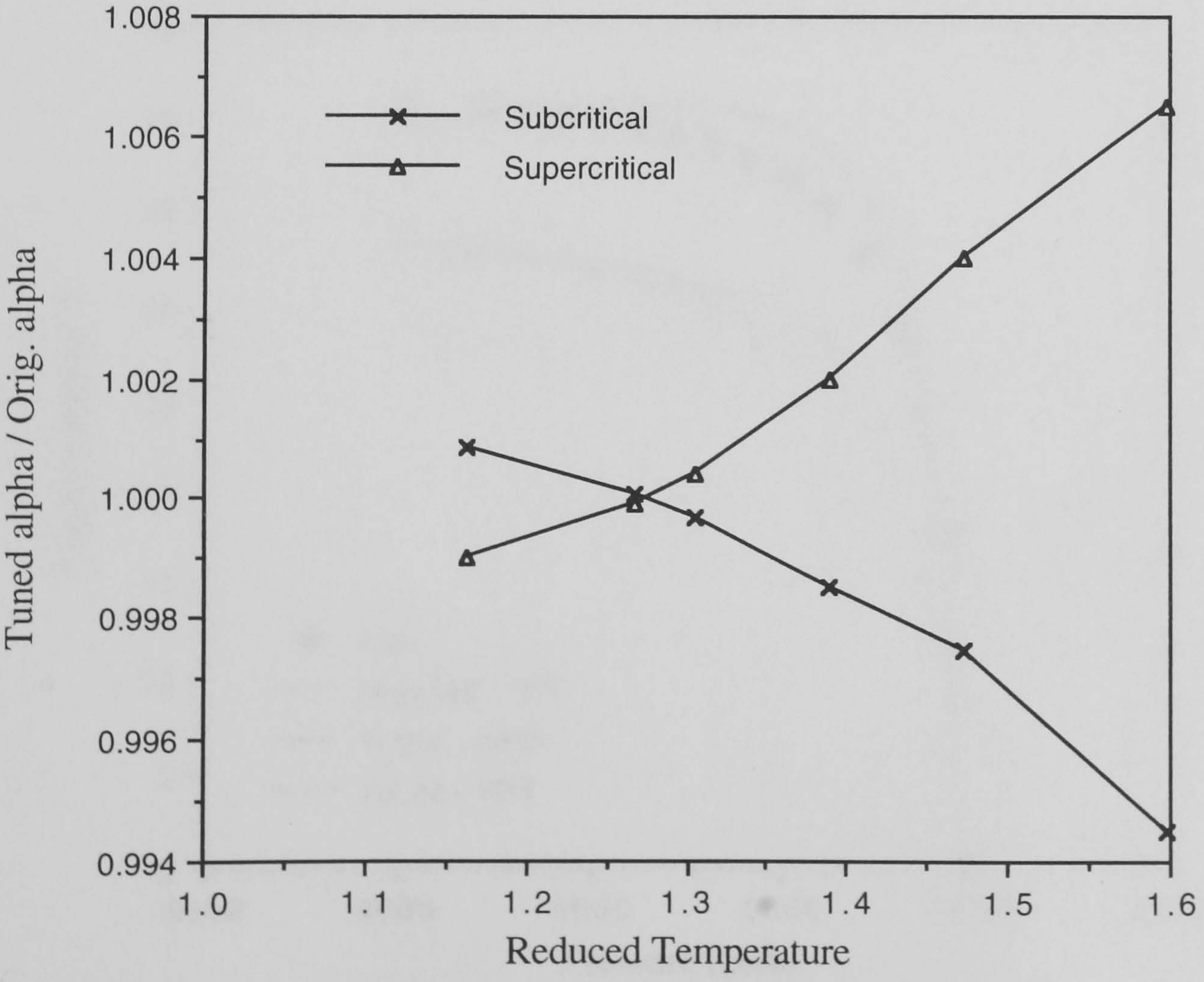

Fig. 3.23 - Variation of Tuned alpha Parameter of Sub and Supercritical Components in the Liquid Phase with Reduced Temperature, 5-component Model Gas Condensate (GMX89-1), VPT EOS.

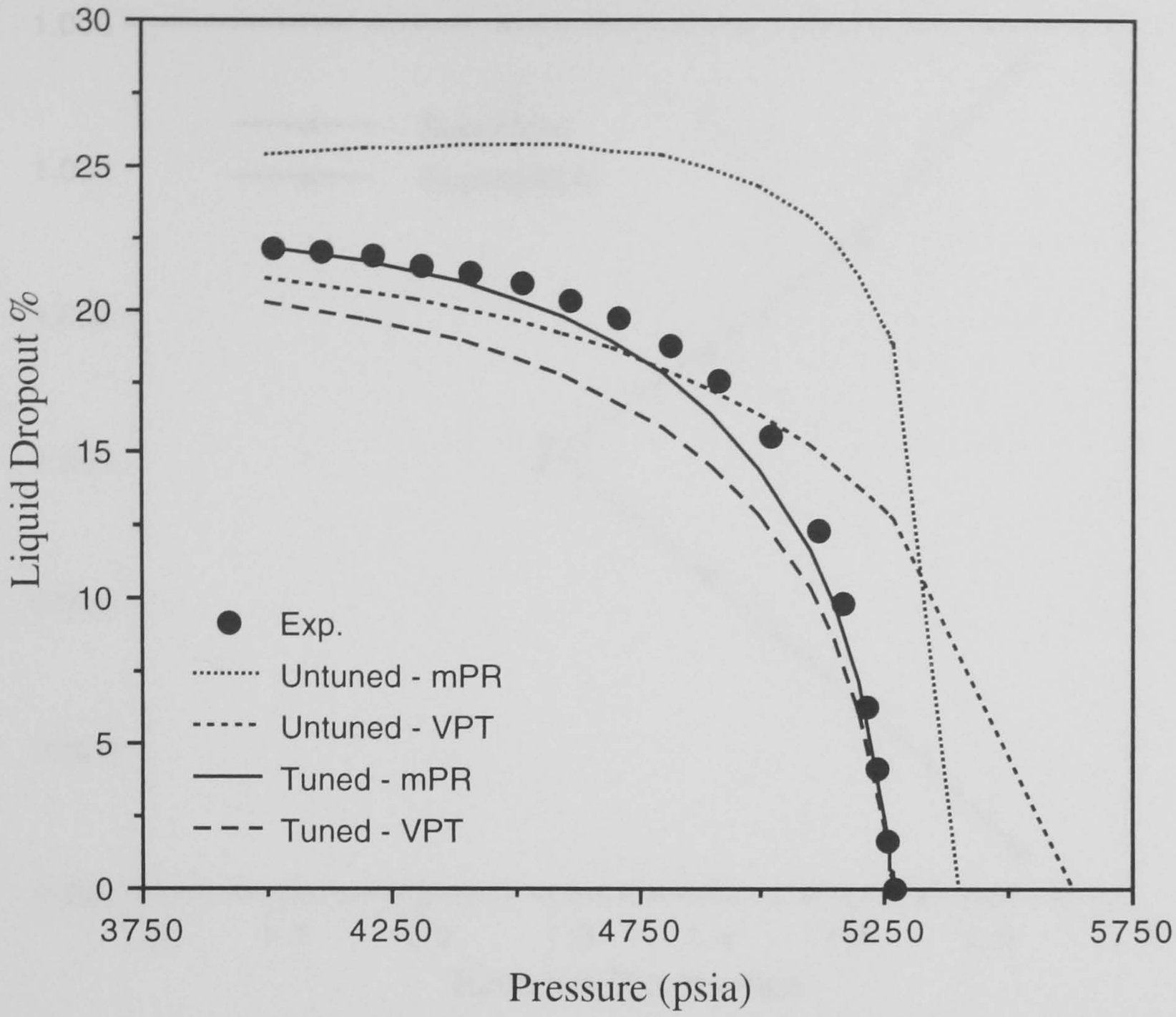

Fig. 3.24 - Liquid Dropout of 20-component Model Gas Condensate (GMX90-1) at 121.1°C.

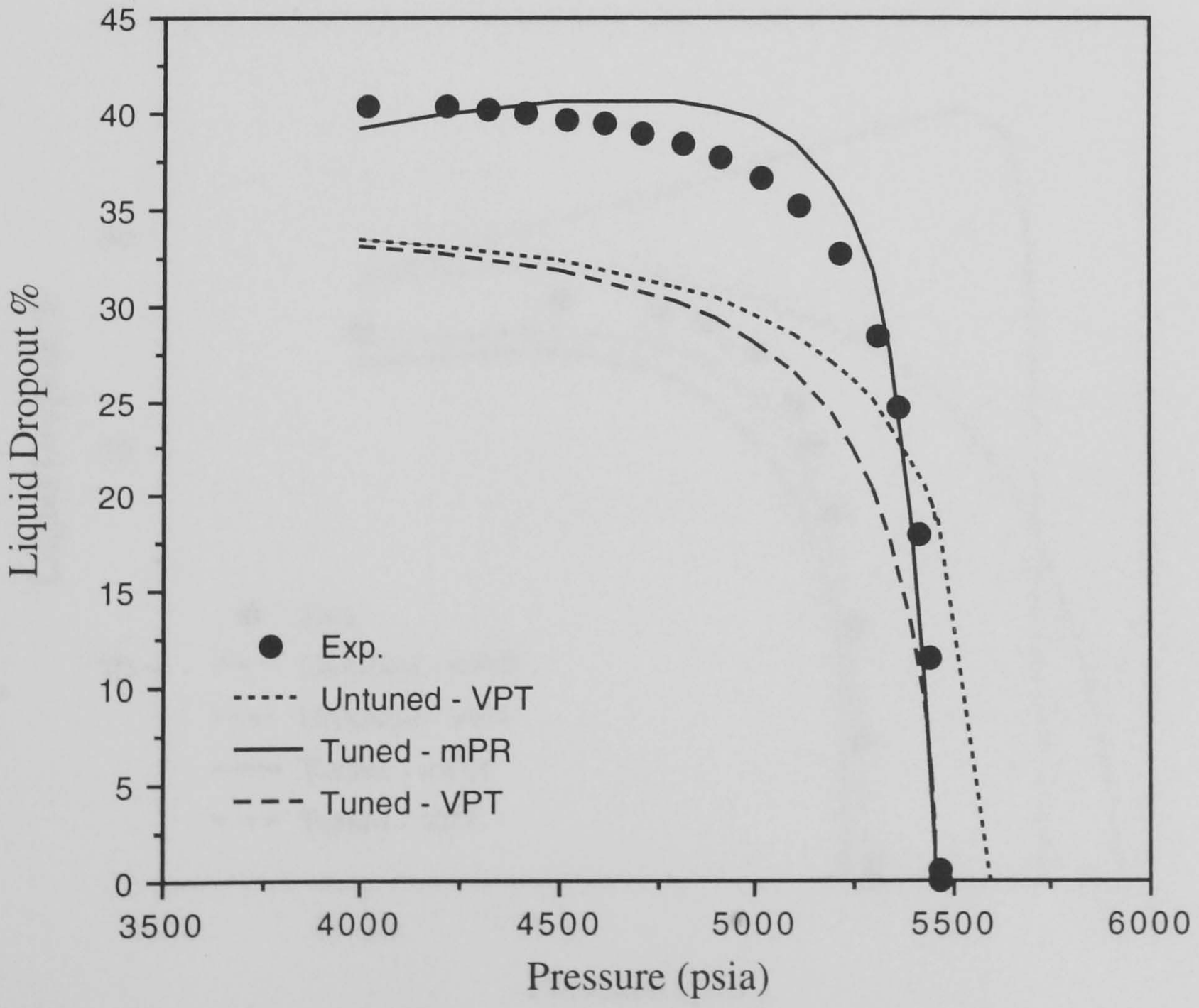

Fig. 3.25 - Liquid Dropout of 20-component Model Gas Condensate (GMX90-1) at 37.7°C.

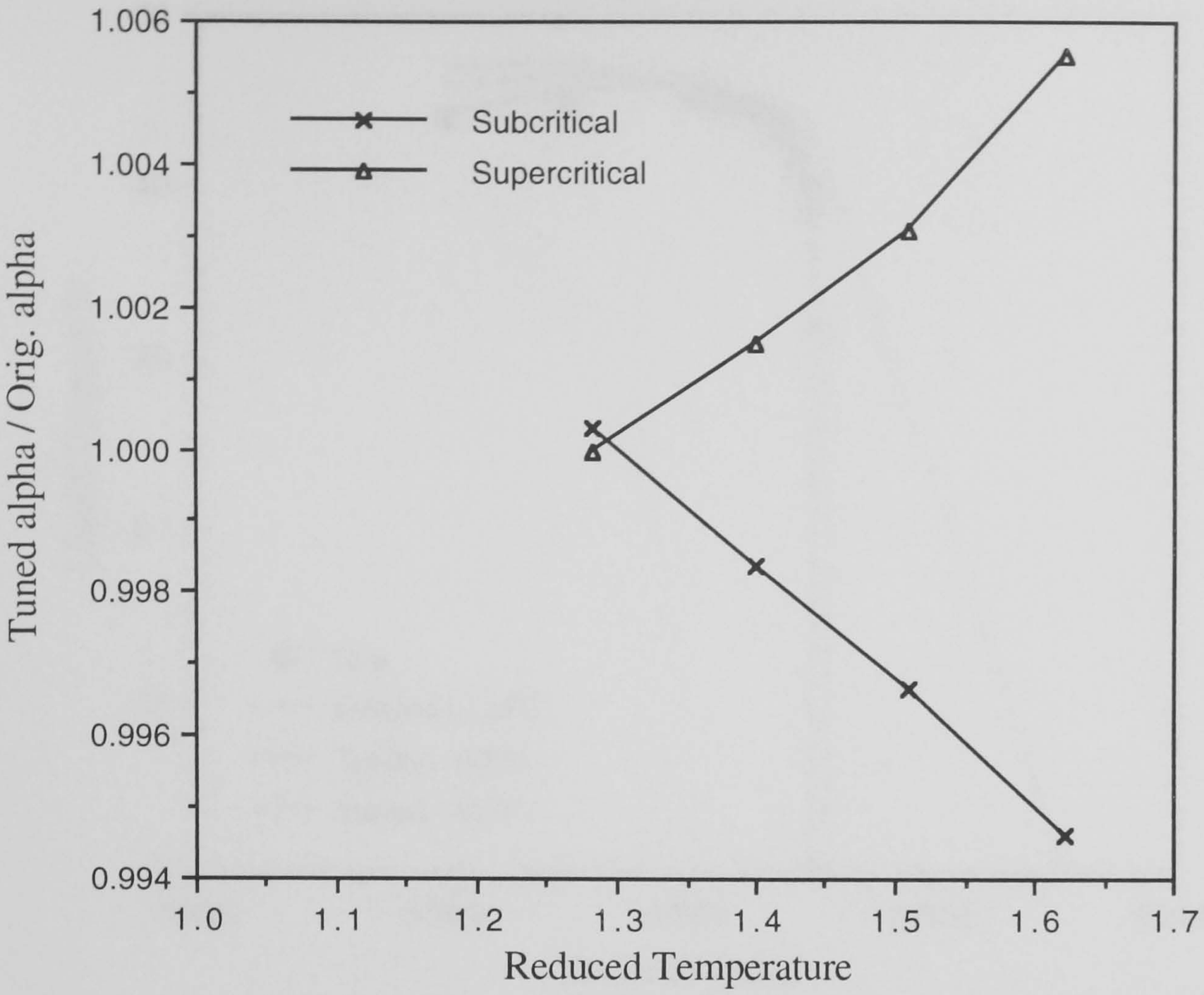

Fig. 3.26 - Variation of Tuned alpha Parameter of Sub and Supercritical Components in the Liquid Phase with Reduced Temperature, 20-component Model Gas Condensate (GMX90-1), VPT EOS.

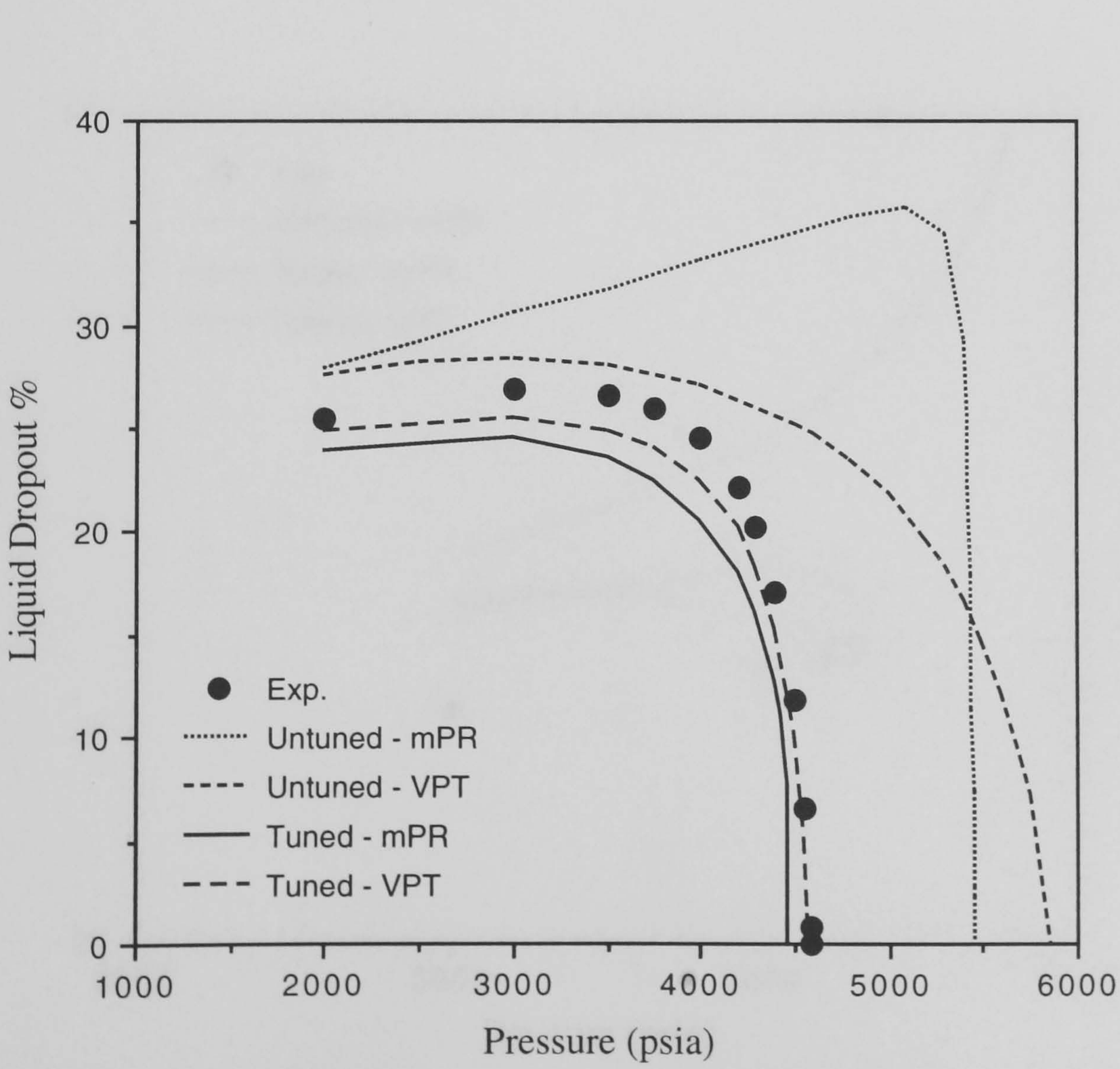

Fig. 3.27 - Liquid Dropout of Near Critical Fluid (NCF) from CCE Test at 140°C.

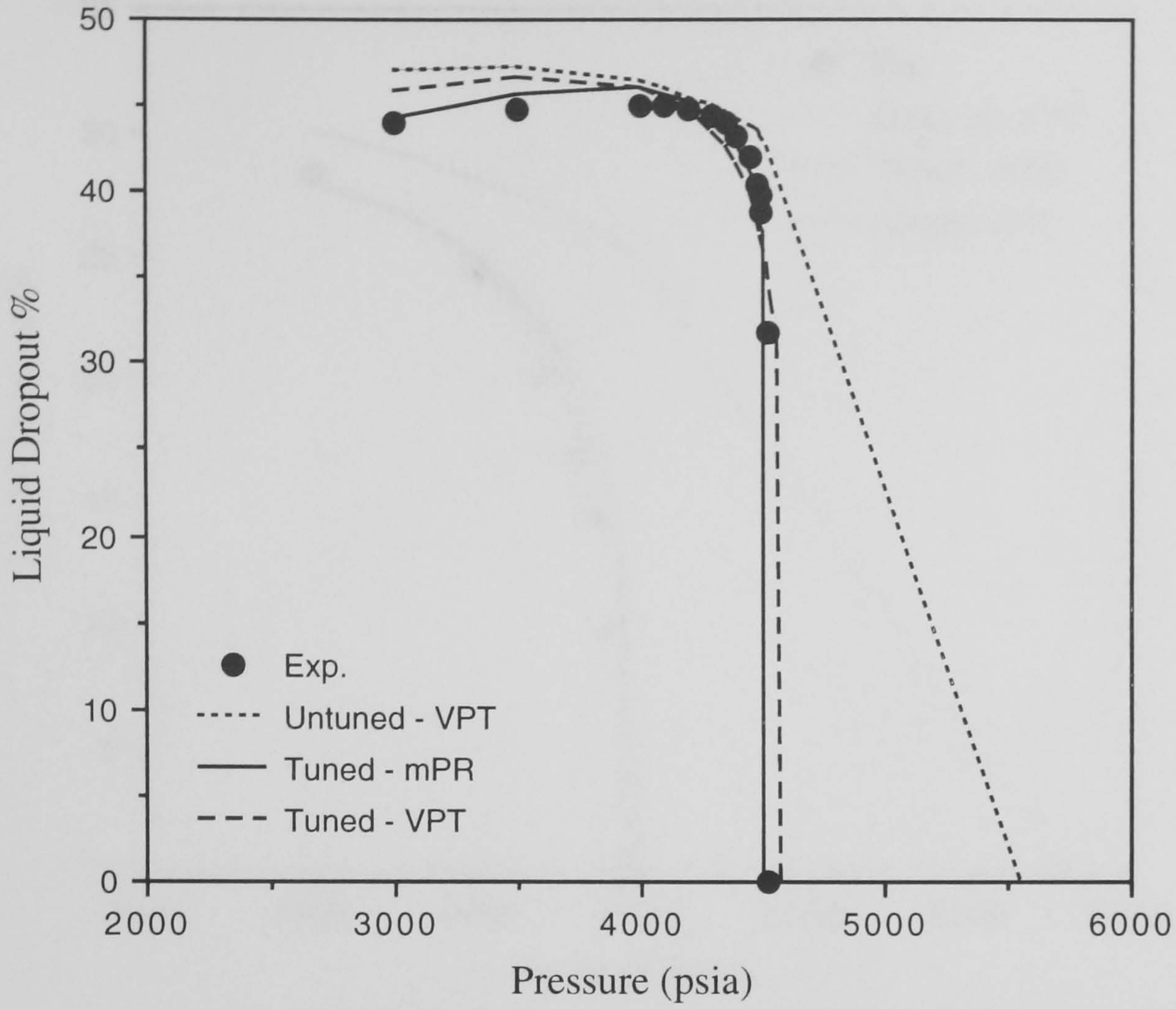

Fig. 3.28 - Liquid Dropout of Near Critical Fluid (NCF) from CCE Test at 50°C.

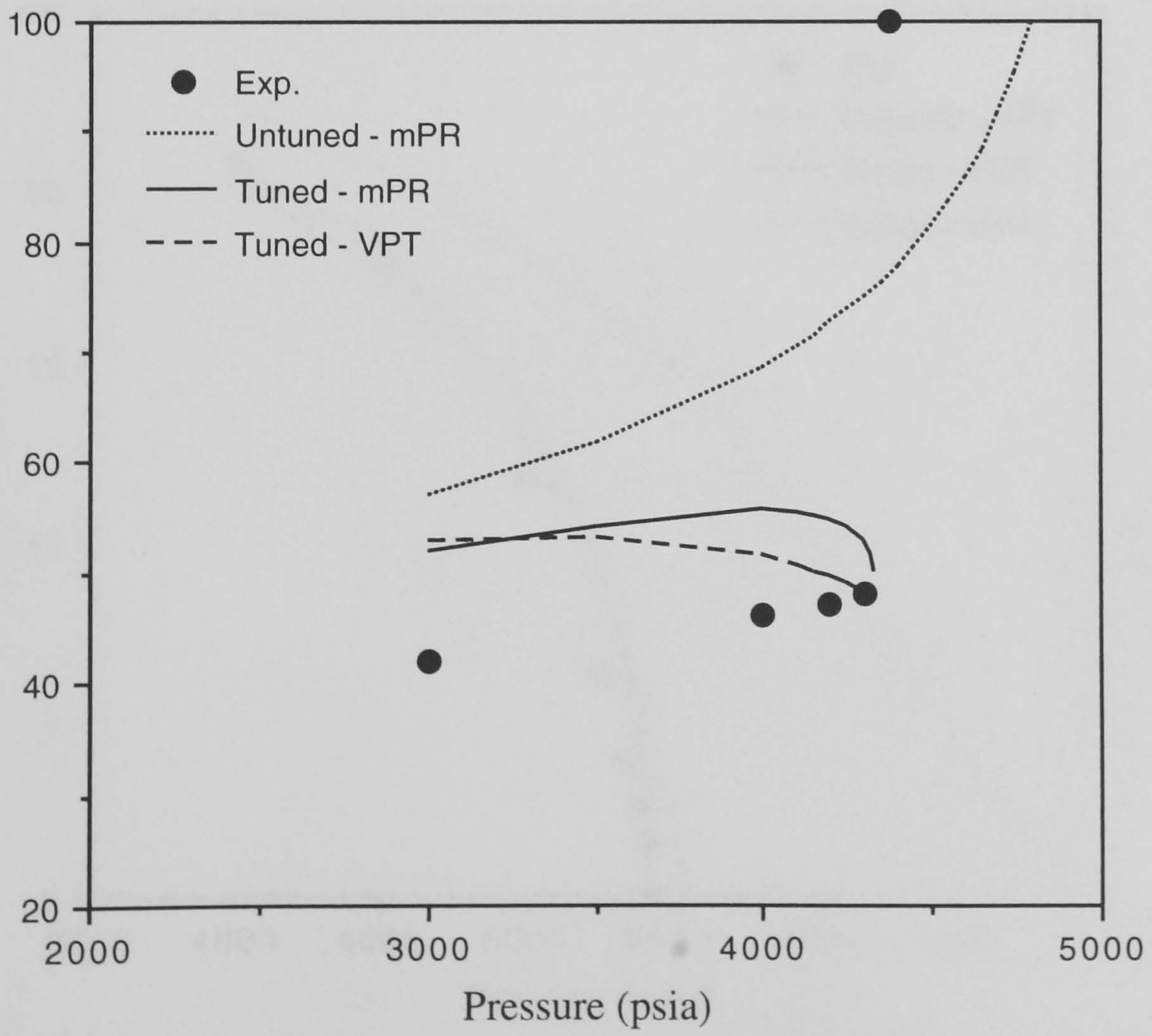

Fig. 3.29 - Liquid Dropout of Near Critical Fluid (NCF) from CCE Test at 25°C.

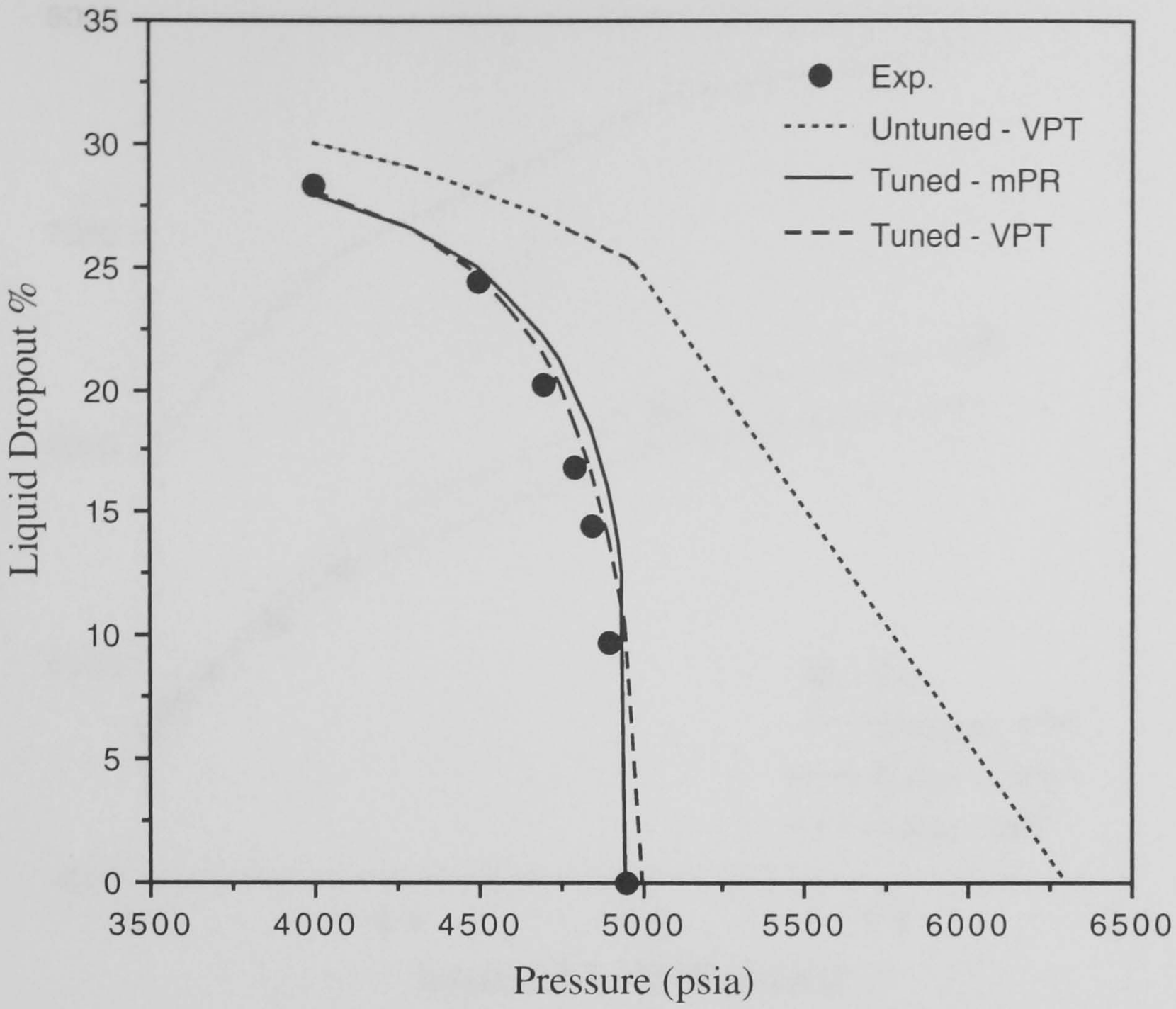

Fig. 3.30 - Liquid Dropout of Near Critical Fluid (NCF) after 0.1285 moles Methane Injected / mole NCF (Stage 3) - CCE Test, 100°C.

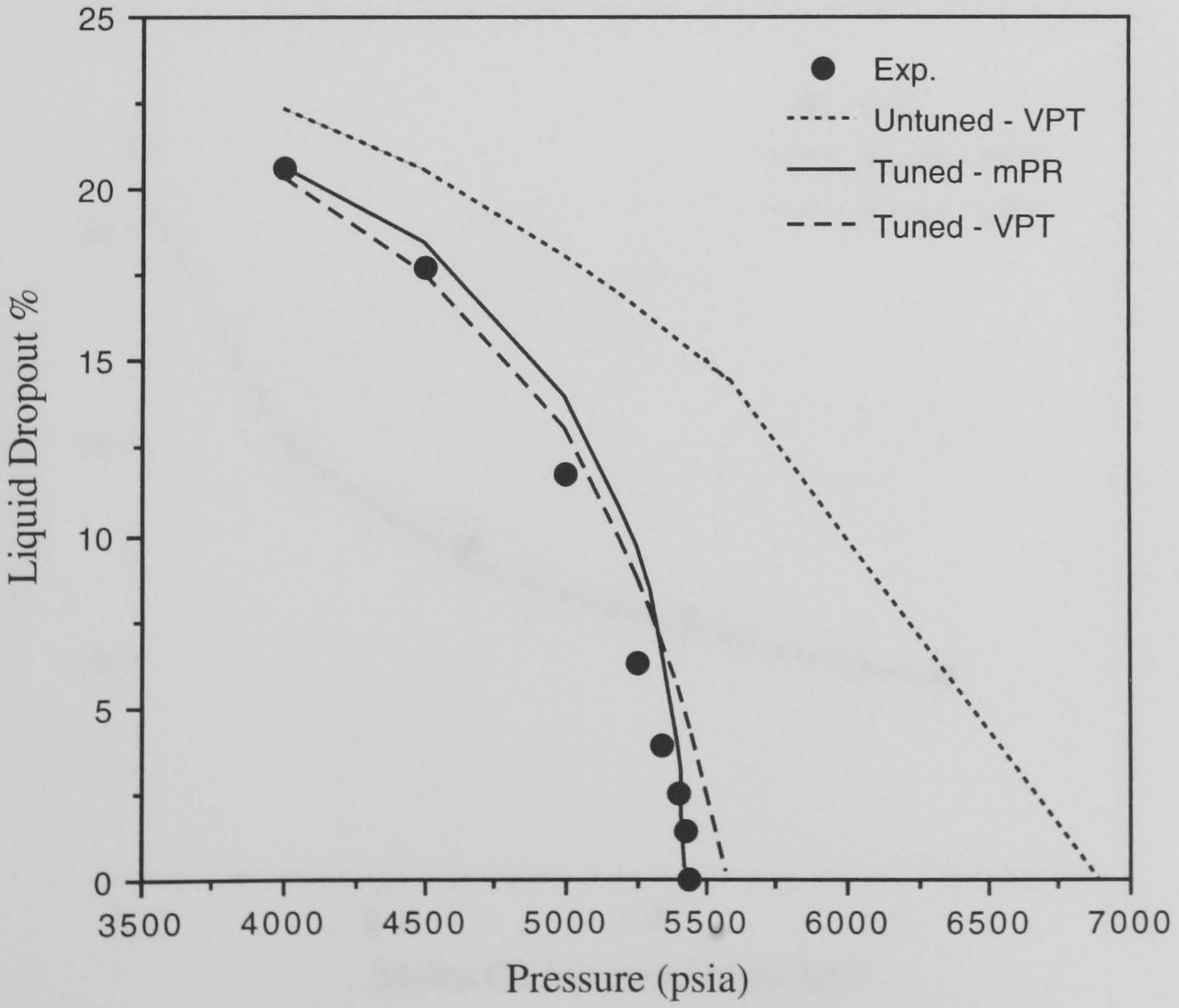

Fig. 3.31 - Liquid Dropout of Near Critical Fluid (NCF) after 0.3928 moles Methane Injected / mole NCF (Stage 5) - CCE Test 100°C.

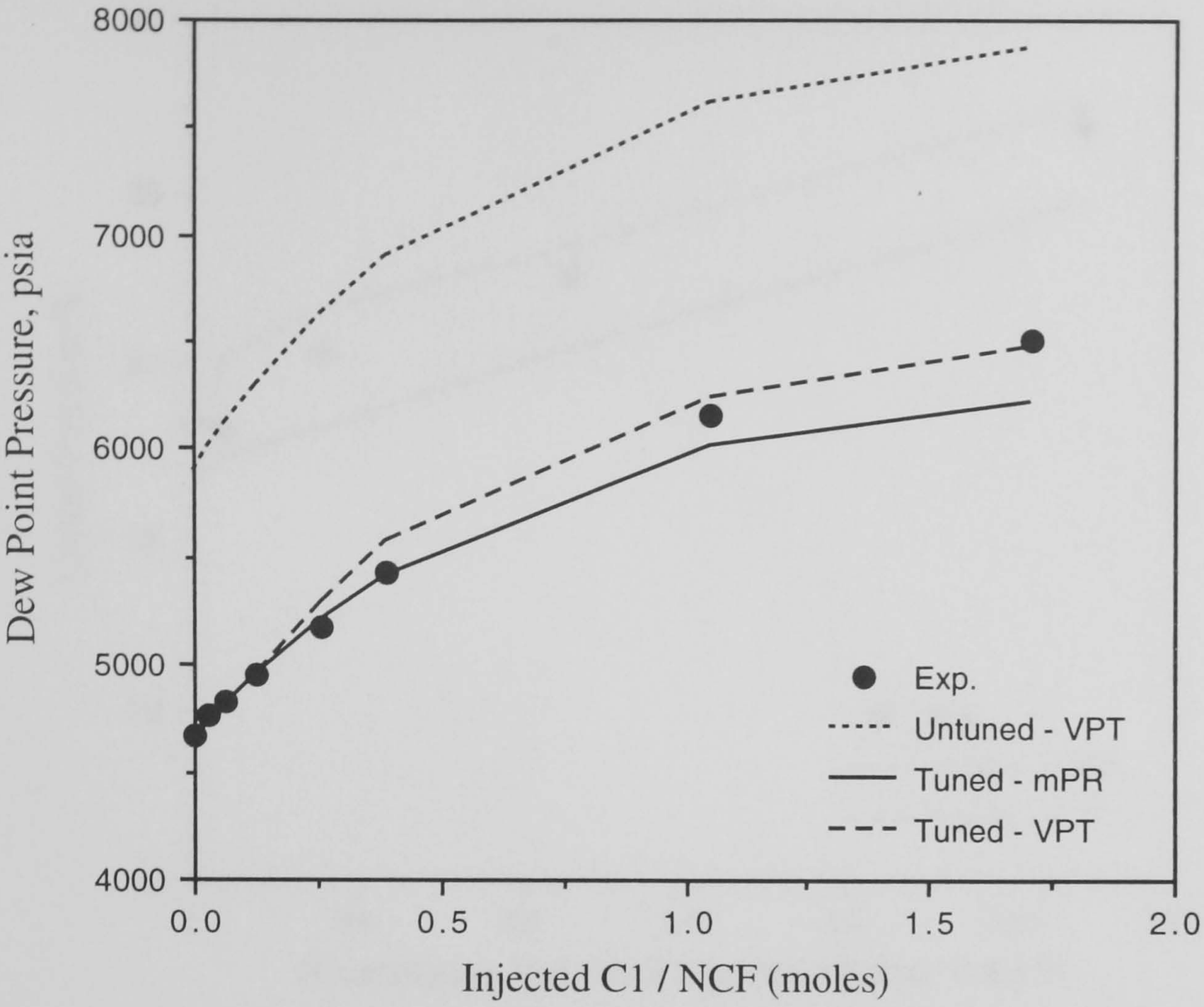

Fig. 3.32 - Variation of the Dew Point Pressure with Methane Injected in Near Critical Fluid (NCF) at 100°C.

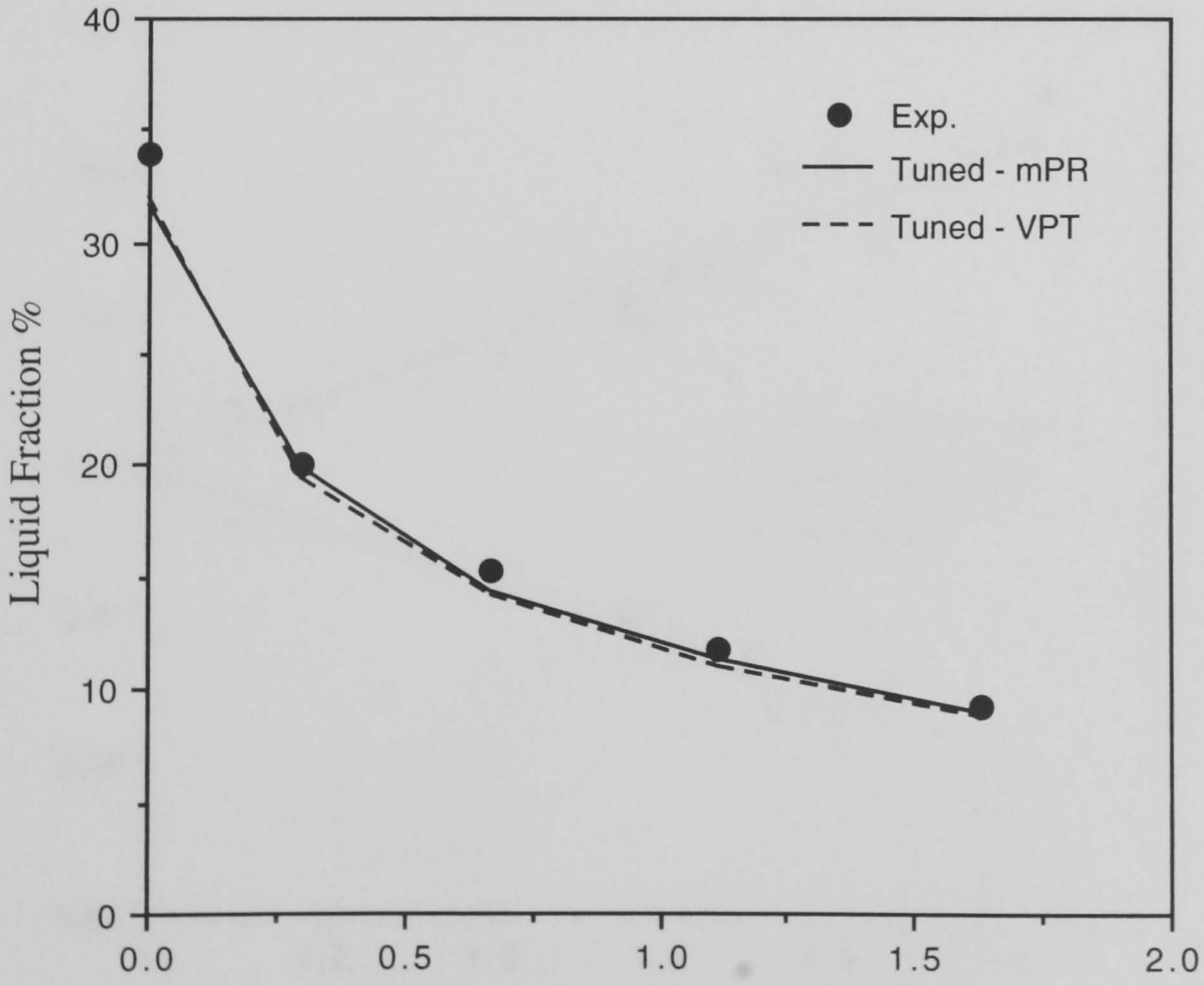

Fig. 3.33 - Liquid Fraction of Near Critical Fluid (NCF) with Methane Cycling at 100°C and 4000 psia.

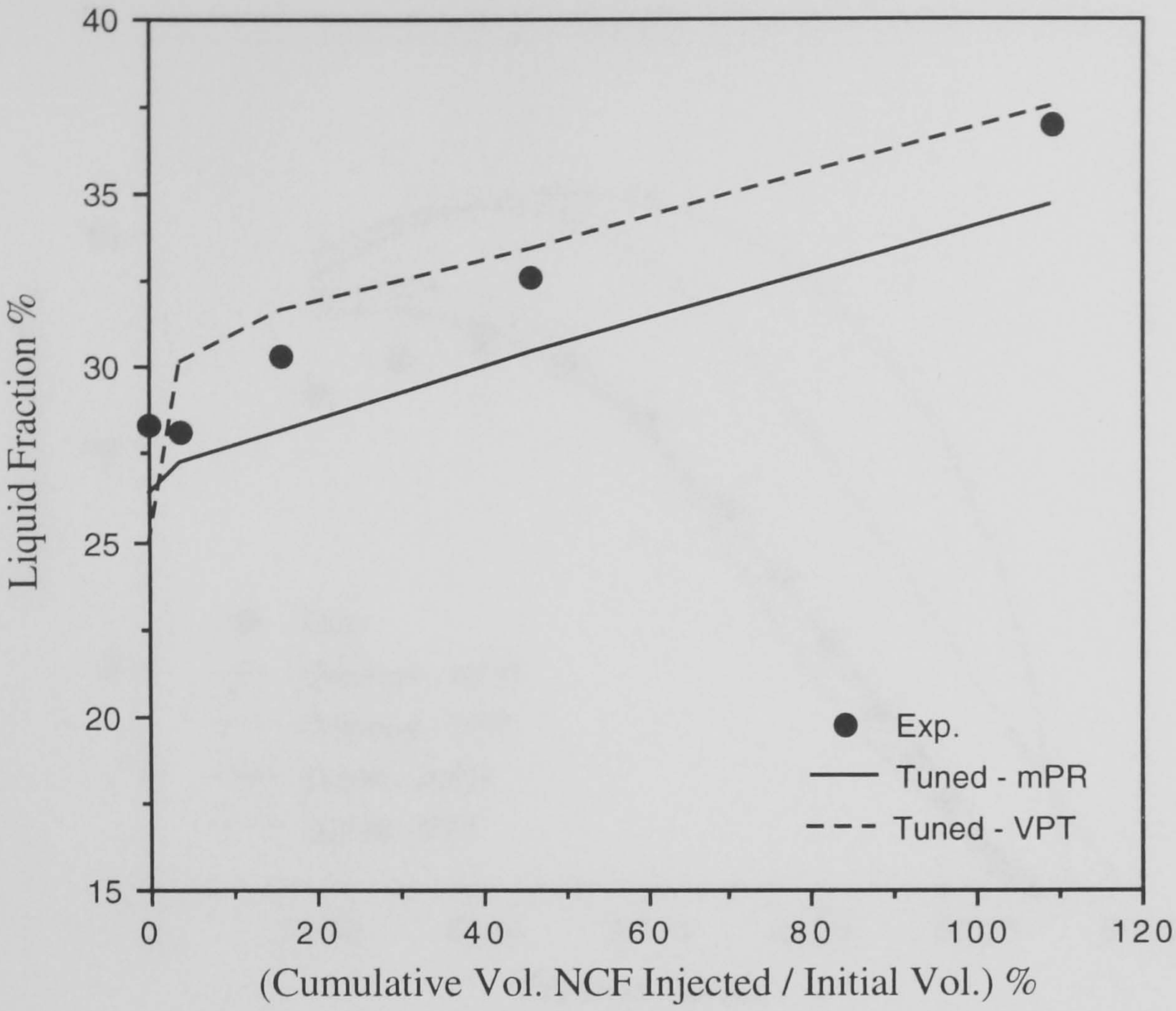

Fig. 3.34 - Liquid Fraction versus Percentage Cumulative Volume NCF Injected / Initial Volume - Condensate Accumulation Near the Well Bore at 100°C and 4550 psia.

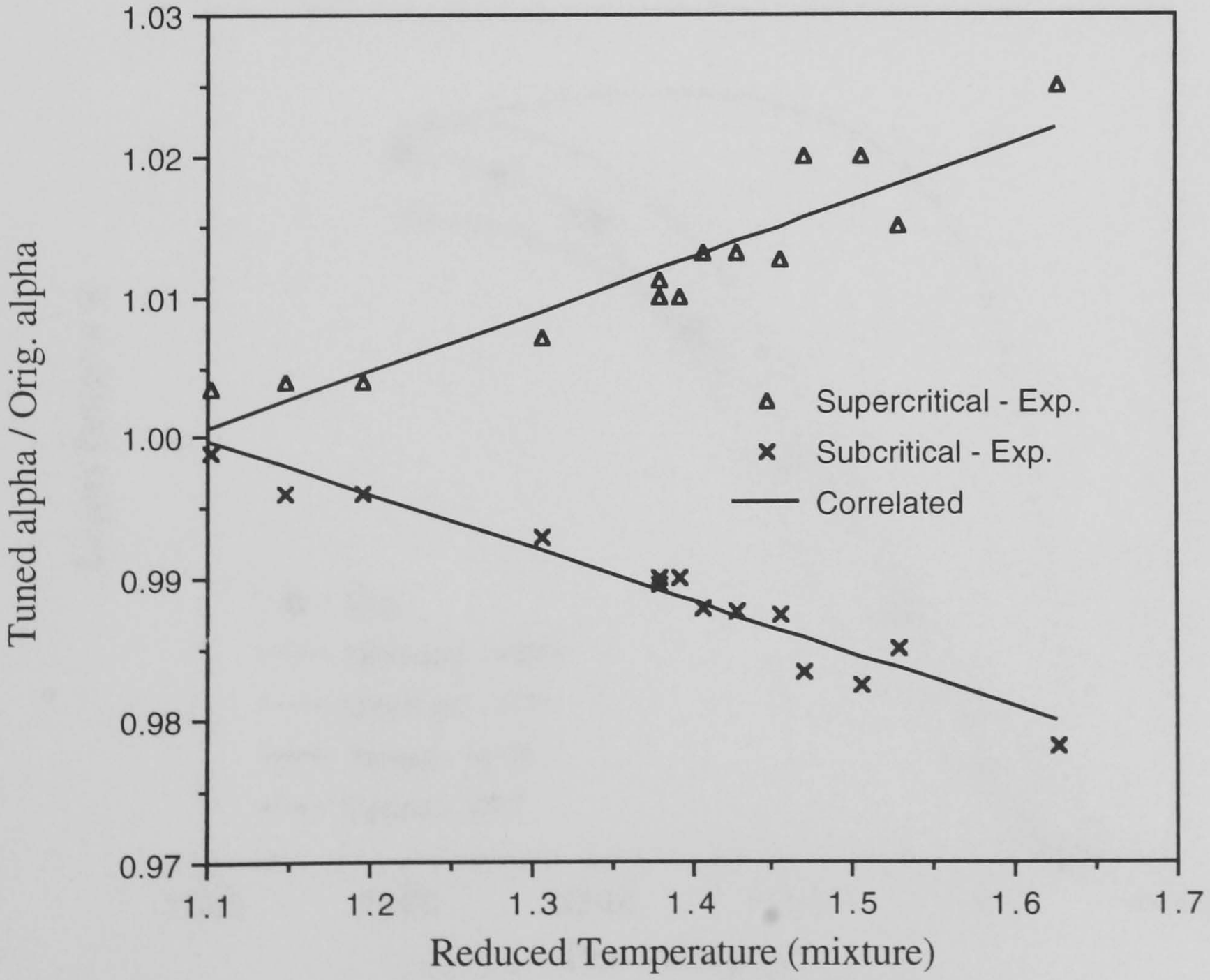

Fig. 3.35 - Variation of Tuned alpha for Sub and Supercritical Components in the Liquid Phase with Reduced Temperature - Near Critical Fluid (NCF), VPT EOS.

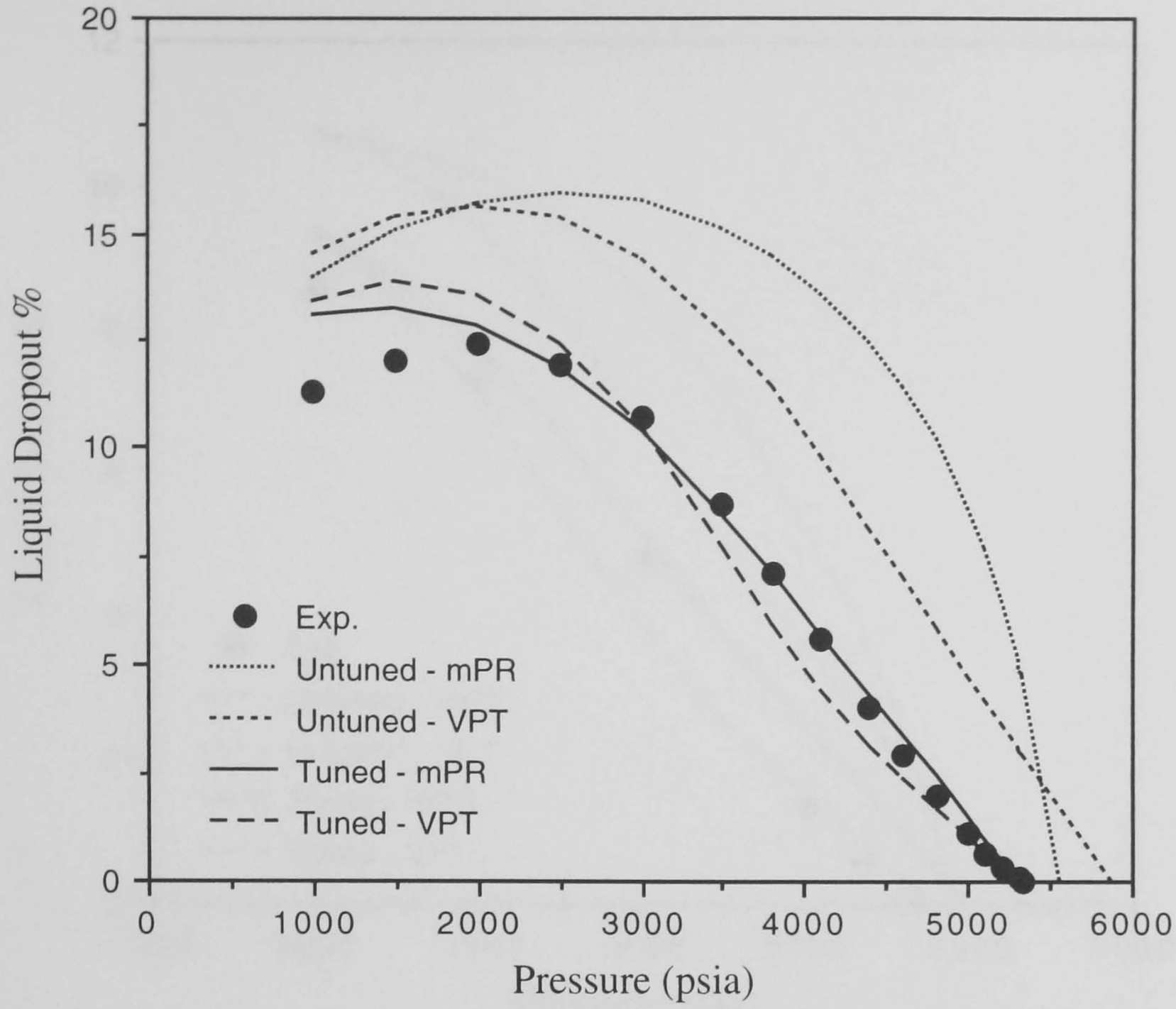

Fig. 3.36 - Liquid Dropout of Gas Condensate GCA94-1 from Constant Composition Expansion (CCE) Test at 110°C.

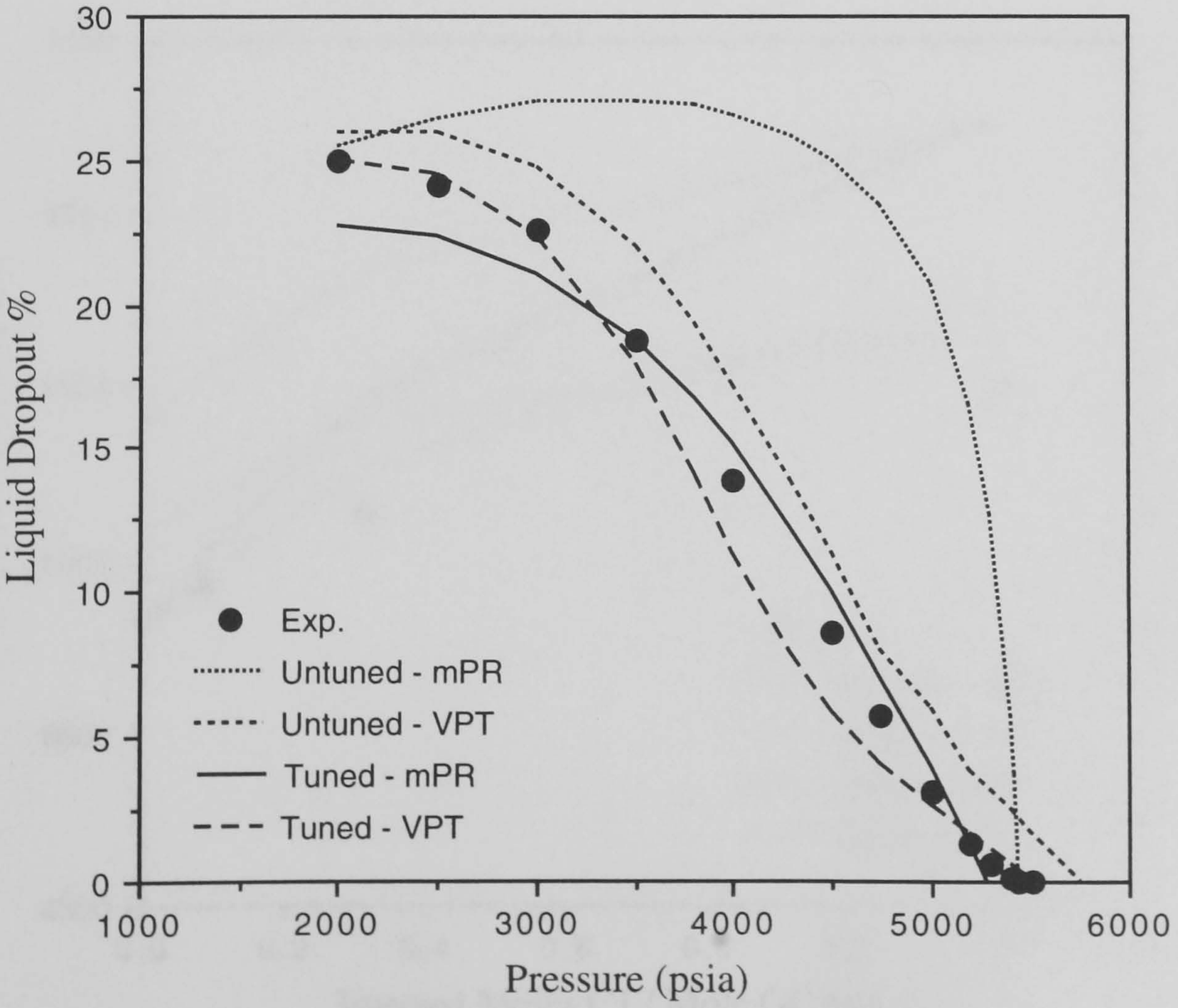

Fig. 3.37 - Liquid Dropout of Gas Condensate GCA94-1 from Constant Composition Expansion (CCE) Test at 50°C.

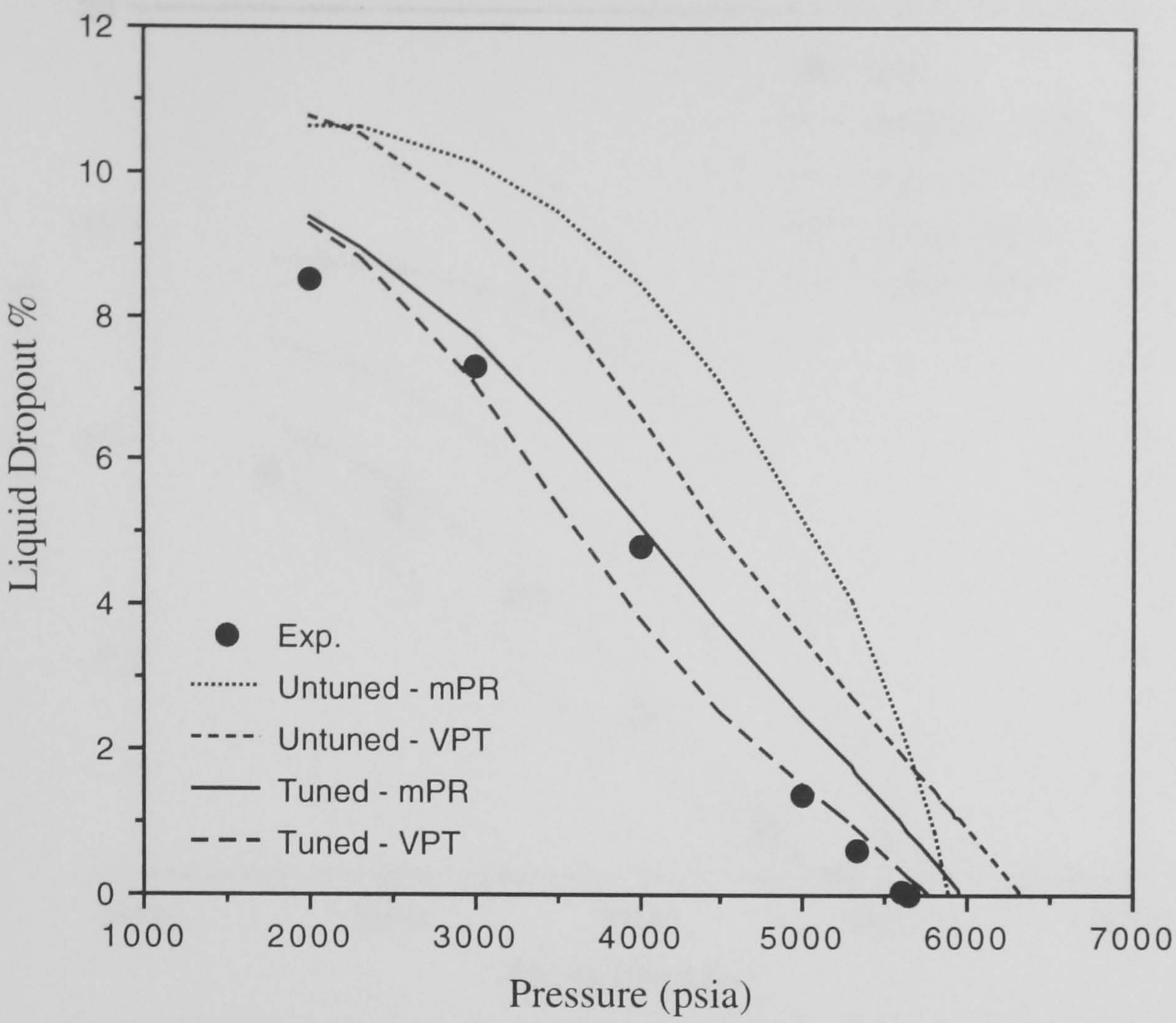

Fig. 3.38 - Liquid Dropout of Gas Condensate GCA94-1 at 110°C, 0.3119 moles C1 Injected / mole GCA94-1.

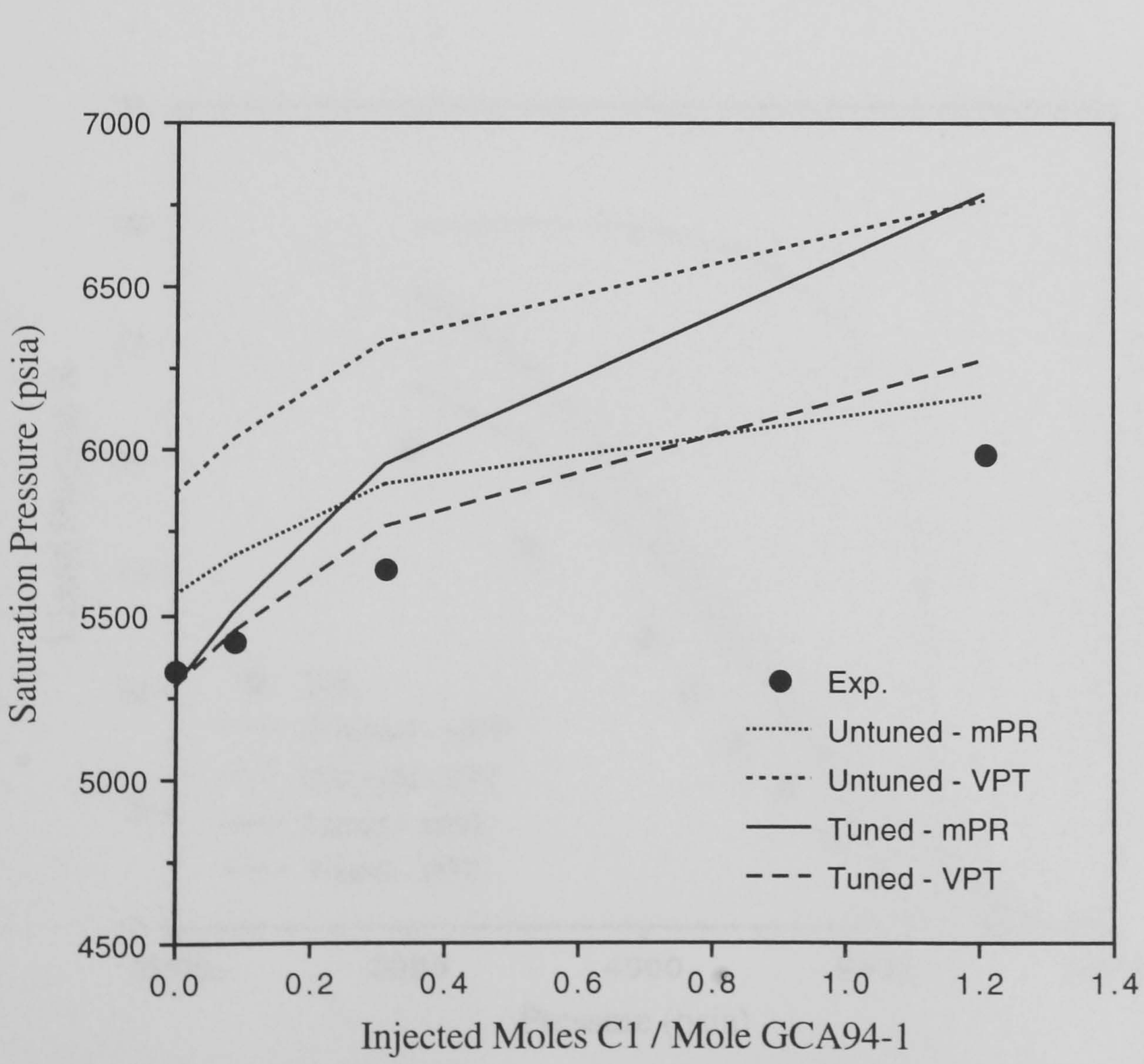

Fig. 3.39 - Variation of Saturation Pressure with Methane Injection into Gas Condensate GCA94-1 at 110°C.

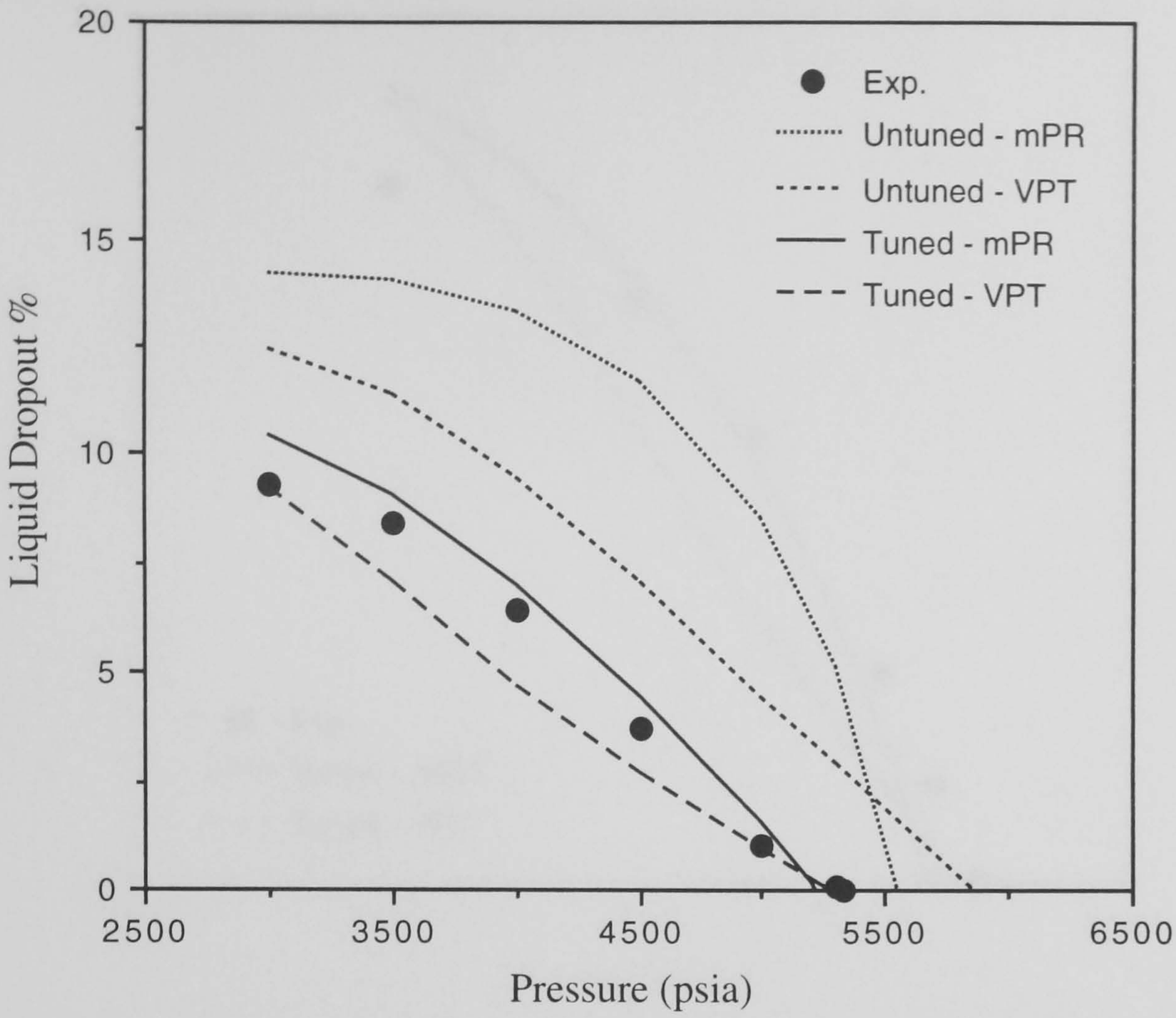

Fig. 3.40 - Liquid Dropout of Gas Condensate GCA94-1 from Constant Volume Depletion (CVD) Test at 110°C.

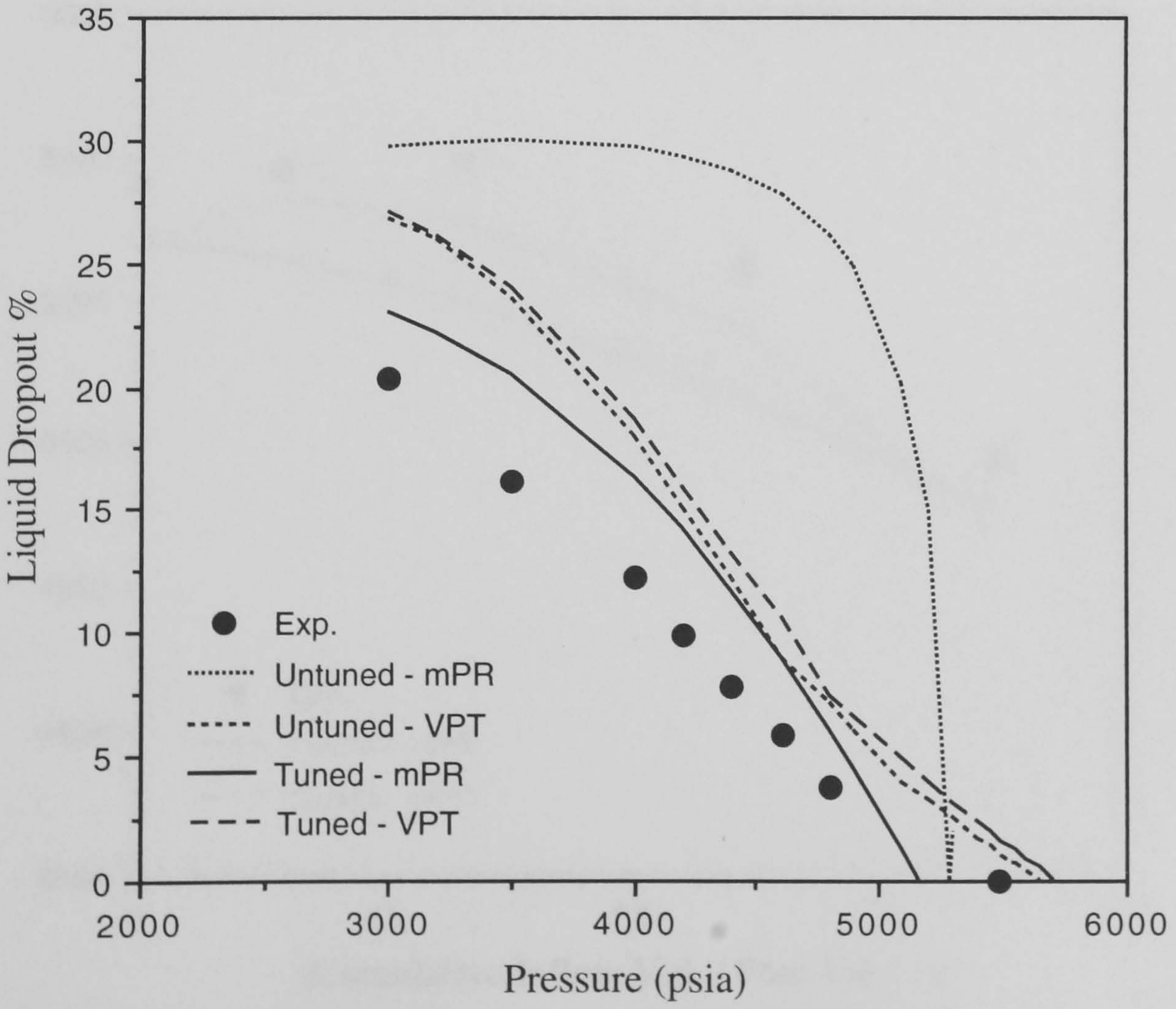

Fig. 3.41 - Liquid Dropout of Gas Condensate GCA94-1 from Constant Composition Expansion (CCE) Test at 37.8°C.

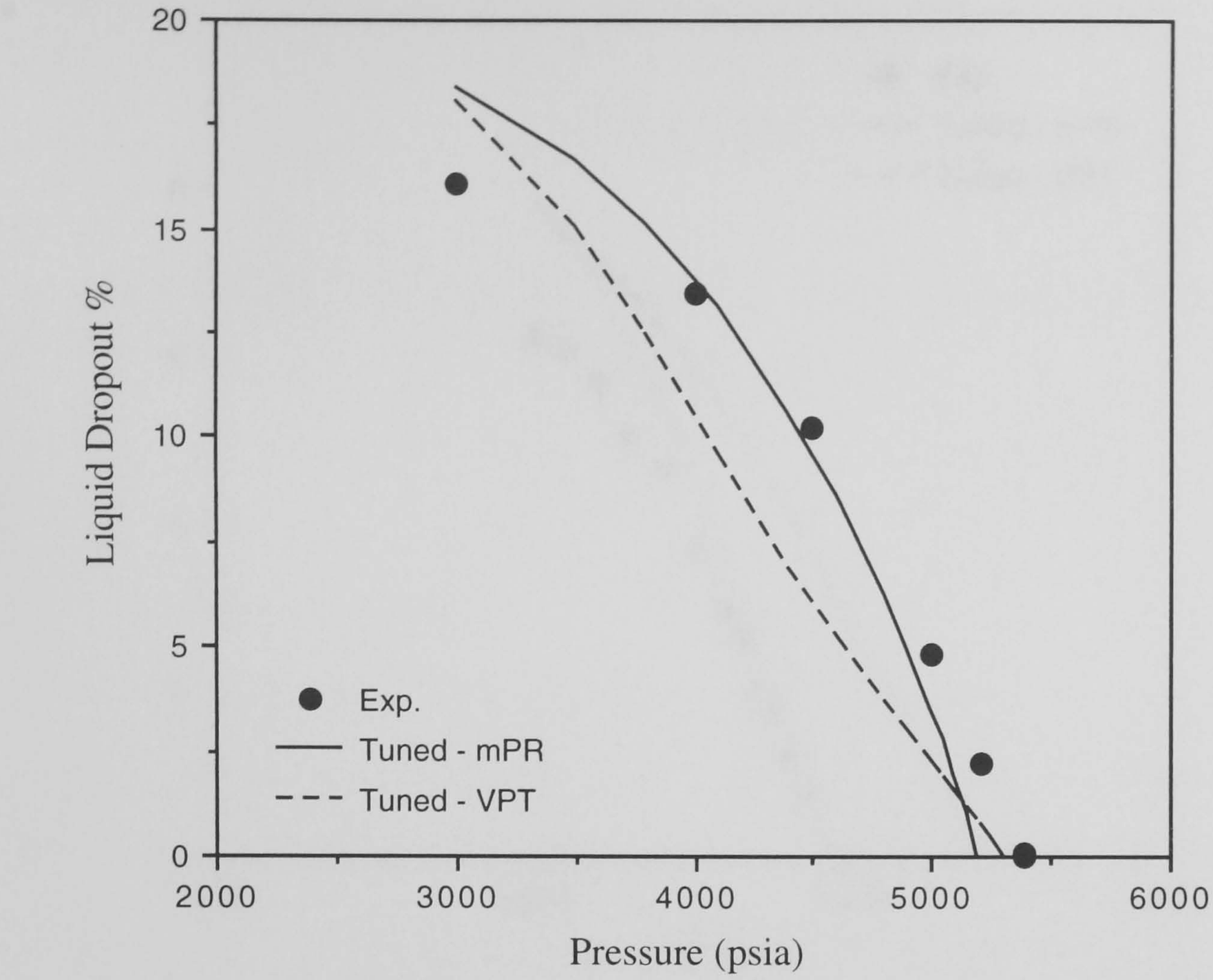

Fig. 3.42 - Condensate Accumulation Near the Welbore Test at 110°C and 3000 psia - Inflow Volume 52.62% Pore Volume, Gas Condensate GCA94-1.

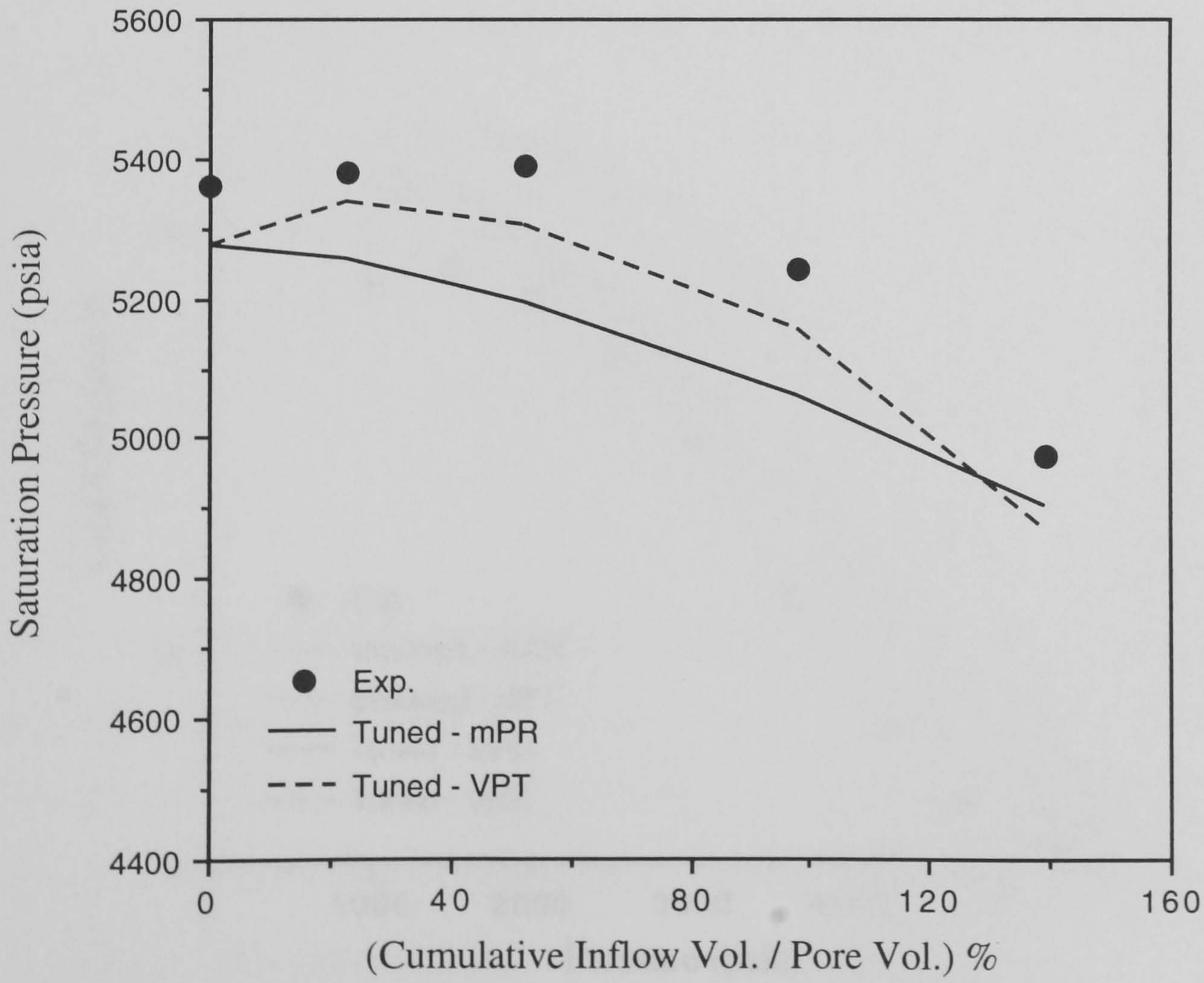

Fig. 3.43 - Variation of Saturation Pressure in Condensate Accumulation Near the Well Bore Test at 110°C and 3000 psia, Gas Condensate GCA94-1.

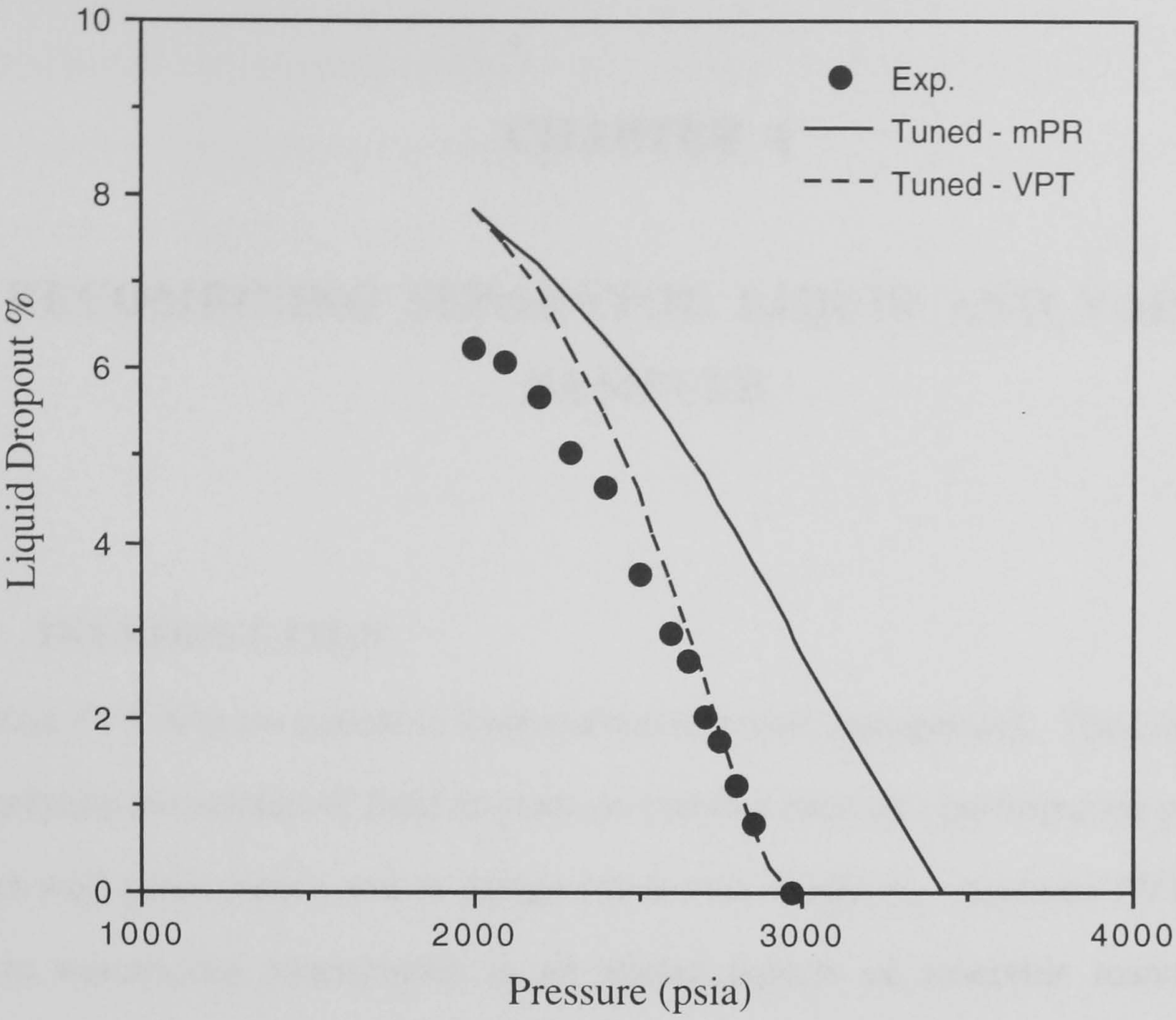

Fig. 3.44 - Constant Composition Expansion (CCE) Test on Depleted Vapour at 37.8°C - Gas Condensate GCA94-1.

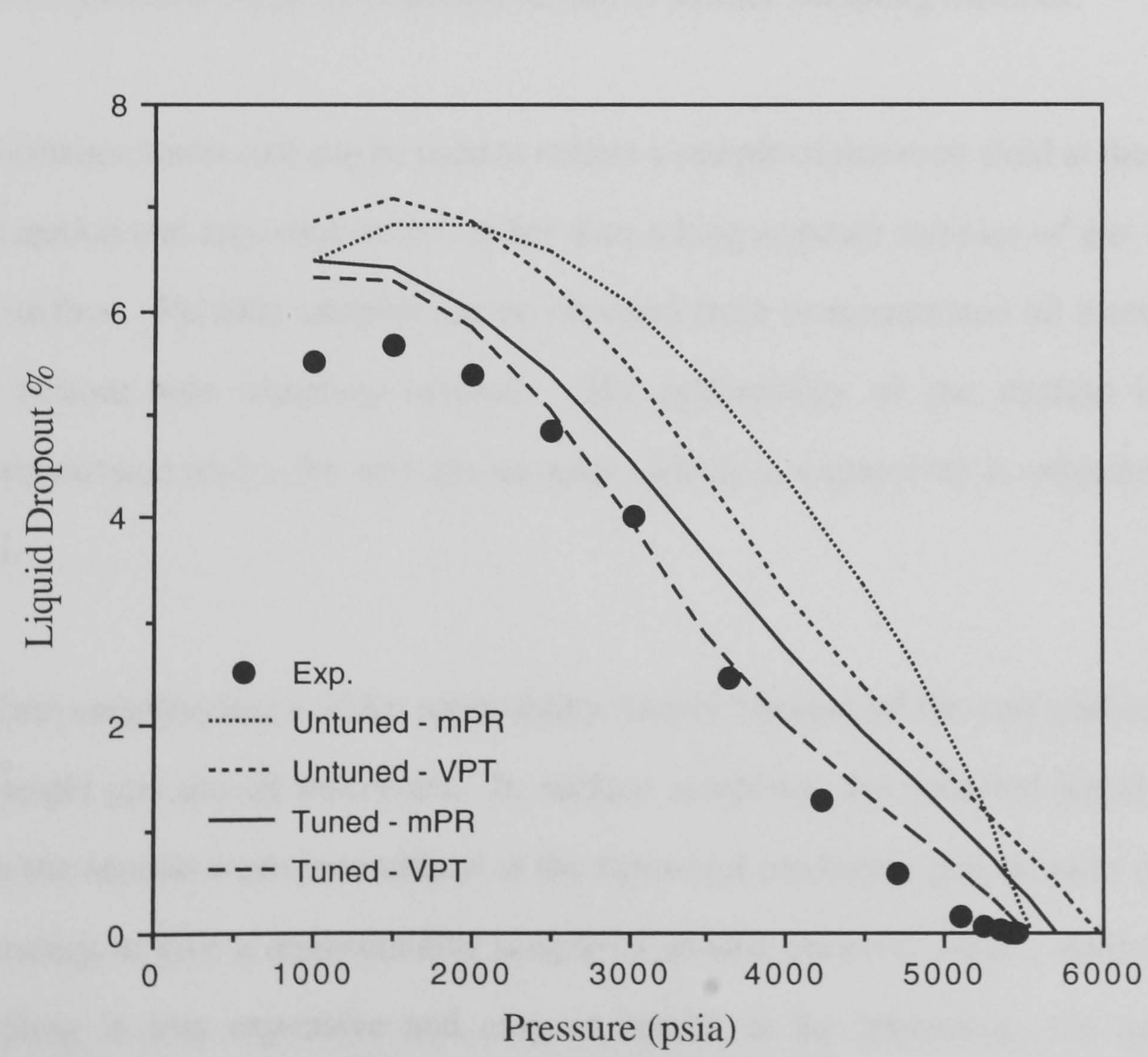

Fig. 3.45 - Liquid Dropout of Gas Condensate GCA94-1 at 110°C, 0.739 moles Gas Injected / mole GCA94-1 - Stage 3.

CHAPTER 4

RECOMBINING SEPARATOR LIQUID AND VAPOUR SAMPLES

4.1 INTRODUCTION

Accurate PVT data are critical in hydrocarbon reservoir management. These data are used to determine the amount of fluid in-place, to conduct reservoir performance prediction, to predict well performance and to design production facilities. Accurate PVT results are vital in minimising uncertainties in all related aspects of reservoir management and associated flow and process calculations. The required PVT data are usually measured in the laboratory by analysing samples of oil and gas from the reservoir. These samples may be provided either by bottom hole and/or surface sampling methods.

A formation tester tool can be used to collect a sample of reservoir fluid at the sand face in exploration and appraisal wells[1], rather than taking separate samples of gas and liquid at the surface. Reliable samples can be obtained from undersaturated oil reservoirs, using this bottom hole sampling method. The applicability of the method is limited to undersaturated reservoirs and the sampler (which is expensive) is subjected to loss in well.

Surface sampling has a wider applicability mainly because of the cost and it can be used to sample gas and oil reservoirs. In surface sampling, the collected liquid and vapour from the separator are recombined at the measured producing gas-oil ratio (GOR) in the laboratory to give a representative sample of in-situ reservoir fluid. Although, surface sampling is less expensive and easy to handle in the laboratory, the quality of the recombined mixture strongly depends on the recombining proportion (GOR). Any uncertainty in separation efficiency and in the measured GOR would directly affect the

composition of the recombined fluid. Any carryover or carry through in the separation could result in unrepresentative samples being taken. The gas / liquid separation during the process of sampling, before or during the sampling, outside or within the sample taker could result in an unrepresentative fluid. For example, if high pressure rich gas from the separator is directed through a throttling valve to an evacuated sample taker, liquid may dropout on the way and may be trapped in the lines that lead to the sample taker. Then, the collected sample could be unrepresentative.

The provided sample (either from recombining and/or bottom hole sampling) is used to perform a variety of standard and non-standard PVT experiments to determine the phase behaviour and physical properties of the fluid. The measured physical properties may directly be used as input data in reservoir simulation (black oil simulation). However, in compositional simulation, these results are used to adjust the equation of state to reasonably reproduce the results of PVT laboratory experiments[2]. Hence accurate PVT data are vital in the modelling of reservoir fluid phase behaviour.

If the top hole flowing pressure is above the saturation pressure, then sampling at wellhead will be adequate. No bottom hole sampling will be needed. If the top hole flowing pressure is below the saturation pressure but the bottom hole flowing pressure is above the saturation pressure, bottom hole sampling may be preferable. If the bottom hole flowing pressure is below the saturation pressure then surface separator sampling will be required.

Sampling undersaturated reservoirs is less troublesome than the other types of reservoirs. When the bottom hole flowing pressure is higher than the saturation pressure of reservoir fluid, either of the sampling methods (bottom hole or surface separator) would provide a representative sample of the reservoir fluid. However, in the case of bottom hole sampling, care needs to be taken to ensure that the draw down pressure required to flow the sample does not allow two phases to be generated. Once the bottom hole flowing pressure drops below the saturation pressure, the fluid changes in two phases at the

vicinity of wellbore and its phase behaviour and composition would constantly change with further pressure decline at the bottom hole. The change in the phase behaviour is more severe in near critical reservoirs. Due to this change in phase behaviour, it may be impossible to get an in-situ representative sample of reservoir fluid. Hence, several methods have been developed to determine the initial reservoir composition, using the collected sample from reservoir[3,4].

The majority of investigators have used the initial saturation pressure of reservoir fluid as a reference point to back calculate the initial reservoir composition. The saturation pressure of oil mixtures can be determined accurately, however there is a large uncertainty in measured dew point pressure of gas condensate samples. Moreover, the dew point of sample may not necessarily be equal to the reservoir fluid dew point.

In this study, a radial 1D compositional reservoir simulation is used to investigate these surface sampling problems from property predictions perspective. Different types of reservoirs from black oil to gas condensate are sampled during normal operational conditions at different times of the reservoir life (undersaturated to depleted). The collected samples are used to back calculate the initial reservoir composition, using the saturation pressure as the matching point. The effect of inaccuracies in the measured GOR (such as carryover, carry through, human error, ...) as well as the uncertainty in measured saturation pressure, on determined initial reservoir composition are also investigated.

4.2 SURFACE SAMPLING

The objective of surface sampling is to collect liquid and vapour from a separator with a measured GOR and to recombine them in the laboratory to obtain a representative sample of the reservoir fluid. As it is the least expensive and easy to handle in laboratory and the best method of sampling when the bottom hole flowing pressure is below the saturation pressure, it has been widely applied by industry to sample different types of reservoirs.

The recombined sample is generally subjected to compositional analysis and various PVT tests to measure the phase behaviour and physical properties of reservoir fluid.

Recombining the separator samples in the proportion of measured GOR would provide a hydrocarbon mixture which is representative of the fluid at the wellhead. If the fluid flows under steady state conditions in the wellbore, the composition of the recombined sample at the wellhead should be the same as the fluid composition at the bottom of the hole. It is obvious that in real practice, the flow conditions may deviate from ideal steady state. Therefore, the recombined sample may not give a true reproduction of the reservoir fluid, but rather a sample which can be used to approximate the properties of reservoir fluid.

Several authors[3,5] have addressed the problems of obtaining a representative sample of a reservoir fluid. Reudelhuber[6] was one of the first investigators who discussed the sampling problems in gas condensate wells. He suggested a practical method to collect samples from a separator at surface and recombine them in the laboratory. He believed that, a well should be produced at a low rate which will result in the minimum pressure draw down at the vicinity of wellbore in the reservoir. The low production rate is consistent with stable flow around the wellbore and may reduce the required period to condition a well prior to sampling. The conditioning period can be varied from several days (for reservoirs with good permeability) to more than a month in tight reservoirs. During the conditioning period the condensate gas ratio (CGR) in the separator should be observed. If there is instability in the CGR, the conditioning period should be extended.

McCain and Alexander[5] have recently investigated the sampling problems of gas condensate wells in homogeneous and layered reservoirs. As part of their analysis, they studied the development of a condensate bank in the vicinity of wellbore. They concluded that the amount of liquid condensate flowing into the wellbore is always slightly less than that of complete stability. Thus, the composition of the production stream will be slightly deficient in heavier compounds. At higher production rates, the

growth in the condensate bank is more rapid and the production stream is more deficient in condensate. They pointed out that, gas condensate wells should be sampled early in the life of the well, say within a month after putting on production. This is more important in layered reservoirs where more rapid growth of condensate bank would happen in the zones with higher permeabilities. They have also mentioned that constant producing GOR at the surface is not necessarily equal to a good or perfect sample. This is particularly true at high production rates where the producing GOR could appear to be constant when the composition of the production stream is not representative of the original reservoir gas.

While the reviewed publications designed procedures to give the best chance of obtaining a representative sample of reservoir fluid at surface, Reffstrup and Olsen[3] studied the physical processes determining the fluid composition during surface sampling under primarily non-ideal conditions for sampling. They used a modified black oil simulator to produce from a low permeability lean gas condensate reservoir. A traditional PVT equation of state package was applied to simulate the recombination of separator samples and effect of liquid dropout. They sampled the reservoir at normal production rate, as they believed that, in practice, samples are often taken during normal operational conditions. The authors showed that the dew point pressure of a well stream (recombined sample) was lower than the initial dew point of reservoir, but higher than the bottom hole pressure. They recommended a method to back calculate the initial reservoir composition by matching the initial reservoir dew point pressure.

Fevang and Whitson[4] extended the Reffstrup and Oslen's method to cover the other types of reservoirs. They used radial 1D and 2D compositional simulation to produce from oil and gas zones independently. They sampled the oil and gas zones and recombined the samples to gas oil contact conditions. They used an oil column composition to determine the initial composition of gas zone (gas reservoirs). They also believe that, due to a lengthy stabilisation period, the samples are generally taken during normal production rate.

The main concern in surface sampling is the recombining proportion of the collected liquid and gas from surface separator. Any uncertainty in the measured GOR in the field directly affects the composition of recombined sample. Imperfect separation in the separator will cause either some liquid to be held up with gas (carryover) or some gas to be produced with liquid (carry through). In the former case, the measured GOR will be higher than the real one, therefore, the recombined sample (using an erroneous GOR) will be lighter in heavy compounds. However, in the second case (carry through), as some gas being produced with the liquid the measured GOR tends to be lower than the real GOR. Using this erroneous GOR, the recombined sample in the laboratory will be heavier than the in-situ reservoir fluid. Some of these errors are cancelled by the richer gas and leaner oil compositions in the carryover case and the opposite in the carry through case. Other sources of uncertainty in sampling such as human error and measurement bias or retrograde condensation in the sample taker system while sampling the rich gas could make the problems more complicated.

Inaccuracy in the compositional analysis of the heavy end, particularly in gas condensate mixtures, should be accounted in composition of reservoir fluid. Gas chromatography techniques[7] are generally applied to determine the composition of collected samples at surface. The sampled gas from surface separator mainly consists of light and intermediate hydrocarbons. Its composition is usually reported up to C_6 or C_7. However, the collected liquid from stock tank is rich in intermediate-heavy and heavy hydrocarbons. The compositions of oil are often reported up to C_6 and the heavy hydrocarbons are lumped as C_{7+}. The condensate samples are commonly analysed to C_{15+} or recently C_{20+}. Although developed methods have greatly improved the compositional analysis of reservoir fluids, uncertainty still exists in the concentration of heavy end in petroleum fractions. In near critical fluids, particularly gas condensate mixtures, the concentration of the heavy end is quite important in determining the dew point pressure of the mixture. Any inaccuracy in the concentration of the heavy end can largely affect the phase properties of gas condensate mixtures.

Inaccuracies in the measured GOR and compositional analysis of stock tank liquid are the two major sources of uncertainties in determining the in-situ representative reservoir fluid composition. Their effect and intensity on the determined composition depend on the type of reservoir fluid (i.e. oil or gas condensate). While the inaccuracy in heavy end composition has a large effect on gas condensate phase behaviour, it has little effect on black oil systems.

In the next section, the various uncertainties have been studied in different types of reservoirs from undersaturated to depleted reservoirs. The problems have also been investigated with various kinds of fluids (i.e. gas condensate and oil mixtures).

4.3 DETERMINATION OF THE INITIAL RESERVOIR FLUID COMPOSITION

The initial reservoir fluid composition is the most important PVT data in compositional reservoir simulation. To obtain a representative sample of initial reservoir fluid, the well should be sampled during early development of the reservoir. Once the average reservoir pressure drops below the initial saturation pressure of reservoir, it is almost impossible to collect a representative sample of the original reservoir fluid. It has been pointed out that the well should be conditioned prior to sampling, which might take a long time in tight reservoirs. Therefore, samples are generally collected at the surface separator during normal operational conditions. Due to this uncertainty, the collected samples are imperfect whereas, they can be adjusted to give a representative sample of initial reservoir composition.

In depleted reservoirs, recombining the collected samples at surface may give a representative sample of in-situ reservoir composition. However, due to the production from the reservoir, the determined composition can be far from the initial reservoir

composition. The collected samples at surface can be modelled and used to back calculate the initial reservoir composition.

In the separator method, which is commonly applied by industry, gas and liquid samples are collected from the surface separator during normal production conditions. The collected samples are recombined in the ratio of measured gas-oil ratio (GOR) at the surface separator. Then, the recombining ratio (GOR) is adjusted to match the initial saturation pressure of reservoir fluid.

In the backward differential depletion (BDD) method, gas and liquid samples are also collected from the surface separator during normal production rate. The samples are recombined in the ratio of measured GOR to determine the composition of the wellhead stream. The recombined mixture is brought to equilibrium at the current average reservoir pressure and temperature. Then the following procedure is used for different reservoir fluids:

* In oil reservoirs, all of the equilibrium gas is removed at constant pressure, then adequate volume of it is re-injected into the liquid to match the initial bubble point pressure of reservoir fluid.

* In gas condensate reservoirs, all of the equilibrium liquid is removed and then adequate volume of it is re-injected into the gas to match the initial dew point pressure of reservoir fluid.

It should be mentioned that if the recombined sample remained single phase (undersaturated) at the current reservoir conditions (it can happen if the recombining GOR was erroneous), the pressure could be reduced to change the mixture to two phases. Then the above mentioned procedure can be applied to the different reservoir fluids.

The bubble point pressure of oil mixtures is a monotonic function of recombining proportion (GOR), i.e., the bubble point pressure of recombined surface samples will increase with increasing GOR. Therefore, in a saturated oil reservoir the bubble point pressure of a recombined sample is generally higher than the bottom hole pressure. In gas condensate reservoirs, the dew point pressure of a recombined mixture is not a monotonic function of GOR[8]. Hence the dew point pressure of recombined mixture can be lower than the bottom hole pressure which may cause one to believe the reservoir is undersaturated.

As the GOR-dew point pressure curve is a dome-like shape in gas condensate mixtures, there is the possibility of having the same dew point pressure with two different GOR's. It is obvious that the calculated composition using the two different GOR's will not be similar, thus their phase behaviour would be significantly different. To investigate the variation of dew point pressure with GOR, a gas condensate sample was flashed to different conditions from surface to the reservoir conditions. Then the resultant liquid was removed and re-mixed with the vapour in different proportions and the dew point pressure of the mixture was determined. The results are summarised in Fig. 4.1. The legend on the Figure shows the logarithm of K-factor of the lightest hydrocarbon (C_1) to that of the heaviest one (plus fraction). It indicates how far from the reservoir conditions the gas condensate was flashed. The high values indicate that the gas condensate was flashed to a condition close to the surface conditions (12.1, separator method), however low values show that the gas condensate was flashed at conditions close to the reservoir conditions (2.9, BDD method). The results show that using the separator method to back calculate the initial reservoir composition, converging to a false composition is more probable in comparison to the BDD method.

Fig. 4.1 shows that in the case of separator method (log(Kl/Kh) = 12.1) adding 4.47 cm^3 of separator liquid to 1000 cm^3 of separator gas would result in a mixture with a dew point pressure of 4633 psia. However, it can be seen that adding 3.24 cm^3 of separator liquid to 1000 cm^3 of separator gas would result in a different mixture with the same dew

point pressure. The above two mixtures were used to perform a constant composition expansion (CCE) test at reservoir temperature. The results are given in Fig. 4.2. It shows that although the dew point pressures of the two mixtures are the same, there is a large difference in the volumetric behaviour of the mixtures. Considering -3% error in the measured dew point pressure, the BDD and separator methods are used to determine the reservoir fluid composition. The determined compositions were used to perform a CCE test at reservoir temperature. The results are also given in Fig. 4.2. It shows that even with -3% error in dew point pressure, the BDD method is superior to the separator method.

4.4 RESERVOIR PERFORMANCE AND SAMPLE CHARACTERISTICS

Saturated reservoirs are the most problematic to be sampled where the bottom hole pressure drops below the saturation pressure as soon as the reservoir is put on production. The reservoir fluid changes into two phases in the vicinity of the wellbore. Due to continuous changes in the composition and phase behaviour of the reservoir fluid with further pressure reduction, the composition of the recombined fluid samples may significantly deviate from the composition of the in-situ reservoir fluid. Hence, the collected samples need to be adjusted to reasonably reproduce the initial reservoir fluid composition.

In depleted reservoirs (if its composition has not been determined early in the life of the reservoir), the reservoir fluid is in two phases as the average reservoir pressure is below the initial saturation pressure of the reservoir fluid. Therefore, recombining the collected samples at surface may give a representative sample of in-situ reservoir composition. However, due to production from the reservoir, the determined composition can be different from the initial reservoir fluid composition. It will be shown in the next section that the BDD method can be used to determine the initial reservoir fluid composition using the collected samples from depleted reservoirs.

Undersaturated reservoirs are less problematic to be sampled in comparison to the other types of reservoirs. As long as the bottom hole pressure is above the saturation pressure of the reservoir, simply recombining the separator samples in the ratio of produced GOR should provide an accurate estimation of the original reservoir fluid.

The sampling uncertainties in determining the initial reservoir composition were investigated in different types of reservoirs at different times of their production life. Liquid and vapour samples were collected at the surface separator during normal operational conditions. Two methods namely, the BDD and separator methods, were applied to back calculate the initial reservoir fluid composition of undersaturated, saturated and depleted reservoirs with known saturation pressure (i.e. to verify the previously determined composition). Inaccuracies in measured saturation pressure and GOR at surface (carryover, carry through, human error, ...) were introduced to the collected samples and their effects were investigated on the determined initial composition of the reservoir fluid. A method was also developed to trace the possible inaccuracies in the measured composition of the reservoir fluid in the laboratory. Different types of reservoir fluids including, black oil, volatile oil, medium-rich and lean gas condensates, were investigated. The results of a volatile oil and a medium-rich gas condensate reservoir fluids are presented.

A radial 1D compositional reservoir simulation, applied to both a volatile oil and gas condensate, was used to investigate the sampling problems. The 3-parameter modification[9] of the Peng-Robinson[10] equation of state was used to perform phase equilibrium calculations. Cavett correlations[11] were used to determine the physical properties of the pseudo components in the reservoir fluid composition. The acentric factors of pseudo components were determined by the Lee-Kesler correlation[12]. The reservoir description and the model grid data are given in Table 4.1.

4.4.1 Volatile Oil Reservoir, LRX89-1

The volatile oil reservoir was undersaturated with an initial pressure being 470 psia above its saturation pressure of 5064.7 psia. The production performance is given in Figs. 4.3 and 4.4. The reservoir is produced for 4000 days, where the GOR increases from 2400 to 8000 SCF/STB. The oil production rate decreases from 6000 to 970 STB/day. The average reservoir pressure and bottom hole pressure drop to 3066 and 2500 psia at 4000 days, respectively. Samples are collected at normal production rate at 10, 200 and 1400 days.

At 10 days, the bottom hole pressure is at 3430 psia, while the average reservoir pressure is well above the initial saturation pressure at 5513 psia. This conditions mimics a undersaturated oil reservoir with a two-phase region in the vicinity of the wellbore. The collected samples at the surface are used to back calculate the initial reservoir composition, using the BDD and separator methods. The results are plotted in Fig. 4.5. As the measured saturation pressure is used to determine the initial reservoir fluid composition, any error in the measurement would affect the determined compositions. The accuracy of the measured bubble point pressure is assumed to be within ±10 psia. The absolute percentage deviations (AD%) in the calculated initial composition of reservoir fluid using the BDD and separator methods with ±10 psia error in reported bubble point pressure are also depicted in Fig. 4.5. The AD% of the separator and BDD methods in the back calculated initial composition are less than 4% and 1%, respectively. The superiority of the BDD method is obvious, although the separator method has also given a good estimation of the initial composition. This is consistent with sampling the reservoir at early time of its life, if the separator method is going to be used to determine the initial reservoir composition. The results also show that the methods are not sensitive to the mentioned inaccuracy in measured saturation pressure.

In Fig. 4.6, the results of the BDD method with ±15% errors in the measured GOR are compared to that of the separator method. It shows that the results of the BDD method with an erroneous GOR are comparable to that of the separator method. The reason is at

CHAPTER 5

CONTAMINATION OF FLUID SAMPLE WITH OIL-BASED MUD FILTRATE

5.1 INTRODUCTION

Bottom hole sampling is an alternative procedure to surface sampling and is widely used to obtain representative samples of reservoir fluids. Bottom hole samples may be obtained from a drill stem test, a well test and/or wireline formation testers (WFT). WFT provides a cost effective means to determine pressure as a function of depth and to recover samples of reservoir fluid from formations at selected depths. However, in the case when oil-based drilling fluids have been used, this information can be hampered by contamination of the reservoir fluid with drilling mud filtrate which will invade the formation during the drilling process. Although, significant efforts have been made in the design of WFT to improve sample recovery, sample quality has improved only marginally[1].

Drilling with oil-based muds have gained world-wide application particularly in offshore environment. Despite many benefits of oil-based drilling muds, they have an adverse effect on the reservoir fluid properties, as their filtrates are miscible with the formation hydrocarbons. Oil-based muds therefore adversely affect fluid properties such as saturation pressure, formation volume factor, gas-liquid ratio and stock tank liquid density. As running WFT is expensive and accurate reservoir fluid properties are needed in reservoir development, it would be essential to determine the accurate composition and phase behaviour of the reservoir fluid from contaminated samples.

In this study different types of real reservoir fluid samples (volatile oil and gas condensate) are deliberately contaminated with an oil-based drilling mud filtrate in the

10 days (very early in life of the reservoir), the collected samples at surface are close to the initial reservoir fluid composition. Therefore, applying the separator method, the results are as good as those of the BDD method with erroneous GOR.

At 200 days, the average reservoir pressure is slightly above the initial saturation pressure with a bottom hole pressure at 2732 psia. The results of determining the initial reservoir composition, using the BDD and separator methods, are illustrated in Figs. 4.7 and 4.8. Comparison of the results at 200 days with those of 10 days shows that the AD% in back calculated initial composition; is almost doubled in the case of the separator method, whereas it has decreased for the BDD method with errors in the measured GOR in the surface separator. Hence, the BDD method should be applied to back calculate the initial composition even with erroneous GOR in the separator.

It was mentioned that in applying the BDD method to determine the initial composition of reservoir, if the recombined sample remains single phase at current reservoir conditions, the pressure can be reduced to change the mixture to two phases. The resultant vapour composition is then used to back calculate the initial reservoir composition. To investigate the sensitivity of the back calculated initial composition to the pressure at which the recombined sample is flashed, the recombined sample from undersaturated reservoir is flashed to 80%, 40% and 20% of the initial saturation pressure. The resultant vapour is applied to back calculate the initial reservoir composition, the results are presented in Fig. 4.9. It shows that better results would be achieved if the mixture is flashed to a condition which is closer to the bubble point of the original system.

At 1400 days, the average reservoir pressure is well below the initial saturation pressure at 4028 psia. This case mimics a depleted / initially undersaturated reservoir (with known saturation pressure). The results of applying the BDD and separator methods to back calculate the initial reservoir composition with ±10 psia error in the initial saturation pressure are shown in Fig. 4.10. The results of determining the initial reservoir composition by introducing ±15% errors in the measured GOR, are given in Fig. 4.11.

As it was expected, the calculated composition by the separator method is highly erroneous and the BDD method should be used to determine the initial composition of the reservoir.

Pressure gradients in the oil column are generally reported by service companies, where they can be used to trace the inaccuracies in the reported compositional analysis by the laboratory. The reported pressure gradient data can be applied to determine the variation of single phase oil density with depth, using the following equation:

$$\frac{\partial \rho}{\partial h} = \frac{1}{g} \frac{\partial P^2}{\partial^2 h} \qquad (4.1)$$

where ρ is density, h is depth, g and P are the gravitational acceleration and pressure, respectively. As it was mentioned, the compositional data of intermediate-heavy and heavy hydrocarbons is liable to errors. A 15% error was introduced in the concentration of C_8-C_{20+} of the sampled stock tank liquid at surface. The liquid was recombined with the associated gas and the BDD method was used to back calculate the initial reservoir composition. The erroneous back calculated and the original compositions were used to determine the variation of single phase density at 1000 ft oil column. The plotted results in Fig. 4.12 shows that whilst there is only 6% deviation in density, a significant difference (about 15%) exists in the slope of calculated single phase densities. Hence, variation of the single phase density with depth (which can be determined from pressure gradient) in oil column can be applied to verify the reported composition. The results also show that the error in concentration of intermediate-heavy and heavy hydrocarbons directly affects the pressure gradient (say 15% error in the mentioned composition would give 15% error in pressure gradient). It should be mentioned that the same results were observed in a black oil reservoir fluid study.

4.4.2 Medium-Rich Gas Condensate Reservoir, GCA94-1

The gas condensate reservoir which was initially saturated, was put on production for 1000 days at a constant gas production rate of 2000 MSCF/day. The bottom hole flowing pressure decreased from 5541 to 5383 psia at 1000 days. The composition of methane and heavy end (C_{20+}) in two phase mixtures at surface and various distances from the wellbore are plotted versus production time in Figs. 4.13 and 4.14, respectively. As they show, the composition at the surface is deficient in heavy ends particularly at 1000 days. Samples were collected from the separator liquid and vapour at 10 and 1000 days during normal operational conditions.

At 10 days, the bottom hole pressure was at 5485 psia (compared to the initial reservoir pressure of 5560 psia), which indicates the early time in the life of the reservoir. Using the BDD and separator methods to back calculate the initial reservoir composition, the results are plotted in Fig. 4.15. It should be mentioned that the uncertainty in the measured dew point pressure of gas condensate mixtures is always higher than the measured saturation pressure of oil mixtures. In this study a ±10 psia error was considered in the measured saturation pressure of the oil mixtures. However, in gas condensate mixtures the error in the measured dew point pressure can be as high as ±3%. Considering the mentioned tolerance in the measured dew point pressure, the calculated initial composition, using the BDD and separator methods are illustrated in Fig. 4.15. The separator method could not reach the dew point pressure with +3% error. The reason is the dew point pressure is not a monotonic function of recombining GOR, particularly in the separator method (see Section 4.3). Fig. 4.15 shows that the BDD method can accurately back calculate the initial reservoir composition, if the dew point pressure is accurately known. However, calculated initial composition using the separator method, can be within 10% error with accurate dew point pressure. It also shows that both methods are sensitive to the uncertainty in the measured dew point pressure.

The calculated initial reservoir composition (with and without error in the initial dew point pressure) and the composition of reservoir fluid at wellhead are used to perform a constant composition expansion (CCE) test at reservoir temperature. The results are presented in Fig. 4.16. It shows that the predicted volumetric properties using the determined initial composition by the separator method are more sensitive to the error in initial dew point pressure than that of the BDD method. It also shows that in early time in the life of the reservoir the composition of the wellhead stream can be used as the initial reservoir fluid composition with a good approximation. However, the BDD method gives perfect results in determining the initial reservoir fluid composition (with correct dew point pressure).

Performing the same study on the collected samples at 1000 days, the same results were experienced. The results of the study on the collected samples at 1000 days are illustrated in Figs. 4.17 and 4.18. They show that the absolute percentage deviation (AD%) in the back calculated initial composition increases with production time in the case of the separator method. However, it is constant or rather the initial reservoir composition can perfectly be back calculated, using the BDD method, even at 1000 days. Fig. 4.18 shows that the composition of wellhead stream is not representative of initial reservoir fluid composition. Hence the BDD method may be applied to determine the initial reservoir fluid composition.

The effect of errors in the measured GOR on the results of the BDD method was investigated. Introducing ±15% errors in the measured GOR of the collected samples at 10 and 1000 days, the initial reservoir composition was determined, using the BDD method. The results are compared to that of the separator method in Figs. 4.19 and 4.20 for the collected samples at 10 and 1000 days, respectively. Fig. 4.19 shows that the BDD method with erroneous GOR has given comparable results to the separator method. However, Fig. 4.20 indicates that the BDD method is superior to the separator method even with erroneous GOR in the separator at surface. Hence, the BDD method should be

applied to determine the initial reservoir composition, either at early or late time in the life of the reservoir.

Regarding tracing the possible error in reported reservoir composition, the same method which was used for oil reservoirs, was applied for gas condensate reservoirs. A 15% error was introduced in the composition of C_8-C_{20+} of stock tank liquid (gas condensate GCA94-1), then the initial reservoir composition was determined using the BDD method. The variation of single phase density with depth was calculated for the erroneous and the original gas compositions. They showed identical slopes for the mentioned variation. Therefore, the method cannot be used for the gas phase in gas condensate reservoirs. However, the method may be applicable in saturated gas condensate reservoirs. If the composition of condensate can be determined from the gas phase, then the method can be applied to determine the variation of single phase condensate density with depth. Unfortunately no procedure has yet been designed to determine the composition of condensate from gas in gas condensate reservoirs.

The separator and BDD methods were also applied to two lean gas condensate reservoirs to determine the initial reservoir fluid composition. The results showed that as the richness of gas condensate system was reduced, the significance of the BDD method was decreased. The results of the BDD method in determining the initial reservoir fluid composition may become similar to those of the separator method for dry gas reservoirs.

4.5 CONCLUSIONS

Any fluid produced from a reservoir should, in principle, provide valuable compositional information. It may not have, however, the same composition as the original reservoir fluid. The main target of this study was to develop a methodology of assessing if a reliable sample has been obtained, and if not what remedial analysis can be carried out. The processes that could contribute to the unreliability of the collected samples at surface are mostly due to changes in phase and flow characteristics in reservoirs. The results of a

numerical study on the use of initial reservoir fluid saturation pressure to evaluate and improve collected surface samples have been presented.

Two methods of adjusting the recombination ratio to match the saturation pressure, namely the separator and the backward differential depletion (BDD) methods have been employed. In the separator method, the collected separator gas and liquid phases are mixed to attain the required saturation pressure. In the BDD method, the separator samples are mixed and then the mixture is brought to equilibrium at conditions close to the saturation pressure, such as the flowing bottom hole conditions. Then, the equilibrated phases are separated at the above equilibrium conditions and recombined in a ratio to attain the saturation pressure. The results show that using the BDD method to determine the initial reservoir fluid composition, samples can be collected during normal operating conditions, without a need for long stabilisation periods prior to sampling. Whereas, the calculated initial reservoir fluid composition using the separator method can be highly erroneous, particularly in near critical saturated reservoirs. As the uncertainty in the measured dew point is more than that of the bubble point pressure, the results are less reliable for gas condensate reservoirs than oil reservoirs.

In gas condensate reservoirs, the dew point pressure of a recombined mixture may increase, decrease, or remain almost unchanged by increasing the recombining gas-liquid ratio (GLR). As the GLR-dew point pressure curve is dome-like shape in gas condensate mixtures, unlike oil mixtures where the bubble point pressure is a monotonic function of the recombining GLR, it is possible to obtain the same dew point pressure with two different GLR's. It is obvious that the composition using the two different GLR's will not be similar, thus, their phase behaviour would be significantly different. The results of this study clearly show that there is far less possibility of converging to a false composition using the BDD method in comparison to the separator method.

The simulated results also show that the variation of single phase density with depth in an oil column may be applied to evaluate the measured composition of hydrocarbon systems, assuming there is no compositional variations with depth within the reservoir.

REFERENCES

1. Kikani, J. and Ratulowski, J., (1996) : "Consistency Check and Reconciliation of PVT Data from Samples Obtained with Formation Testers Using EOS Models", SPE paper 36743, presented at the 71th Annual Technical Conference and Exhibition held in Denver, Colorado, Oct. 6-9.

2. Final Report, Reservoir Fluid Studies, January 1997. Heriot-Watt University, Department of Petroleum Engineering, Report No : PVT/97/1.

3. Reffstrup, J. and Olsen, H., (1994) : "Evaluation of PVT Data from Low Permeability Gas Condensate Reservoirs", North Sea Oil and Gas Reservoirs - III, Kluwer Academic Press, 289 - 296.

4. Fevang, Ø. and Whitson C.H., (1994) : "Accurate Insitu Compositions in Petroleum Reservoirs", SPE paper 28829, presented at the European Petroleum Conference held in London, UK, Oct. 25-27.

5. McCain, W.D. Jr. and Alexander, R.A., (1992) : "Sampling Gas-Condensate Wells", *SPERE*, August, 358-362.

6. Reudelhuber, F.O., (1954) : "Separator Sampling of Gas-Condensate Reservoirs", *Oil and Gas J.*, June, 138-140.

7. Osjard, E.H., Ronningsen, H.P. and Tau, L., (1985) : "Distribution of Weight. Density and Molecular Weight in Crude Oil Derived from Computerized Capillary GC Analysis", *J. High Res. Chromat. & Chromat. Commun.*, Oct., **8**, 683-690.

8. Standing, M.B., (1977) : *Volumetric and Phase Behaviour of Oil Field Hydrocarbon Systems*, 9th printing, Society of Petroleum Engineers of AIME, Dallas.

9. Jhaveri, B.S. and Youngren, G.K., (1988) : "Three-Parameter Modification of the Peng-Robinson Equation of State to Improve Volumetric Predictions", *SPERE*, Aug., 1033-1040.

10. Peng, D.-Y. and Robinson, D.B., (1976) : "A New Two-Constant Equation of State", *Ind. Eng. Chem. Fundam.*, **15**(1), 59-64.

11. Cavett, R.H., (1962) : "Physical Data for Distillation Calculations, Vapour-Liquid Equilibria", Proc. 27th API Meeting, San Francisco, 351-366.

12. Lee, B.I., and Kesler, M.G., (1975) : "A Generalized Thermodynamic Correlation Based on Three-Parameter Corresponding States", *AIChE J.*, **21**, 510-527.

Table 4.1 : Reservoir Description and Numerical Grid Data.

Rock Compressibility	1.0 E-5	psi^{-1}
Reservoir height	200	ft
Porosity	0.225	
Absolute Permeability r-direction	4.8	md
Absolute Permeability θ-direction	4.8	md
Absolute Permeability Z-direction	4.8	md
No. of Blocks in r-direction	20	
No. of Blocks in θ-direction	1	
No. of Blocks in Z-direction	1	
Max. reservoir radius	3000	ft
Radial well grid, block size	0.53, 0.36, 0.50, 0.76, 1.20, 1.85, 2.87 4.46, 6.93, 10.77, 16.71, 25.96, 40.30, 61.81, 98.00, 150.96, 234.44, 364.08, 565.39, 878.02, 534.10	

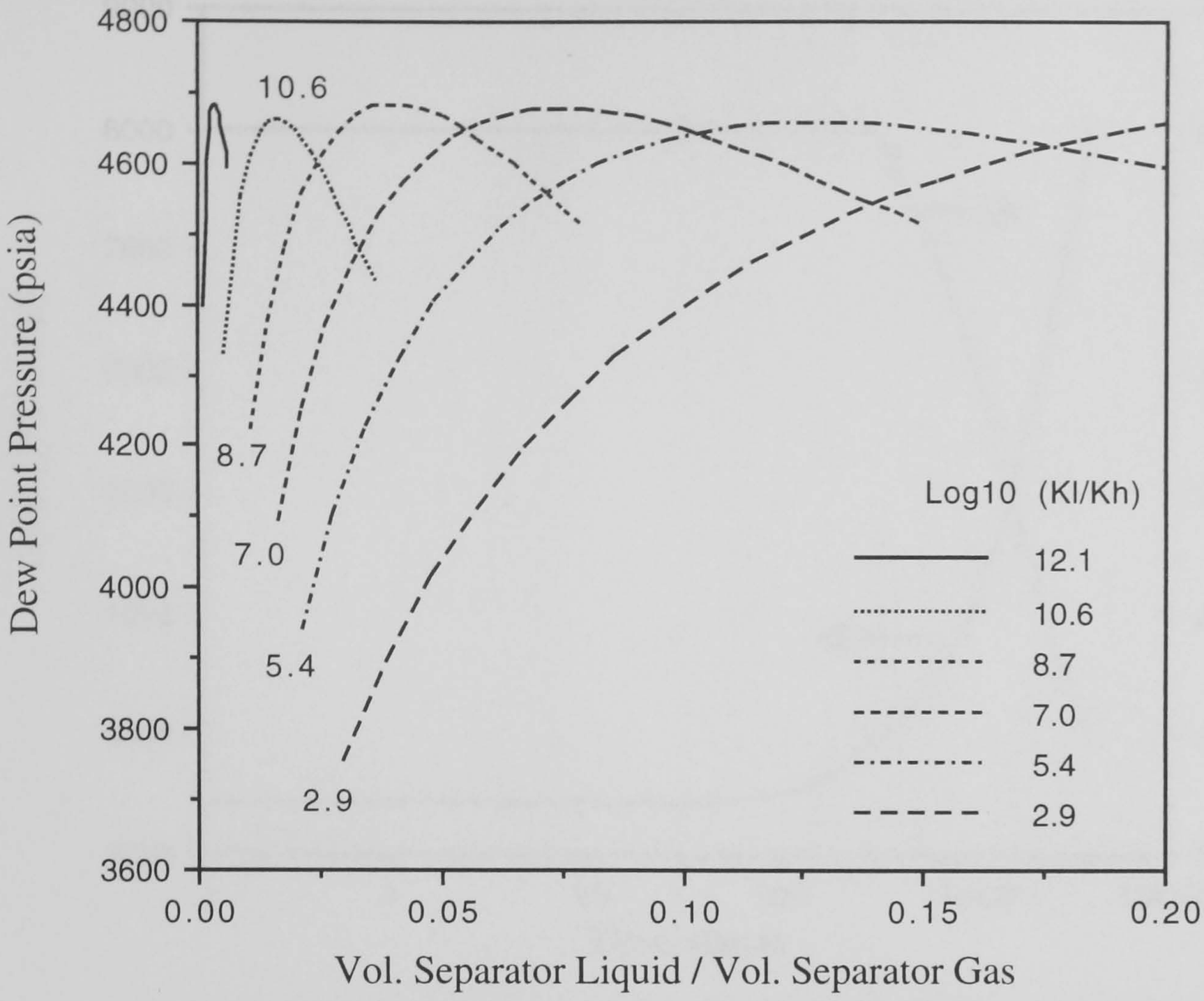

Fig. 4.1 - Predicted Dew Point Pressure of Recombined Separator Liquid and Gas.

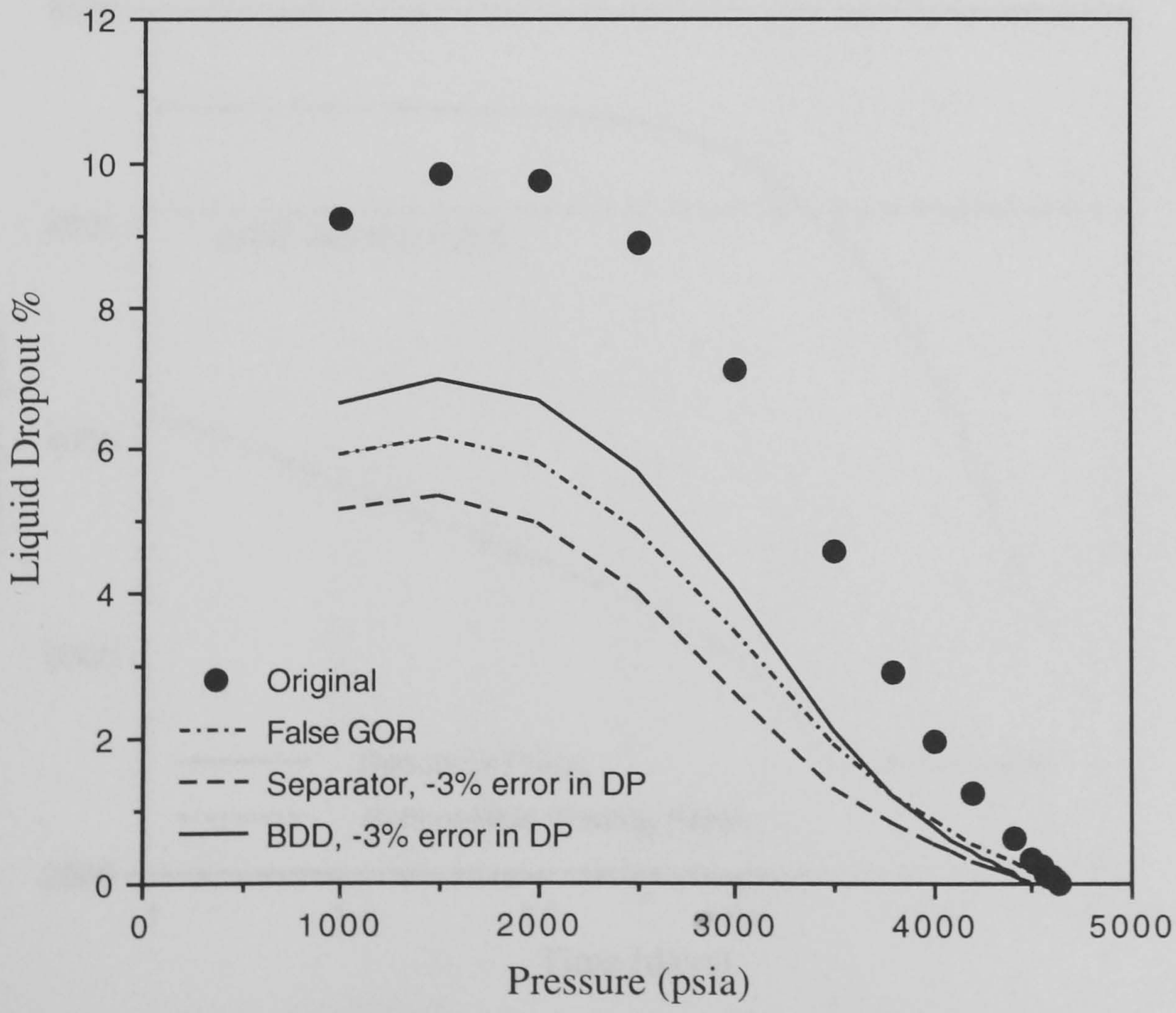

Fig. 4.2 - Predicted Liquid Dropout from Constant Composition Expansion (CCE) Test at 110°C, a Gas Condensate Mixture.

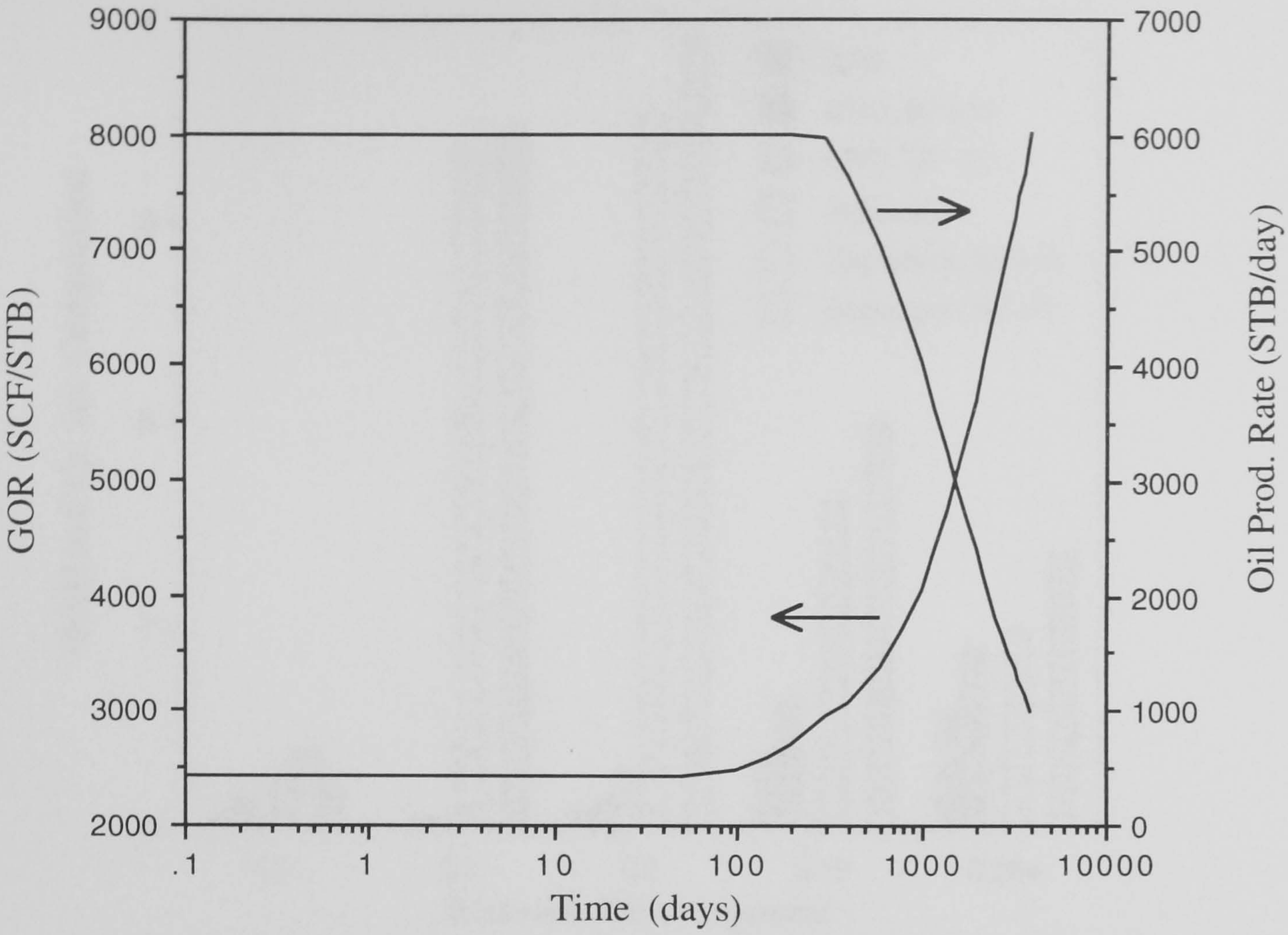

Fig. 4.3 - Variation of Gas-Oil Ratio and Oil Production Rate at Surface with Production Time, Initially Undersaturated, Volatile Oil LRX89-1.

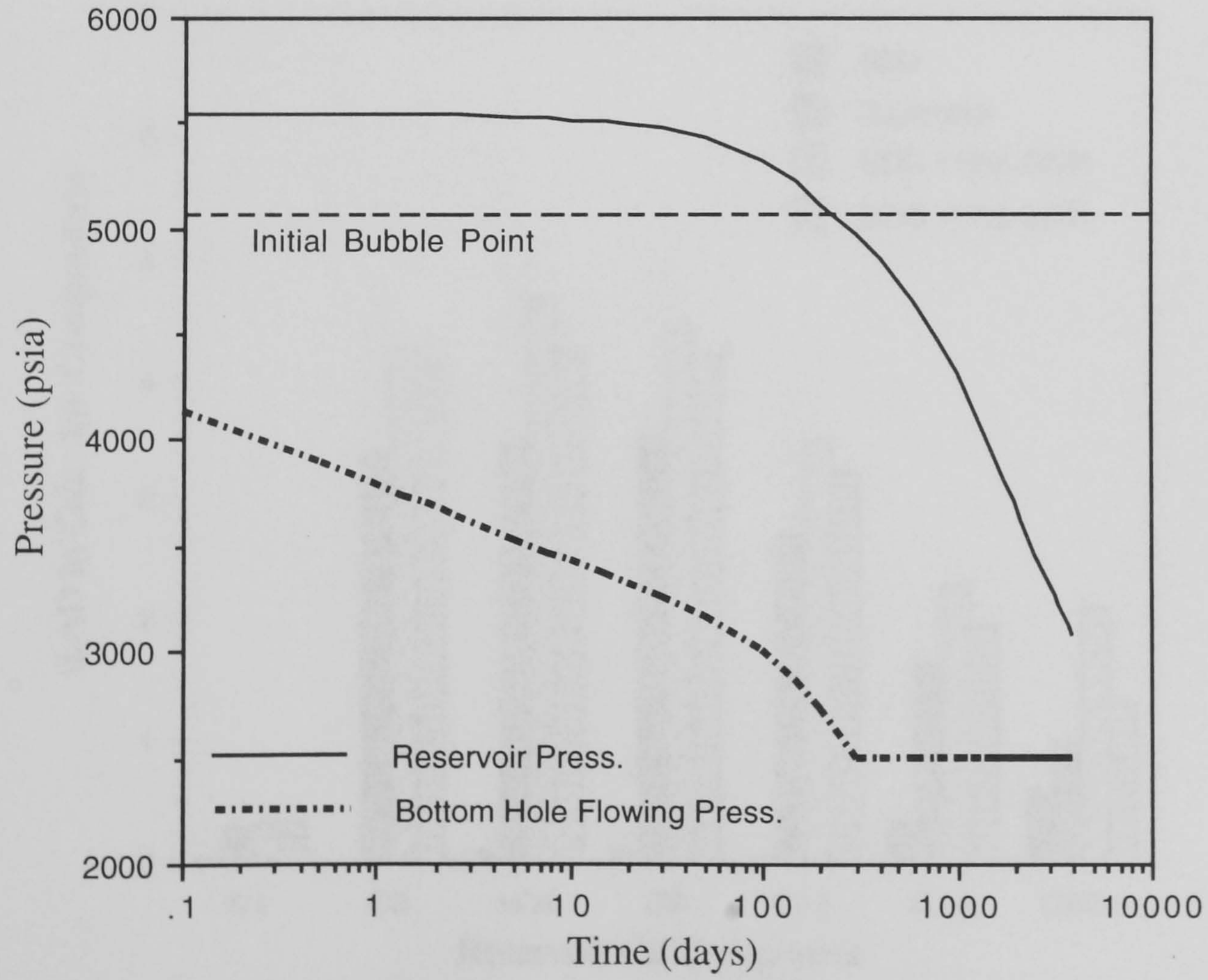

Fig. 4.4 - Variation of Bottom Hole Flowing Pressure and Average Reservoir Pressure with Production Time, Initially Undersaturated, Volatile Oil LRX89-1.

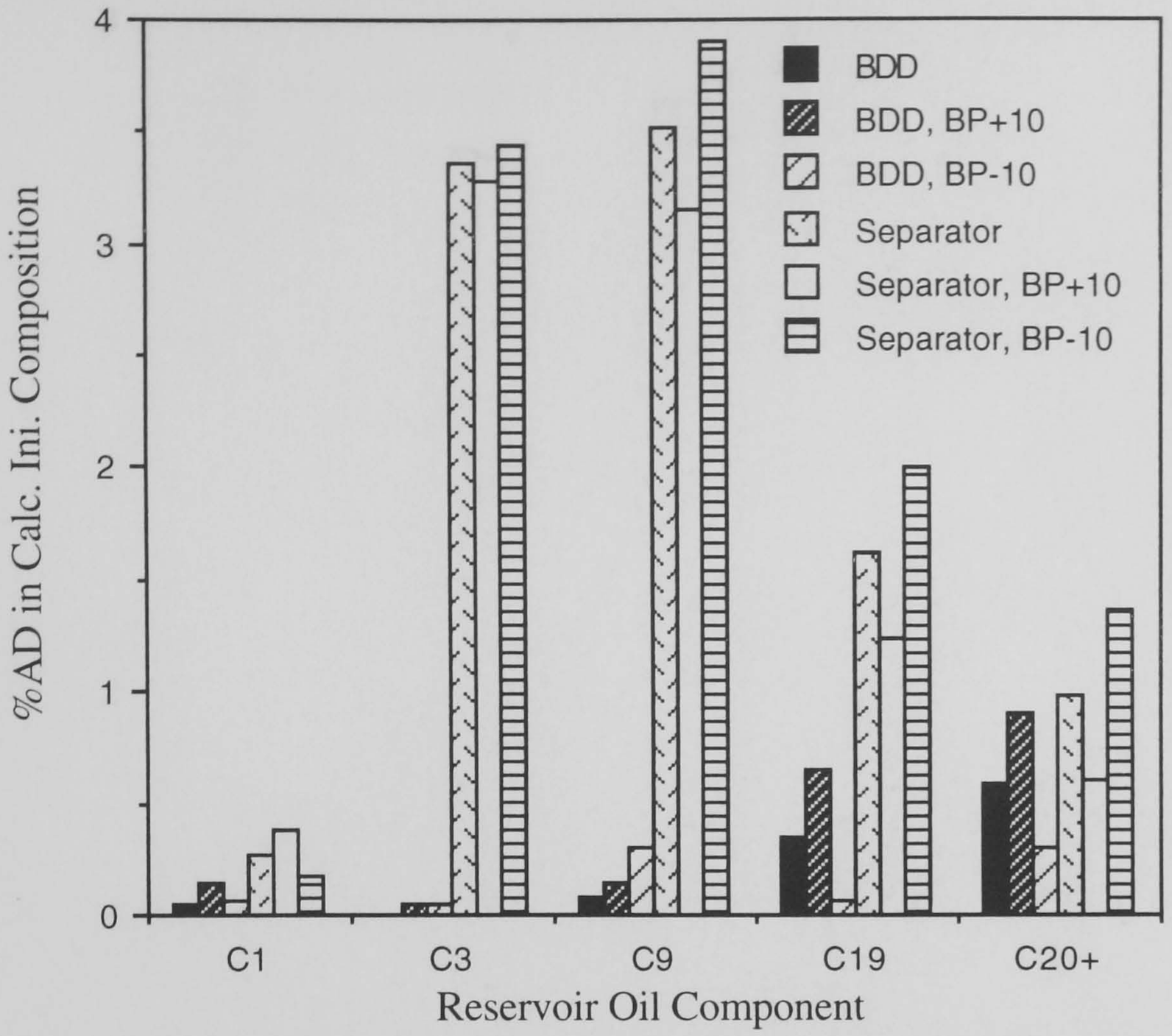

Fig. 4.5 - Absolute Percentage Deviation in Back Calculated Initial Composition of the Reservoir after 10 Days Production, Initially Undersaturated, Volatile Oil LRX89-1.

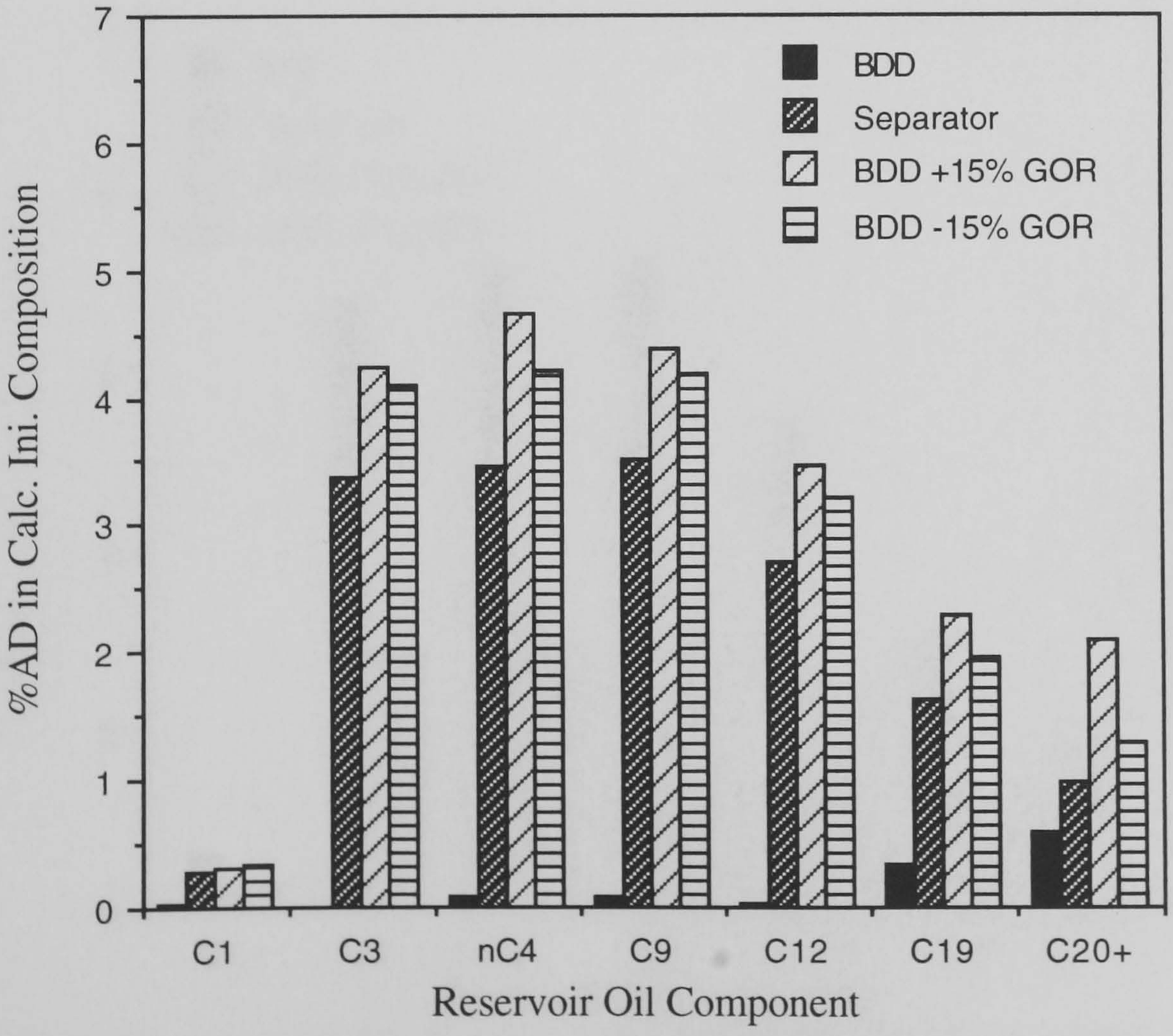

Fig. 4.6 - %AD in Determined Initial Composition after 10 Days Production, with Carryover and Carry Through Errors, Initially Undersaturated, Volatile Oil LRX89-1.

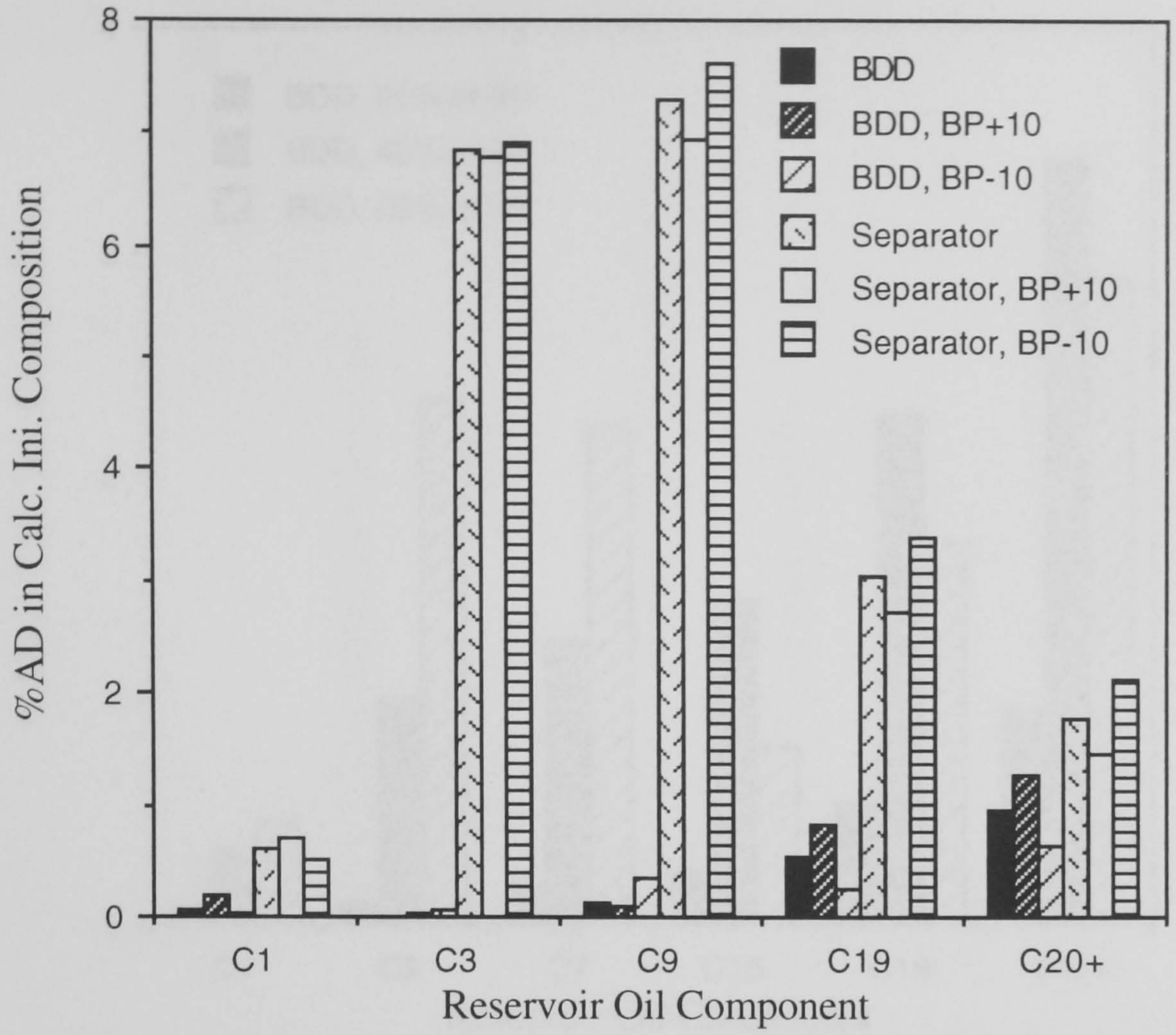

Fig. 4.7 - Absolute Percentage Deviation in Back Calculated Initial Composition of the Reservoir after 200 Days Production, Initially Undersaturated, Volatile Oil LRX89-1.

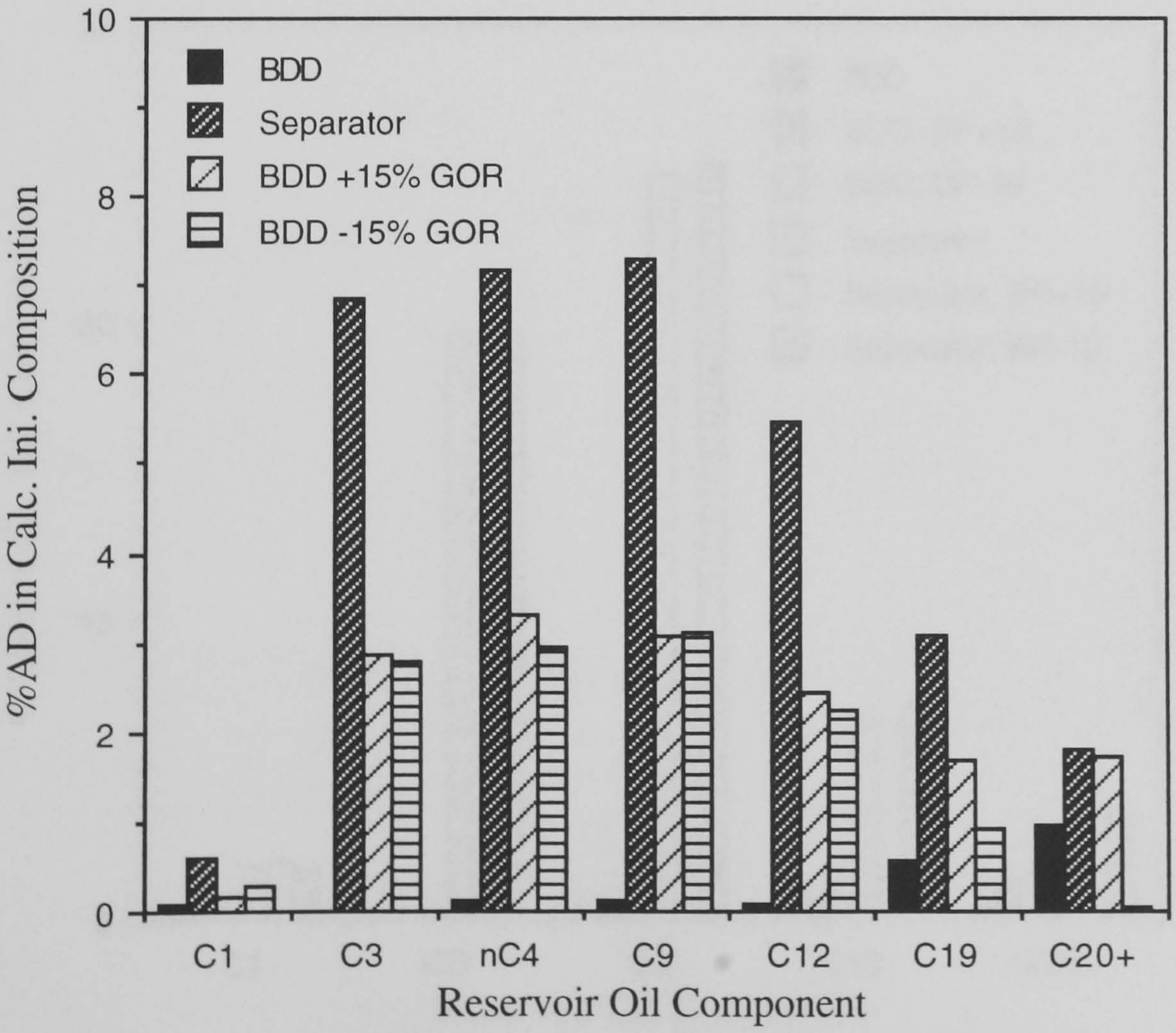

Fig. 4.8 - %AD in Determined Initial Composition after 200 Days Production, with Carryover and Carry Through Errors, Initially Undersaturated, Volatile Oil LRX89-1.

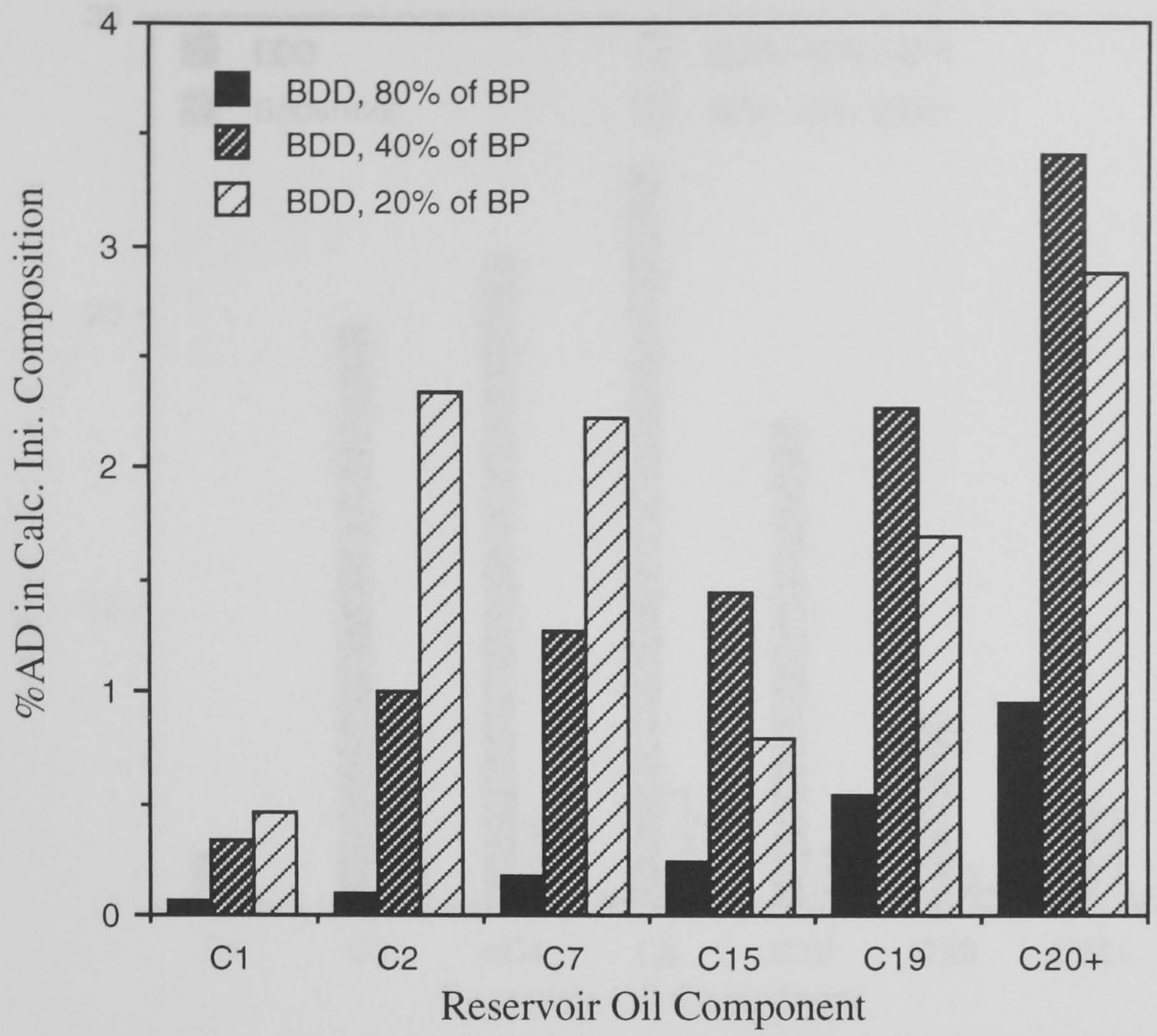

Fig. 4.9 - %AD in Determined Initial Composition with BDD Method by Flashing to Different Pressures, Initially Undersaturated, Volatile Oil LRX89-1.

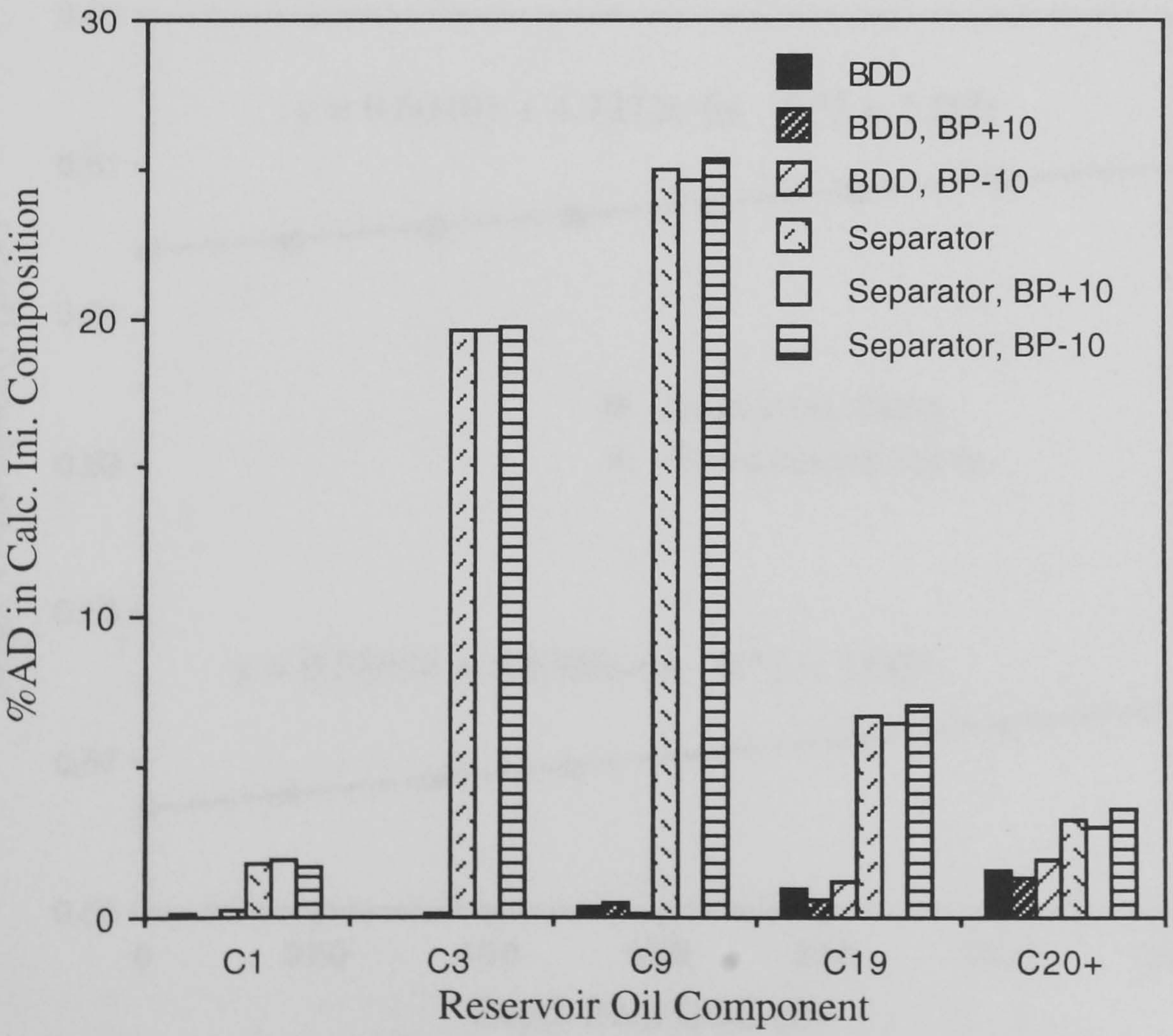

Fig. 4.10 - Absolute Percentage Deviation in Back Calculated Initial Composition of the Reservoir after 1400 Days Production, Initially Undersaturated, Volatile Oil LRX89-1.

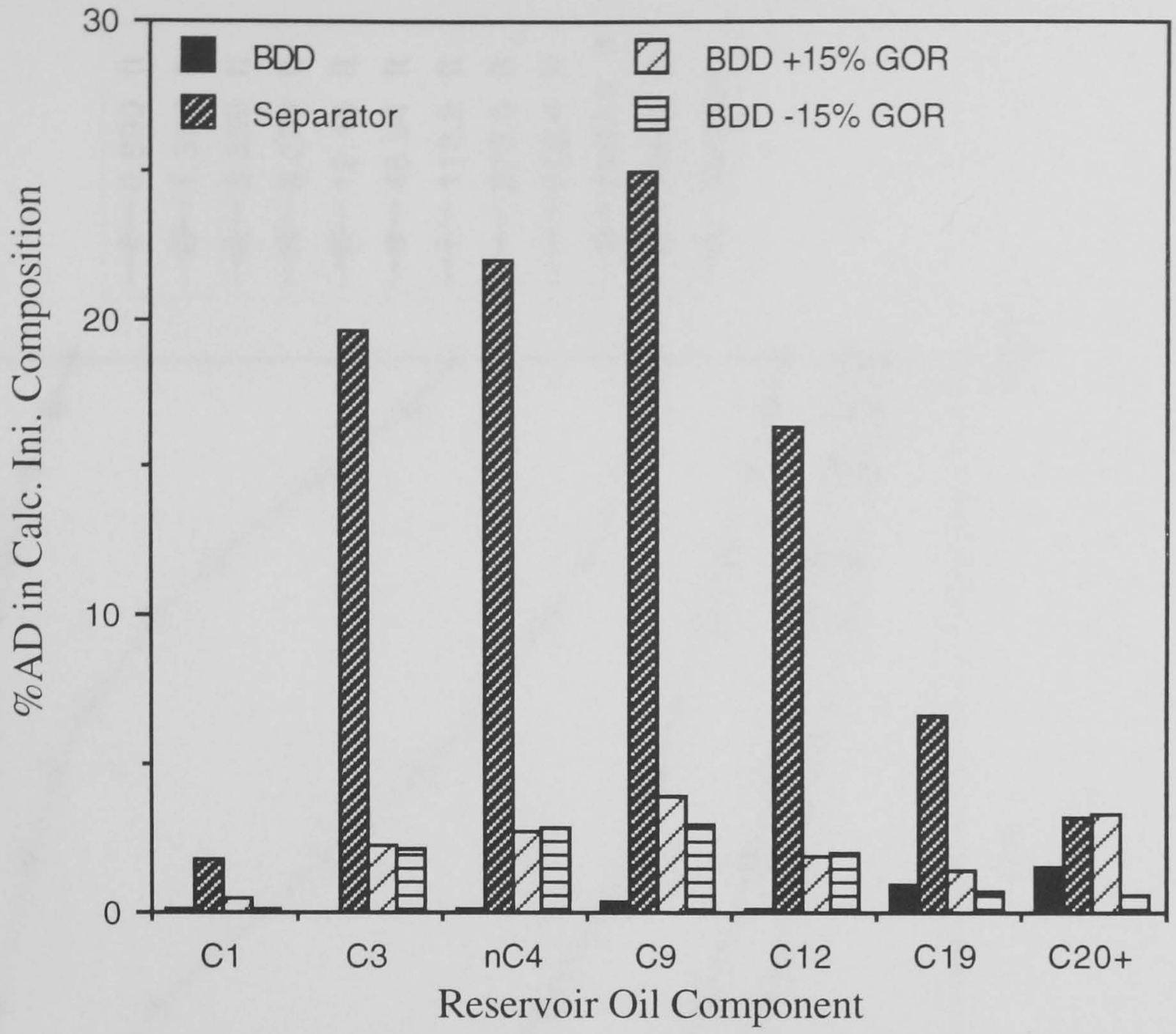

Fig. 4.11 - %AD in Determined Initial Composition after 1400 Days Production, with Carryover and Carry Through Errors, Initially Undersaturated, Volatile Oil LRX89-1.

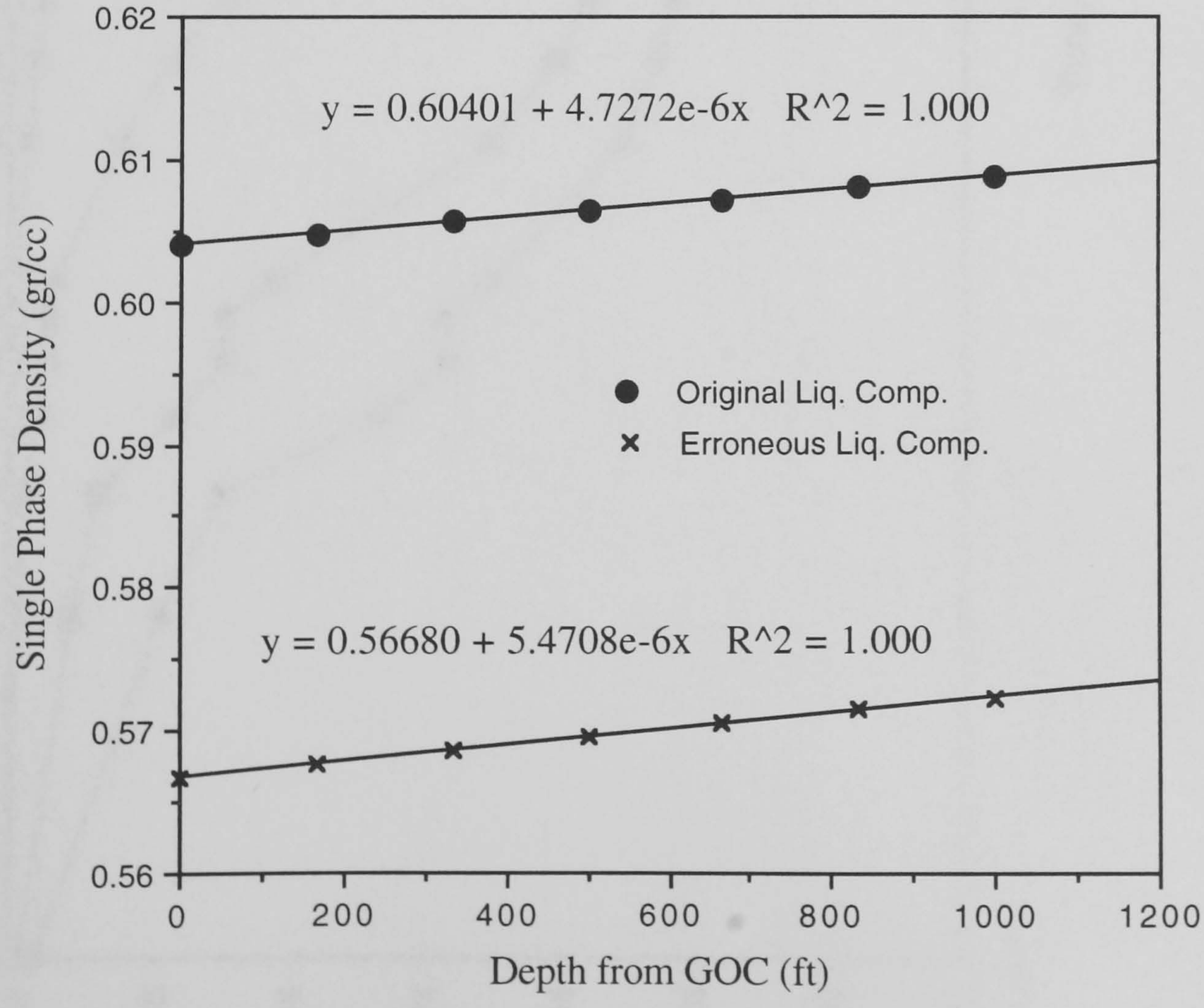

Fig. 4.12 - Variation of Single Phase Density with Depth in Oil Column, Volatile Oil LRX89-1.

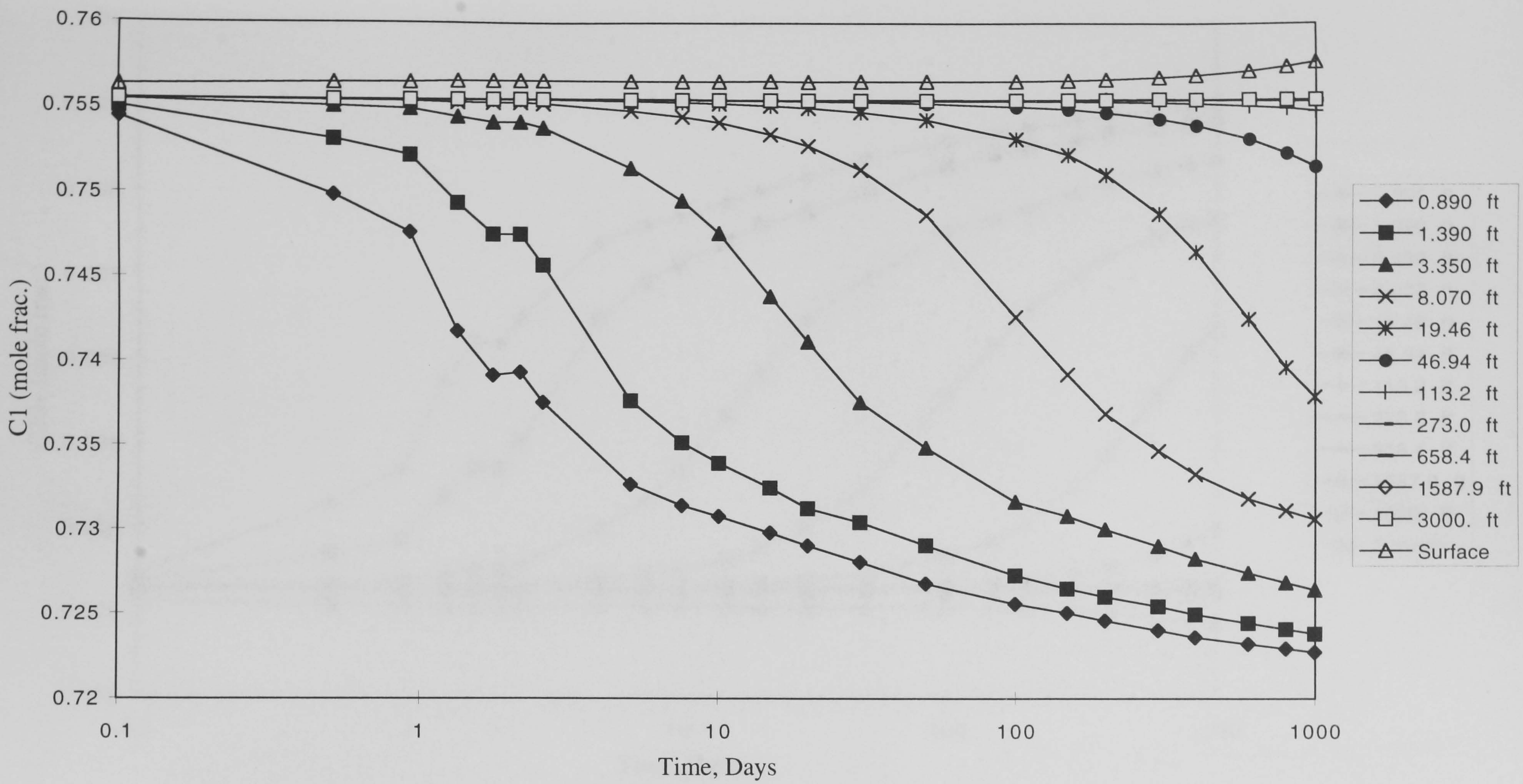

Fig. 4.13 - Variation of Overall Fluid Composition in Grid Block, Gas Condensate GCA94-1.

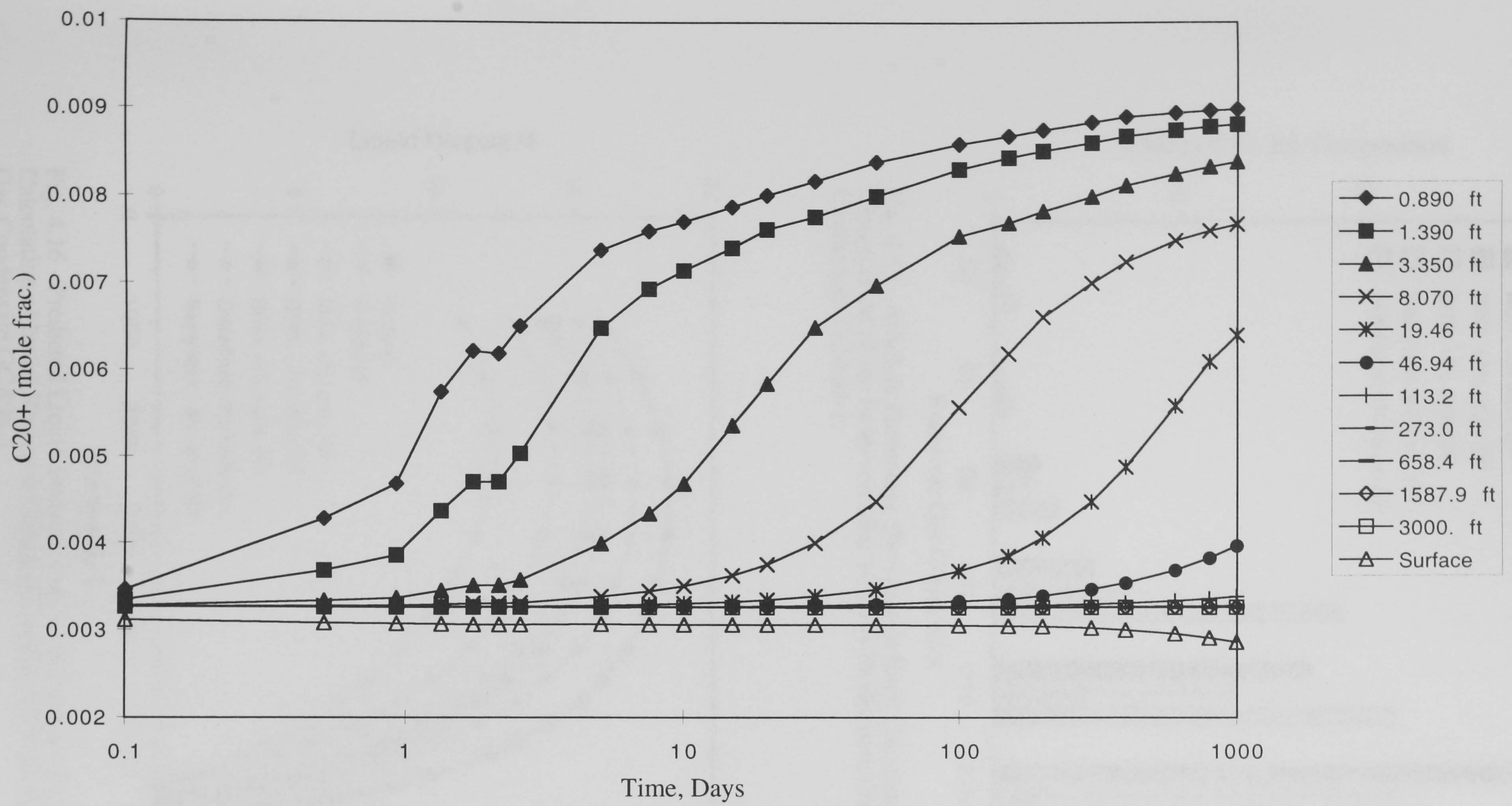

Fig. 4.14 - Variation of Overall Fluid Composition in Grid Block, Gas Condensate GCA94-1.

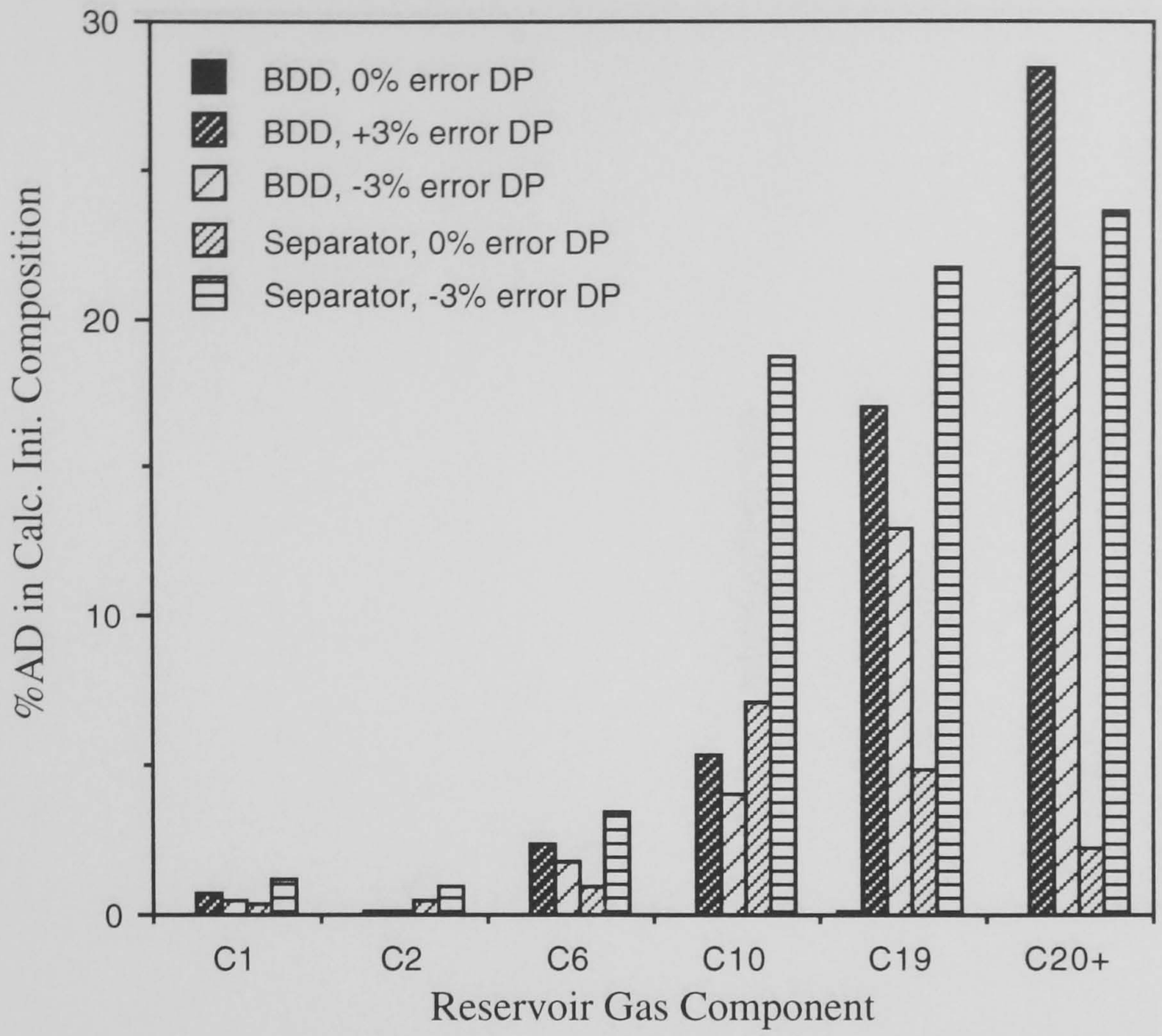

Fig. 4.15 - Absolute Percentage Deviation in Back Calculated Initial Composition of the Reservoir after 10 Days Production, Gas Condensate GCA94-1.

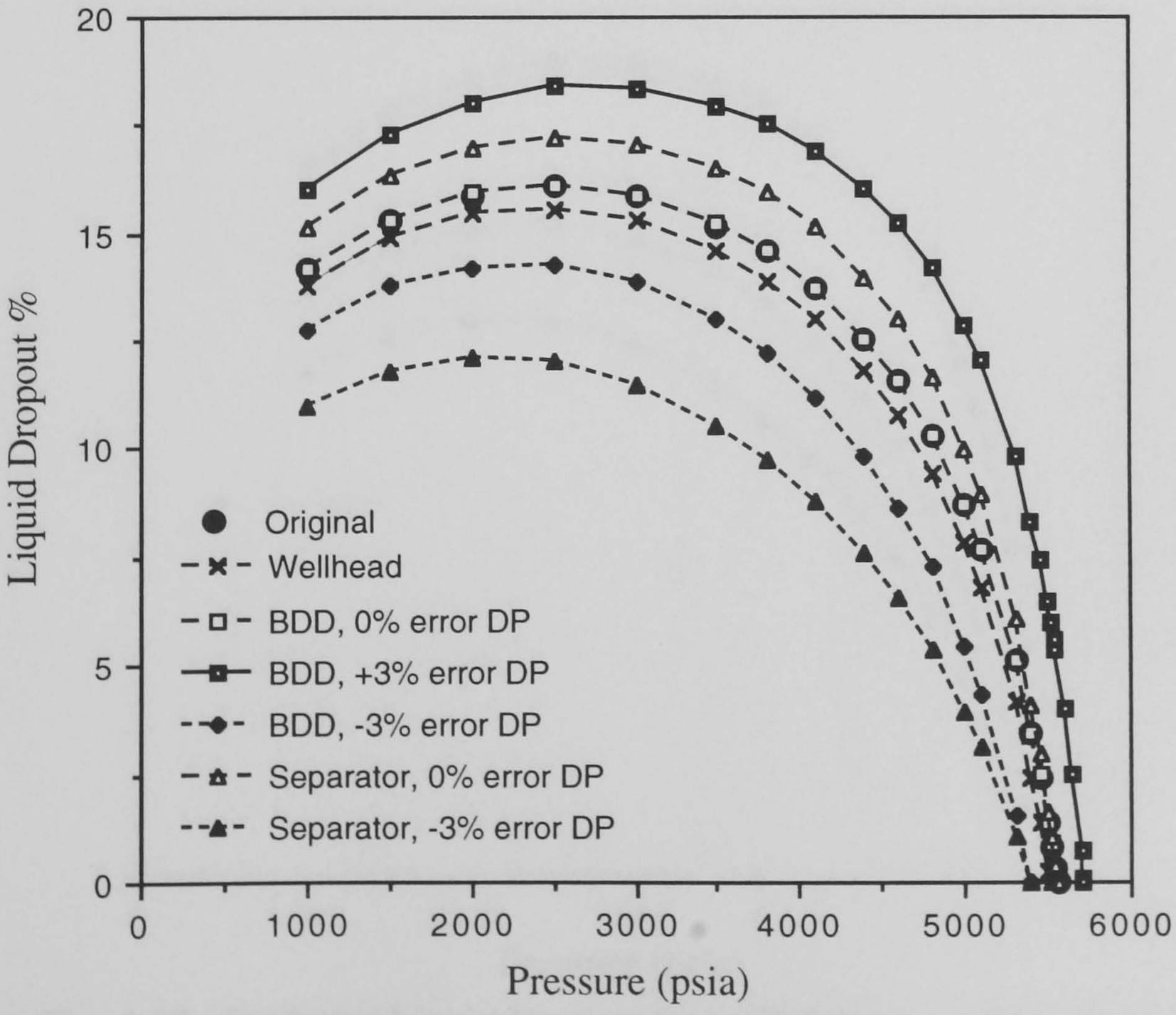

Fig. 4.16 - Predicted Liquid Dropout from CCE Test at 110°C, Back Calculation of Initial Reservoir Composition after 10 Days Production, Gas Condensate GCA94-1.

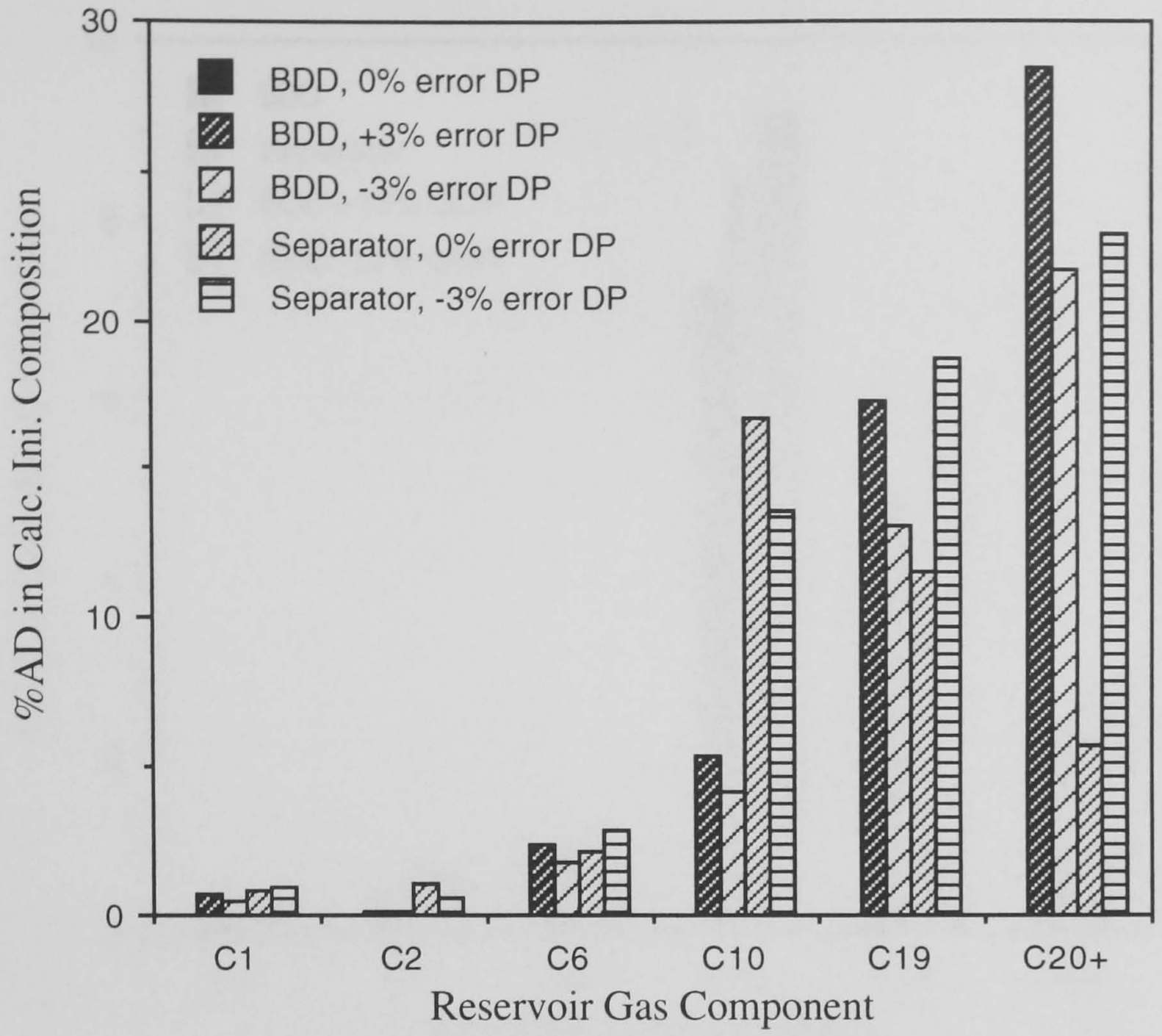

Fig. 4.17 - Absolute Percentage Deviation in Back Calculated Initial Composition of the Reservoir after 1000 Days Production, Gas Condensate GCA94-1.

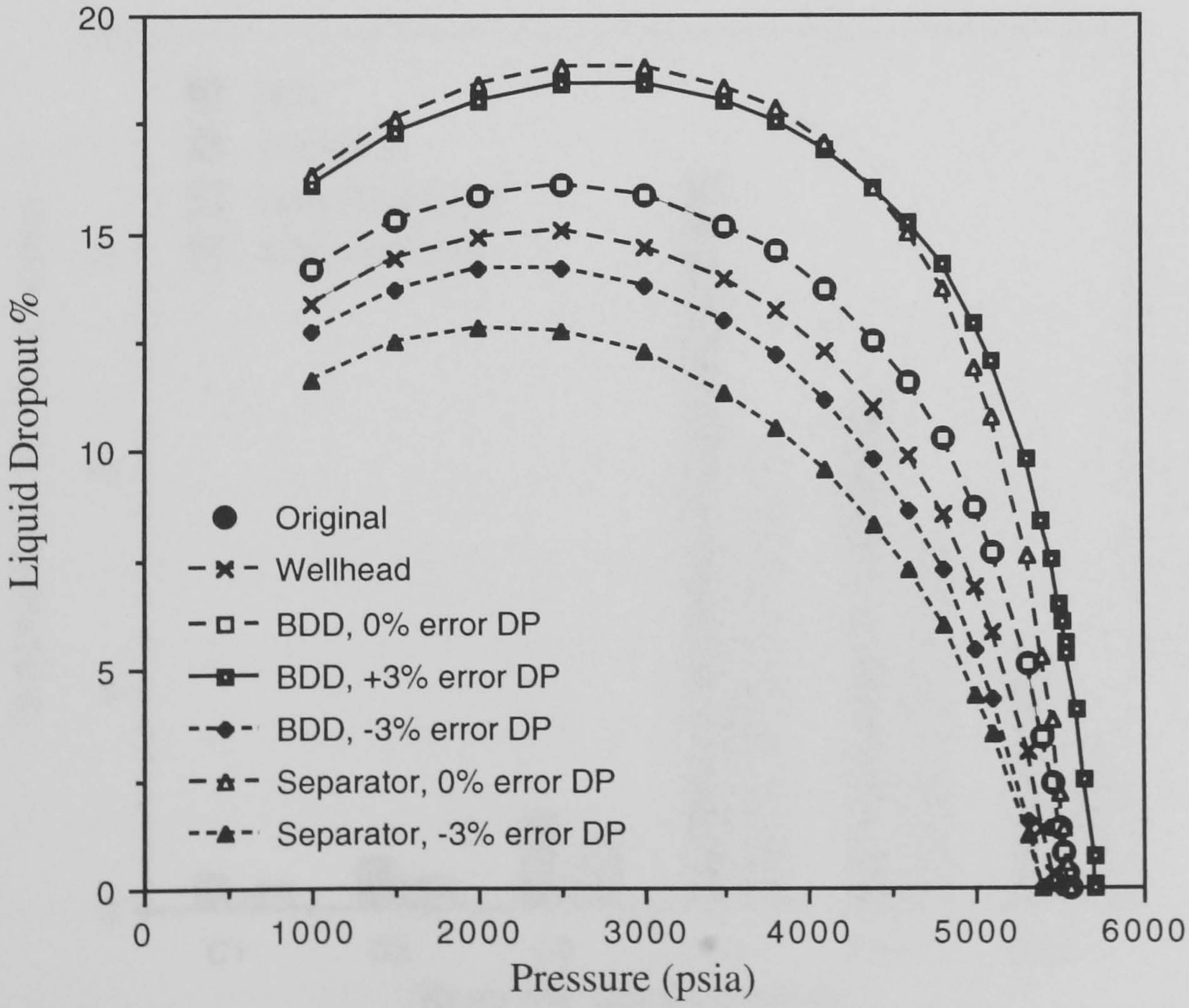

Fig. 4.18 - Predicted Liquid Dropout from CCE Test at 110°C, Back Calculation of Initial Reservoir Composition after 1000 Days Production, Gas Condensate GCA94-1.

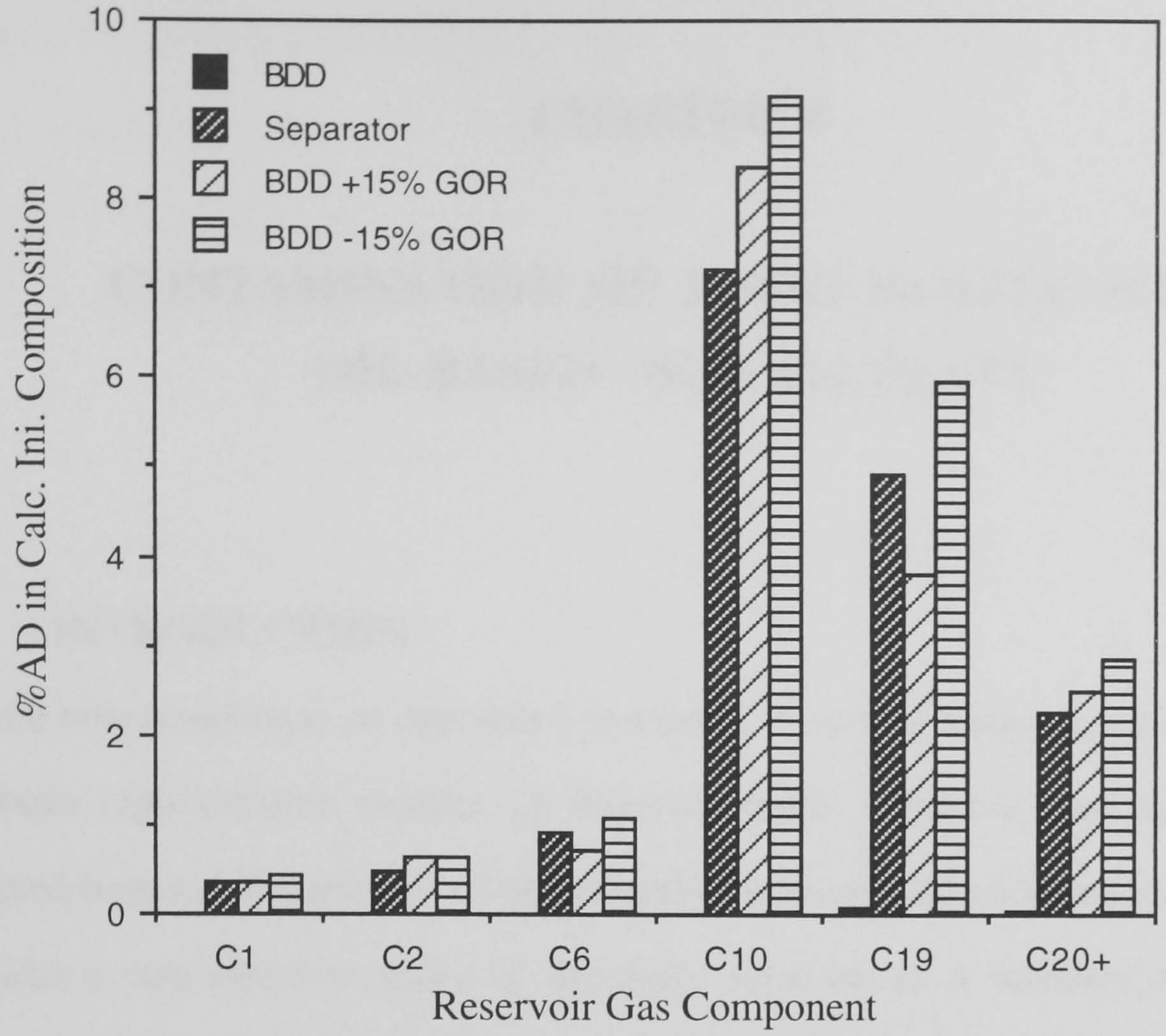

Fig. 4.19 - %AD in Determined Initial Composition after 10 Days Production, with Carryover and Carry Through Errors, Gas Condensate GCA94-1.

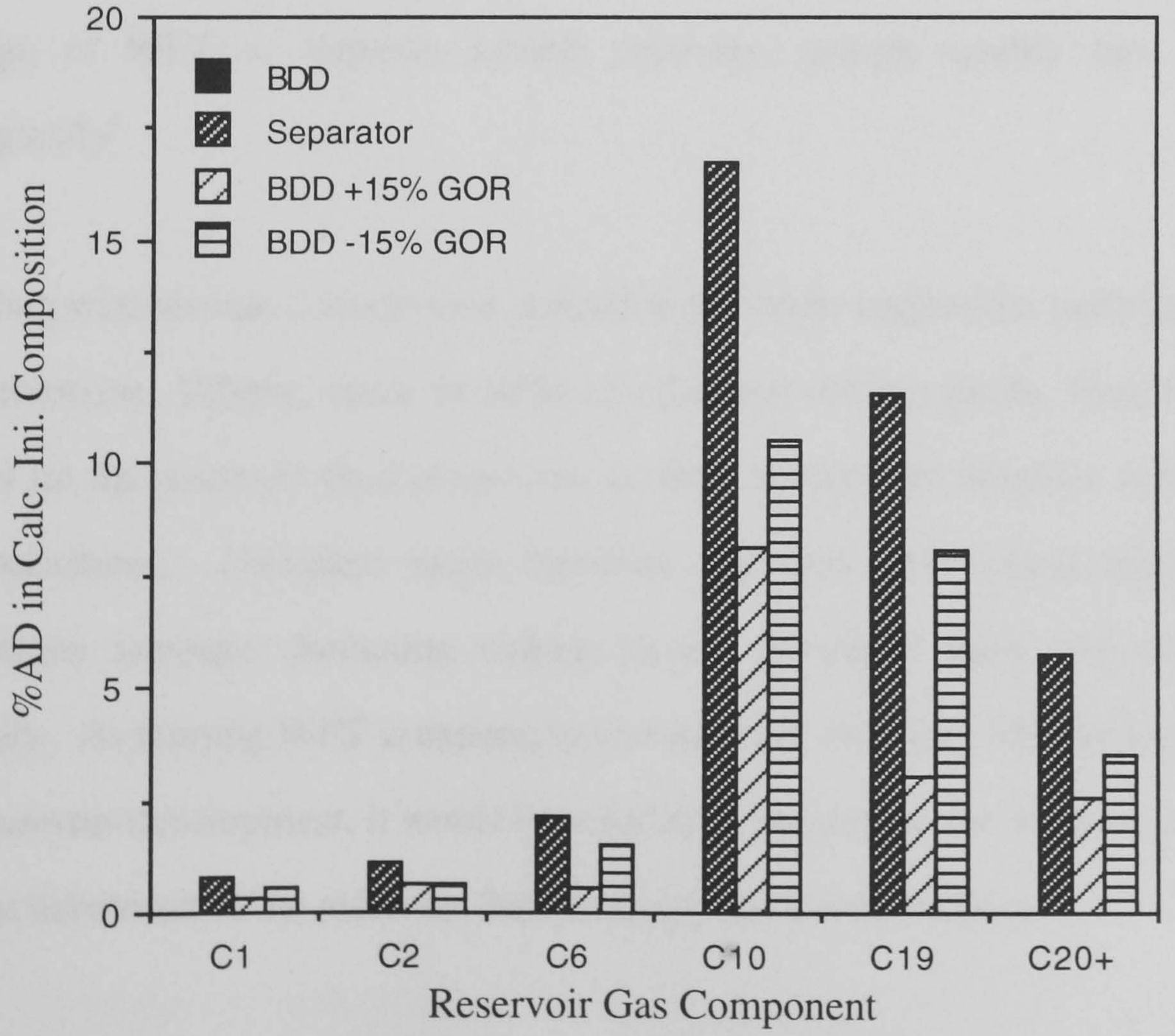

Fig. 4.20 - %AD in Determined Initial Composition after 1000 Days Production, with Carryover and Carry Through Errors, Gas Condensate GCA94-1.

range of 1% to 20% on a volumetric basis. A method has been developed to determine the original composition of the reservoir fluid from contaminated samples. The measured phase behaviour of the contaminated samples are used to tune an EOS, where the model will be applied to predict the volumetric properties of the original reservoir fluid.

5.2 CONTAMINATION OF RESERVOIR FLUIDS WITH MUD FILTRATE

Hydrocarbon-based fluids (natural or synthetic oils) are generally used in oil-based muds to drill a well. As these fluids are soluble in the reservoir fluid, they can impair the fluid sample. Analysis of the contaminated sample is feasible, but identifying the properties of the reservoir fluid free of the contamination is not easily accomplished. Despite the significant need in the petroleum industry to predict the phase behaviour and volumetric properties of uncontaminated reservoir fluid from a contaminated bottom hole sample, the issue has rarely been addressed in the literature.

MacMillan et al.[2] have recently developed a method to predict reservoir fluid phase behaviour from properties of contaminated samples. They purposely contaminated three reservoir oil samples with a synthetic-based drilling mud filtrate in a range of 10% to 25% on a volumetric basis. A gamma distribution function was fitted to the C_{7+} portion of composition of the contaminated samples, where the composition of contaminants showed a significant deviation to the trend of gamma distribution. They excluded the contaminants and retrieved the original reservoir fluid composition. Using a tuned EOS to predict the phase behaviour of retrieved composition, they concluded that the saturation pressure of decontaminated samples could be calculated within 4% error.

To determine the original composition of reservoir fluid from contaminated samples, we have employed a slightly different approach which is simpler than the above mentioned procedure. It has been shown that an exponential relationship exists between the molar composition of C_{8+} portion of real reservoir fluids and the corresponding molecular

weights[3,4]. In other words, if the molar composition of C_{8+} is plotted against molecular weight, it would give a straight line on a semi-logarithmic scale. The exponential distribution function is indeed a specific form of the general gamma distribution function[5].

In this study, different types of real reservoir fluids are contaminated with an oil-based drilling mud filtrate which is mainly C_{14} (Tetradecene) and C_{16} (Hexadecene). The composition of the mud filtrate is given in Table 5.1. Plotting the molar composition of C_{8+} portion of the contaminated samples against their molecular weight on a semi-logarithmic scale, yields peaks would be seen in the composition of C_{14} and C_{16} (contaminants). An exponential distribution function (linear function on semi-logarithmic scale) is fitted to the data after excluding the composition of contaminants from the fluid composition. The fitted function can be used to estimate the composition of C_{14} and C_{16} of the reservoir fluid. The retrieved composition may be used along with those of contaminated samples to back calculate the composition of mud filtrate and the level of contamination. Although, no contaminants other than the mud filtrate are introduced into the system, in real cases the comparison of the calculated composition of mud filtrate with those of the original one, can reveal whether the mud filtrate was in contact with other fluids prior to contaminating the reservoir fluid sample.

The modified Peng-Robinson (mPR, Chapter 2) EOS is used to perform phase equilibrium calculations in the contamination study. Initially, the mPR EOS is tuned to the experimental data of contaminated samples, using the temperature dependency of the attractive term (α parameter) of the components in the liquid phase as regression variables (see Section 3.5). The tuned EOS model is then applied to the retrieved composition to predict the phase behaviour and volumetric properties of the original reservoir fluid. The developed method is applied to contaminated samples of volatile oil and gas condensate mixtures at reservoir and surface conditions and the results are discussed.

5.2.1 Volatile Oil LRA97-1

The volatile oil (LRA97-1) was a real volatile reservoir oil with bubble point pressure values of 4965 and 4550 psia at reservoir (100°C) and separator (37.8°C) conditions, respectively. The fluid (LRA97-1) was used to carry out constant composition expansion (CCE) tests at reservoir and separator conditions. The volatile oil (LRA97-1) was purposely contaminated with the oil-based mud filtrate in the range of 5.3% to 20% on a volumetric basis. The contaminated samples were then subjected to a constant composition expansion (CCE) test at reservoir temperature in the laboratory. The measured liquid fraction values of the original, 5.3%, 10% and 20% (by volume) contaminated samples are plotted against pressure in Fig. 5.1. The experimental results show that contamination of the volatile oil (LRA97-1) with oil-based mud filtrate would lower the bubble point pressure whereas it would increase the liquid fraction at all subsequent pressures. The mPR EOS was individually tuned to the measured experimental data of the original, 5.3%, 10% and 20% contaminated samples, using the α parameter of the liquid phase as regression variables. The tuning results are also depicted in Fig. 5.1. It can be seen that the tuned EOS predictions are in good agreement with the reported experimental data. The variation of bubble point pressure of the volatile oil (LRA97-1) at reservoir conditions with the level of contamination is given in Fig. 5.2. It shows that a 20% contamination could reduce the bubble point pressure as much as 22%.

The molar composition of C_9-C_{19} of 5.3%, 10% and 20% contaminated samples are plotted against molecular weight on a semi-logarithmic scale in Fig. 5.3. It can be seen that the molar compositions of contaminants (C_{14} and C_{16}) show a distinctive deviation in comparison to the linear trend of the rest of components. Excluding the contaminants from the contaminated samples of the reservoir fluid, an exponential distribution function (linear in semi-logarithmic scale) is fitted to the experimental data. The fitted function is used to estimate the molar composition of C_{14} and C_{16} of the original reservoir fluid. The calculated original reservoir fluid compositions from different levels of contamination are respectively given in Tables 5.2, 5.3 and 5.4 for 5.3%, 10% and 20% contamination. The results indicate that the molar composition of C_{14} and C_{16} of the original composition

could be calculated within 6% error regardless of level of contamination. In other words, the level of contamination has no effect on the retrieved composition of reservoir fluid.

Comparing the retrieved composition with those of the contaminated ones, the composition of the oil-based mud filtrate and the level of contamination can be back calculated. The calculation results are given in corresponding Tables for different levels of contamination. The percentage deviation in back calculating the mud filtrate composition and the level of contamination are shown in Fig. 5.4. It indicates that at high levels of contamination (say higher than 10% by volume), the mud filtrate composition and the level of contamination could be back calculated within 1.5% error, however, at low levels of contamination the percentage deviation would exponentially increase. It might be due to the fact that the composition of the C_{8+} portion of the real reservoir fluid deviates from a perfect exponential behaviour and shows anomalies particularly in the molar composition of C_{14} and C_{16}. The deviation can be a large value in comparison to the level of contamination, particularly at low ranges. It should be mentioned that the anomalies may affect the back calculated composition of mud filtrate and the level of contamination, but (as it will be seen) they do not have a major impact on the predicted properties of original reservoir fluids, using the retrieved composition.

The determined mud filtrate composition could reveal whether the mud filtrate was in contact with other fluids prior to contaminating the reservoir fluid sample. If the mud filtrate was in contact with other fluids its composition and the ratio of components could be different from the original composition.

The tuned EOS models to the experimental data of 5.3%, 10% and 20% contaminated samples were used to predict the phase behaviour of the original reservoir fluid in reservoir conditions, using retrieved composition from different levels of contamination. The predicted results are compared with those of the experimentally measured values in Figs. 5.5 and 5.6. The results of tuning the EOS to the measured liquid fraction values of the original fluid are also shown in Fig. 5.5. It shows that the predicted liquid fractions

of the retrieved compositions are in good agreement with the experimental values, particularly at low pressures (less than 3500 psia). Approaching the bubble point pressure the predicted liquid fractions are deviated slightly from measured experimental ones. However, the predicted liquid fractions of the retrieved compositions match the tuning results of the original fluid. Therefore, the deviation in predicting the liquid fraction of the original fluid at higher pressures (close to bubble point) is due to inability of the EOS to give a perfect match to the experimental data of the original fluid. As it is shown in Fig. 5.6, the deviation in predicting the bubble point pressure of original reservoir fluid, using the retrieved composition, increases with the level of contamination. For example, using the retrieved composition from 20% contaminated sample, the bubble point pressure can be determined within 3.5% error.

As was pointed out earlier the retrieved compositions from different levels of contamination were similar and the level of contamination had no effect on the retrieved composition. Therefore, an increase in error of the predicted bubble point pressure of original reservoir fluid, using the retrieved compositions, resulted from tuning of the EOS. The mPR EOS was tuned to the experimental data of the 20% (by volume) contaminated sample which behaved like a low-volatile mixture. Removing the contaminants, the de-contaminated sample would behave like a high-volatile oil. The tuned parameters to the experimental data of the low-volatile oil are not necessarily valid for a high-volatile oil system. Hence, using the adjusted EOS to predict the phase behaviour and volumetric properties of the original reservoir fluid, the predictions can be affected by the level of tuning of EOS, rather than the level of contamination.

The contamination of the volatile oil (LRA97-1) with the oil-based mud filtrate was also investigated at surface conditions. The original and the 5.3% (volume) contaminated samples were used to perform CCE tests at 37.8°C in the laboratory. The measured liquid fractions are plotted against pressure in Fig. 5.7. Contamination of the volatile oil (LRA97-1) with 5.3% (volume) oil-based mud filtrate at this temperature reduced the bubble point pressure of the original fluid by 6.8%. The mPR EOS was individually

adjusted to the experimental data of the original and contaminated samples, where the results are also illustrated in Fig. 5.7. It can be seen that the tuned results match the measured values very well. The tuned EOS to the experimental data of the contaminated sample, was applied to predict the phase behaviour of the retrieved composition at 37.8°C. The results are shown in Fig. 5.8. The tuned results of EOS, using the original composition, are also given in Fig. 5.8. It shows that the predicted liquid fractions of the original reservoir fluid, using the retrieved composition, are in close agreement with those of the original values. The predicted liquid fractions of the retrieved composition also coincide with the tuned results of the original fluid.

The volatile oil (LRA97-1) and the contaminated samples were used to perform a two-stage separator test, using the tuned EOS models. The effect of contamination on the formation volume factor is illustrated in Fig. 5.9. As it was expected, contamination with the oil-based mud filtrate reduced the formation volume factor. Contamination had the same effect on the gas-oil ratio and the stock tank oil density (Fig. 5.10). As the density of mud filtrate is less than the density of stock tank oil, contamination of reservoir fluid decreases the stock tank oil density. The gas-oil ratio is highly affected by contamination whereas stock tank oil density is the least sensitive property to the contamination with the oil-based mud filtrate. Contamination of the volatile oil (LRA97-1) with 20% (volume) oil-based mud filtrate decreased the gas-oil ratio by 32%, however, it decreased the stock tank oil density by only 0.3%. The tuned EOS models were also applied to predict the volumetric behaviour of the original reservoir fluid at separator conditions, using the retrieved composition from different levels of contamination. The results are depicted in Fig. 5.11, where it shows that all the properties of the original reservoir fluid from a separator test (i.e. the formation volume factor, the gas-oil ratio and the stock tank oil density) could be determined within less than 0.5% error.

5.2.2 Gas Condensate GCA94-1

Gas condensate (GCA94-1) is a medium-rich gas condensate at a reservoir temperature of 110°C. The fluid was contaminated with 1%, 3%, 5%, 10% and 20% oil-based drilling

mud filtrate on a volumetric basis (the composition of mud filtrate is given in Table 5.1). The original and the contaminated samples were used to carry out CCE tests at 110°C, using the mPR EOS to perform the phase equilibrium calculations. No experimental data have been generated on the volumetric behaviour of contaminated samples. The predicted liquid dropouts of the original and the contaminated samples from the CCE test are illustrated in Fig. 5.12. It shows that the contamination of the gas condensate (GCA94-1) with the oil-based mud filtrate (mainly C_{14} and C_{16}) would increase the dew point pressure as well as liquid dropout of the system at all subsequent pressures. It can also be seen that 10% (by volume) contamination with the oil-based mud filtrate would dramatically change the phase behaviour of the fluid (GCA94-1) from a gas condensate to a very volatile oil. The effect of contamination with the oil-based mud filtrate on saturation pressure of the gas condensate (GCA94-1) is demonstrated in Fig. 5.13. The fluid behaved as a gas condensate up to 5% (by volume) contamination, however, it changed to a very volatile oil mixture at 10% contamination. The dew point pressure increased with the level of contamination, whereas the bubble point pressure decreased with further contamination with mud filtrate (10% and 20% contamination). The variation of saturation density with level of contamination is shown in Fig. 5.14. There is almost a linear increment in the density of the saturated fluid with percentage of contamination.

The original and the contaminated samples were also used to conduct a two-stage separator test. Contamination had a large impact on the gas-liquid ratio where a 20% contamination (by volume) with the oil-based mud filtrate caused 62% reduction in the gas-liquid ratio. The variation of gas-liquid ratio with the level of contamination is illustrated in Fig. 5.15. The effect of contamination on the stock tank liquid density and the formation volume factor are shown in Fig. 5.16. The formation volume factor of the 10% and 20% contaminated samples are only depicted in this Figure as the original and the other contaminated samples behave like a gas condensate mixture. Fig. 5.16 shows that contamination could dramatically decrease the formation volume factor of very volatile oil mixtures, however it had the least effect on the stock tank liquid density. As it can be seen, the stock tank liquid density non-linearly increases with the level of

contamination and a 20% contamination with the oil-based mud filtrate has an impact of 3.7% increase in the stock tank liquid density.

To determine the composition of the original gas condensate (GCA94-1), the molar composition of C_8-C_{19} of the contaminated samples are plotted against molecular weight in Fig. 5.17 for 1%, 3%, 5%, 10% and 20% contamination (by volume). Excluding the molar composition of contaminants (C_{14} and C_{16}) an exponential distribution function is fitted to the compositional data. The fitted function is used to predict the molar composition of C_{14} and C_{16} of the original reservoir fluid where the results are given in Tables 5.5 to 5.9 for different levels of contamination. As it was expected, the level of contamination had no effect on the retrieved composition and the original molar composition of C_{14} and C_{16} are determined with -20.4% and +21.4% error from all levels of contamination, respectively. Using the retrieved composition to perform a CCE test, the predicted liquid dropout values are compared to those of original fluid in Fig. 5.18. It shows that although there is -20.4% and +21.4% deviation in the molar composition of C_{14} and C_{16} of the retrieved composition, the volumetric behaviour of the retrieved composition is in close agreement with that of the original fluid.

The retrieved composition was also applied to conduct a two-stage separator test. The results are compared with those of original fluid in Table 5.10. It shows that the volumetric behaviour of the original fluid could be predicted, using the retrieved composition. The reason for such good results, is the reliability of the method in retrieving the original composition from contaminated samples and using untuned EOS to predict the phase behaviour and volumetric properties of the retrieved composition.

Comparing the retrieved composition with those of contaminated samples the molar composition of mud filtrate and the level of contamination could be back calculated. The calculation results are given in Tables 5.5 to 5.9 for different levels of contamination. The results of back calculating the mud filtrate composition and the level of contamination are summarised in Fig. 5.19. It demonstrates that at high levels of contamination (say

higher than 10% by volume) the mentioned properties can be back calculated within a reasonable deviation (say less than 5% error). However, at low level of contamination the error in determining the composition of mud filtrate and the level of contamination would increase exponentially. Therefore, at low level of contamination, it can be quite misleading if the results are used as criteria to investigate whether the mud filtrate has been in contact with other fluids prior to contaminating the reservoir fluid sample.

5.3 CONCLUSIONS

The impact of contamination with an oil-based mud filtrate on the phase behaviour and volumetric properties of reservoir fluids including, volatile oil and gas condensate samples, have been investigated. A practical method has been developed to determine the composition of the original reservoir fluid from contaminated samples.

A volatile oil sample was contaminated with an oil-based mud filtrate (mainly C_{14} and C_{16}) at different volume percentages of the contaminant equal 5.3, 10.0 and 20.0 at 6000 psia and 100°C. The contamination dramatically reduced the bubble point pressure of the system almost linearly with the volume percentage of the contaminant.

It has been demonstrated that an exponential relationship exists between the molar composition of C_{8+} portion of real reservoir fluids and corresponding molecular weight. This feature of natural fluids can be used to calculate the original reservoir fluid composition and determine the level contamination. The mole fraction of all the components in the original oil, except the contaminants (C_{14} and C_{16}), are calculated with a deviation of about 0.08%, which is of the order of 0.00001 mole fraction for most compounds. The deviation for C_{14} and C_{16} groups were 0.06 and 0.03 mole% at 10% contamination level. Such deviations are within the error bands of fluid analysis and are of little significance to oil systems.

A phase behaviour model using the modified Peng-Robinson (mPR) EOS was tuned to the experimental data of the contaminated samples. The tuned model was used to predict the phase behaviour and properties of the original fluid, using the retrieved composition from contaminated samples. The results clearly demonstrated that if contamination did not cause a big shift on the phase diagram (i.e. changing from a gas condensate to an oil system), the tuned EOS to the contaminated samples could reasonably predict the phase behaviour of the original fluid.

The developed approach has also been applied to a gas condensate system at different contamination levels up to 20% by volume at the reservoir conditions. The predicted results by the phase behaviour model show that contamination with the oil-based mud filtrate can dramatically affect the phase behaviour of the gas condensate systems. In this study a 10% contamination (on volumetric basis) has changed the phase behaviour of the gas condensate to a very volatile oil system. Applying the developed method to the contaminated samples, the retrieved compositions are in good agreement with the original composition.

REFERENCES

1. Michaels, J., Moody, M. and Shwe, S., (1995) : "Wireline Fluid Sampling", SPE paper 30610, presented at the SPE Annual Technical Conference and Exhibition held in Dallas, 22-25 October.

2. MacMillan, D.J., Ginley, G.M. and Dembicki, H., (1997) : "How to Obtain Reservoir Fluid Properties from an Oil Sample Contaminated with Synthetic Drilling Mud", SPE paper 38852, presented at the SPE Annual Technical Conference and Exhibition held in San Antonio, Texas, 5-8 October.

3. Katz, D., (1983) : "Overview of Phase Behaviour in Oil and Gas Production", *JPT*, June, 1205-1214.

4. Pedersen, K., Thomassen, P. and Fredenslund, A., (1982) : "Phase Equilibria and Separation Processes", Report SEP 8207, Inst. of Kemiteknik, Denmark Tekniske Højskole, July.

5. Whitson, C.H., (1983) : "Characterizing Hydrocarbon Plus Fraction", *SPEJ*, August, 683-694.

Table 5.1 : Composition of Oil-based Drilling Mud Filtrate.

Component	Mole%	MW
Tetradecene (C_{14})	69.00	196.4
Hexadecene (C_{16})	31.00	224.4

Table 5.2 : Contamination of Volatile Oil LRA97-1 with Oil-based Mud Filtrate, 5.3% Volumetric, at 6000 psia and 100°C.

Name	Mole% Contam.	Mole% Read	Mole% Calculated	Mole% Original	%Deviation
C1	54.574	54.574	55.862	55.904	-0.08
C2	9.640	9.640	9.868	9.875	-0.08
C3	5.529	5.529	5.660	5.664	-0.08
iC4	1.166	1.166	1.194	1.195	-0.07
nC4	2.076	2.076	2.125	2.127	-0.08
iC5	1.200	1.200	1.229	1.230	-0.08
nC5	2.099	2.099	2.149	2.150	-0.08
C6	1.799	1.799	1.841	1.843	-0.07
C7	2.131	2.131	2.181	2.183	-0.07
C8	2.456	2.456	2.514	2.516	-0.08
C9	1.725	1.725	1.766	1.767	-0.07
C10	1.487	1.487	1.523	1.524	-0.08
C11	1.153	1.153	1.180	1.181	-0.08
C12	0.839	0.839	0.859	0.859	-0.07
C13	1.071	1.071	1.096	1.097	-0.08
C14	**2.393**	**0.792**	**0.811**	**0.770**	**5.37**
C15	0.739	0.739	0.756	0.757	-0.07
C16	**1.321**	**0.617**	**0.631**	**0.598**	**5.60**
C17	0.426	0.426	0.436	0.436	-0.08
C18	0.497	0.497	0.509	0.509	-0.07
C19	0.512	0.512	0.524	0.524	-0.08
C20+	5.166	5.166	5.288	5.292	-0.08
	Sum	**97.695**	**100.000**		
Moles	Removed	2.305			

Mole% Contam. : Molar composition of contaminated sample.

Mole% Read : Estimated molar composition of C_{14} and C_{16} of the uncontaminated sample from semi-logarithmic plot.

Mole% Calculated : Calculated molar composition of uncontaminated sample.

Mole% Original : Original molar composition of reservoir fluid.

Table 5.2 : Continued... (5.3% Contamination)
Determination of Mud Filtrate Composition and Level of Contamination.

Name	Mole% Contam.	Mole% Read	Moles Removed	Mud-Mole% Calculated	Mud-Mole% Original	%Deviation
C14	2.393	0.792	1.601	**69.44**	69.00	0.64
C16	1.321	0.617	0.704	**30.56**	31.00	-1.42
			2.305	100.00		

Fluid	Moles-mix	MW	Mass-mix (gr)	Density (gr/cc)	Vol.-mix (cc)	Vol.%
LRA97-1	97.695	65.42	6391.23	0.57	11212.68	94.86
Mud Filtrate	2.305	205.08	472.65	0.778	607.52	**5.14**
					11820.20	

Mole% Contam : Molar composition of C_{14} and C_{16} in contaminated sample.
Mole% Read : Estimated molar composition of C_{14} and C_{16} of uncontaminated reservoir fluid from semi-logarithmic plot.
Moles Removed : Number of moles of C_{14} and C_{16} removed from 100 moles of contaminated sample.
Vol.% : Calculated level of contamination (volumetric) at initial conditions of 6000 psia and 100°C.

Table 5.3 : Contamination of Volatile Oil LRA97-1 with Oil-based Mud Filtrate, 10.0% Volumetric, at 6000 psia and 100°C.

Name	Mole% Contam.	Mole% Read	Mole% Calculated	Mole% Original	%Deviation
C1	53.324	53.324	55.862	55.904	-0.08
C2	9.419	9.419	9.867	9.875	-0.08
C3	5.402	5.402	5.659	5.664	-0.08
iC4	1.140	1.140	1.194	1.195	-0.07
nC4	2.029	2.029	2.125	2.127	-0.07
iC5	1.173	1.173	1.229	1.230	-0.07
nC5	2.051	2.051	2.149	2.150	-0.07
C6	1.758	1.758	1.841	1.843	-0.07
C7	2.082	2.082	2.181	2.183	-0.07
C8	2.400	2.400	2.514	2.516	-0.08
C9	1.685	1.685	1.766	1.767	-0.07
C10	1.454	1.454	1.523	1.524	-0.07
C11	1.126	1.126	1.180	1.181	-0.08
C12	0.820	0.820	0.859	0.859	-0.07
C13	1.046	1.046	1.096	1.097	-0.08
C14	**3.918**	**0.774**	**0.811**	**0.770**	**5.37**
C15	0.722	0.722	0.756	0.757	-0.07
C16	**2.001**	**0.603**	**0.631**	**0.598**	**5.60**
C17	0.416	0.416	0.436	0.436	-0.07
C18	0.485	0.485	0.508	0.509	-0.08
C19	0.500	0.500	0.524	0.524	-0.08
C20+	5.048	5.048	5.288	5.292	-0.08
	Sum	**95.458**	**100.000**		
Moles	Removed	4.542			

Mole% Contam. : Molar composition of contaminated sample.

Mole% Read : Estimated molar composition of C_{14} and C_{16} of the uncontaminated sample from semi-logarithmic plot.

Mole% Calculated : Calculated molar composition of uncontaminated sample.

Mole% Original : Original molar composition of reservoir fluid.

Table 5.3 : Continued... (10.0% Contamination)
Determination of Mud Filtrate Composition and Level of Contamination.

Name	Mole% Contam.	Mole% Read	Moles Removed	Mud-Mole% Calculated	Mud-Mole% Original	%Deviation
C14	3.918	0.774	3.144	**69.22**	69.00	0.32
C16	2.001	0.603	1.398	**30.78**	31.00	-0.71
			4.542	100.00		

Fluid	Mole-mix	MW	Mass-mix (gr)	Density (gr/cc)	Vol.-mix (cc)	Vol.%
LRA97-1	95.458	65.42	6244.86	0.57	10955.89	90.15
Mud Filtrate	4.542	205.08	931.49	0.778	1197.29	**9.85**
					12153.18	

Mole% Contam : Molar composition of C_{14} and C_{16} in contaminated sample.
Mole% Read : Estimated molar composition of C_{14} and C_{16} of uncontaminated reservoir fluid from semi-logarithmic plot.
Moles Removed : Number of moles of C_{14} and C_{16} removed from 100 moles of contaminated sample.
Vol.% : Calculated level of contamination (volumetric) at initial conditions of 6000 psia and 100°C.

Table 5.4 : Contamination of Volatile Oil LRA97-1 with Oil-based Mud Filtrate, 20.0% Volumetric, at 6000 psia and 100°C.

Name	Mole% Contam.	Mole% Read	Mole% Calculated	Mole% Original	%Deviation
C1	50.441	50.441	55.862	55.904	-0.08
C2	8.910	8.910	9.868	9.875	-0.08
C3	5.110	5.110	5.659	5.664	-0.08
iC4	1.078	1.078	1.194	1.195	-0.08
nC4	1.919	1.919	2.125	2.127	-0.07
iC5	1.109	1.109	1.229	1.230	-0.08
nC5	1.940	1.940	2.149	2.150	-0.07
C6	1.663	1.663	1.841	1.843	-0.08
C7	1.970	1.970	2.181	2.183	-0.07
C8	2.270	2.270	2.514	2.516	-0.08
C9	1.594	1.594	1.766	1.767	-0.08
C10	1.375	1.375	1.523	1.524	-0.07
C11	1.065	1.065	1.180	1.181	-0.08
C12	0.775	0.775	0.859	0.859	-0.08
C13	0.990	0.990	1.096	1.097	-0.08
C14	**7.437**	**0.732**	**0.811**	**0.770**	**5.37**
C15	0.683	0.683	0.756	0.757	-0.08
C16	**3.569**	**0.570**	**0.631**	**0.598**	**5.60**
C17	0.394	0.394	0.436	0.436	-0.07
C18	0.459	0.459	0.509	0.509	-0.07
C19	0.473	0.473	0.524	0.524	-0.07
C20+	4.775	4.775	5.288	5.292	-0.08
	Sum	**90.296**	**100.000**		
Moles	Removed	9.704			

Mole% Contam. : Molar composition of contaminated sample.

Mole% Read : Estimated molar composition of C_{14} and C_{16} of the uncontaminated sample from semi-logarithmic plot.

Mole% Calculated : Calculated molar composition of uncontaminated sample.

Mole% Original : Original molar composition of reservoir fluid.

Table 5.4 : Continued... (20.0% Contamination)
Determination of Mud Filtrate Composition and Level of Contamination.

Name	Mole% Contam.	Mole% Read	Moles Removed	Mud-Mole% Calculated	Mud-Mole% Original	%Deviation
C14	7.437	0.732	6.705	**69.10**	69.00	0.14
C16	3.569	0.570	2.999	**30.90**	31.00	-0.31
			9.704	100.00		

Fluid	Mole-mix	MW	Mass-mix (gr)	Density (gr/cc)	Vol.-mix (cc)	Vol.%
LRA97-1	90.296	65.42	5907.18	0.57	10363.47	80.20
Mud Filtrate	9.704	205.08	1990.06	0.778	2557.91	**19.80**
					12921.38	

Mole% Contam : Molar composition of C_{14} and C_{16} in contaminated sample.
Mole% Read : Estimated molar composition of C_{14} and C_{16} of uncontaminated reservoir fluid from semi-logarithmic plot.
Moles Removed : Number of moles of C_{14} and C_{16} removed from 100 moles of contaminated sample.
Vol.% : Calculated level of contamination (volumetric) at initial conditions of 6000 psia and 100°C.

Table 5.5 : Contamination of Gas Condensate GCA94-1 with Oil-based Mud Filtrate, 1.0% Volumetric, at 6000 psia and 110°C.

Name	Mole% Contam.	Mole% Read	Mole% Calculated	Mole% Original	%Deviation
N2	1.020	1.020	1.024	1.024	0.03
C1	75.318	75.318	75.600	75.574	0.03
CO2	2.082	2.082	2.090	2.089	0.03
C2	7.353	7.353	7.381	7.378	0.03
C3	3.753	3.753	3.767	3.766	0.03
iC4	0.532	0.532	0.534	0.534	0.04
nC4	1.362	1.362	1.368	1.367	0.04
iC5	0.440	0.440	0.441	0.441	0.03
nC5	0.611	0.611	0.613	0.613	0.03
C6	0.829	0.829	0.832	0.832	0.04
C7	1.401	1.401	1.406	1.406	0.03
C8	1.396	1.396	1.402	1.401	0.04
C9	0.851	0.851	0.854	0.854	0.03
C10	0.539	0.539	0.541	0.541	0.04
C11	0.383	0.383	0.384	0.384	0.03
C12	0.295	0.295	0.296	0.296	0.04
C13	0.245	0.245	0.246	0.246	0.05
C14	**0.538**	**0.243**	**0.244**	**0.306**	**-20.40**
C15	0.220	0.220	0.221	0.221	0.06
C16	**0.226**	**0.148**	**0.148**	**0.122**	**21.45**
C17	0.108	0.108	0.108	0.108	0.00
C18	0.0945	0.0945	0.095	0.095	0.06
C19	0.078	0.078	0.078	0.078	-0.01
C20+	0.325	0.325	0.326	0.326	0.04
	Sum	**99.627**	**100.000**		
Moles	Removed	0.373			

Mole% Contam. : Molar composition of contaminated sample.

Mole% Read : Estimated molar composition of C_{14} and C_{16} of the uncontaminated sample from semi-logarithmic plot.

Mole% Calculated : Calculated molar composition of uncontaminated sample.

Mole% Original : Original molar composition of reservoir fluid.

Table 5.5 : Continued... (1.0% Contamination)
Determination of Mud Filtrate Composition and Level of Contamination.

Name	Mole% Contam.	Mole% Read	Moles Removed	Mud-Mole% Calculated	Mud-Mole% Original	%Deviation
C14	0.538	0.243	0.295	**78.98**	69.00	14.46
C16	0.226	0.148	0.078	**21.02**	31.00	-32.18
			0.373	100.00		

Fluid	Mole-mix	MW	Mass-mix (gr)	Density (gr/cc)	Vol.-mix (cc)	Vol.%
GCA94-1	99.627	28.71	2860.78	0.3254	8791.58	98.89
Mud Filtrate	0.373	205.08	76.56	0.778	98.41	**1.11**
					8889.99	

Mole% Contam : Molar composition of C_{14} and C_{16} in contaminated sample.

Mole% Read : Estimated molar composition of C_{14} and C_{16} of uncontaminated reservoir fluid from semi-logarithmic plot.

Moles Removed : Number of moles of C_{14} and C_{16} removed from 100 moles of contaminated sample.

Vol.% : Calculated level of contamination (volumetric) at initial conditions of 6000 psia and 110°C.

Table 5.6 : Contamination of Gas Condensate GCA94-1 with Oil-based Mud Filtrate, 3.0% Volumetric, at 6000 psia and 110°C.

Name	Mole% Contam.	Mole% Read	Mole% Calculated	Mole% Original	%Deviation
N2	1.013	1.013	1.024	1.024	0.04
C1	74.798	74.798	75.600	75.574	0.03
CO2	2.068	2.068	2.090	2.089	0.04
C2	7.302	7.302	7.380	7.378	0.03
C3	3.727	3.727	3.767	3.766	0.03
iC4	0.529	0.529	0.534	0.534	0.03
nC4	1.353	1.353	1.368	1.367	0.04
iC5	0.436	0.436	0.441	0.441	0.04
nC5	0.607	0.607	0.613	0.613	0.03
C6	0.824	0.824	0.832	0.832	0.04
C7	1.392	1.392	1.407	1.406	0.04
C8	1.387	1.387	1.401	1.401	0.03
C9	0.845	0.845	0.854	0.854	0.03
C10	0.535	0.535	0.541	0.541	0.03
C11	0.380	0.380	0.384	0.384	0.05
C12	0.293	0.293	0.296	0.296	0.05
C13	0.244	0.244	0.246	0.246	0.04
C14	**1.010**	**0.241**	**0.244**	**0.306**	**-20.40**
C15	0.219	0.219	0.221	0.221	0.02
C16	**0.438**	**0.147**	**0.148**	**0.122**	**21.45**
C17	0.107	0.107	0.108	0.108	0.04
C18	0.094	0.094	0.095	0.095	0.01
C19	0.077	0.077	0.078	0.078	0.04
C20+	0.323	0.323	0.326	0.326	0.05
	Sum	**98.939**	**100.000**		
Moles	Removed	1.061			

Mole% Contam. : Molar composition of contaminated sample.

Mole% Read : Estimated molar composition of C_{14} and C_{16} of the uncontaminated sample from semi-logarithmic plot.

Mole% Calculated : Calculated molar composition of uncontaminated sample.

Mole% Original : Original molar composition of reservoir fluid.

Table 5.6 : Continued... (3.0% Contamination)
Determination of Mud Filtrate Composition and Level of Contamination.

Name	Mole% Contam.	Mole% Read	Moles Removed	Mud-Mole% Calculated	Mud-Mole% Original	%Deviation
C14	1.010	0.241	0.769	**72.49**	69.00	5.06
C16	0.438	0.147	0.291	**27.51**	31.00	-11.26
			1.060	100.00		

Fluid	Mole-mix	MW	Mass-mix (gr)	Density (gr/cc)	Vol.-mix (cc)	Vol.%
GCA94-1	98.940	28.71	2841.04	0.3254	8730.92	96.90
Mud Filtrate	1.060	205.08	217.53	0.778	279.60	**3.10**
					9010.52	

Mole% Contam : Molar composition of C_{14} and C_{16} in contaminated sample.
Mole% Read : Estimated molar composition of C_{14} and C_{16} of uncontaminated reservoir fluid from semi-logarithmic plot.
Moles Removed : Number of moles of C_{14} and C_{16} removed from 100 moles of contaminated sample.
Vol.% : Calculated level of contamination (volumetric) at initial conditions of 6000 psia and 110°C.

Table 5.7 : Contamination of Gas Condensate GCA94-1 with Oil-based Mud Filtrate, 5.0% Volumetric, at 6000 psia and 110°C.

Name	Mole% Contam.	Mole% Read	Mole% Calculated	Mole% Original	%Deviation
N2	1.006	1.006	1.024	1.024	0.04
C1	74.264	74.264	75.600	75.574	0.03
CO2	2.053	2.053	2.090	2.089	0.04
C2	7.250	7.250	7.381	7.378	0.03
C3	3.701	3.701	3.767	3.766	0.03
iC4	0.525	0.525	0.534	0.534	0.03
nC4	1.343	1.343	1.367	1.367	0.03
iC5	0.433	0.433	0.441	0.441	0.04
nC5	0.602	0.602	0.613	0.613	0.04
C6	0.818	0.818	0.832	0.832	0.04
C7	1.382	1.382	1.406	1.406	0.03
C8	1.377	1.377	1.401	1.401	0.03
C9	0.839	0.839	0.854	0.854	0.03
C10	0.532	0.532	0.541	0.541	0.03
C11	0.377	0.377	0.384	0.384	0.02
C12	0.291	0.291	0.296	0.296	0.05
C13	0.242	0.242	0.246	0.246	0.02
C14	**1.495**	**0.239**	**0.244**	**0.306**	**-20.40**
C15	0.217	0.217	0.221	0.221	0.05
C16	**0.657**	**0.145**	**0.148**	**0.122**	**21.44**
C17	0.106	0.106	0.108	0.108	0.01
C18	0.093	0.093	0.095	0.095	0.08
C19	0.077	0.077	0.078	0.078	-0.03
C20+	0.320	0.320	0.326	0.326	0.02
	Sum	**98.233**	**100.000**		
Moles	Removed	1.767			

Mole% Contam. : Molar composition of contaminated sample.

Mole% Read : Estimated molar composition of C_{14} and C_{16} of the uncontaminated sample from semi-logarithmic plot.

Mole% Calculated : Calculated molar composition of uncontaminated sample.

Mole% Original : Original molar composition of reservoir fluid.

Table 5.7 : Continued... (5.0% Contamination)
Determination of Mud Filtrate Composition and Level of Contamination.

Name	Mole% Contam.	Mole% Read	Moles Removed	Mud-Mole% Calculated	Mud-Mole% Original	%Deviation
C14	1.495	0.239	1.256	**71.08**	69.00	3.02
C16	0.657	0.145	0.511	**28.92**	31.00	-6.71
			1.767	100.00		

Fluid	Mole-mix	MW	Mass-mix (gr)	Density (gr/cc)	Vol.-mix (cc)	Vol.%
GCA94-1	98.233	28.71	2820.75	0.3254	8668.58	94.90
Mud Filtrate	1.767	205.08	362.42	0.778	465.83	**5.10**
					9134.41	

Mole% Contam : Molar composition of C_{14} and C_{16} in contaminated sample.
Mole% Read : Estimated molar composition of C_{14} and C_{16} of uncontaminated reservoir fluid from semi-logarithmic plot.
Moles Removed : Number of moles of C_{14} and C_{16} removed from 100 moles of contaminated sample.
Vol.% : Calculated level of contamination (volumetric) at initial conditions of 6000 psia and 110°C.

Table 5.8 : Contamination of Gas Condensate GCA94-1 with Oil-based Mud Filtrate, 10.0% Volumetric, at 6000 psia and 110°C.

Name	Mole% Contam.	Mole% Read	Mole% Calculated	Mole% Original	%Deviation
N2	0.987	0.987	1.024	1.024	0.04
C1	72.862	72.862	75.600	75.574	0.03
CO2	2.014	2.014	2.090	2.089	0.03
C2	7.113	7.113	7.381	7.378	0.03
C3	3.631	3.631	3.767	3.766	0.04
iC4	0.515	0.515	0.534	0.534	0.03
nC4	1.318	1.318	1.368	1.367	0.04
iC5	0.425	0.425	0.441	0.441	0.04
nC5	0.591	0.591	0.613	0.613	0.03
C6	0.802	0.802	0.832	0.832	0.03
C7	1.356	1.356	1.407	1.406	0.04
C8	1.351	1.351	1.401	1.401	0.03
C9	0.823	0.823	0.854	0.854	0.04
C10	0.522	0.522	0.541	0.541	0.04
C11	0.370	0.370	0.384	0.384	0.03
C12	0.285	0.285	0.296	0.296	0.04
C13	0.237	0.237	0.246	0.246	0.05
C14	**2.769**	**0.235**	**0.244**	**0.306**	**-20.40**
C15	0.213	0.213	0.221	0.221	0.05
C16	**1.229**	**0.143**	**0.148**	**0.122**	**21.46**
C17	0.104	0.104	0.108	0.108	0.01
C18	0.092	0.092	0.095	0.095	0.04
C19	0.075	0.075	0.078	0.078	0.03
C20+	0.314	0.314	0.326	0.326	0.03
	Sum	**96.379**	**100.000**		
Moles	Removed	3.621			

Mole% Contam. : Molar composition of contaminated sample.

Mole% Read : Estimated molar composition of C_{14} and C_{16} of the uncontaminated sample from semi-logarithmic plot.

Mole% Calculated : Calculated molar composition of uncontaminated sample.

Mole% Original : Original molar composition of reservoir fluid.

Table 5.8 : Continued... (10.0% Contamination)

Determination of Mud Filtrate Composition and Level of Contamination.

Name	Mole% Contam.	Mole% Read	Moles Removed	Mud-Mole% Calculated	Mud-Mole% Original	%Deviation
C14	2.769	0.235	2.534	**70.00**	69.00	1.44
C16	1.229	0.143	1.086	**30.00**	31.00	-3.22
			3.620	100.00		

Fluid	Mole-mix	MW	Mass-mix (gr)	Density (gr/cc)	Vol.-mix (cc)	Vol.%
GCA94-1	96.380	28.71	2767.52	0.3254	8504.97	89.91
Mud Filtrate	3.620	205.08	742.64	0.778	954.55	**10.09**
					9459.52	

Mole% Contam : Molar composition of C_{14} and C_{16} in contaminated sample.

Mole% Read : Estimated molar composition of C_{14} and C_{16} of uncontaminated reservoir fluid from semi-logarithmic plot.

Moles Removed : Number of moles of C_{14} and C_{16} removed from 100 moles of contaminated sample.

Vol.% : Calculated level of contamination (volumetric) at initial conditions of 6000 psia and 110°C.

Table 5.9 : Contamination of Gas Condensate GCA94-1 with Oil-based Mud Filtrate, 20.0% Volumetric, at 6000 psia and 110°C.

Name	Mole% Contam.	Mole% Read	Mole% Calculated	Mole% Original	%Deviation
N2	0.945	0.945	1.024	1.024	0.03
C1	69.736	69.736	75.600	75.574	0.03
CO2	1.928	1.928	2.090	2.089	0.03
C2	6.808	6.808	7.381	7.378	0.03
C3	3.475	3.475	3.767	3.766	0.03
iC4	0.493	0.493	0.534	0.534	0.04
nC4	1.261	1.261	1.367	1.367	0.03
iC5	0.407	0.407	0.441	0.441	0.03
nC5	0.566	0.566	0.613	0.613	0.03
C6	0.768	0.768	0.832	0.832	0.03
C7	1.297	1.297	1.406	1.406	0.04
C8	1.293	1.293	1.402	1.401	0.04
C9	0.788	0.788	0.854	0.854	0.03
C10	0.499	0.499	0.541	0.541	0.03
C11	0.354	0.354	0.384	0.384	0.02
C12	0.273	0.273	0.296	0.296	0.02
C13	0.227	0.227	0.246	0.246	0.04
C14	**5.611**	**0.225**	**0.244**	**0.306**	**-20.39**
C15	0.204	0.204	0.221	0.221	0.02
C16	**2.507**	**0.137**	**0.148**	**0.122**	**21.48**
C17	0.100	0.100	0.108	0.108	0.08
C18	0.088	0.088	0.095	0.095	0.08
C19	0.072	0.072	0.078	0.078	0.07
C20+	0.301	0.301	0.326	0.326	0.03
	Sum	**92.244**	**100.000**		
Moles	Removed	7.756			

Mole% Contam. : Molar composition of contaminated sample.

Mole% Read : Estimated molar composition of C_{14} and C_{16} of the uncontaminated sample from semi-logarithmic plot.

Mole% Calculated : Calculated molar composition of uncontaminated sample.

Mole% Original : Original molar composition of reservoir fluid.

Table 5.9 : Continued... (20.0% Contamination)
Determination of Mud Filtrate Composition and Level of Contamination.

Name	Mole% Contam.	Mole% Read	Moles Removed	Mud-Mole% Calculated	Mud-Mole% Original	%Deviation
C14	5.611	0.225	5.386	**69.45**	69.00	0.65
C16	2.507	0.137	2.370	**30.55**	31.00	-1.44
			7.756	100.00		

Fluid	Mole-mix	MW	Mass-mix (gr)	Density (gr/cc)	Vol.-mix (cc)	Vol.%
GCA94-1	92.244	28.71	2648.78	0.3254	8140.07	79.93
Mud Filtrate	7.756	205.08	1590.65	0.778	2044.54	**20.07**
					10184.61	

Mole% Contam : Molar composition of C_{14} and C_{16} in contaminated sample.

Mole% Read : Estimated molar composition of C_{14} and C_{16} of uncontaminated reservoir fluid from semi-logarithmic plot.

Moles Removed : Number of moles of C_{14} and C_{16} removed from 100 moles of contaminated sample.

Vol.% : Calculated level of contamination (volumetric) at initial conditions of 6000 psia and 110°C.

Table 5.10 : Separator Test Results of Original and Retrieved Compositions of Gas Condensate GCA94-1.

Property	Original	Retrieved	%Deviation
Gas-Liquid Ratio (SCF/STB)	9097	9156	+0.65
Stock Tank Liquid Density (gr/cc)	0.7730	0.7728	-0.03

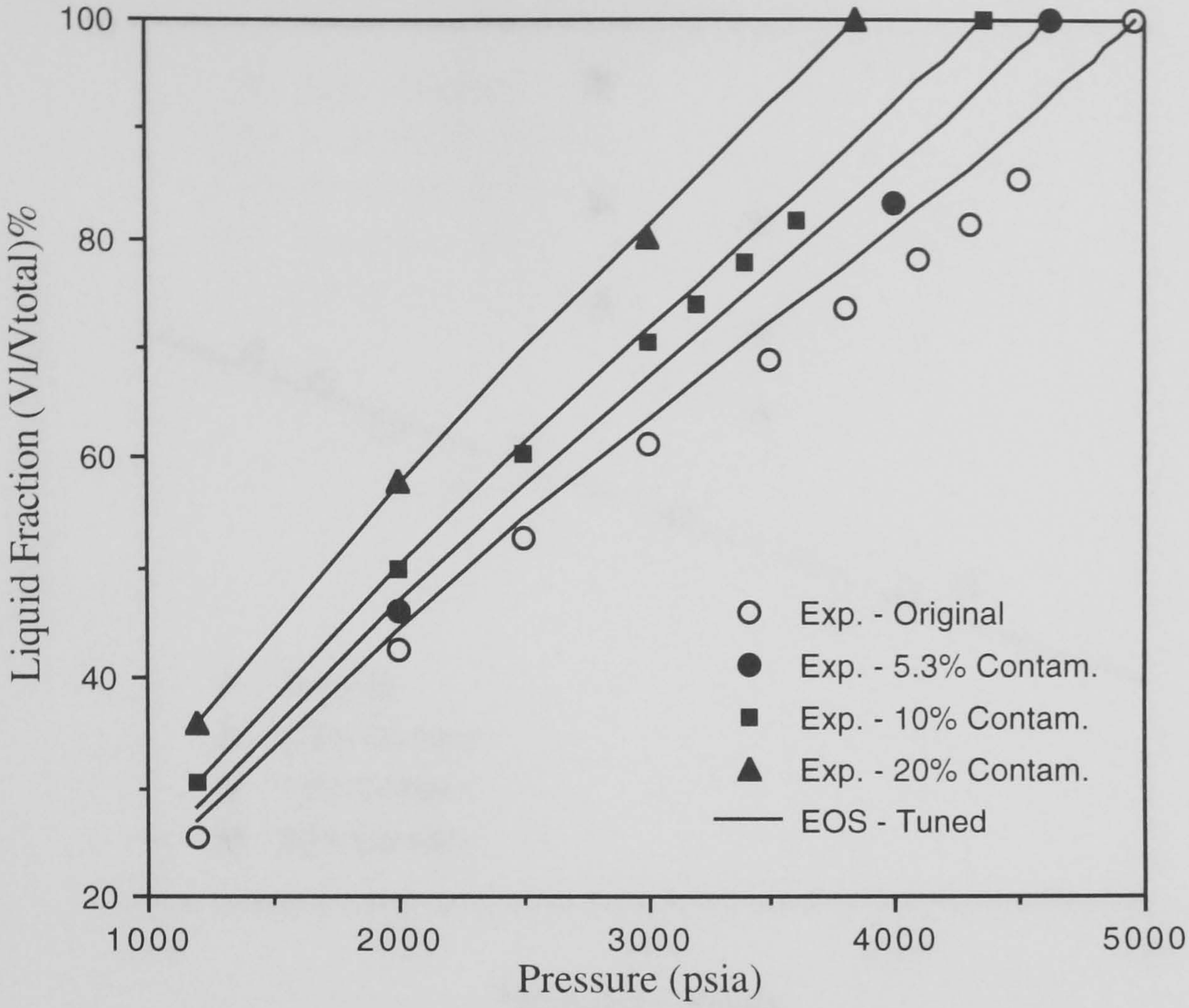

Fig. 5.1 - Phase Behaviour of Volatile Oil LRA97-1 Contaminated with 5.3%, 10% and 20% (Volume) Oil-based Mud Filtrate, Constant Composition Expansion (CCE) Test at 100°C.

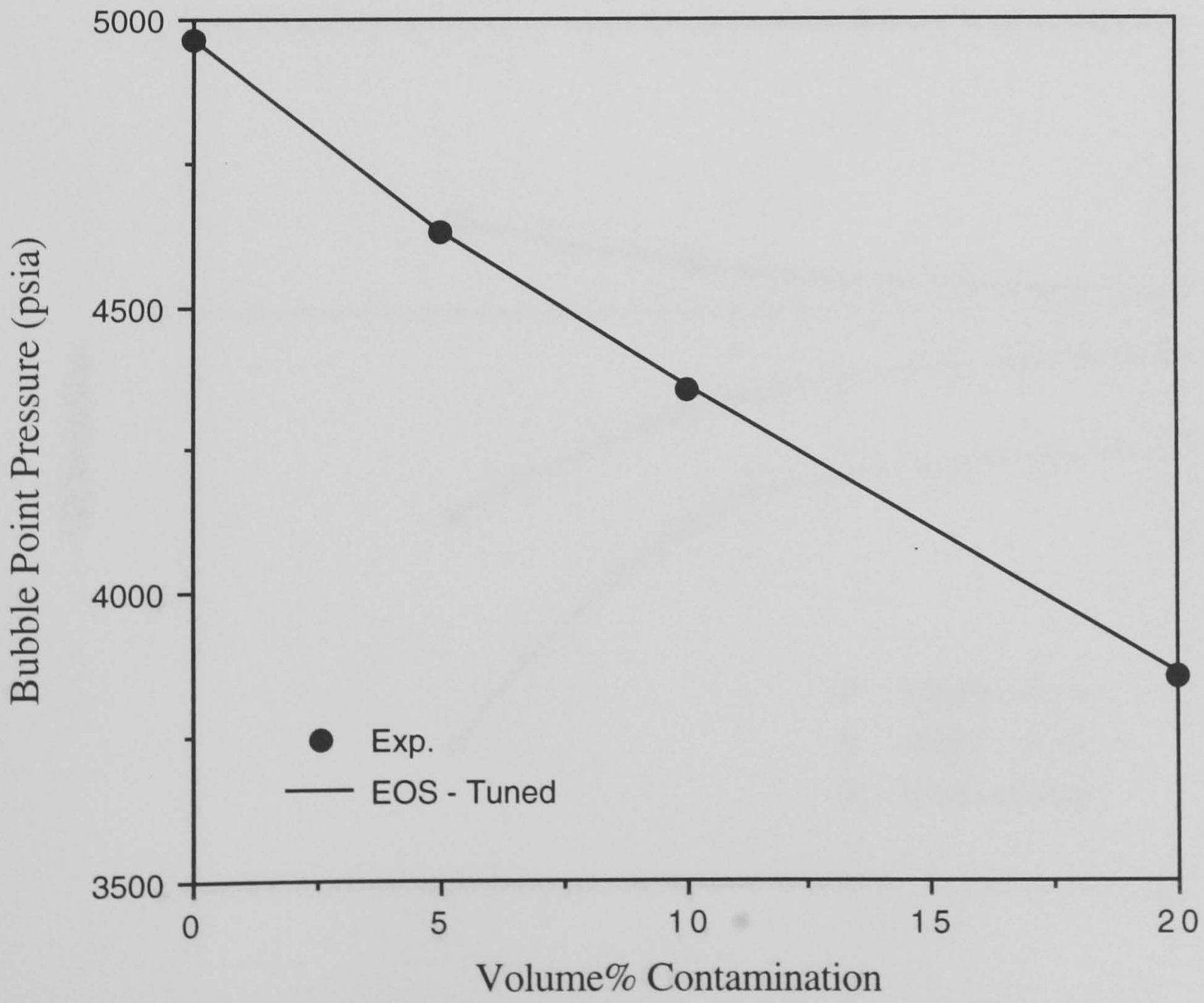

Fig. 5.2 - Effect of Contamination with Oil-based Mud Filtrate on Bubble Point Pressure, Volatile Oil LRA97-1, 100°C.

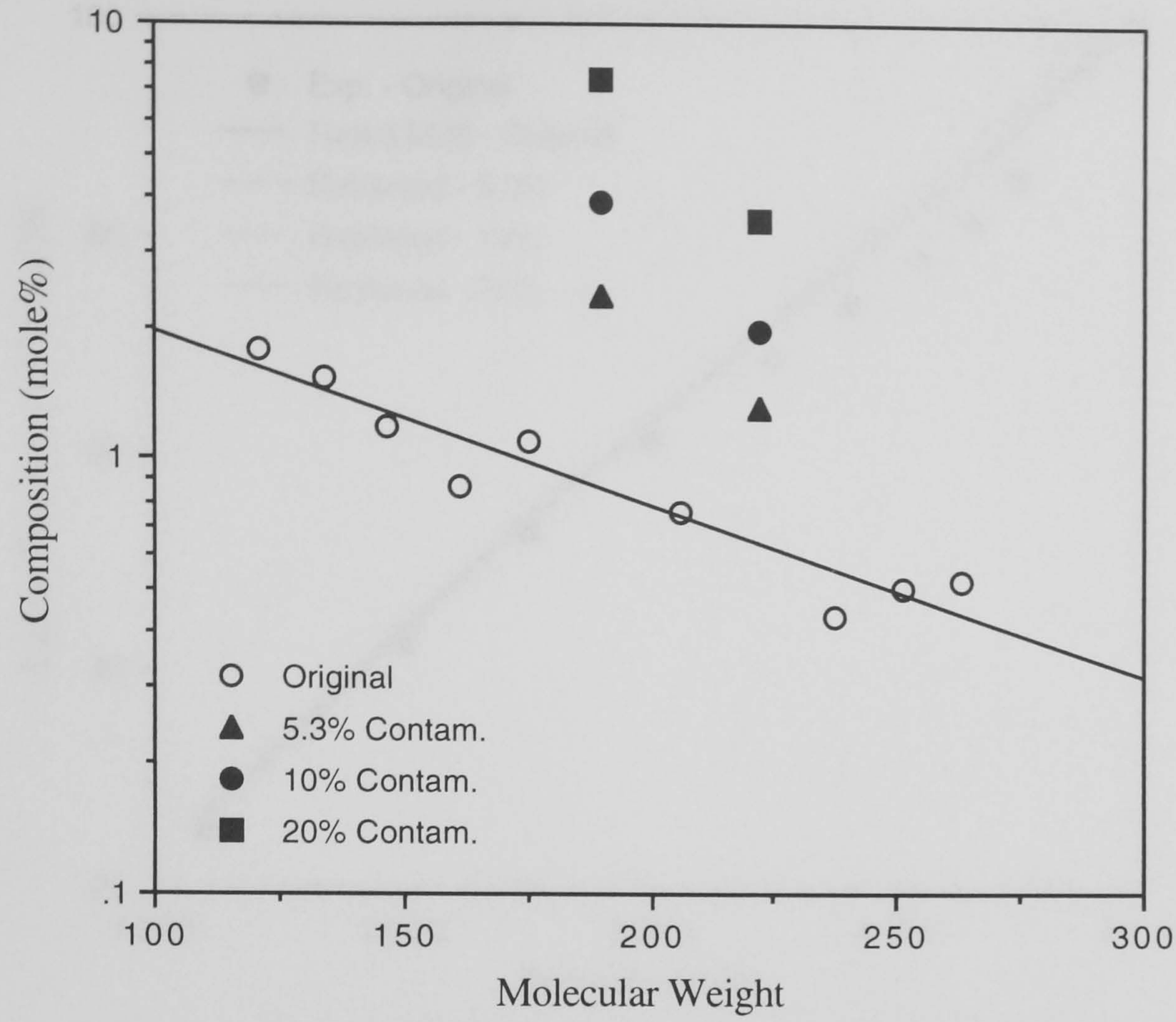

Fig. 5.3 - Composition of Volatile Oil LRA97-1 Contaminated with 5.3%, 10% and 20% (Volumetric) Oil-based Mud Filtrate, C9-C19.

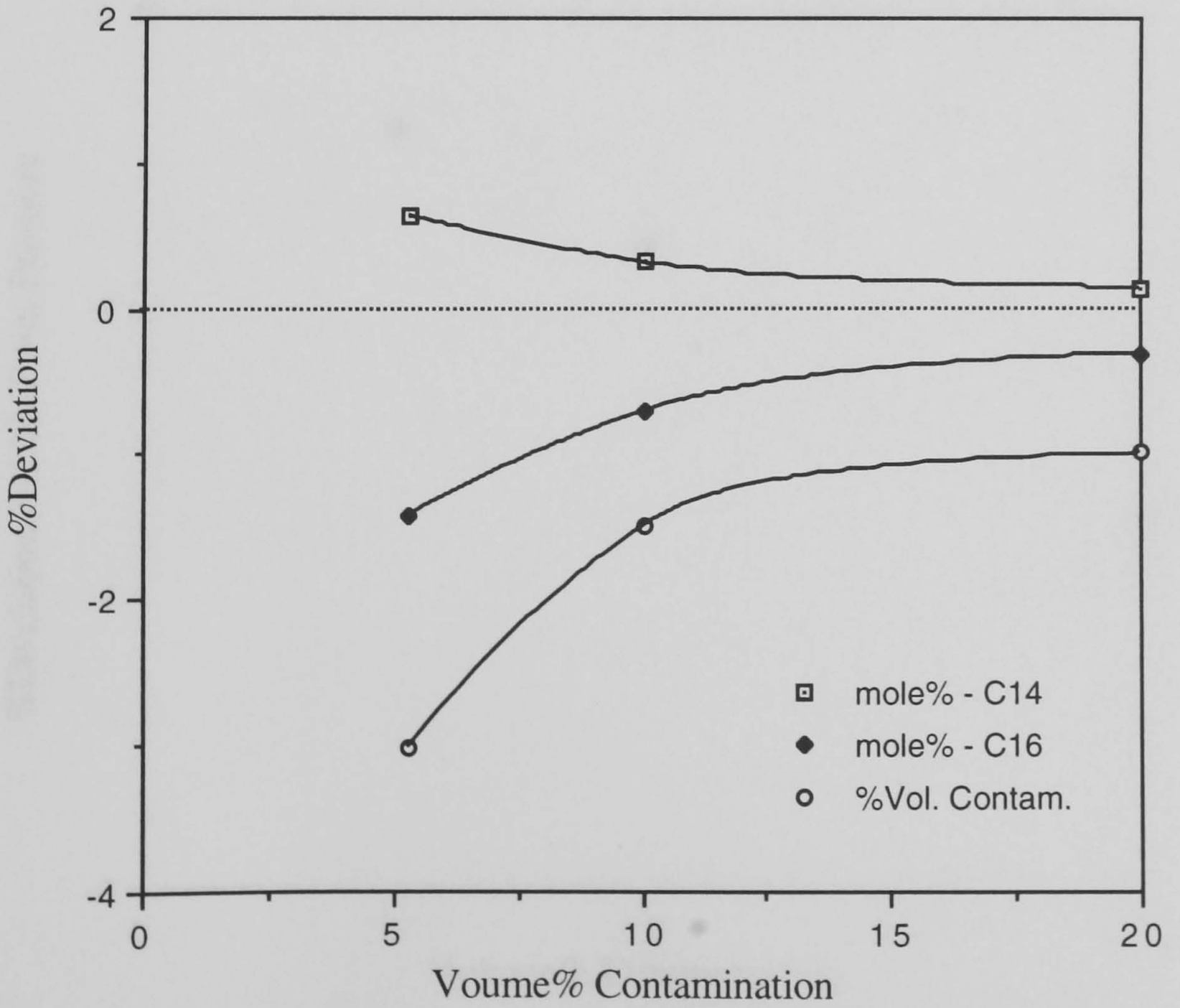

Fig. 5.4 - %Deviation in Determining Mud Filtrate Composition and Level of Contamination, Volatile Oil LRA97-1.

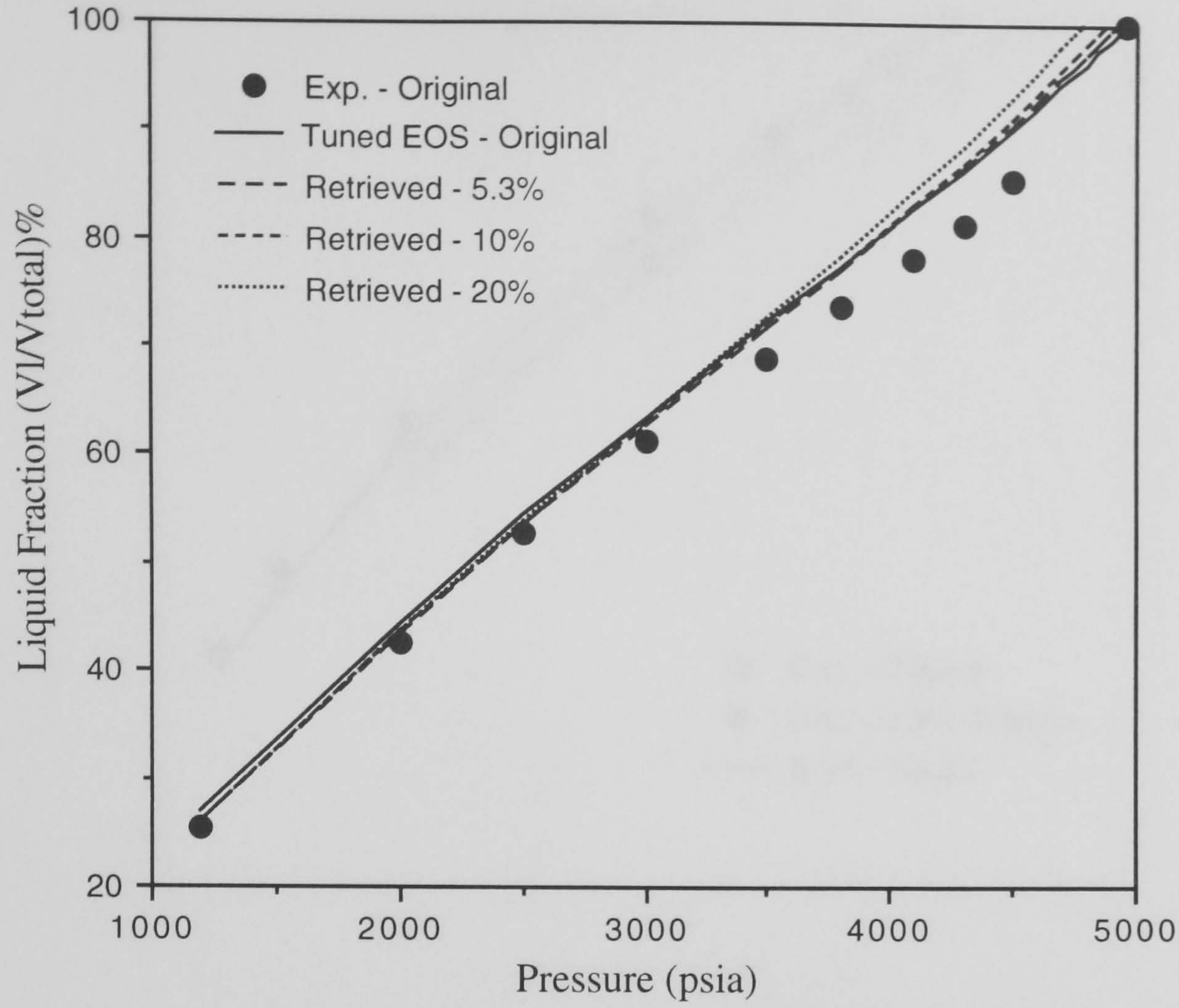

Fig. 5.5 - Volumetric Behaviour of the Original and Retrieved Compositions from Contaminated Samples, Volatile Oil LRA97-1, Constant Composition Expansion (CCE) Test at 100°C.

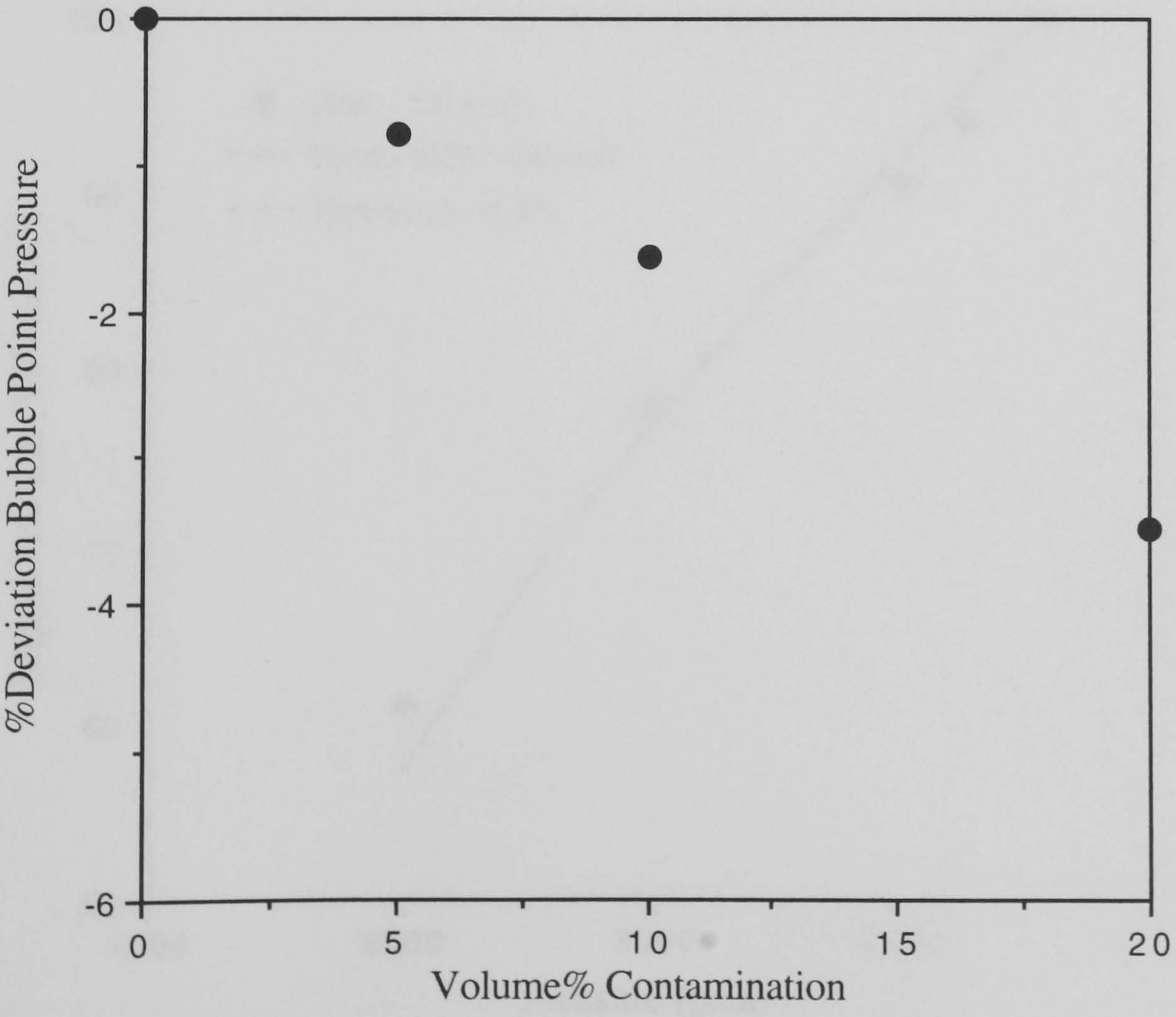

Fig. 5.6 - %Deviation in Bubble Point Pressure of Retrieved Composition from Contaminated Samples with Different Level of Contamination at 100°C, Volatile Oil LRA97-1.

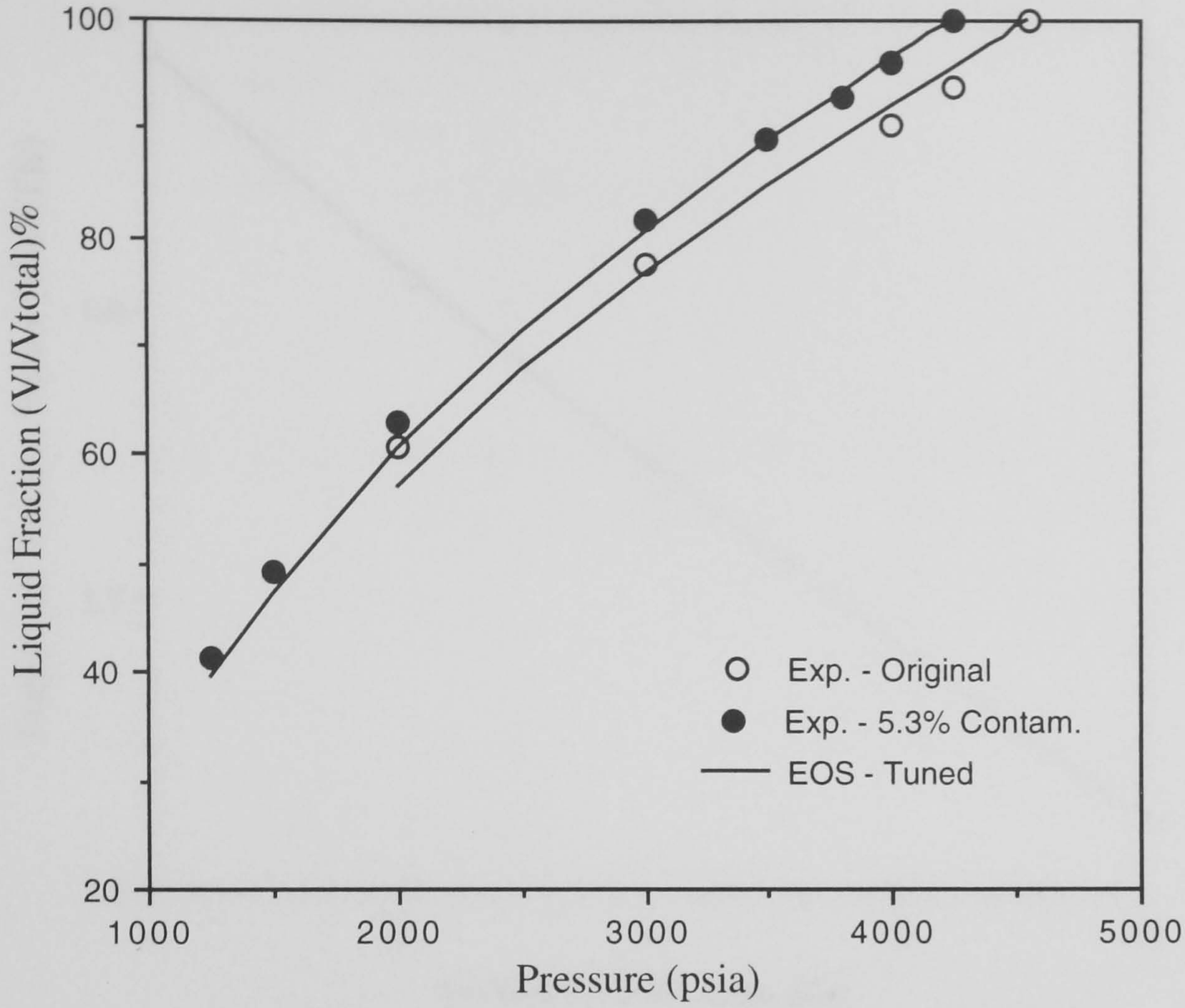

Fig. 5.7 - Phase Behaviour of Volatile Oil LRA97-1 Contaminated with 5.3% (Volume) Oil-based Mud Filtrate, Constant Composition Expansion (CCE) Test at 37.8°C.

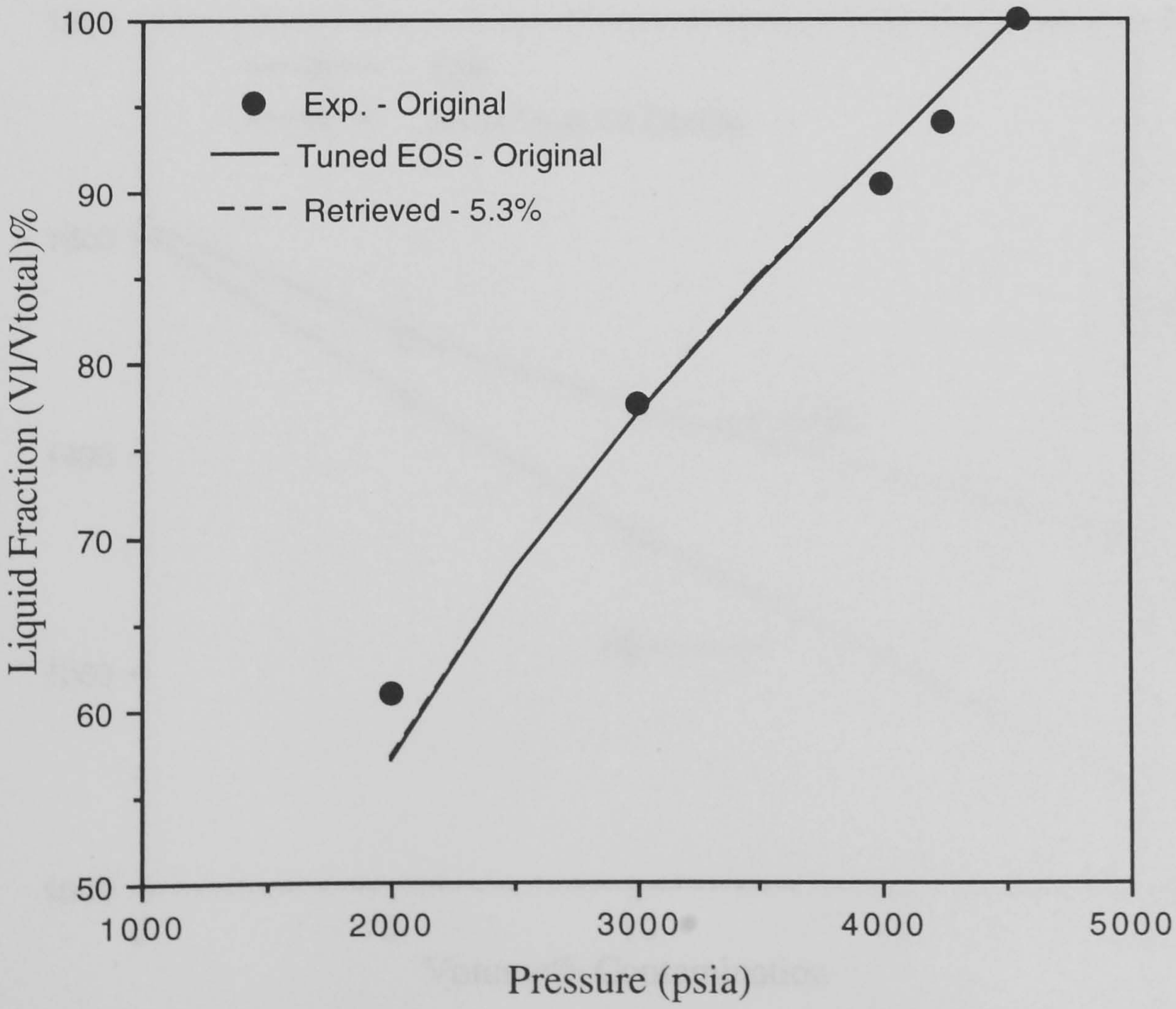

Fig. 5.8 - Volumetric Behaviour of the Original and Retrieved Compositions from Contaminated Sample, Volatile Oil LRA97-1, CCE Test at 37.8°C.

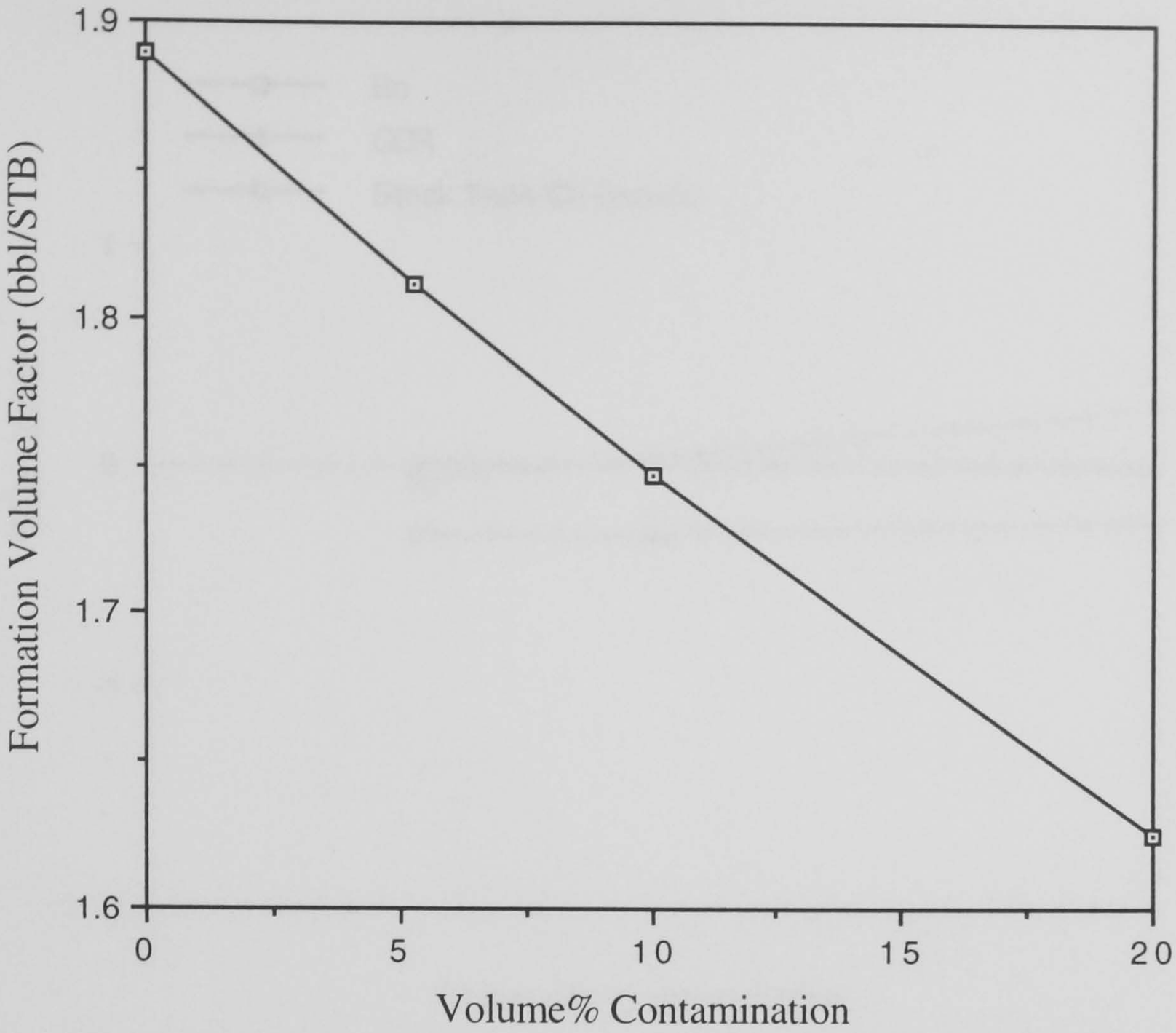

Fig. 5.9 - Effect of Contamination with Oil-based Mud Filtrate on Formation Volume Factor, Separator Test, Volatile Oil LRA97-1.

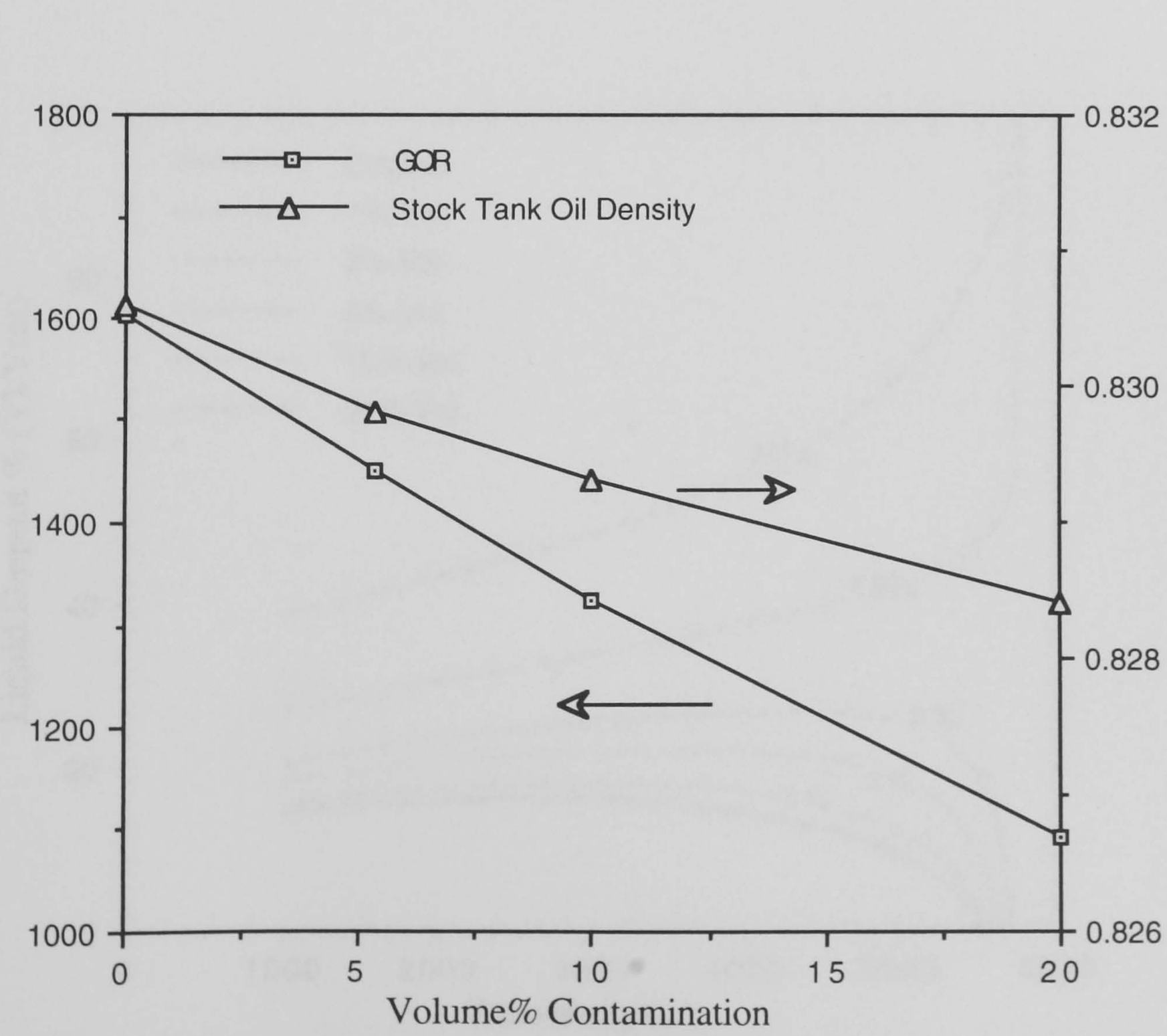

Fig. 5.10 - Effect of Contamination with Oil-based Mud Filtrate on GOR and Stock Tank Oil Density, Separator Test, Volatile Oil LRA97-1.

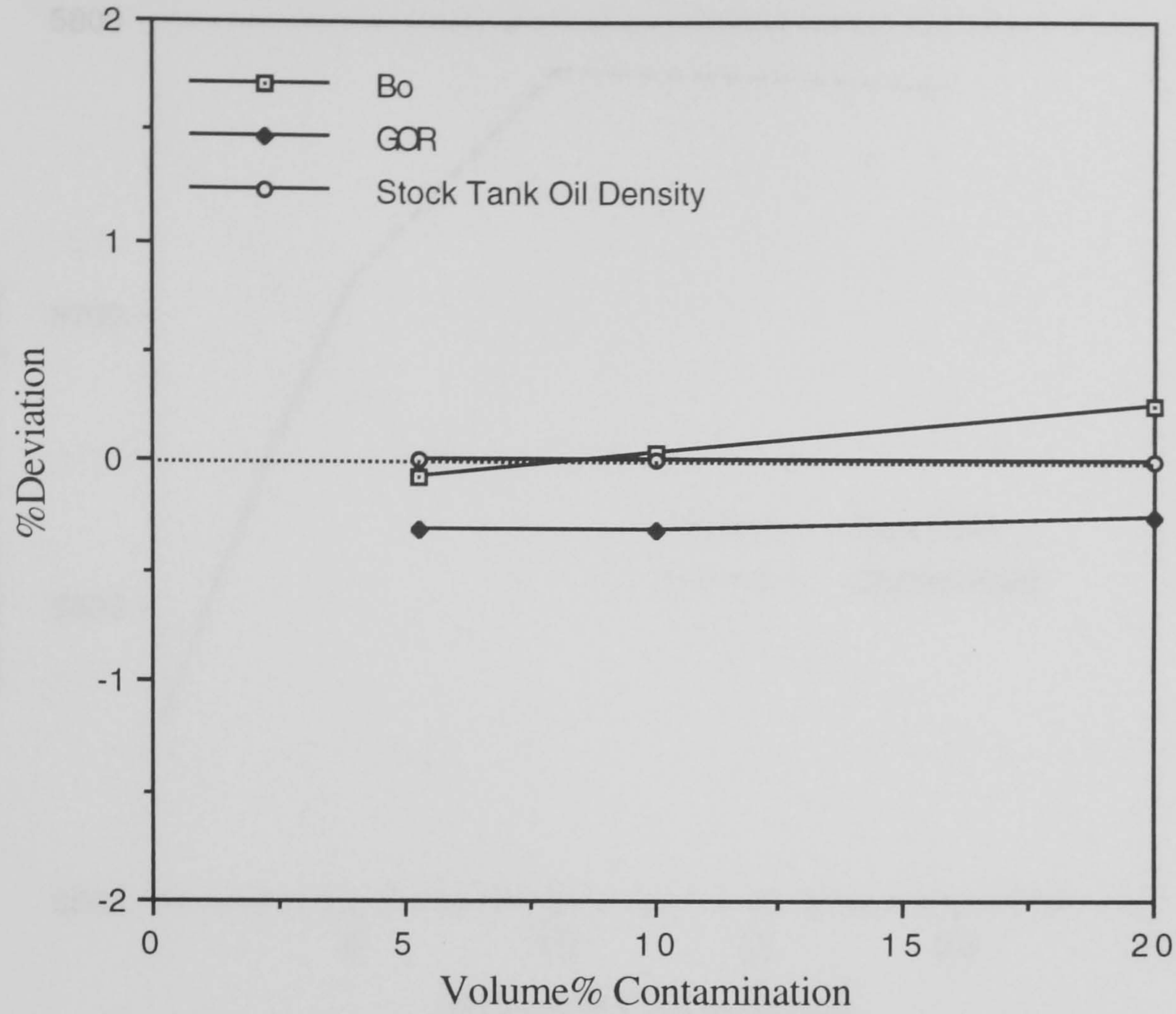

Fig. 5.11 - %Deviation in Calculated Properties of Original Fluid Using Retrieved Composition from Different Level of Contamination, Volatile Oil LRA97-1.

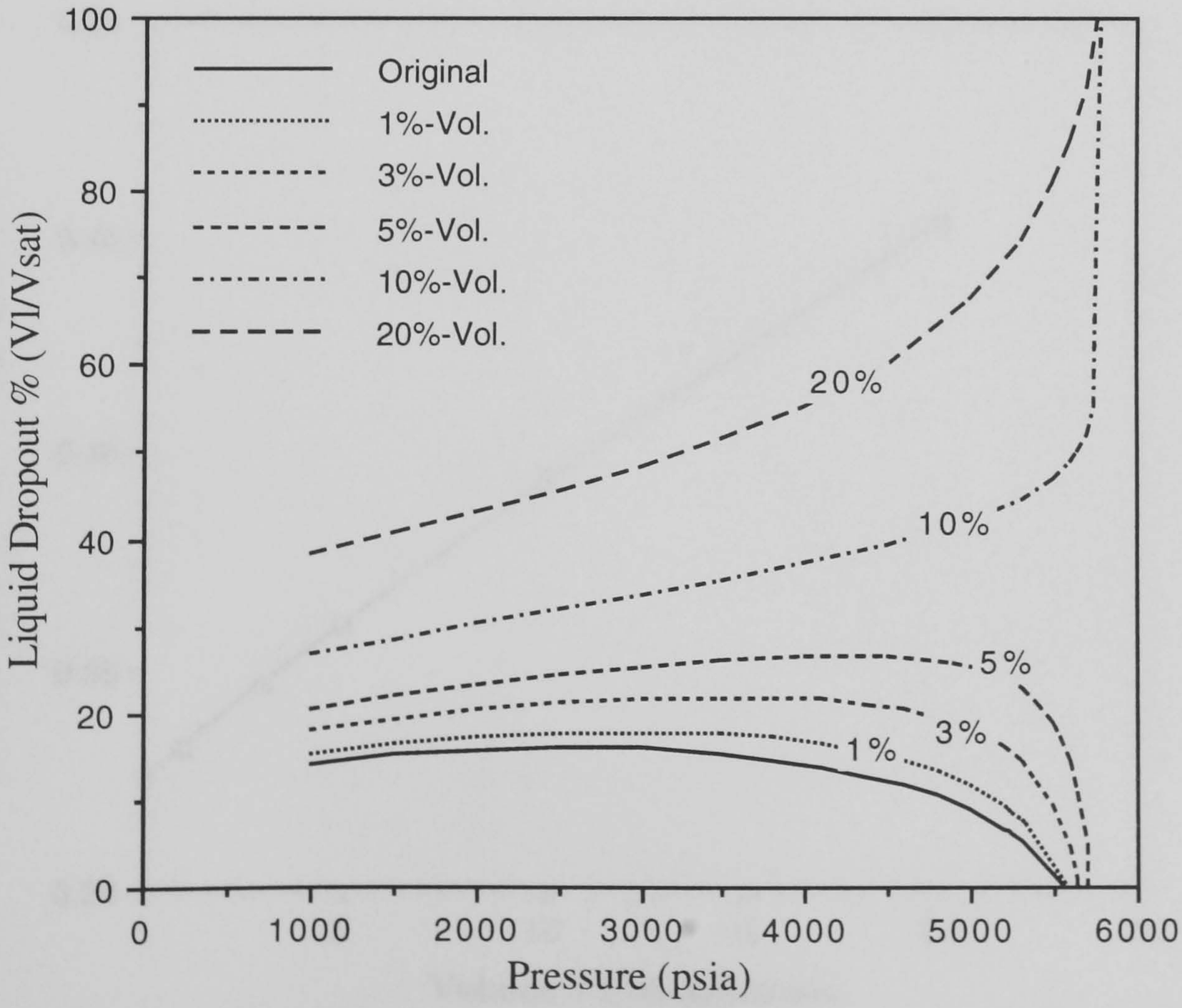

Fig. 5.12 - Volumetric Behaviour of Gas Condensate GCA94-1 Contaminated with 1%, 3%, 5%, 10% and 20% (Volumetric basis) Oil-based Mud Filtrate, Constant Composition Expansion (CCE) Test at 110°C.

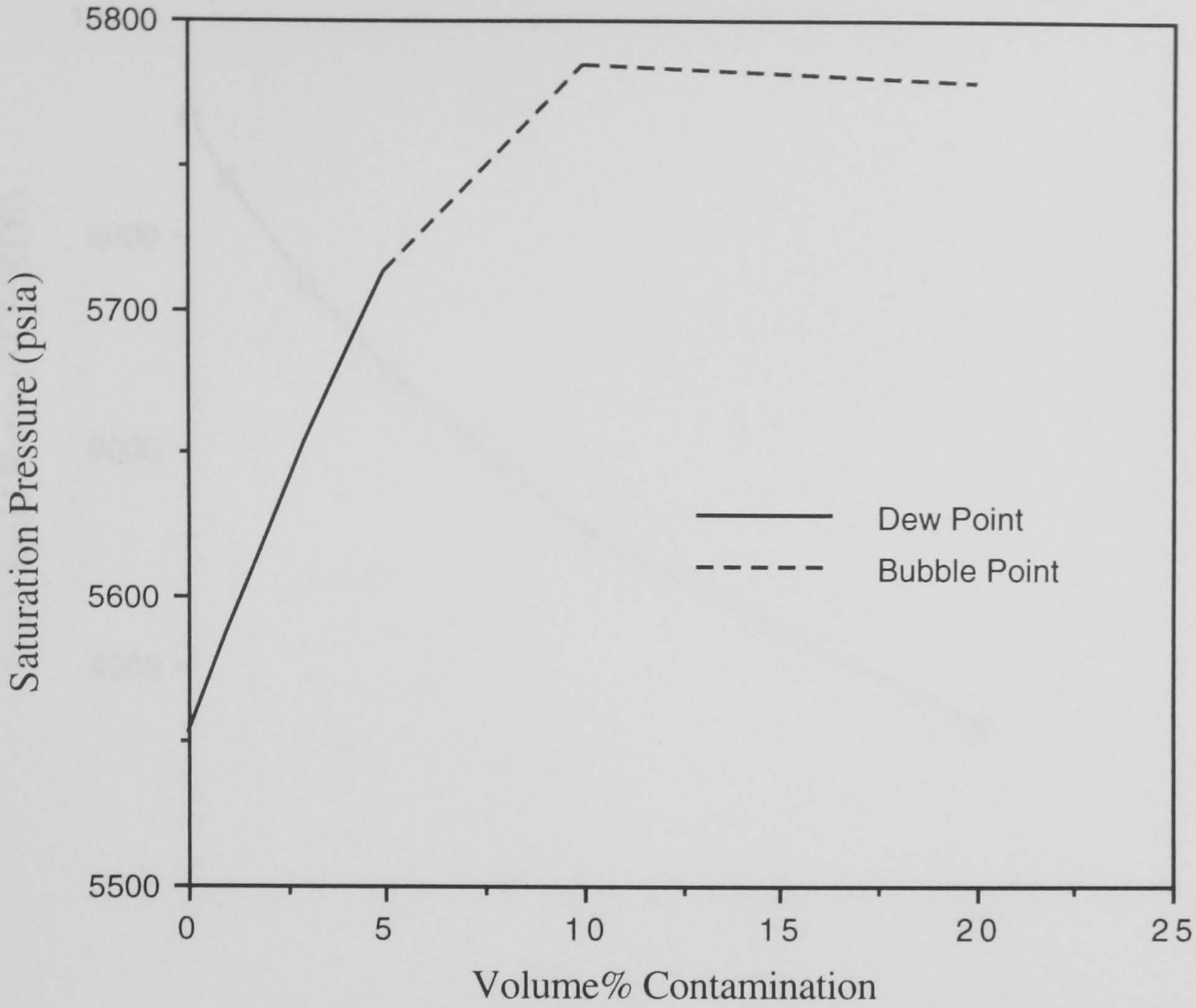

Fig. 5.13 - Effect of Contamination with Oil-based Mud Filtrate on Saturation Pressure, Gas Condensate GCA94-1, 110°C.

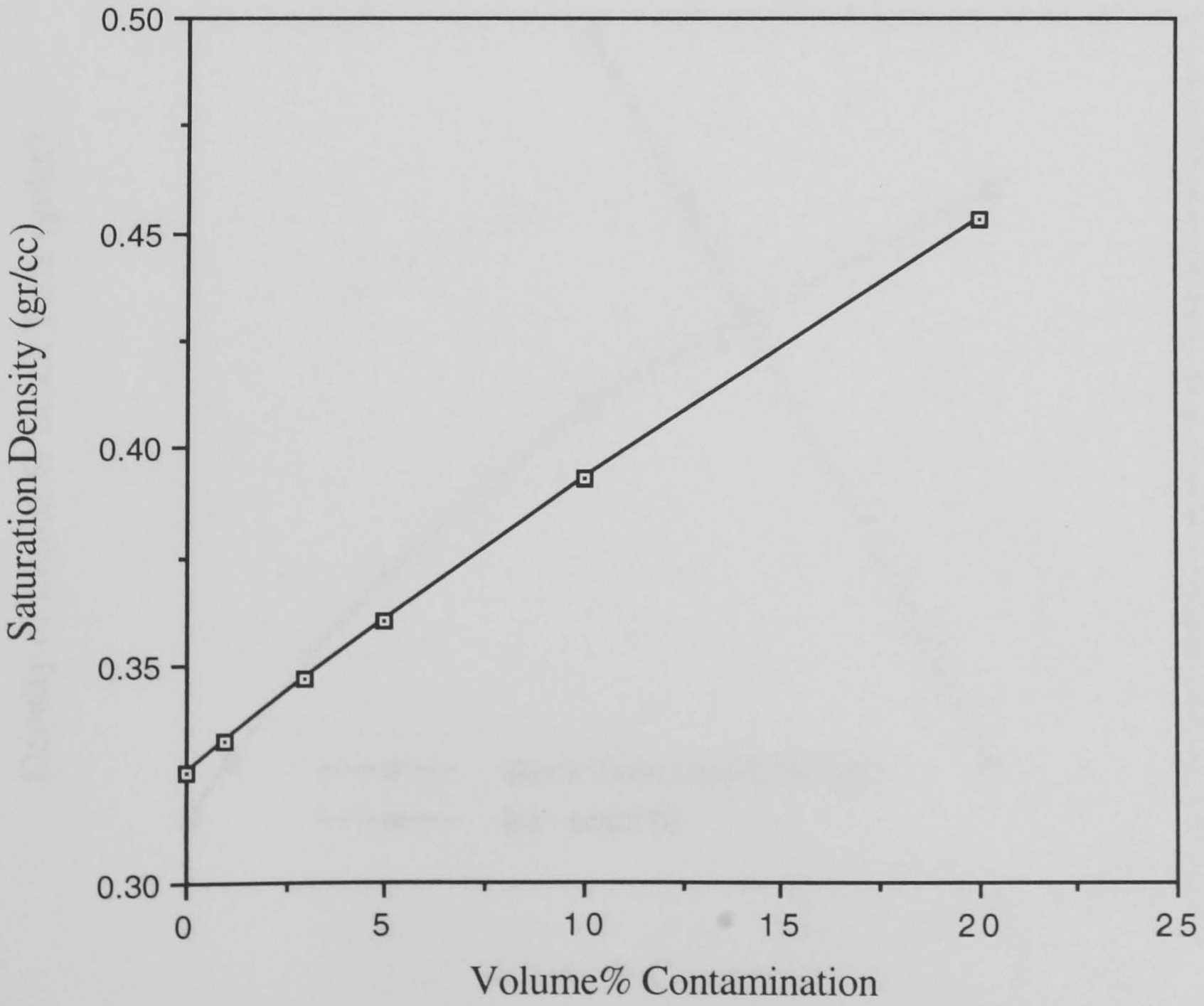

Fig. 5.14 - Effect of Contamination with Oil-based Mud Filtrate on Saturated Gas Density, Gas Condensate GCA94-1, 110°C.

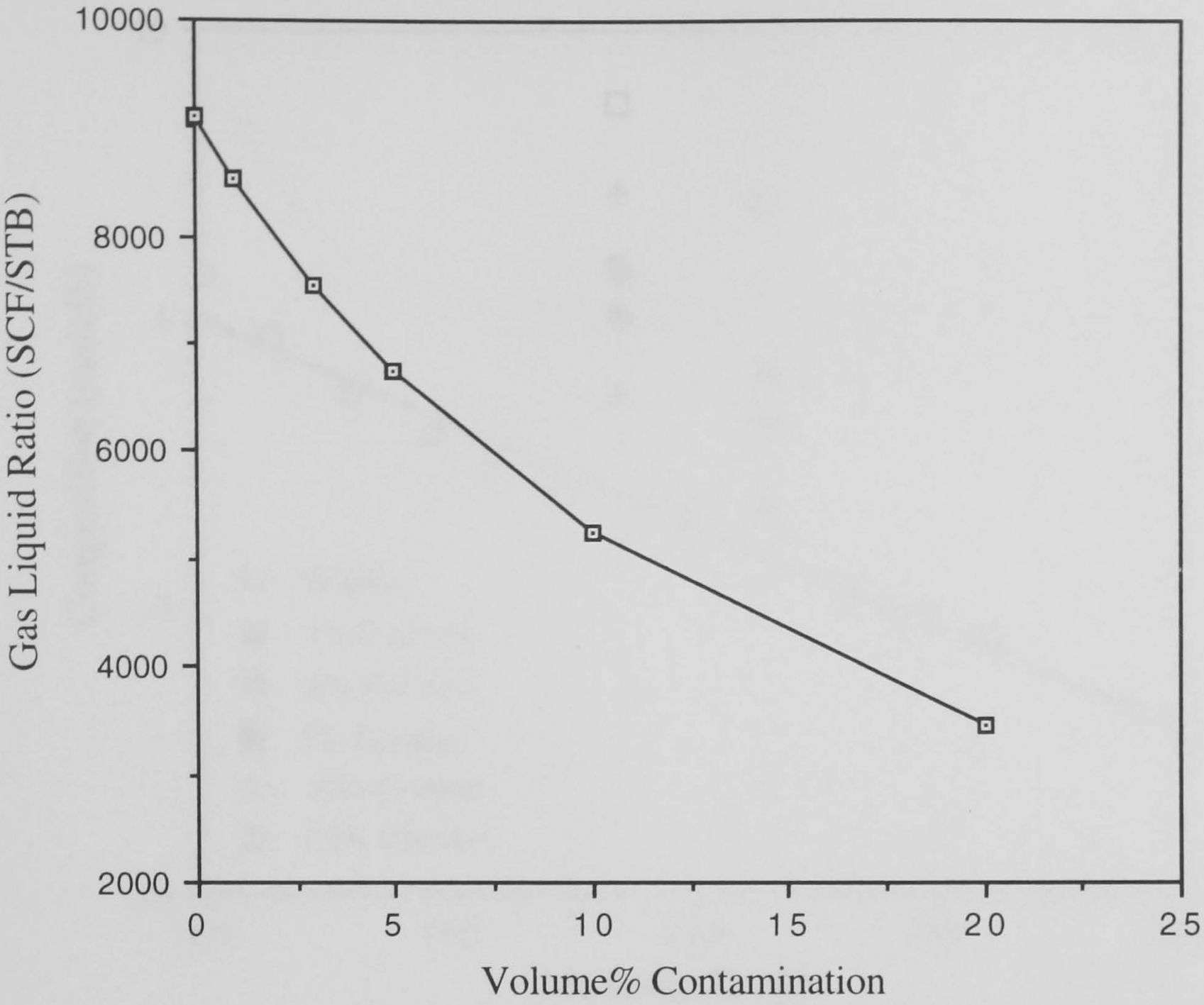

Fig. 5.15 - Effect of Contamination with Oil-based Mud Filtrate on Gas-Liquid Ratio, Gas Condensate GCA94-1.

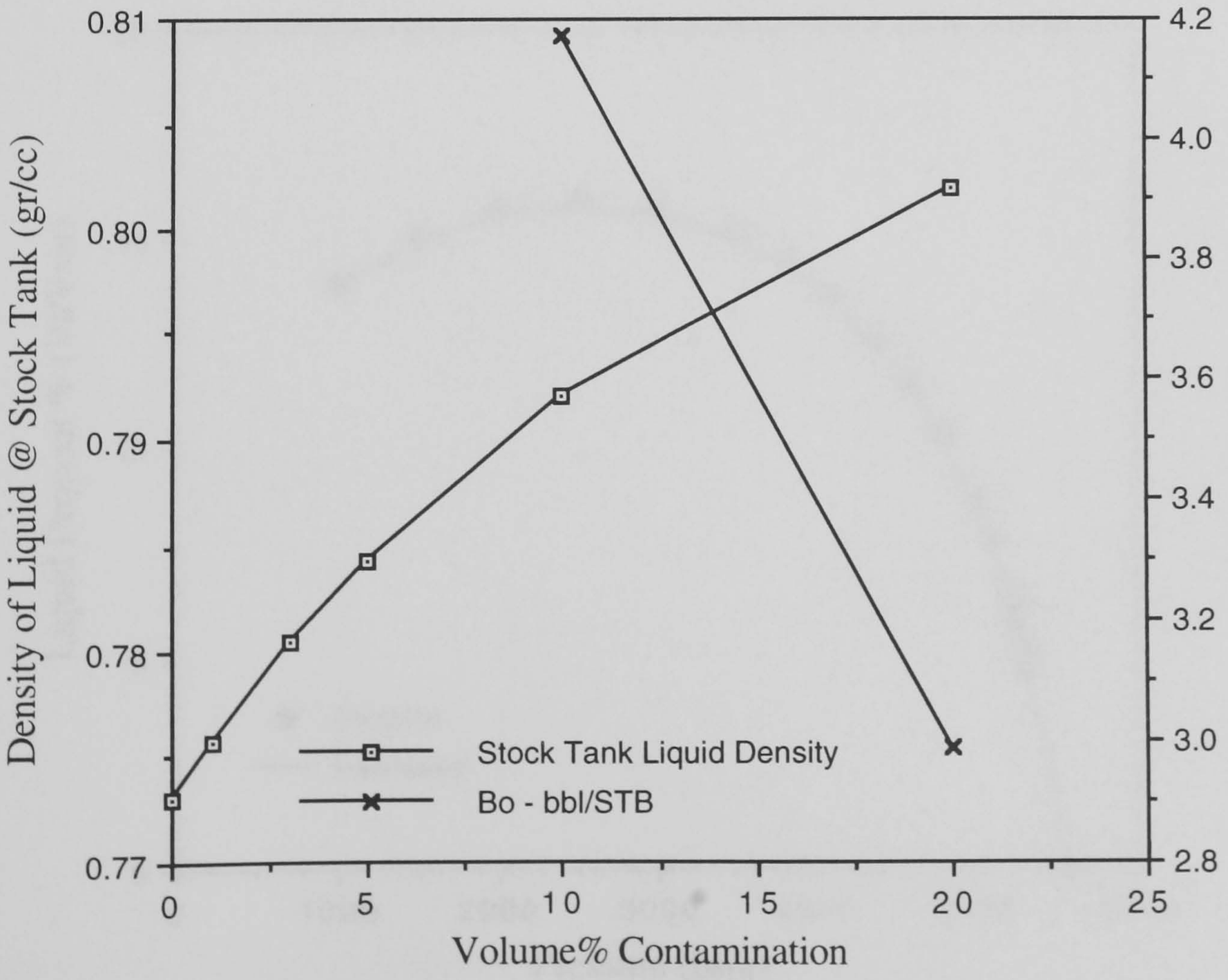

Fig. 5.16 - Effect of Contamination with Oil-based Mud Filtrate on Stock Tank Liquid Density and Formation Volume Factor, Gas Condensate GCA94-1.

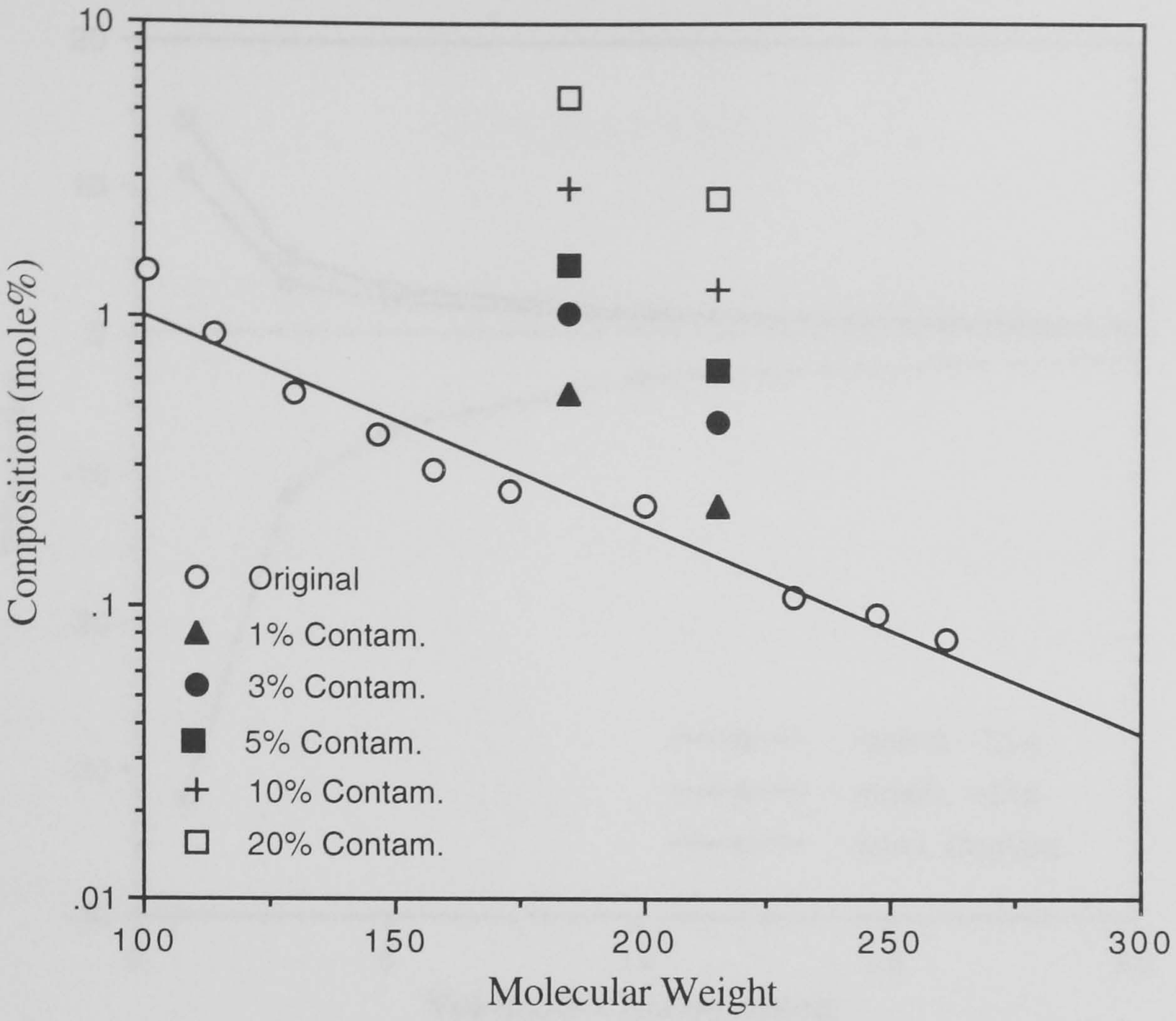

Fig. 5.17 - Composition of Gas Condensate GCA94-1 Contaminated with 1%, 3%, 5%, 10% and 20% (Volumetric) Oil-based Mud Filtrate, C8-C19.

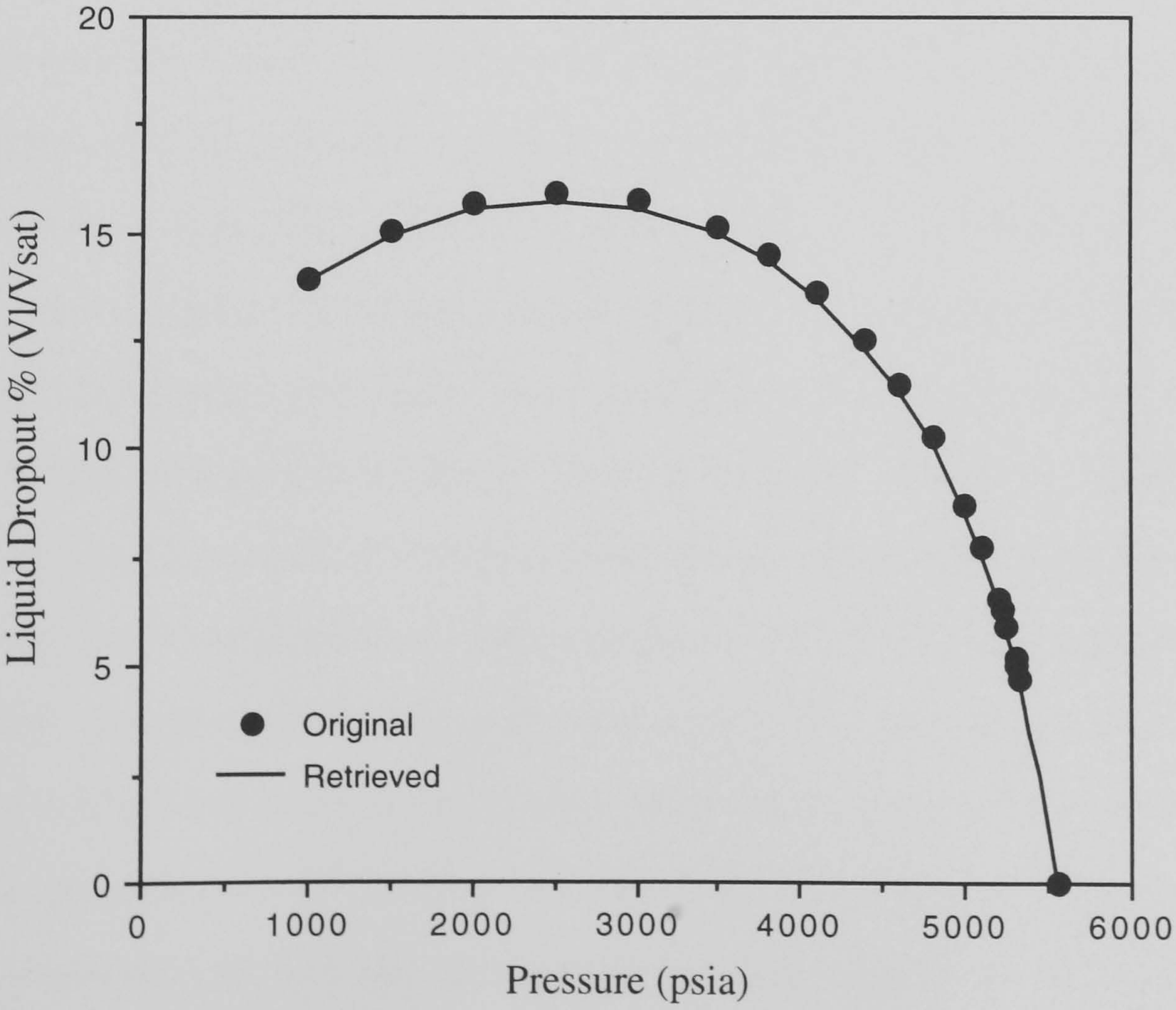

Fig. 5.18 - Predicted Liquid Dropout of Original and Retrieved Composition, Gas Condensate GCA94-1, CCE Test at 110°C.

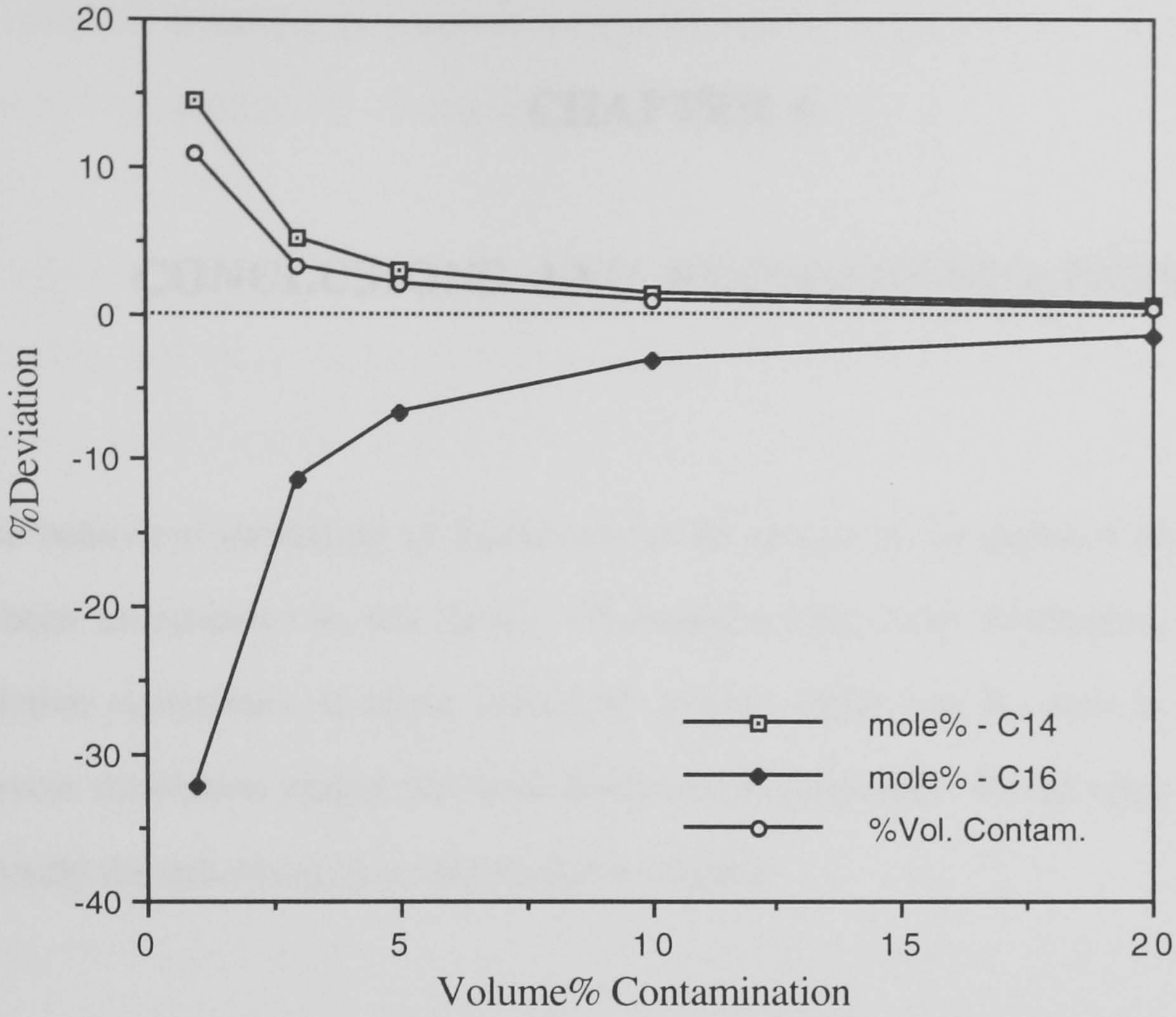

Fig. 5.19 - %Deviation in Determining Mud Filtrate Composition and Level of Contamination, Gas Condensate GCA94-1.

CHAPTER 6

CONCLUSIONS AND RECOMMENDATIONS

Phase behaviour modelling of fluids over wide ranges of temperature and composition has been investigated in this thesis. Techniques have been developed to improve the predictive capabilities of phase behaviour models which can be used in compositional reservoir simulation studies for field development proposes. Based upon the results of this study the following conclusions can be drawn.

6.1 CONCLUSIONS

An integrated modelling of fluid phase behaviour within the reservoir, flow lines and surface facilities has been developed in this study. The approach is based on using no binary interaction parameters (BIP) in the mixing rules of the equation of state (EOS), allowing rapid flash calculations (RFC) for mixtures described by a large number of components. In the RFC method, the number of equations to be solved in phase split calculation is reduced to three for a two-parameter EOS, regardless of the number of components describing the fluid. These equations can then be solved either by successive substitution or Newton type methods. The computational time (CPU) of the RFC method has been compared to those of conventional methods which solve a set of N+1 equations (N = number of components), to determine phase equilibrium. The computational time of the RFC method was markedly lower than those of the conventional ones in all cases. When the fluid was described by a large number of components, the computational time of the quasi-Newton (QN) method was higher by more than two orders of magnitude. The results also showed that approaching the critical region, the CPU time increased, more severely with the QN method than with the other methods. Although, the above conclusions are expected to be general, the time saving by incorporating the RFC method

in a reservoir simulator is expected to depend on the model algorithms, particularly the mathematical methods of solving the governing equations.

The application of the rapid flash calculation (RFC) method to gas condensate systems resulted in lack of convergence in most cases. The method is modified in this study by iterating on EOS parameters for the liquid phase instead of the vapour phase used for oil systems. The modified RFC method was found to be more robust than the conventional formulation using quasi-Newton (QN) method for gas condensate systems.

The deterioration of the predictive capability of EOS for gas condensate and volatile oil systems was investigated in this study. The lack of reliability of the models for gas condensate fluids can be attributed to the high impact of heavy compounds on the phase behaviour of these fluids and the presence of the large concentration of supercritical components. To improve the mentioned deficiencies, a more reliable method has been developed to determine the temperature dependency of the attractive term (α parameter) in EOS. Vapour pressure data of pure compounds from the triple point to the critical point, and saturation pressure data of binary systems which include a supercritical component were used to develop a new α function for the Peng-Robinson EOS. The developed function provided more reliable values for supercritical components, such as methane, and accounted for the lack of binary interaction parameters (BIP). The new α function is linearly related to the acentric factor at constant reduced temperature, therefore, it can be extrapolated to heavy petroleum fractions with high acentric factors. The average absolute percentage deviation in predicting the saturation pressure of 32 synthetic and real reservoir fluids over a wide range of temperature by the Peng-Robinson EOS using the original α function with and without BIP, m' (Eq 2.50) and the new α function were 7.4%, 12.9%, 6.3% and 4.5%, respectively.

Binary interaction parameters (BIP) are generally used as regression variables in tuning processes. An important contribution of this study has been the demonstration of the fact that EOS can be tuned as effectively without using BIP, hence allowing the use of the

rapid flash calculation (RFC) method. To calibrate phase behaviour models against the experimental data of fluids without using BIP in the mixing rules, two practical tuning methods namely, conventional and integrated, have been developed in this study.

In the conventional tuning approach, the properties of the heavy end of reservoir fluids are used as regression variables to match the experimental data of fluids at reservoir and surface conditions. The concentration and properties of the heavy end (or plus fraction) are the most doubtful information among the input data of EOS. The ability and flexibility of the conventional tuning method have been demonstrated in this study by matching the experimental data of volatile systems (i.e. volatile oil and gas condensate), and the results have been compared with those of other tuning models reported in the literature.

In the integrated tuning method, the temperature dependency of the attractive term of EOS in the liquid phase is used as the tuning parameter to match the experimental data of fluids over wide ranges of temperature and composition, including near critical conditions. Adjusting the α parameter of components in the liquid phase is physically justifiable, where the effect of temperature on attraction between molecules in the liquid phase is different from that of the vapour phase. Approaching the critical point, the attraction between molecules in the liquid phase becomes similar to that of the vapour phase, therefore, the adjusted α parameter approached that of the vapour at the critical point. The integrated tuning method has successfully been applied to match the PVT data of different types of fluids including model and real reservoir fluids, within wide ranges of temperature and composition.

To improve phase densities predictions, a new method has been developed in this study to determine the shift parameter of petroleum fractions as well as light hydrocarbons in the 3-parameter modification of Peng-Robinson EOS. The new shift parameter correlation is linear with acentric factor at constant reduced temperature, hence it can be extrapolated to heavy petroleum fractions. The proposed method can predict the phase densities of near critical fluids more accurately than the leading method in the literature. Two adjustable

parameters have been considered in the new method which can be used to further improve phase density prediction.

The inaccuracies in the measured gas-liquid ratio in surface sampling of undersaturated, saturated and depleted reservoirs have been investigated in this work using compositional models. Liquid and vapour samples were collected at the surface separator during normal operational conditions, where two-phase flow occurs in the reservoir near the wellbore. The collected samples were used to determine the initial reservoir composition, using the backward differential depletion (BDD) and separator methods. The BDD method provided a reliable sample representing the initial reservoir composition. Consequently, long stabilisation periods are not needed prior to sampling. This is particularly important for gas condensate reservoirs with low permeabilities. The conventional separator method could lead to highly erroneous results, particularly for near critical saturated reservoirs.

The investigation also indicated that variation of single phase density with depth in the oil column may be used to evaluate the measured composition of the collected sample, assuming no compositional variations with depth within the reservoir.

The impact of sample contamination with an oil-based mud filtrate on the phase behaviour and volumetric properties of reservoir fluids including, volatile oil and gas condensate systems, has also been investigated. The results show that contamination may dramatically change the phase behaviour of reservoir fluids to the extent of changing gas condensate to a volatile oil mixture. A simple and practical method has been developed in this study to determine the original composition of the reservoir fluid from contaminated samples. The method is based on the observed trend that an exponential distribution function can be fitted to the compositional analysis of C_{8+} portion of uncontaminated reservoir fluid composition. The method is general and it can be applied to different types of reservoir fluids, and highly contaminated samples.

The measured PVT data of the contaminated sample is used to develop the phase behaviour model and applied to predict the properties of the original reservoir fluid using the retrieved composition. The results clearly demonstrated that if contamination did not result in a major shift of the phase diagram (i.e. changing the fluid from a gas condensate to an oil system), the tuned EOS to contaminated samples could reasonably predict the phase behaviour of the original fluid. The results also indicated that the level of contamination had no effect on the retrieved composition of the original fluid. This demonstrates the robustness of the method.

6.2 RECOMMENDATIONS FOR FUTURE WORK

The rapid flash calculation method (RFC) is based upon using no binary interaction parameters (BIP) in the mixing rules of EOS. To extend the applicability of the RFC method for systems which requires BIP, such as water and solid phase equilibrium, it is recommended to modify the RFC method to include the required BIP for some specific components. The inclusion of BIP will however increase the number of equations to be solved in phase equilibrium calculations. Therefore, it may increase the computational time of flash calculations to the extent of making it comparable with the conventional methods.

It has been shown that the temperature dependency of the attractive term (α parameter) in the Peng-Robinson (PR) EOS is linear with acentric factor at constant reduced temperature. Based on this linearity a new α function has been developed for the PR EOS in this study, improving the phase behaviour prediction without using binary interaction parameter (BIP). It would be worth-while to develop the same type of α function for other models such as the Valderrama modification of Patel and Teja EOS.

A new method has been developed in this study to determine the shift parameters of petroleum fractions as well as light hydrocarbons, which has improved phase density prediction. The new method has adjustable parameters for multicomponent systems for

further improvement. It is suggested to correlate the adjustable parameters with properties of hydrocarbon mixtures.

The tuned EOS to the experimental data of contaminated samples is generally applied to the retrieved composition to predict the properties of the original (free of contamination) reservoir fluid. Although, the predicted results are within acceptable accuracy in most cases, the tuned parameters may not be valid for the retrieved composition, particularly if the retrieved composition is a near critical fluid. Therefore, an investigation on the relation of tuned parameters of the EOS with the contamination level may result in an improved method.

It was shown in this study that the variation of single phase density with depth in the oil column can be applied to evaluate the measured composition of hydrocarbon system. The application of the method can be extended to gas condensate reservoirs if the composition of the condensate at gas-oil contact can be determine from gas phase composition.

APPENDIX A

SOLUTION TO FUGACITY COEFFICIENT EQUATION

The fugacity coefficient of pure compounds can be expressed by the following equation:

$$\ln\phi = Z - 1 - \ln Z + \frac{1}{RT}\int_{\infty}^{V}\left(\frac{RT}{V} - P\right)dV \qquad (A.1)$$

However, the fugacity coefficient of each component in a mixture can be written in the following form:

$$\ln\phi_i = \frac{1}{RT}\int_{v}^{\infty}\left[\left(\frac{\partial P}{\partial n_i}\right)_{T,v,n_{j\neq i}} - \frac{RT}{v}\right]dv - \ln Z \qquad (2.7)$$

An equation of state is required to determine the pressure and the derivative of the pressure with respect to the number of moles in Equations A.1 and 2.7, respectively. A general cubic equation of state is used to determine the fugacity coefficients which is given in Equation A.2:

$$P = \frac{RT}{V-b} - \frac{a}{V^2 + uV - w^2} \qquad (A.2)$$

A.1 PURE COMPOUNDS

Applying the general cubic equation of state (Eq A.2) to the fugacity coefficient of pure compounds (Eq A.1) results in:

$$\ln\phi = Z - 1 - \ln Z + \frac{1}{RT}\int_{\infty}^{V}\left(\frac{RT}{V} - \frac{RT}{V-b} + \frac{a}{V^2 + uV - w^2}\right)dV \qquad (A.3)$$

The integral in Equation A.3 can be separated to three integrals:

$$\frac{1}{RT}\int_{\infty}^{V}\frac{RT}{V}dV = \ln(V)\Big|_{\infty}^{V} = \ln V - \lim_{V\to\infty}\underbrace{\ln V}_{} \qquad (A.4)$$

$$\frac{-1}{RT}\int_{\infty}^{V}\frac{RT}{V-b}dV = -\ln(V-b)\Big|_{\infty}^{V} = -\ln(V-b) + \lim_{V\to\infty}\underbrace{\ln(V-b)}_{} \qquad (A.5)$$

$$\frac{1}{RT}\int_{\infty}^{V}\frac{a}{V^2 + uV - w^2}dV = \frac{1}{RT}\int_{\infty}^{V}\frac{a}{(V+R_1)(V+R_2)}dV$$

$$R_1 = \frac{u - \sqrt{u^2 + 4w^2}}{2} \quad \text{and} \quad R_2 = \frac{u + \sqrt{u^2 + 4w^2}}{2}$$

$$= \frac{a}{RT}\frac{1}{R_1 - R_2}\ln\frac{V+R_2}{V+R_1}\Big|_{\infty}^{V} = \frac{a}{RT}\frac{1}{-\sqrt{u^2+4w^2}}\ln\frac{2V + u + \sqrt{u^2+4w^2}}{2V + u - \sqrt{u^2+4w^2}}$$

$$= \frac{-A}{\sqrt{U^2+4W^2}}\ln\frac{2Z + U + \sqrt{U^2+4W^2}}{2Z + U - \sqrt{U^2+4W^2}} \qquad (A.6)$$

where $Z = \frac{PV}{RT}$, $A = \frac{Pa}{R^2T^2}$, $U = \frac{Pu}{RT}$ and $W = \frac{Pw}{RT}$

Applying Equations A.4, A.5 and A.6 in Equation A.3 results in:

$$\ln\phi = Z - 1 - \ln Z + \ln V - \lim_{V\to\infty}\underbrace{\ln V}_{} - \ln(V-b) + \lim_{V\to\infty}\underbrace{\ln(V-b)}_{} - \frac{A}{\sqrt{U^2+4W^2}}\ln\frac{2Z + U + \sqrt{U^2+4W^2}}{2Z + U - \sqrt{U^2+4W^2}} \qquad (A.7)$$

$$\ln V - \lim_{V\to\infty}\underbrace{\ln V} - \ln(V-b) + \lim_{V\to\infty}\underbrace{\ln(V-b)} = \ln\frac{V}{V-b} + \lim_{V\to\infty}\underbrace{\ln\frac{V-b}{V}} \qquad (A.8)$$

$$= \ln\frac{V}{V-b} = \ln\frac{Z}{Z-B} = \ln Z - \ln(Z-B)$$

where $B = \frac{Pb}{RT}$. Substituting Equation A.8 in Equation A.7 results in:

$$\ln\phi = Z - 1 - \ln(Z-B) - \frac{A}{\sqrt{U^2+4W^2}}\ln\frac{2Z+U+\sqrt{U^2+4W^2}}{2Z+U-\sqrt{U^2+4W^2}} \qquad (A.9)$$

A.2 MIXTURES

The derivative of pressure with respect to the number of moles at constant T, v and $n_{j\neq i}$ in fugacity coefficient of components in the mixture (Eq 2.7) can be determined from the general cubic equation of state (Eq A.2):

$$\left(\frac{\partial P}{\partial n_i}\right)_{T,v,n_{j\neq i}} = \frac{RT(v-nb) + nRT\dfrac{\partial(nb)}{\partial n_i}}{(v-nb)^2} - \frac{\dfrac{\partial(n^2a)}{\partial n_i}(v^2+nuv-n^2w^2) - \left[v\dfrac{\partial(nu)}{\partial n_i} - 2nw\dfrac{\partial(nw)}{\partial n_i}\right]n^2a}{(v^2+nuv-n^2w^2)^2} \qquad (A.10)$$

Substituting Equation A.10 into Equation 2.7, the fugacity coefficient of components in the mixture can be written in the following form:

$$\ln\phi_i = \frac{1}{RT}\int_v^\infty \left[\frac{RT(v-nb)+nRT\dfrac{\partial(nb)}{\partial n_i}}{(v-nb)^2}\right]dv -$$

$$\frac{1}{RT}\int_v^\infty \left[\frac{\dfrac{\partial(n^2a)}{\partial n_i}(v^2+nuv-n^2w^2)-\left[v\dfrac{\partial(nu)}{\partial n_i}-2nw\dfrac{\partial(nw)}{\partial n_i}\right]n^2a}{(v^2+nuv-n^2w^2)^2}+\frac{RT}{v}\right]dv - \ln Z \qquad (A.11)$$

The integral in Equation A.11 can be separated to several integrals:

$$\frac{1}{RT}\int_v^\infty \frac{RT(v-nb)}{(v-nb)^2}\,dv = \ln(v-nb)\Big|_v^\infty \qquad (A.12)$$

$$\frac{1}{RT}\int_v^\infty \frac{nRT\dfrac{\partial(nb)}{\partial n_i}}{(v-nb)^2}\,dv = \frac{-n\dfrac{\partial(nb)}{\partial n_i}}{v-nb}\Bigg|_v^\infty = \frac{-nb_i}{v-nb}\Big|_v^\infty = \frac{nb_i}{v-nb} \qquad (A.13)$$

$$\frac{1}{RT}\int_v^\infty \frac{-RT}{v}dv = -\ln v\Big|_v^\infty \qquad (A.14)$$

A.12 and A.14 result in:

$$\ln(v-nb)\Big|_v^\infty - \ln v\Big|_v^\infty = \ln\frac{v-nb}{v}\Bigg|_v^\infty = \ln\frac{v}{v-nb} \qquad (A.15)$$

$$\frac{1}{RT}\int_v^\infty \frac{-\dfrac{\partial(n^2a)}{\partial n_i}(v^2+nuv-n^2w^2)}{(v^2+nuv-n^2w^2)^2}dv = \frac{-\dfrac{\partial(n^2a)}{\partial n_i}}{RT}\int_v^\infty \frac{dv}{(v+R_1)(v+R_2)}$$

$$R_1 = \frac{nu-\sqrt{(nu)^2+4(nw)^2}}{2} \quad \text{and} \quad R_2 = \frac{nu+\sqrt{(nu)^2+4(nw)^2}}{2}$$

$$= \frac{-\dfrac{\partial(n^2a)}{\partial n_i}}{RT} \frac{1}{R_1 - R_2} \ln \frac{v + R_2}{v + R_1}\Bigg|_v^\infty$$

$$= \frac{-\dfrac{\partial(n^2a)}{\partial n_i}}{RT\sqrt{(nu)^2 + 4(nw)^2}} \ln \frac{2v + nu + \sqrt{(nu)^2 + 4(nw)^2}}{2v + nu - \sqrt{(nu)^2 + 4(nw)^2}} \qquad (A.16)$$

$$\frac{1}{RT}\int_v^\infty \frac{\left(v\dfrac{\partial(nu)}{\partial n_i} - 2nw\dfrac{\partial(nw)}{\partial n_i}\right) n^2a}{(v^2 + nuv - n^2w^2)^2} dv \qquad (A.17)$$

The above integral (A.17) can be solved by fraction decomposition method. To simplify the integral, it is assumed that $\dfrac{\partial(nu)}{\partial n_i} = q_1$, $2nw\dfrac{\partial(nw)}{\partial n_i} = q_2$ and $-R_1$ and $-R_2$ are roots of second order polynomial in the denominator:

$$R_1 = \frac{nu - \sqrt{(nu)^2 + 4(nw)^2}}{2} \quad \text{and} \quad R_2 = \frac{nu + \sqrt{(nu)^2 + 4(nw)^2}}{2}$$

Therefore, the fraction in A.17 can be written in the following form:

$$\frac{q_1v - q_2}{(v^2 + nuv - n^2w^2)^2} = \frac{q_1v - q_2}{(v + R_1)^2(v + R_2)^2} = \frac{D_1}{v + R_1} + \frac{D_2}{(v + R_1)^2} + \frac{D_3}{v + R_2} + \frac{D_4}{(v + R_2)^2}$$

where $D_1 = \dfrac{-q_1(R_1 + R_2) - 2q_2}{(R_1 - R_2)^3}$, $D_2 = \dfrac{-q_1R_1 - q_2}{(R_1 - R_2)^2}$

$D_3 = \dfrac{q_1(R_1 + R_2) + 2q_2}{(R_1 - R_2)^3}$, $D_4 = \dfrac{-q_1R_2 - q_2}{(R_1 - R_2)^2}$ (A.18)

Applying Equation A.18 in A.17, it results in:

$$\frac{n^2a}{RT}\int_v^\infty \frac{q_1v-q_2}{(v+R_1)^2(v+R_2)^2}dv =$$

$$\frac{n^2a}{RT}\left[\int_v^\infty \frac{-q_1(R_1+R_2)-2q_2}{(v+R_1)(R_1-R_2)^3}dv \;+\; \int_v^\infty \frac{-q_1R_1-q_2}{(v+R_1)^2(R_1-R_2)^2}dv\right]+$$

$$\frac{n^2a}{RT}\left[\int_v^\infty \frac{q_1(R_1+R_2)+2q_2}{(v+R_2)(R_1-R_2)^3}dv \;+\; \int_v^\infty \frac{-q_1R_2-q_2}{(v+R_2)^2(R_1-R_2)^2}dv\right]$$

$$= \frac{-n^2a[q_1(R_1+R_2)+2q_2]}{RT(R_1-R_2)^3}\ln(v+R_1)\Big|_v^\infty \;+\; \frac{-n^2a(q_1R_1+q_2)}{RT(R_1-R_2)^2}\frac{-1}{(v+R_1)}\Big|_v^\infty \;+$$

$$\frac{n^2a[q_1(R_1+R_2)+2q_2]}{RT(R_1-R_2)^3}\ln(v+R_2)\Big|_v^\infty \;+\; \frac{-n^2a(q_1R_2+q_2)}{RT(R_1-R_2)^2}\frac{-1}{(v+R_2)}\Big|_v^\infty$$

$$= \frac{n^2a[q_1(R_1+R_2)+2q_2]}{RT(R_1-R_2)^3}\left(\ln(v+R_2)\Big|_v^\infty - \ln(v+R_1)\Big|_v^\infty\right) \;+$$

$$\frac{n^2a(q_1R_1+q_2)}{RT(R_1-R_2)^2}\frac{1}{v+R_1}\Big|_v^\infty \;+\; \frac{n^2a(q_1R_2+q_2)}{RT(R_1-R_2)^2}\frac{1}{v+R_2}\Big|_v^\infty$$

$$= \frac{n^2a[q_1(R_1+R_2)+2q_2]}{RT(R_1-R_2)^3}\ln\frac{v+R_1}{v+R_2} \;+$$

$$\frac{-n^2a}{RT(R_1-R_2)^2}\frac{2q_1R_1R_2+2q_2v+(R_1+R_2)(q_1v+q_2)}{(v+R_1)(v+R_2)} \qquad \text{(A.19)}$$

Substituting A.13, A.15, A.16 and A.19 into Equation A.11 and knowing $R_1R_2=-(nw)^2$, would result in:

$$\ln\phi_i = \frac{nb_i}{v-nb} + \ln\frac{v}{v-nb} - \ln Z + \frac{-\frac{\partial(n^2a)}{\partial n_i}}{RT\sqrt{(nu)^2+4(nw)^2}}\ln\frac{2v+nu+\sqrt{(nu)^2+4(nw)^2}}{2v+nu-\sqrt{(nu)^2+4(nw)^2}} +$$

$$\frac{n^2a\left(\frac{\partial(nu)}{\partial n_i}(nu)+4nw\frac{\partial(nw)}{\partial n_i}\right)}{RT\left(-\sqrt{(nu)^2+4(nw)^2}\right)^3}\ln\frac{2v+nu-\sqrt{(nu)^2+4(nw)^2}}{2v+nu+\sqrt{(nu)^2+4(nw)^2}} +$$

$$\frac{-n^2a}{RT\left(-\sqrt{(nu)^2+4(nw)^2}\right)^2}\;\frac{2\frac{\partial(nu)}{\partial n_i}(-n^2w^2)+2\left(2nw\frac{\partial(nw)}{\partial n_i}\right)v+nu\left(\frac{\partial(nu)}{\partial n_i}v+2nw\frac{\partial(nw)}{\partial n_i}\right)}{v^2+nuv-n^2w^2}$$

If

$$A_i' = \frac{1}{n\,a}\left[\frac{\partial(n^2a)}{\partial n_i}\right]_{T,n_{j\neq i}} \qquad B_i' = \frac{1}{b}\left[\frac{\partial(nb)}{\partial n_i}\right]_{T,n_{j\neq i}}$$

$$U_i' = \frac{1}{u}\left[\frac{\partial(nu)}{\partial n_i}\right]_{T,n_{j\neq i}} \qquad W_i' = \frac{1}{w}\left[\frac{\partial(nw)}{\partial n_i}\right]_{T,n_{j\neq i}}$$

Then, the above equation can be written in the following form;

$$\ln\phi_i = -\ln(Z-B) + \frac{B_i'\,B}{Z-B} + \frac{A}{\sqrt{U^2+4W^2}}\left[A_i' - \frac{U_i'\,U^2+4W_i'W^2}{U^2+4W^2}\right]\times$$
$$\ln\left[\frac{2Z+U-\sqrt{U^2+4W^2}}{2Z+U+\sqrt{U^2+4W^2}}\right] - A\left[\frac{2(2Z+U)W_i'W^2+(UZ-2W^2)U_i'U}{\left(Z^2+UZ-W^2\right)\left(U^2+4W^2\right)}\right] \qquad (A.20)$$

where;

$$A=\frac{P\,a}{(RT)^2}\quad,\quad B=\frac{P\,b}{RT}\quad,\quad U=\frac{P\,u}{RT}\quad,\quad W=\frac{P\,w}{RT}\quad,\quad Z=\frac{P\,V}{RT}$$

APPENDIX B

FUGACITY COEFFICIENTS IN THE RAPID FLASH CALCULATION METHOD

The two-parameter PR EOS has the form;

$$P = \frac{RT}{V - b} - \frac{a}{V^2 + 2bV - b^2} \qquad (B.1)$$

where P, T and V are pressure, temperature and molar volume respectively. The two mixture parameters a and b can be determined from Equations 3.1 and 3.2, using pure compound parameters.

Fugacity coefficients in the PR EOS can be calculated from Equation B.2;

$$Ln\phi_i = \frac{b_i}{b}\left(\frac{PV}{RT} - 1\right) - Ln\left(\frac{P}{RT}(V - b)\right) - \frac{a}{2\sqrt{2}\,bRT} \times Ln\left(\frac{V + (1+\sqrt{2})b}{V + (1-\sqrt{2})b}\right) \times \left(\frac{2\sum_{j=1}^{N}(a_i a_j)^{0.5} y_j}{a} - \frac{b_i}{b}\right) \qquad (B.2)$$

Substituting Equation 3.14 in the PR EOS (Eq B.1) and Equation B.2, the fugacity coefficient expression can be written;

$$Ln\phi_i = q_0 + q_1 a_i' + q_2 b_i \qquad (B.3)$$

where q_0, q_1 and q_2 depend on a', b, T and P only. The expressions for the coefficients are;

$$q_0 = - \mathrm{Ln}\left(\frac{P}{RT}(V - b)\right) \tag{B.4a}$$

$$q_1 = - \frac{a'}{\sqrt{2}\, bRT} \mathrm{Ln}\left(\frac{V + (1 + \sqrt{2})b}{V + (1 - \sqrt{2})b}\right) \tag{B.4b}$$

$$q_2 = \frac{1}{b}\left(\frac{PV}{RT} - 1\right) + \frac{a'}{2b} q_1 \tag{B.4c}$$

The calculated fugacity coefficients can be used to determine the K-factors;

$$K_i = \frac{\phi_i^L}{\phi_i^V} = \frac{y_i}{x_i} \tag{B.5}$$

APPENDIX C

PRESSURE-VOLUME-TEMPERATURE (PVT) EXPERIMENTS

PVT experiments were conducted in the PVT laboratory at Heriot-Watt University, Department of Petroleum Engineering to investigate the phase behaviour of reservoir fluids within reservoir and surface facilities. The common PVT tests included:

Constant Composition Expansion (CCE)

Constant Volume Depletion (CVD)

Differential Liberation (DL)

Separator Test

Some unconventional experiments were also carried out in this laboratory which were used to simulate improved oil recovery processes in the reservoir. The unconventional PVT tests that were used in this study are as follows:

Gas Injection / Gas Cycling

Condensate Accumulation Near the Wellbore

Multiple-Contact

All the experiments could numerically be modelled by a series of successive flash calculations. The differential liberation (DL) test is usually carried out on oil samples, however, the constant volume depletion (CVD) test is specifically used to model the fluid behaviour in a gas condensate reservoir during recovery by pressure depletion. The constant composition expansion (CCE) and separator tests could be applied to both oil and gas condensate samples.

Two experimental facilities were used to measure phase behaviour and volumetric properties of fluids in this laboratory. A gas condensate experimental cell (Fig. C.1) was used to carry out PVT tests on gas condensate samples at reservoir conditions. A

vapour-liquid equilibrium (VLE) cell (Fig. C.2) was used to perform PVT tests at separator and reservoir conditions.

The gas condensate cell had a test pressure of 26000 psi and a maximum working pressure of 17600 psi. It consisted of two chambers connected by a narrow neck. The upper chamber had a volume of 4.0 litres where the lower chamber had a volume of half a litre. The connecting neck had a diameter of 1.0 cm and it was used to allow visual inspection of the fluid being studied, as two sapphire windows mounted on either side of the neck. A light source shone through the windows and the image was picked up by a borescope and then a colour video camera. The facilities provided a clean image of rising liquid at the vapour-liquid interface which was used for interfacial tension measurement. The entire cell was enclosed in a thermostatically controlled enclosure which had an operating limit of -20°C to +200°C. The temperature was controlled by a high precision temperature controller which could maintain the cell temperature to ±0.05°C. The temperature was measured by a high precision platinum resistance thermometer to an accuracy of ±0.025°C. The density of liquid and vapour could be measured through a high pressure, high temperature densitometer which had a maximum working pressure of 10000 psi. The density loop could also be used to transfer a sample of fluid to a HP Gas Chromatograph through valves V1, S1 and S2. The set up called "Direct Sampling System (DSS)" was used to measure the composition of fluid. Pressure was measured by a high pressure resonating quartz crystal transducer to an accuracy of ±0.001 psi.

Fig. C.2 gives the general layout of the main compartments in the VLE experimental facility. The VLE experimental facility consisted of two cells and the volume of each cell was 200 cm^3. The majority of these components were held inside a temperature controlled air bath, the temperature of which could be maintained to ±0.1°C with an upper temperature limit of about 110°C. The upper pressure limitation is approximately 5500 psi, which was governed by the operational limit of the direct compositional sampling valves. The pressure can be controlled to an accuracy of ±0.6 psi. The liquid and vapour densities were measured to an accuracy of ±0.0003 and ±0.0005 g/cm^3, respectively,

using an oscillating U tube density cell. A capillary tube viscometer was housed in the VLE experimental facilities which could measure the viscosity of the liquid and vapour to an accuracy of 1.8%-3.8% and 4%, respectively.

C.1 CONSTANT COMPOSITION EXPANSION (CCE)

The gas condensate experimental facility (Fig. C.1) was used to carry out the CCE tests at reservoir conditions in this laboratory. The CCE test was performed to determine the saturation pressure (bubble point or dew point) and liquid dropout behaviour of the fluid. A sample of the reservoir fluid (200 cm^3 single phase) was placed in the cell at a pressure greater than the saturation pressure of the fluid. The pressure was reduced in a stepwise manner by removing mercury from the upper chamber of the cell and the total volume and density of the fluid were recorded at each pressure. At pressures lower than the saturation pressure, the volume of liquid and vapour phases were measured to an accuracy of ±0.01 cm^3. The liquid and vapour densities were also measured which could be used to check the material balance. The accuracy of measured densities were ±0.0005 gr/cm^3. By plotting the pressure against the total volume, the saturation pressure and volume were determined. All values of the total volume were divided by the saturation volume and the results were reported as *relative volume*. The volume of liquid dropout was reported as percentage of the total volume (the liquid percentage) or as a percentage of the saturation volume (the liquid dropout).

C.2 CONSTANT VOLUME DEPLETION (CVD)

The CVD tests were performed in this laboratory, using the gas condensate experimental facility (Fig. C.1). The CVD test was used to simulate the pressure depletion of a reservoir below the dew point pressure. A sample of reservoir fluid (180 cm^3 single phase) was loaded into the cell and it was allowed to stabilise at the study temperature and at a pressure well above the expected saturation pressure. The volume of sample at the saturation pressure (V_{sat}) was used as reference volume in this test. The sample was taken

to a pressure below the dew point pressure and stabilised to ensure equilibrium was attained. The volume of liquid and vapour were recorded. The vapour and liquid compositions and densities were measured using the direct sampling system (DSS). The total volume was reduced to V_{sat} by removing gas from the system at constant pressure. The volume of the removed gas was also measured at cell conditions. The above procedure was repeated for several times until a minimum test pressure (usually 2000 psi) was reached, after which the quality and composition of the gas and retrograde liquid remaining in the cell were measured.

C.3 DIFFERENTIAL LIBERATION (DL)

The VLE experimental facility (Fig. C.2) was used to carry out the DL tests. The DL test was conducted to investigate the pressure depletion of an oil reservoir below the bubble point pressure. A single phase sample of fluid (180 cm^3) was charged into the VLE cell and it was stabilised at study temperature and a pressure above the bubble point pressure. The pressure was reduced in a stepwise manner, usually 10 to 15 pressure levels, and all the liberated gas was removed and its volume was measured to an accuracy of ± 0.01 cm^3. The volume of oil at each pressure step was also measured. As it is shown in Fig. C.2, the VLE experimental facility consisted of two cells located in a temperature controlled air-bath. By transferring the sample from one cell to another one through the density loop at constant pressure, the density and composition of the sample were measured using the density cell and the direct sampling system (DSS), respectively. The above procedure was continued to atmospheric pressure where the volume of the residual oil was measured and converted to a volume at standard conditions.

C.4 SEPARATOR TEST

The separator test was carried out to simulate the phase behaviour of reservoir fluids throughout production facilities at the surface. A portion of reservoir fluid sample (180 cm^3) was charged into the cell at reservoir temperature and its saturation pressure. Then,

the single phase sample was expelled from the cell at constant pressure and it was flashed through a multi-stage separation system, with each separation stage at fixed pressure and temperature. The temperature was measured to an accuracy of ±0.1°C. The pressure could be controlled within ±0.6 psi. The liberated gas from every stage was removed and its volume and density were measured to an accuracy of ±0.01 cm^3 and ±0.0005 gr/cm^3, respectively. The volume of the remaining liquid in the stock tank stage (lab temperature and pressure) was also recorded.

C.5 GAS INJECTION / GAS CYCLING

Gas injection or gas cycling test was performed to investigate improved oil (condensate) recovery processes by injecting gas into a reservoir. Once the reservoir fluid sample (160 cm^3) was introduced into the cell, its pressure was reduced to a pre-defined point and then allowed to stabilise (to simulate the primary depletion). Volumetric readings were recorded together with compositions and densities of both phases using the density cell and the DSS. Then, a volume of gas (say 10 cm^3 at cell conditions) was injected into the cell at a pressure slightly above the sample pressure (to ensure that it flows into the cell). The resultant vapour was allowed to contact the liquid at the original test pressure until equilibrium attained. Once the sample reached its equilibrium, volumetric readings were recorded. The saturation pressure of the mixture was also determined by performing a CCE test. An important part of the data collected from this test was the reduction of the liquid volume as the volume of injected gas increases. This indicated an extra recovery of liquid possible by the gas cycling of the system. In the gas cycling test, once all the required readings were recorded, vapour was removed from the cell to return the total sample volume back to the volume prior to the injection of the gas. Again, the sample was allowed to equilibrate and volumetric and density readings were taken. The process was then repeated until there was no significant change in the liquid volume.

In the gas injection test, gas was injected into the cell but vapour was not then removed. More gas was simply injected into the cell at each stage and saturation pressure, phase

volumes and densities were recorded. The volume of injected gas was incrementally increased with each subsequent injection.

C.6 CONDENSATE ACCUMULATION NEAR THE WELLBORE

This test was performed to simulate and therefore to investigate the build-up of condensate liquid around the wellbore as single phase reservoir fluid passed through a lower pressure region surrounding the wellbore.

A portion of reservoir fluid was loaded into the gas condensate cell. The volume of the fluid was recorded at the dew point pressure and this volume was then taken as the constant volume (V_0) to which the system was returned after each reservoir fluid injection. The pressure was then reduced to just below the saturation pressure by expanding the system. The fluid depleted back to the constant volume (V_0) by removing vapour from the cell after which the saturation pressure was re-measured. Next, some single phase reservoir fluid was injected into the cell at the test temperature and the system was stabilised at the same pressure as prior to the injection. The liquid and vapour volumes and densities were measured before the system was depleted back to the constant volume. The saturation pressure was then measured again prior to the next injection of single phase reservoir fluid. This procedure was performed a number of times, with an increased volume of reservoir fluid being injected each time. The test was completed when the volume of condensate left in the cell results in the system changed from a gas condensate to a liquid system.

The condensate accumulation near the wellbore test could also be performed in a different manner without the need to physically inject large volumes of single phase reservoir fluid. The above described procedure was suitable for rich gas condensate systems with relatively high liquid dropout. However, for fluids with low to medium liquid dropout behaviour (say below 15% maximum liquid dropout) the changes in fluid properties and behaviour were not as pronounced if the above procedure would be used. In order to

produce the greatest changes in fluid behaviour, it was preferable to have as much original liquid in place as possible at the start of the test. Therefore, the sample pressure was depleted to its maximum liquid dropout point prior to the removal of the vapour in incrementally increasing amounts. After each removal of the vapour, the system was returned to single phase and the saturation pressure and volumetric properties of the system were determined by performing a constant composition expansion (CCE) test. As the system was in equilibrium prior to and during the removal of the vapour, when the system returned to the original pressure after CCE, the properties of the system would be unchanged from their original values regardless of how much vapour was removed. However, as the volume of vapour decreased at each stage of the test, the liquid percentage (the percentage of liquid to total sample volume) increased. Therefore, the system would eventually revert from a gas condensate to a liquid system as it moved through the critical point.

C.7 MULTIPLE-CONTACT

Multiple-contact processes were used to simulate the relative movement of the injected gas in the reservoir during a gas injection process. The multiple-contact processes were divided into forward-contact and backward-contact tests.

Multiple forward contact (MFC) test simulates the conditions at the front of the injection gas. A known volume (180 cm^3) of oil was introduced into the cell and it was stabilised at study temperature and pressure. A known volume of injection gas was contacted with the oil and the volumes, densities and compositions of the equilibrated phases were measured. The density cell could measure the density of liquid and vapour to an accuracy of ± 0.0003 and ± 0.0005 gr/cm^3, respectively. The accuracy of volumetric readings were ± 0.01 cm^3. The equilibrated gas at each contact was used in the next contact with fresh reservoir oil, simulating the advancing injection gas in a reservoir. The above procedure was continued until the injection gas became either miscible with the fresh oil or achieved equilibrium without significant changes of compositions.

Multiple backward contact (MBC) test simulates the tail of the injection zone. The test was similar to the forward contacts, but the equilibrated oil at each contact was used in the next contact with fresh injection gas. The experiment provided valuable information on the vaporisation effect of the injection gas.

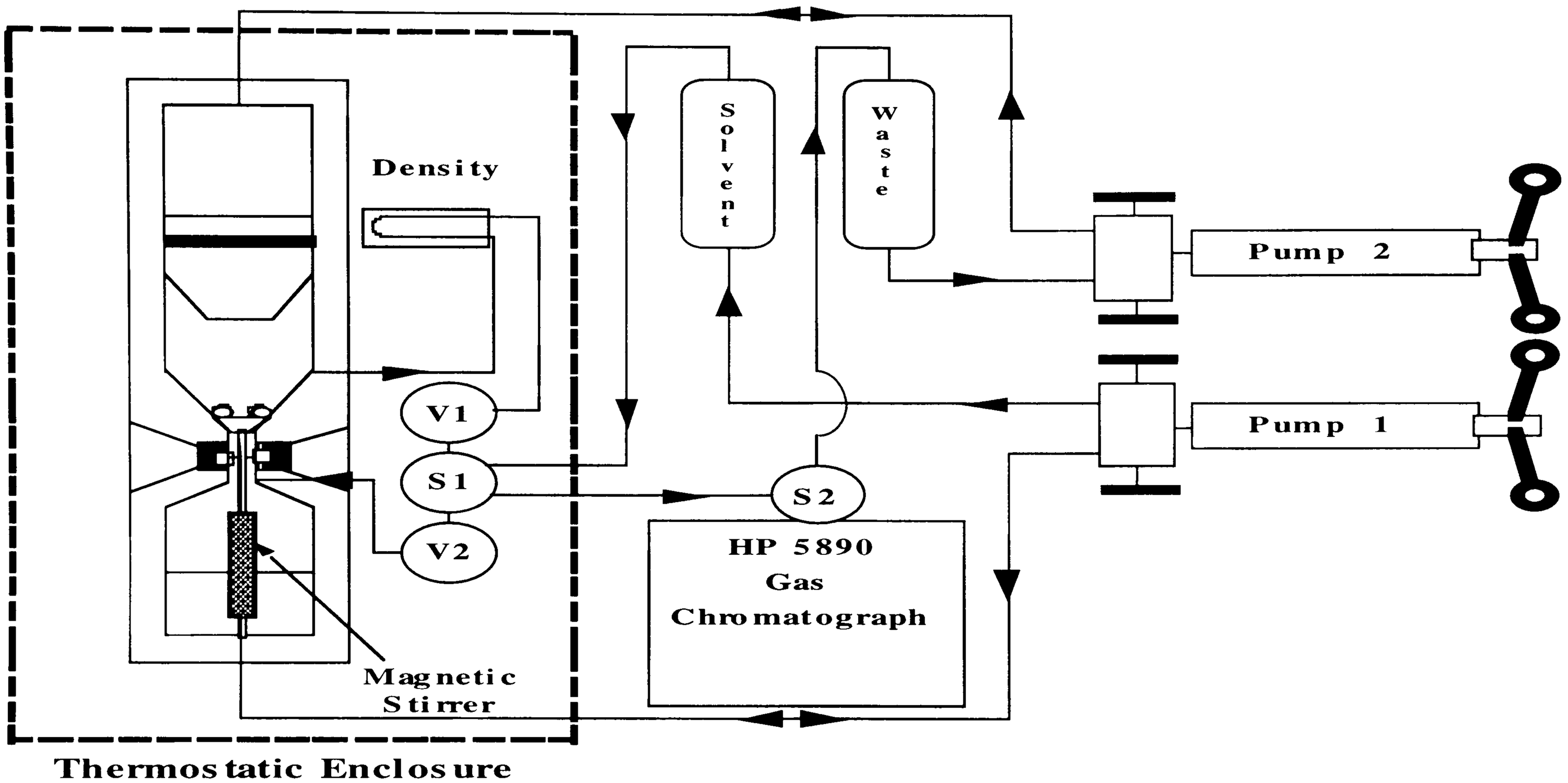

Fig. C.1 - Schematic Illustration of the Gas Condensate Experimental Facility.

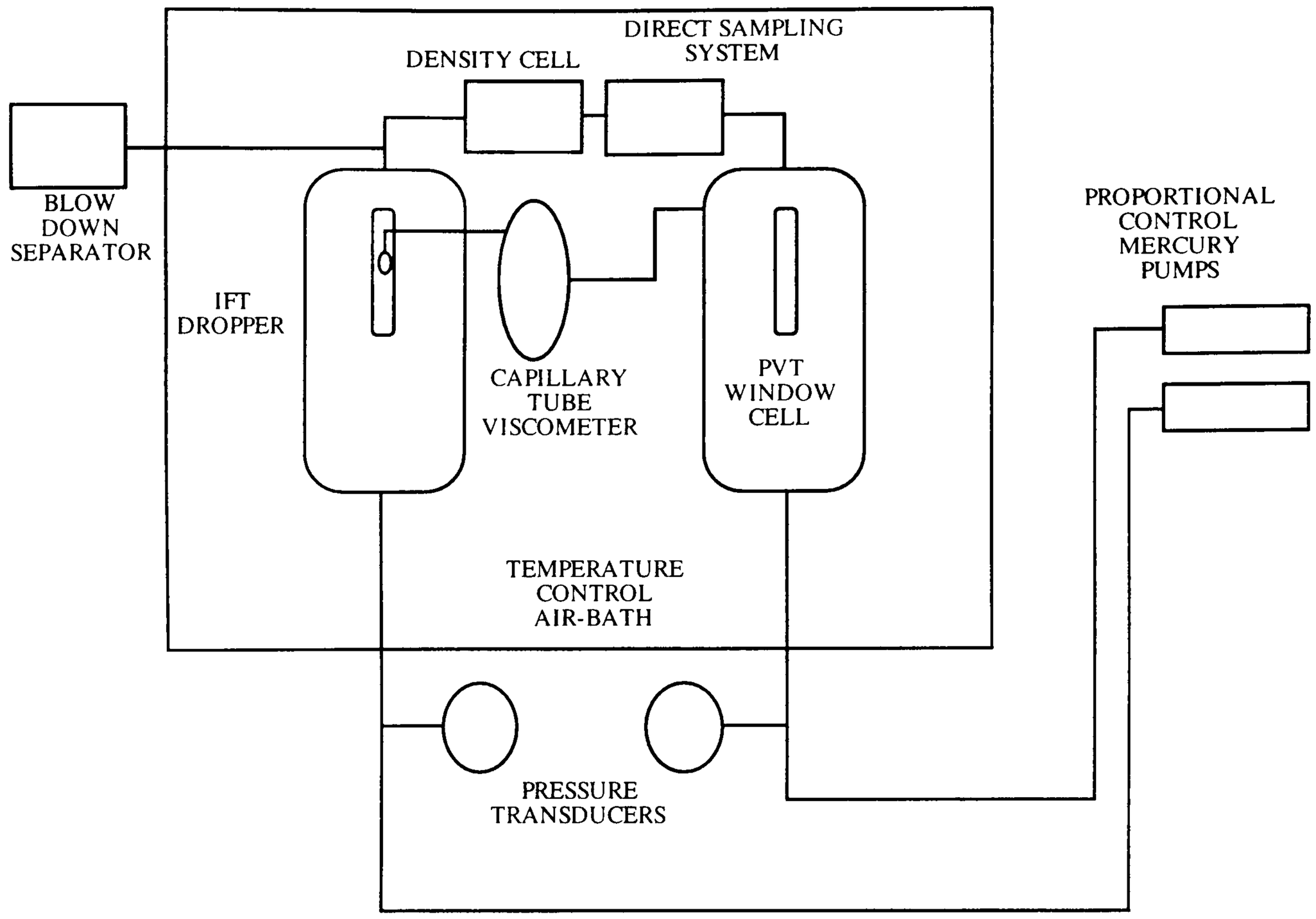

Fig. C.2 - Schematic Representation of the VLE Experimental Facility.